ISBN 978-82-326-2638-0 (printed version)
ISBN 978-82-326-2639-7 (electronic version)
ISSN 1503-8181

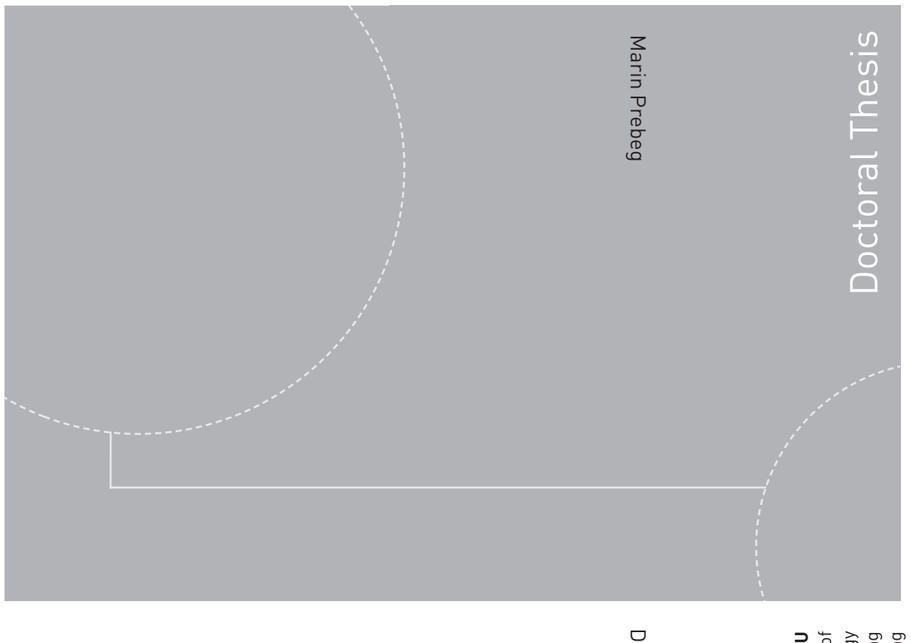

Doctoral theses at NTNU, 2017:285

Marin Prebeg

Large Time Step Methods for Hyperbolic Conservation Laws

NTNU
Norwegian University of
Science and Technology
Faculty of Engineering
Department of Energy and Process Engineering

Doctoral theses at NTNU, 2017:285

NTNU
Norwegian University of
Science and Technology

NTNU
Norwegian University of
Science and Technology

Marin Prebeg

Large Time Step Methods for Hyperbolic Conservation Laws

Thesis for the degree of Philosophiae Doctor

Trondheim, September 2017

Norwegian University of Science and Technology
Faculty of Engineering
Department of Energy and Process Engineering

NTNU
Norwegian University of
Science and Technology

NTNU
Norwegian University of Science and Technology

Thesis for the degree of Philosophiae Doctor

Faculty of Engineering
Department of Energy and Process Engineering

ISBN 978-82-326-2638-0 (printed version)
ISBN 978-82-326-2639-7 (electronic version)
ISSN 1503-8181

Doctoral theses at NTNU, 2017:285

Printed by Skipnes Kommunikasjon as

Abstract

Large Time Step (LTS) finite volume methods are presented, analyzed and applied to one-dimensional hyperbolic conservation laws.

The HLL (Harten–Lax–van Leer) and HLLC (HLL–Contact) schemes are extended to LTS-HLL(C) schemes. The LTS-HLL-type schemes for scalar conservation laws are defined in the numerical viscosity, flux-difference splitting and wave propagation form, and TVD conditions on wave velocity estimates are determined. It is shown that the LTS-HLL-type schemes contain some already existing LTS methods such as the LTS-Roe and LTS-Lax-Friedrichs, and that they allow us to deduce LTS extensions of other methods, such as the Rusanov and Engquist-Osher schemes. The LTS-HLL(C) schemes for systems of conservation laws are developed by standard field-by-field decomposition. Numerical results suggest that the computational efficiency of LTS methods depends on the type of problem under consideration. In certain cases LTS methods for nonlinear systems of equations yield increased accuracy, efficiency and convergence rate compared to standard methods.

Entropy stability of LTS-HLL-type schemes is analyzed. We use modified equation analysis to gain insight into numerical diffusion in LTS-HLL-type schemes and to conjecture about entropy stability of LTS methods. Theoretical results obtained through the modified equation analysis are in agreement with numerical results for both scalar conservation laws and the Euler equations.

Positivity preservation in LTS methods is investigated. We show that the positivity preserving conditions for LTS methods are stronger than for standard methods. We describe different ways positivity can be lost in LTS-HLL-type schemes for the Euler equations, and we propose a simple way to increase the robustness of the LTS-HLL-type schemes by adding numerical diffusion. Numerical investigations show that LTS-HLL-type schemes successfully handle test cases for positivity preservation, and where the positivity is lost we can improve the robustness by adding numerical diffusion.

In addition, we applied the LTS-Roe scheme to a two-fluid model and focused on the treatment of the boundary conditions and the source terms. It is shown that stability and accuracy of the solution can be greatly improved by appropriate treatment of boundary conditions and source terms.

Preface

The work presented in this thesis was carried out in the period from September 2014 to July 2017, at the Department of Energy and Process Engineering at the Norwegian University of Science and Technology. The project has been funded through the SIMCOFLOW project, carried out by the SINTEF Materials and Chemistry. I gratefully acknowledge the financial support from the Research Council of Norway (project no. 234126/30).

I wish to thank my supervisor, Professor Bernhard Müller, for allowing and encouraging me to pursue my own ideas, while ensuring that I stay on planned schedule and agreed deadlines. I am especially thankful for a lot of patience during the beginning of my PhD when I had a lot to learn and catch up with. I would like to thank my co-supervisor Tore Flåtten for all our scientific and nonscientific discussions. I am especially thankful for teaching me countless mathematical concepts and tools and for having endless faith in our work even when I didn't. I wish to thank my co-supervisor Marica Pelanti for arranging my stay at ENSTA ParisTech and for being a great host during my six months stay in Paris. My stay in Paris has been a valuable experience both professionally and personally. Further, Marica's knowledge on HLL(C) schemes has been an invaluable asset when I first started to work with this schemes. I also wish to thank my co-supervisor Ernst Arne Meese. We did not collaborate closely, but I appreciated our discussions and interest in my work.

These three years would have been much less fun without all my co-workers from the Department of Energy and Process Engineering. I am very thankful for all Green Room breaks, movie nights, dinners and skiing trips, but most of all, thank you for sharing with me the joys and excitement of doing sweet science. There are too many people to name them all, and I will point out Øyvind, Ehsan, Eskil and Anna who had a misfortune of sharing an office and an apartment with me.

Lastly, I wish to thank all my friends back home in Croatia for not forgetting me during my long absences, and I wish to thank Martina for her endless support in all my endeavors.

Trondheim, September 2017
Marin Prebeg

Contents

Contents iv

1. Introduction 1
- 1.1. Motivation . . . 1
- 1.2. Historical overview . . . 3
- 1.3. Goals and thesis outline . . . 5

2. Background 9
- 2.1. Mathematical models . . . 10
  - 2.1.1. Scalar conservation laws . . . 10
  - 2.1.2. Systems of conservation laws . . . 12
- 2.2. Finite volume methods for scalar conservation laws . . . 14
  - 2.2.1. Standard methods . . . 15
  - 2.2.2. Convergence and entropy stability . . . 17
  - 2.2.3. CFL condition . . . 22
  - 2.2.4. Large Time Step methods . . . 23
  - 2.2.5. Convergence and entropy stability . . . 26
- 2.3. Finite volume methods for systems of conservation laws . . . 29
  - 2.3.1. Convergence and entropy stability . . . 31

3. LTS-HLL-type schemes 33
- 3.1. Constructing the LTS-HLL and LTS-HLLC schemes . . . 33
  - 3.1.1. Standard HLL scheme for scalar conservation laws . . . 35
  - 3.1.2. Convergence and entropy stability . . . 40
  - 3.1.3. LTS-HLL scheme for scalar conservation laws . . . 44
  - 3.1.4. A class of LTS one-parameter methods . . . 46
  - 3.1.5. Convergence and entropy stability . . . 49
  - 3.1.6. LTS-HLL(C) schemes for systems of conservation laws 51
  - 3.1.7. Choice of the wave velocity estimates S_L and S_R . . . 52

3.2. Entropy stability 54
3.2.1. Entropy violation 55
3.2.2. Modified equation analysis 56
3.2.3. A class of one-parameter modified equations 57
3.3. Positivity preservation 62
3.3.1. Monotonicity 62
3.3.2. Positivity preservation 64

4. Multiphase flow modeling **67**
4.1. Mathematical modeling of two-phase flow 67
4.1.1. Two-fluid model 68
4.2. Numerical modeling of two-phase flow 71
4.2.1. Treatment of the boundary conditions 72
4.2.2. Treatment of the source terms 74

5. Conclusions and outlook **75**
5.1. Conclusions 75
5.2. Future outlook 77

Bibliography **79**

A. Research papers **93**
A.1. My publications 93
A.2. Journal paper 1 [P3] 97
A.3. Journal paper 2 [P2] 125
A.4. Journal paper 3 [P4] 149
A.5. Conference paper 1 [P5] 177
A.6. Conference paper 2 [P1] 185

I like mathematics because it is not human and has nothing particular to do with this planet or with the whole accidental universe – because, like Spinoza's God, it won't love us in return.

Bertrand Russell

1 Introduction

This thesis studies finite volume methods for hyperbolic conservation laws. In particular, we study Large Time Step (LTS) methods, unconditionally stable, explicit multi-point finite volume methods and their application to scalar conservation laws, the Euler equations and two-fluid model.

We start by giving a motivation for our work, by presenting a brief historical overview of the Large Time Step methods and by outlining the goals and structure of this thesis.

1.1. Motivation

Hyperbolic conservation laws are widely used to model a variety of physical phenomena, such as fluid dynamics, geophysics, biomechanics, electrodynamics, magnetohydrodynamics, astrophysics, etc. They are also heavily used in modeling multiphase flow phenomena [125, 138, 94], which is of particular interest for the SIMCOFLOW project [96][1]. In this thesis, we consider already existing models and focus on numerical methods for hyperbolic conservation laws rather than on physical modeling. To simplify the analysis, we mostly use simpler models (such as the Euler equations)

[1] The PhD project is a part of the research project *SIMCOFLOW – a framework for complex 3D multiphase and multi physics flows* carried out by SINTEF Materials and Chemistry from July 2014 until June 2017 and funded by the Research Council of Norway.

instead of more complicated multiphase flow models. However, we believe that the numerical tools developed here should be applicable to a wide class of hyperbolic problems.

In that respect, the motivation for our work on LTS methods is twofold. First, the final goal of every numerical method should be to solve a real-life problems or help us develop numerical methods for such problems. In order to describe the capacity of a particular method to do that, we often evaluate the method in terms of accuracy, efficiency and robustness.

When it comes to the accuracy, the current state of the art tools for hyperbolic conservation laws are ENO and WENO methods [122]. However, these methods may be quite expensive in terms of computing time, and even with continuous advances in computational power, many practical applications still require a trade-off between accuracy and efficiency. In addition, for highly nonlinear problems including discontinuities, WENO methods will not necessarily be more accurate and efficient than second-order methods [45].

The computational efficiency of a numerical method is strongly influenced by a number of things. One of them is the time integration method, where the main division is made between explicit and implicit time integration methods. Explicit methods are associated with higher accuracy and simpler implementation, but their efficiency and stability are limited by the CFL (Courant–Friedrichs–Lewy) condition. Implicit methods are not limited by the CFL condition and may be very efficient, but they are associated with a number of different difficulties, most important being the excessive diffusion and more complicated implementation. In addition, a development of modern supercomputers in the direction of parallel computing favors explicit methods, since they are parallelized more easily than implicit ones [107].

Further, high-order methods are usually less robust than first-order methods [151]. One property of robust methods is positivity preservation, which is still an active area of research for high-order methods. For instance, at this year's SIAM CSE conference[2], there was a dedicated session on *Positivity Preserving and Invariant Domain Preserving Methods*, where many of the talks addressed these issues for high-order methods. Some of the more recent publications include [151, 152, 61, 19, 121]. Hence, simpler methods may be more convenient when we are dealing with very complex

[2]SIAM Conference on Computational Science and Engineering, February 27–March 3, 2017, Atlanta, Georgia, USA.

flows, such as multiphase flow models or flows with strong source terms.

Unfortunately, there is always a trade-off between the accuracy, efficiency and robustness. Considering the great variety of problems where CFD (Computational Fluid Dynamics) is applied, there is a growing demand for methods with a different balance between these properties. In this thesis, we study LTS methods, a class of explicit methods not limited by the CFL condition, thereby providing a potential increase in efficiency, while preserving the advantages of explicit methods.

The second reason to study explicit multi-point methods is to gain better understanding of explicit methods in general. Namely, almost the complete theory of explicit finite volume methods assumes standard (3-point) methods.[3] By studying the concepts such as stability, numerical diffusion, total variation, modified equation and entropy stability in the multi-point methods one may gain better insight into these concepts in standard methods. And while multi-point methods are often seen as an extension of standard methods, it might be fruitful to view standard methods as a special case of the multi-point methods. Hence, we believe that studying explicit multi-point methods is a valuable exercise regardless whether one plans to use a CFD code that includes such methods or not.

1.2. Historical overview

Large Time Step methods studied in this thesis have been introduced by LeVeque in a series of papers between 1982 and 1985 [79, 80, 81]. Therein, the Godunov [43] and the Roe scheme [120] were extended to the LTS-Godunov and the LTS-Roe schemes and applied to scalar conservation laws and the Euler equations. In 1988, LeVeque extended the LTS-Godunov scheme to second-order accuracy and into two dimensions for arbitrary grids [82]. Through the years, these ideas have been recognized and used by a number of authors. Herein, we present the most important contributions in chronological order.

Parallel to LeVeque's work, Brenier [12] developed a framework of unconditionally stable explicit methods which includes the LTS methods of LeVeque and an LTS extension of the Engquist-Osher scheme [36], while Lucier [93] studied the error bounds in different schemes, including the LTS-Godunov scheme by LeVeque.

[3] Throughout the thesis, we use the term *standard methods* to denote explicit 3-point finite volume methods.

In 1992, Elliot and Chaundhry used these ideas to model two-dimensional dam-break flows [35], while in 1994 García-Navarro and Priestley [41] used the LTS-Roe scheme in their work on semi-Lagrangian methods for the shallow water equations. At the same time, in 1993, Wang and Warnecke investigated the entropy consistency in different LTS methods [144, 145]. In 1995, further applications of the LTS methods included front tracking methods based on wave propagation by LeVeque and Shyue [86] and semi-implicit methods by Klein [68].

From 2001 to 2004, there was a focus on investigating more mathematical properties of LTS methods: Helzel and Warnecke [55] and Wang et al. [146] studied the entropy stability of the LTS-Godunov scheme, Huang et al. [62] investigated the error bounds for the LTS-Glimm scheme and Tang and Warnecke [133] studied the monotonicity of (2K+1)-point schemes.

This period of numerical analysis of LTS methods was followed by a new wave of research mostly focused on the application of existing LTS methods and their extension to two- and three-dimensional problems. From 2006 to today, Morales-Hernández, Murillo, García-Navarro and co-workers [105, 99, 101, 100, 102] published a number of papers in which the LTS-Roe scheme is applied to the shallow water equations. Therein, the main focus has been on the treatment of the source terms, boundary conditions and multidimensional extensions, including arbitrary grids. In 2014, Xu et al. [148] applied the LTS-Godunov scheme to the shallow water equations. Further applications of the LTS-Godunov scheme in recent years include the three-dimensional Euler equations by Qian and Lee [117], high speed combustion waves by Tang et al. [134], and Maxwell's equations by Makwana and Chatterjee [95], while Lindqvist and Lund [90] applied the LTS-Roe scheme to two-phase flow model.

In 2016, Lindqvist et al. [91] studied the TVD property of LTS methods and showed that the LTS-Roe and the LTS-Lax-Friedrichs schemes are the least and most diffusive TVD LTS methods, respectively. This thesis heavily builds on the theoretical framework developed in [91]. In addition, the ideas developed in [91] have been further explored by a sequence of masters students at the author's university: Bore [10] investigated high-order LTS methods, while Solberg [124] and Nygaard [108] studied LTS methods with inherent mechanisms for introducing numerical diffusion.

In addition to LTS methods, there is a number of other approaches on how to relax the CFL condition in the explicit methods. The interested reader is referred to the research on semi-Lagrangian schemes [44, 126, 41, 49, 48, 75], front-tracking methods studied by Holden and co-workers [56,

58, 57], different approaches by Corrias et al. [20, 21], Leonard [76, 77, 78], Qiu and Shu [119] and Thompson and Moeller [135], and a version of LTS method developed by Harten [51] and further explored by Qian and Lee [118], Hussain et al. [63] and Siddiqui et al. [123]. Herein, we do not explore these any further.

1.3. Goals and thesis outline

The majority of the LTS methods discussed above are extensions of the Godunov and Roe schemes. The major disadvantage of the Godunov scheme is that it is computationally very expensive and cumbersome to implement for systems of equations, while the Roe scheme is not entropy stable and it is not positivity preserving. In fact, the LTS-Roe scheme leads to entropy violations even more often than the standard Roe scheme [91]. The LTS-Lax-Friedrichs scheme [91] is extremely diffusive and it is of interest only as a theoretical result and a building block for more sophisticated methods.

These observations motivated the question if it is possible to construct the LTS extensions of other schemes and what would be the properties of such solvers. In particular, we focused on the HLL and HLLC schemes. The HLL (Harten–Lax–van Leer) scheme is a very simple and efficient Riemann solver proposed by Harten et al. [53] in 1983. In addition to its simplicity and efficiency, the HLL scheme may be tuned to be entropy stable and positivity preserving. A more sophisticated extension, the HLLC (HLL–Contact) scheme, was proposed by Toro et al. [139] in 1994. Today, the HLL and HLLC schemes are widely used in a number of different fields, such as multiphase flow modeling [149, 137, 136, 115, 28, 27, 92], relativistic flows and magnetohydrodynamics [67, 88, 98, 97, 69, 59], shallow water equations [2] and radiative transfer [9]. For more references we refer to the book by Toro [138].

The development, analysis and application of the LTS-HLL(C) schemes are major themes of this thesis. In particular, our goals are:

- Develop LTS extensions of the HLL and HLLC schemes.
- Study entropy stability of the LTS-HLL(C) schemes.
- Study positivity preservation of the LTS-HLL(C) schemes.
- Study boundary and source term treatment in the LTS methods.

The thesis outline and contributions can be summarized as follows: in chapter 2 we present the mathematical models we solve, we outline the framework of the numerical methods we will consider, and we present the existing LTS methods. In chapter 3 we present the main results:

- In section 3.1 we develop LTS extensions of the HLL and HLLC schemes. We develop the LTS-HLL-type schemes, we determine their numerical viscosity and flux-difference splitting coefficients, and we investigate their convergence. This new class of schemes allows us to deduce some already existing LTS methods such as the LTS-Roe and LTS-Lax-Friedrichs, and it allows us to deduce LTS extensions of other methods, such as the Rusanov and Engquist-Osher schemes. Parts of this section are adapted from our second journal paper *Large Time Step HLL and HLLC Schemes* [P2].

- In section 3.2 we study entropy stability of LTS-HLL-type schemes. We use modified equation analysis to investigate how entropy violations occur in the LTS-HLL-type schemes and how can they be avoided. Parts of this section are adapted from our second conference paper *Numerical Viscosity in Large Time Step HLL-type Schemes* [P1].

- In section 3.3 we study monotonicity and positivity preservation of LTS-HLL(C) schemes. We determine monotonicity conditions on numerical flux function of an LTS method, and we show that positivity preserving conditions in LTS methods are stronger than in standard methods. We investigate different ways how is positivity lost in the LTS-HLL scheme, and we propose a simple way to increase robustness of the scheme by adding numerical diffusion. This section closely follows our third journal paper *Monotonicity and Positivity Preservation in Large Time Step Methods* [P4].

In addition to the work on the LTS-HLL(C) schemes, we applied the LTS-Roe scheme to a one-dimensional two-fluid model and focused on the treatment of the source terms and the boundary conditions. By introducing a new type of boundary conditions and by treating source terms in a similar way as Morales-Hernández, Murillo, García-Navarro and co-workers [105, 99, 101, 100, 102], we are able to notably improve accuracy of the solution. These results are presented in chapter 4. Content of chapter 4 corresponds to our first journal paper *Large Time Step Roe Scheme for a Common 1D Two-Fluid Model* [P3], and our first conference paper *Boundary and Source Term*

Treatment in the Large Time Step Method for a Common Two-Fluid Model [P5]. Finally, chapter 5 closes with conclusions and comments regarding possible further research directions.

In the presentation of the thesis results, we aimed to give a structured overview of our findings, but also tried to depict the order in which our work was done and how it was motivated.

Never any knowledge was delivered in the same order it was invented.

Sir Francis Bacon

2 Background

We present the mathematical models we will be considering and the numerical methods we will be using.

First, we present a general scalar conservation law and the Euler equations. The multiphase flow model will be presented in chapter 4. The properties of the solution to the scalar conservation law are presented in more detail, with a focus on the uniqueness of the solution and entropy conditions.

We then present the numerical methods we will use. We begin with the standard methods for scalar conservation laws and consider their numerical viscosity and flux-difference splitting forms. Convergence and entropy stability of the numerical methods are discussed following the standard literature. We do not aim to provide a comprehensive overview of numerical methods for the hyperbolic conservation laws. Instead, we focus on those parts that play an important role in the understanding and development of LTS methods. The methods are then extended to the LTS framework along the lines of Lindqvist et al. [91]. Main ideas of the LTS methods are presented, together with the already existing LTS methods.

Finally, both standard and LTS methods are extended to systems of conservation laws following the standard field-by-field decomposition.

The content of this chapter up to section 2.2.4 on the LTS methods heavily builds on the existing literature, and we refer to the books by Godlewski

and Raviart [42], LeVeque [83, 84], Toro [138], Trangenstein [142] and Dafermos [24] for more detailed reading.

2.1. Mathematical models

2.1.1. Scalar conservation laws

We consider the initial value problem for the scalar conservation law:

$$u_t + f(u)_x = 0, \qquad x \in \mathbb{R},\, t \in \mathbb{R}^+, \tag{2.1a}$$

$$u(x,0) = u_0(x), \tag{2.1b}$$

where $u \in \mathbb{R}$ is a conserved variable, $f(u) : \mathbb{R} \to \mathbb{R}$ is a strictly convex (or concave) flux function[1], and u_0 is the initial data.[2] It is known that solutions to the initial value problem (2.1) may develop discontinuous solutions even when the initial data is smooth. To allow for discontinuous solutions we consider weak solutions that satisfy (2.1) in the sense of distributions. A function $u(x,t)$ is a weak solution of (2.1) if it satisfies:

$$\int_0^\infty \int_{-\infty}^{+\infty} (u\varphi_t + f(u)\varphi_x)\,\mathrm{d}x\mathrm{d}t + \int_{-\infty}^{+\infty} u_0(x)\varphi(x,0)\mathrm{d}x = 0, \tag{2.2}$$

for all test functions $\varphi \in C_0^1$, i.e. for all continuously differentiable functions with compact support. However, there are infinitely many weak solutions $u(x,t)$ that satisfy (2.1) in a weak sense. The correct, unique weak solution to (2.1) is the same as the solution to the parabolic equation:

$$u_t + f(u)_x = \nu u_{xx}, \quad \nu > 0, \tag{2.3}$$

in the limit when $\nu \to 0$, where ν is a small parameter acting as a viscosity. In order to determine if a particular weak solution $u(x,t)$ is the unique weak solution, we usually determine the so-called *entropy condition* for (2.1) and check if the weak solution $u(x,t)$ satisfies this condition. This can be done in different ways, and examples of such conditions include the Lax entropy condition [73], Oleinik's entropy condition [109], Kružkov entropies [70] and entropy functions [73]. Here, we focus on the entropy

[1] Here and throughout the thesis, we will be considering only strictly convex (i.e. $f''(u) > 0$) or strictly concave (i.e. $f''(u) < 0$) flux functions.

[2] We follow the common notation where subscripts x and t denote partial derivatives with respect to x and t, respectively.

functions, because they will be used later when we discuss the numerical methods.

The basic idea is to define an *entropy function* $\eta(u)$ such that it is a convex function of u (i.e. $\eta''(u) > 0$) and a corresponding *entropy flux* $\psi(u)$ such that:

$$\psi'(u) = \eta'(u) f'(u). \tag{2.4}$$

Then it can be shown that the function $u(x,t)$ is the unique weak solution (or *entropy solution*) of the scalar conservation law (2.1) if the inequality:

$$\eta(u)_t + \psi(u)_x \leq 0, \tag{2.5}$$

holds in a weak sense, see LeVeque [83, p. 39].

Another important property of the unique weak solution to (2.1) is that it respects a strict *maximum principle*. Namely, if:

$$m = \min_x \left(u_0(x)\right), \quad M = \max_x \left(u_0(x)\right), \tag{2.6}$$

then:

$$u(x,t) \in [m, M] \quad \forall \quad x, t. \tag{2.7}$$

This property will play an important role later on when we discuss monotone methods for scalar conservation laws and positivity preserving methods for systems of equations.

For our purposes, we assume that the unique weak solution is known and want to know whether the numerical method converges to this solution.

The one-dimensional Riemann problem

In order to gain additional insight into the properties of the solution to the scalar conservation law (2.1), we consider a Riemann problem for (2.1):

$$u(x,0) = \begin{cases} u_{\mathrm{L}} & \text{for} \quad x < 0, \\ u_{\mathrm{R}} & \text{for} \quad x > 0, \end{cases} \tag{2.8}$$

which is simply the conservation law (2.1) with a piecewise constant initial data with a single discontinuity. By assuming a strictly convex flux function $f(u)$ the solution to the Riemann problem is either:

- a shock:

$$u(x,t) = \begin{cases} u_{\mathrm{L}} & \text{for} \quad x < st, \\ u_{\mathrm{R}} & \text{for} \quad x > st, \end{cases} \tag{2.9}$$

where $s(u_L, u_R)$ is the shock speed given by the Rankine–Hugoniot condition:

$$s = \frac{f(u_R) - f(u_L)}{u_R - u_L}, \tag{2.10}$$

- or a rarefaction wave:

$$u(x,t) = \begin{cases} u_L & \text{for} \quad x \leq f'(u_L)t, \\ (v(x/t)) & \text{for} \quad f'(u_L)t \leq x \leq f'(u_R)t, \\ u_R & \text{for} \quad x \geq f'(u_R)t, \end{cases} \tag{2.11}$$

where:

$$f'\left(v(x/t)\right) = \frac{x}{t}. \tag{2.12}$$

The structure of the solution for the Riemann problem (2.8) is closely related to the fact that (2.1) has infinitely many weak solutions. Namely, it is possible to construct weak solutions of (2.1) with the initial data (2.8) that satisfy (2.1) in a weak sense, but are not the solution to the viscous equation (2.3) in the vanishing viscosity limit.

The same difficulty is observed with numerical methods. When we numerically solve (2.1) with discrete initial data (2.8), a numerical method may converge to weak solution of (2.1) that is not the solution to the viscous equation (2.3) in the vanishing viscosity limit. We will return to this later on when we consider entropy stability of numerical methods.

2.1.2. Systems of conservation laws

We consider the hyperbolic system of conservation laws:

$$\mathbf{U}_t + \mathbf{F}(\mathbf{U})_x = 0, \qquad x \in \mathbb{R},\, t \in \mathbb{R}^+, \tag{2.13a}$$

$$\mathbf{U}(x,0) = \mathbf{U}_0(x), \tag{2.13b}$$

where $\mathbf{U} \in \mathbb{R}^N$ $(1 < N \in \mathbb{N})$ is a vector of conserved variables, $\mathbf{F}(\mathbf{U}) : \mathbb{R}^N \to \mathbb{R}^N$ is a flux function, and $\mathbf{U}_0$ is the initial data. We can also write (2.13) in a quasilinear form as:

$$\mathbf{U}_t + \mathbf{A}(\mathbf{U})\mathbf{U}_x = 0, \tag{2.14}$$

where:

$$\mathbf{A}(\mathbf{U}) = \frac{\partial \mathbf{F}(\mathbf{U})}{\partial \mathbf{U}}, \tag{2.15}$$

is the Jacobian matrix of $\mathbf{F}(\mathbf{U})$. We assume that the system of equations (2.14) is hyperbolic, i.e. the Jacobian matrix (2.15) has real eigenvalues and linearly independent eigenvectors.

Hyperbolic systems of conservation laws suffer from the same difficulties as the scalar conservation laws, i.e. they may develop discontinuous solutions and we have to look for a unique solution among all weak solutions. The unique entropy solution is determined in a similar fashion as for the scalar conservation law, namely we look for an entropy condition for the system of conservation laws and check if the particular weak solution satisfies this entropy condition.

In general, the entropy conditions for systems of conservation laws are notably more difficult than for scalar conservation laws. For more details we refer to the literature from the beginning of this chapter and the work by Tadmor [129, 130, 131, 132] and references therein. For our purposes, we will once again assume that the unique weak solution is known and we will only be interested in whether the numerical method converges to this solution.

The Euler equations

The Euler equations can be written in the form (2.13) by defining:

$$\mathbf{U} = \begin{bmatrix} \rho \\ \rho v \\ E \end{bmatrix}, \qquad \mathbf{F}(\mathbf{U}) = \begin{bmatrix} \rho v \\ \rho v^2 + p \\ v(E+p) \end{bmatrix}, \tag{2.16}$$

where ρ, v, E, p denote the density, velocity, total energy density and the pressure, respectively. The total energy density E is given as:

$$E = \rho e + \frac{1}{2}\rho v^2, \tag{2.17}$$

where e is a specific internal energy defined by an equation of state:

$$e = e\left(\rho, p\right), \tag{2.18}$$

which depends on the gas under consideration. In this thesis, we will consider only *ideal gas* for which:

$$e = \frac{p}{\rho\left(\gamma - 1\right)}. \tag{2.19}$$

Throughout the thesis we will use $\gamma = 1.4$ for air. Alternatively, we may write the Euler equations (2.16) in the form (2.14) by defining the Jacobian matrix $\mathbf{A}(\mathbf{U})$ (see LeVeque [84, p. 300]). The eigenvalues of the Jacobian matrix $\mathbf{A}(\mathbf{U})$ for the Euler equations are:

$$\lambda_1 = v - a, \quad \lambda_2 = v, \quad \lambda_3 = v + a, \tag{2.20}$$

where $a = \sqrt{\gamma p/\rho}$ is the speed of the sound.

Remark 1. It is possible to define the Riemann problem (2.8) for the Euler equations and study structure of the solution in a similar fashion as for the scalar conservation law. We omit such analysis here and refer to Lax [73], LeVeque [85] and Toro [138] for detailed analysis of the Riemann problem for the Euler equations.

2.2. Finite volume methods for scalar conservation laws

We start by dividing the spatial domain into intervals with increment $\Delta x = x_{j+1/2} - x_{j-1/2}$, and the time domain into intervals with increment $\Delta t = t^{n+1} - t^n$. We then integrate the conservation law (2.1) over the control volume $\left[x_{j-1/2}, x_{j+1/2}\right] \times \left[t^n, t^{n+1}\right]$ to obtain:

$$\int_{x_{j-1/2}}^{x_{j+1/2}} u(x, t^{n+1}) \mathrm{d}x = \int_{x_{j-1/2}}^{x_{j+1/2}} u(x, t^n) \mathrm{d}x + \int_{t^n}^{t^{n+1}} f(u(x_{j-1/2}, t)) \mathrm{d}t - \int_{t^n}^{t^{n+1}} f(u(x_{j+1/2}, t)) \mathrm{d}t, \tag{2.21}$$

which is telling us that the conserved variable inside a cell changes only due to the flow over its boundaries. By approximating the exact cell average of the exact solution as:

$$u_j^n \approx \frac{1}{\Delta x} \int_{x_{j-1/2}}^{x_{j+1/2}} u\left(x, t^n\right) \mathrm{d}x, \tag{2.22}$$

and by approximating the time averaged flux function of the exact solution at the interface $x_{j+1/2}$ as:

$$F_{j+1/2}^n \approx \frac{1}{\Delta x} \int_{t^n}^{t^{n+1}} f(u(x_{j+1/2}, t)) \mathrm{d}t, \tag{2.23}$$

we can write (2.21) in the conservation form:

$$u_j^{n+1} = u_j^n - \frac{\Delta t}{\Delta x}\left(F_{j+1/2}^n - F_{j-1/2}^n\right). \tag{2.24}$$

Unfortunately, $u\left(x_{j\mp1/2}, t\right)$ changes in time and most of the time we cannot evaluate the integral (2.23) exactly. Instead, we evaluate it by using an exact or approximate Riemann solver.

2.2.1. Standard methods

In order to solve (2.1) numerically, Godunov [43] assumes a piecewise constant initial data:

$$u(x, t^n) = u_j^n, \quad x_{j-1/2} \le x < x_{j+1/2}, \tag{2.25}$$

which leads to a local Riemann problem defined at each interface. Then, u_j^{n+1} is updated by exactly solving (2.1) with initial data (2.25):

$$u_j^{n+1} = \frac{1}{\Delta x}\int_0^{\Delta x/2} \widetilde{u}_{j-1/2}^{\text{God}}\left(x/\Delta t\right) \mathrm{d}x + \frac{1}{\Delta x}\int_{-\Delta x/2}^{0} \widetilde{u}_{j+1/2}^{\text{God}}\left(x/\Delta t\right) \mathrm{d}x, \tag{2.26}$$

where $\widetilde{u}_{j-1/2}^{\text{God}}\left(x/t\right)$ is the exact solution to the local Riemann problem at the cell interface $x_{j-1/2}$, and where we assumed that the time step Δt is such that the waves from the Riemann problems do not interact. We note that we can obtain (2.24) from (2.26), revealing the definition of $F_{j+1/2}$ as:

$$F_{j+1/2}^{\text{God}} = F(u_j, u_{j+1}) = f\left(\widetilde{u}_{j+1/2}^{\text{God}}(0)\right). \tag{2.27}$$

Unfortunately, solving the Riemann problem exactly becomes extremely expensive once we move to nonlinear systems of equations, especially for complex equations of state. Thus, we consider (2.1) with initial data (2.25) and we seek an approximation to the flux (2.23). In this chapter we consider two different ways to approximate the flux function (2.23): *numerical viscosity* (NV) form and *flux-difference splitting* (FDS) form.

Numerical viscosity

In the section above, we discretized (2.1) in conservation form:

$$u_j^{n+1} = u_j - \frac{\Delta t}{\Delta x}\left(F_{j+1/2} - F_{j-1/2}\right), \tag{2.28}$$

where the numerical flux function is usually defined as:

$$F_{j+1/2} = \frac{1}{2}\left(f_j + f_{j+1}\right) - \frac{1}{2}Q_{j+1/2}(u_{j+1} - u_j), \tag{2.29}$$

where $f_j = f\left(u_j\right)$ and $Q_{j+1/2}$ is the numerical viscosity coefficient.[3] We require that the numerical flux function is Lipschitz continuous and consistent in the sense that:

$$F\left(u, u\right) = f(u). \tag{2.30}$$

In this form, the method is completely determined by the numerical viscosity coefficient:

$$Q_{\text{Roe}} = |\lambda| \qquad \text{: Roe} \tag{2.31a}$$
$$Q_{\text{LxF}} = \Delta x/\Delta t \qquad \text{: Lax-Friedrichs} \tag{2.31b}$$
$$Q_{\text{Rus}} = \max\left(|\lambda_j|, |\lambda_{j+1}|\right) \qquad \text{: Rusanov} \tag{2.31c}$$
$$Q_{\text{E-O}} = \frac{1}{u_{j+1} - u_j}\int_{u_j}^{u_{j+1}} \left|f'(u)\right| \mathrm{d}u \qquad \text{: Engquist-Osher} \tag{2.31d}$$
$$Q_{\text{God}} = \frac{f_j + f_{j+1} - 2\mathcal{M}_{j+1/2}(f(u))}{u_{j+1} - u_j} \qquad \text{: Godunov} \tag{2.31e}$$
$$Q_{\text{L-W}} = \lambda^2 \Delta t/\Delta x \qquad \text{: Lax-Wendroff} \tag{2.31f}$$

where $\lambda_j = f'(u_j)$, $\lambda = \lambda_{j+1/2}$ is the shock speed at the interface $x_{j+1/2}$ determined by the Rankine–Hugoniot condition:

$$\lambda_{j+1/2} = \begin{cases} \left(f(u_{j+1}) - f(u_j)\right) / \left(u_{j+1} - u_j\right) & \text{if} \quad u_{j+1} - u_j \neq 0, \\ f'(u_j) & \text{if} \quad u_{j+1} - u_j = 0, \end{cases} \tag{2.32}$$

and $\mathcal{M}_{j+1/2}(f(u))$:

$$\mathcal{M}_{j+1/2}\left(f(u)\right) = \begin{cases} \min\limits_{u \in \mathcal{R}_{j+1/2}} f(u) & \text{if} \quad u_j < u_{j+1}, \\ \max\limits_{u \in \mathcal{R}_{j+1/2}} f(u) & \text{if} \quad u_j \geq u_{j+1}, \end{cases} \tag{2.33}$$

where:

$$\mathcal{R} = \left[\min\left(u_j, u_{j+1}\right), \max\left(u_j, u_{j+1}\right)\right]. \tag{2.34}$$

[3] From now on, we omit time index n because we consider only explicit methods.

Flux-difference splitting

Another way to discretize (2.1) is by flux-difference splitting:

$$u_j^{n+1} = u_j - \frac{\Delta t}{\Delta x}\left(A^+_{j-1/2}\Delta u_{j-1/2} + A^-_{j+1/2}\Delta u_{j+1/2}\right), \tag{2.35}$$

where $A^{\pm}_{j\mp1/2}$ are the flux-difference splitting coefficients, and where we introduced $\Delta u_{j-1/2} = u_j - u_{j-1}$. In this form, the method is completely determined by the flux-difference splitting coefficients:

$$A^{\pm}_{\text{Roe}} = \pm\max\left(0, \pm\lambda\right) \quad : \text{Roe} \tag{2.36a}$$

$$A^{\pm}_{\text{LxF}} = \frac{1}{2}\left(\lambda \pm \frac{\Delta x}{\Delta t}\right) \quad : \text{Lax-Friedrichs} \tag{2.36b}$$

$$A^{\pm}_{\text{Rus}} = \frac{1}{2}\left(\lambda \pm \max\left(|\lambda_j|, |\lambda_{j+1}|\right)\right) \quad : \text{Rusanov} \tag{2.36c}$$

$$A^{\pm}_{\text{E-O}} = \frac{1}{u_{j+1} - u_j}\int_{u_j}^{u_{j+1}} \left(f'(u)\right)^{\pm} \mathrm{d}u \quad : \text{Engquist-Osher} \tag{2.36d}$$

$$A^{\pm}_{\text{God}} = \frac{1}{2}\left(\lambda \pm \frac{f_j + f_{j+1} - 2\mathcal{M}_{j+1/2}\left(f(u)\right)}{u_{j+1} - u_j}\right) \quad : \text{Godunov} \tag{2.36e}$$

$$A^{\pm}_{\text{L-W}} = \frac{1}{2}\lambda\left(1 \pm \lambda\frac{\Delta t}{\Delta x}\right) \quad : \text{Lax-Wendroff} \tag{2.36f}$$

There is a one-to-one mapping between the numerical viscosity (2.31) and the flux-difference splitting coefficients (2.36) such that:

$$A^{\pm} = \frac{1}{2}\left(\lambda \pm Q\right) \quad \text{and} \quad Q = A^+ - A^-. \tag{2.37}$$

We will denote the methods in (2.31) and (2.36) as *one-parameter* methods.

2.2.2. Convergence and entropy stability

In this section we address two important questions associated with the numerical methods (2.31):

- how do we know that a numerical method (2.31) converges to the solution of the scalar conservation law (2.1);
- and since there are infinitely many weak solutions of (2.1), even if the numerical method converges, how do we know that it converges to the unique weak solution satisfying the entropy condition?

To answer these questions we consider the conservation form (2.28) and note that it is much more than just a convenient way to write the scheme in the numerical viscosity form. Namely, Lax and Wendroff [74] proved that if a conservative and consistent numerical method converges, then it converges to a weak solution of the scalar conservation law (2.1). Unfortunately, the Lax-Wendroff theorem itself says nothing about whether a method converges, and it says even less about the uniqueness of the solution.

To address these two questions, we recall that (2.31) are one-parameter methods, completely determined by the numerical viscosity coefficient Q. Therefore, our two questions can be summarized as – what choice of Q guarantees convergence to the unique weak solution satisfying the entropy condition?

Convergence

We start by considering the Lax-Wendroff theorem and addressing the question of conservation, consistency and convergence.

For the methods (2.31), the requirement to be written in conservation form is satisfied by the definition of (2.28), while the consistency can be shown by using the modified equation. Namely, the first-order accurate methods (2.31a)–(2.31e) give a second-order accurate approximation to the equation (see [91]):

$$u_t + f(u)_x = \frac{1}{2}\frac{\Delta x^2}{\Delta t}\left[\left(\frac{\Delta t}{\Delta x}\bar{Q} - c^2\right)u_x\right]_x, \tag{2.38}$$

where $\bar{Q} = Q(u,u)$ and $c = f'(u)\Delta t/\Delta x$. It can be shown that by using any Q from (2.31a)–(2.31e) in (2.38), by keeping $c = \text{const.}$ and passing $\Delta x \to 0$ we recover the scalar conservation law (2.1). The same property can be shown for the second-order accurate Lax-Wendroff method (2.31f).

In order to prove the convergence, we need to show that the scheme is stable in some appropriate sense. Herein, we will use the form of nonlinear stability called the *total variation stability*. A weak solution to the scalar conservation laws (2.1) has the following property (see Harten [50]):

$$\mathrm{TV}\left(u\left(\cdot,t_2\right)\right) \leq \mathrm{TV}\left(u\left(\cdot,t_1\right)\right), \quad t_2 \geq t_1, \tag{2.39}$$

where TV is the *total variation* of an arbitrary function $u(x)$:

$$\mathrm{TV}(u) = \lim_{\delta} \sup \frac{1}{\delta}\int_{-\infty}^{\infty} |u(x) - u(x-\delta)|\,\mathrm{d}x, \tag{2.40}$$

where for smooth $u(x)$ we can write:

$$\mathrm{TV}(u) = \int_{-\infty}^{\infty} \left|u'(x)\right| \mathrm{d}x. \tag{2.41}$$

Equation (2.39) is telling us that the total variation of solution is non-increasing in time. Hence, it is natural to enforce this requirement on the numerical method.

Definition 1 (Harten [50][4])**.** *A two-level method is called total variation diminishing (TVD) if, for any set of data u^n, the values u^{n+1} computed by the method satisfy:*

$$TV(u^{n+1}) \leq TV\left(u^n\right), \tag{2.42}$$

where the discrete total variation is defined as:

$$TV\left(u^n\right) = \sum_{j=-\infty}^{\infty} |u_{j+1}^n - u_j^n|. \tag{2.43}$$

We note that for $\mathrm{TV}(u^n)$ to be finite, one must assume $u_j^n = \text{const.}$ as $j \to \pm\infty$ (see [85, 138]). Hence, it follows from the Lax-Wendroff theorem that if the methods (2.31) are TVD, then we expect they converge to some weak solution of the scalar conservation law. This can be determined using the classical result:

Theorem 1 (Harten [50], Tadmor [128])**.** *A 3-point conservative scheme in the form* (2.28) *is unconditionally TVD if and only if:*

$$\left|\lambda_{j+1/2}\right| \leq Q_{j+1/2} \leq \frac{\Delta x}{\Delta t}, \quad \forall\, j. \tag{2.44}$$

It can be shown that methods (2.31a)–(2.31e) are TVD, while the Lax-Wendroff method (2.31f) is not. We can also see that the lower and upper bounds are in fact the Roe and Lax-Friedrichs schemes:

$$Q_{\mathrm{Roe}} \leq Q \leq Q_{\mathrm{LxF}}. \tag{2.45}$$

[4]The TVD concept has been introduced by Harten [50], while the Definition 1 is taken verbatim from LeVeque [84].

Entropy stability

Following the Lax-Wendroff theorem, a conservative, consistent and TVD scheme converges to a weak solution of the conservation law. However, we still do not know if the method converges to the entropy solution. If the method converges to the entropy solution, we say that the method is *entropy stable*.

Since the numerical method is completely determined by the numerical viscosity coefficient Q, it is no surprise that the concept of entropy stability is directly related to the numerical viscosity coefficient Q. This is not a coincidence, and it has a deeper meaning – the unique weak solution we wish to obtain is the limit solution of the parabolic equation (2.3) which contains a certain amount of physical viscosity.

In order to see how are solutions to (2.1) and (2.3) related, we recall that the parabolic equation (2.3) contains a viscosity ν:

$$u_t + f(u)_x = \nu u_{xx}, \quad \nu > 0. \tag{2.46}$$

It is precisely this viscosity that guarantees that (2.46) has only one solution, and it is precisely the lack of this viscosity that causes (2.1) to have discontinuous solutions and forces us to consider all weak solutions as possible solutions to (2.1).[5]

However, the modified equation (2.38) shows that when we solve (2.1) with a first-order accurate method, we are actually solving the following equation with second-order accuracy:

$$u_t + f(u)_x = \frac{1}{2}\frac{\Delta x^2}{\Delta t}\left[Du_x\right]_x, \tag{2.47}$$

where we introduce the inherent numerical diffusion:

$$D = \frac{\Delta t}{\Delta x}\bar{Q} - c^2. \tag{2.48}$$

The right-hand side of (2.47) has the same effect as the right-hand side of (2.46). Hence, by solving (2.1) we are actually more accurately solving the viscous equation (2.47) in which the viscosity is introduced by the numerical method. This suggests that a certain amount of numerical diffusion

[5] *La nature ne fait jamais des sauts* (French for "Nature does not make jumps") – Gottfried Leibniz, in New Essays, IV, 16. Leibniz's axiom sums up a crux of the matter with the hyperbolic conservation laws (2.1) – by neglecting viscosity, we allow jumps, which leads to difficulties otherwise not encountered in real world.

should guarantee convergence to the unique weak solution satisfying the entropy condition. The critical question is how much numerical diffusion do we need to make sure that the method converges to the unique weak solution satisfying the entropy condition?

The Godunov scheme plays a central role in answering this question. The Godunov scheme solves the Riemann problem exactly, and it can be shown that it converges to the entropy solution [110, 127]. Osher [110] and Tadmor [127] showed that any scheme with more numerical diffusion than the Godunov scheme also converges to the entropy solution. Such scheme are denoted as *E-schemes* and they satisfy the inequality:

$$\operatorname{sgn}\left(u_j - u_{j-1}\right)\left[F^{\mathrm{E}}_{j-1/2} - F^{\mathrm{God}}_{j-1/2}\right] \leq 0, \tag{2.49}$$

or in terms of the numerical viscosity coefficient (2.31):

$$Q_{\mathrm{God}} \leq Q_{\mathrm{E}} \leq Q_{\mathrm{LxF}}, \tag{2.50}$$

where Q_{E} is the numerical viscosity coefficient of an E-scheme, and the upper bound has to hold due to the TVD condition (2.44). Among the schemes considered in (2.31), the Lax-Friedrichs, Rusanov and Engquist-Osher schemes are E-schemes, while the Roe and Lax-Wendroff schemes are not.

Another way to obtain convergence to the entropy solution is to supplement a scheme that is not entropy stable, such as the Roe scheme, with an entropy fix. Then it is sufficient to show that the new scheme satisfies a discrete version of the entropy inequality (2.5):

$$\eta(u_j^{n+1}) \leq \eta(u_j) - \frac{\Delta t}{\Delta x}\left(\psi_{j+1/2} - \psi_{j-1/2}\right), \tag{2.51}$$

where $\psi_{j+1/2} = \psi(u_j, u_{j+1})$ is the numerical entropy flux. A number of different entropy fixes can be found in [84], but they are all designed for standard methods and they are not suited to resolve the entropy violations which we encounter in LTS methods. Therefore, we do not consider these in much detail.

The third way to ensure convergence to the entropy solution is by showing that the scheme is *monotone*. We recall that in addition to being entropy stable, the unique weak solution to the scalar conservation law (2.1) satisfies the strict maximum principle (2.7). If the numerical scheme satisfies this property on a discrete level, namely for:

$$m = \min_j(u_j^0), \quad M = \max_j(u_j^0), \tag{2.52}$$

if the numerical scheme ensures that:

$$u_j^n \in [m, M] \quad \forall \quad j, n, \tag{2.53}$$

we say that the scheme is maximum-principle-satisfying. Monotone schemes are maximum-principle-satisfying and their properties will be studied in section 3.3 (p. 63). Among the schemes considered earlier (2.31), the Godunov, Lax-Friedrichs, Rusanov and Engquist-Osher schemes are monotone, while the Roe and Lax-Wendroff schemes are not. An important feature of the monotone schemes is that they are E-schemes and that they are at best first-order accurate [110]. More details on E-schemes and monotone schemes, including proofs of statements above, can be found in the books by Godlewski and Raviart [42] and Trangenstein [142].

2.2.3. CFL condition

We saw that the TVD condition led to a lower bound on the numerical viscosity coefficient, corresponding to the Roe scheme. Further, E-schemes imposed a stronger lower bound on the numerical viscosity coefficient, corresponding to the Godunov scheme.

The upper bound of the TVD condition (2.44) is due to the CFL (Courant–Friedrichs–Lewy) condition. Namely, the time step Δt in the standard methods given by discretizations (2.28) and (2.35) is limited by:

$$\bar{C} = \max_x |\lambda(x,t)| \frac{\Delta t}{\Delta x} \leq 1, \tag{2.54}$$

which enforces that information from interface cannot travel more than a single cell during a single time step. This is due to the fact that the numerical flux function (2.29) depends only on neighboring cells:

$$F_{j+1/2} = F\left(u_j, u_{j+1}\right), \tag{2.55}$$

which leads to a standard (3-point) method:

$$u_j^{n+1} = u\left(u_{j-1}, u_j, u_{j+1}\right). \tag{2.56}$$

The central topic of this thesis are explicit methods not limited by the CFL condition (2.54). Namely, standard methods may be interpreted as a special case of the $(2k+1)$-point methods, where the parameter k defines the size of the stencil. For standard methods $k = 1$, yielding a 3-point

methods. We may relax the CFL condition (2.54) by increasing the domain of dependence:

$$u_j^{n+1} = u\left(u_{j-k}, \ldots, u_{j+k}\right), \tag{2.57}$$

which leads to a new CFL condition:

$$\bar{C} = \max_x |\lambda(x,t)| \frac{\Delta t}{\Delta x} \leq k, \tag{2.58}$$

where k is any positive integer. These ideas were originally introduced by LeVeque [79, 80, 81] and used by a number of authors through the years (see section 1.2 *Historical overview* for more details). Herein, we follow Lindqvist et al. [91] who were (to the best of our knowledge) the first to give closed forms of the numerical viscosity and flux-difference splitting coefficients for LTS methods.

2.2.4. Large Time Step methods

For the LTS methods considered here, the basic conservation form (2.28) is still valid, and it is the numerical flux function that is changed. The LTS extension of the numerical viscosity form (2.29) is:

$$F_{j+1/2} = \frac{1}{2}\left(f_j + f_{j+1}\right) - \frac{1}{2}\sum_{i=-\infty}^{\infty} Q^i_{j+1/2+i} \Delta u_{j+1/2+i}, \tag{2.59}$$

and the LTS extension of the flux-difference splitting form (2.35) is:

$$u_j^{n+1} = u_j - \frac{\Delta t}{\Delta x}\sum_{i=0}^{\infty}\left(A^{i+}_{j-1/2-i}\Delta u_{j-1/2-i} + A^{i-}_{j+1/2+i}\Delta u_{j+1/2+i}\right), \tag{2.60}$$

where newly introduced indices will be explained below, and where we introduce the convention:

$$Q^i = A^{i\pm} = 0 \quad \text{for} \quad |i| \geq k. \tag{2.61}$$

We note that (2.59) differs from [91] in a sense that we scale Q^i by $\Delta x/\Delta t$. In order to see how is the numerical flux function of an LTS method (2.59) related to the standard numerical flux function (2.29), and how is the LTS flux-difference splitting (2.60) related to the standard flux-difference splitting (2.35), we consider Figure 2.1.

In the numerical flux function (2.59), the infinite sum contains contributions to the numerical flux function from different interfaces. The subscript

of Q describes the absolute cell interface position, while the superscript describes the relative cell interface position with respect to the interface $x_{j+1/2}$. Hence, $Q^i_{j+1/2+i}$ tells us how the numerical viscosity coefficient Q from the interface $x_{j+1/2+i}$ contributes to the numerical flux function at the interface $x_{j+1/2}$, which is $|i|$ cells away. This is illustrated in Figure 2.1a.

In the flux-difference splitting form (2.60), two infinite sums contain contributions to the flux differences from different interfaces. The subscript of A describes the absolute cell interface position, while the superscript describes the relative cell interface position with respect to interfaces $x_{j-1/2}$ and $x_{j+1/2}$. Hence, $A^{i+}_{j-1/2-i}$ tells us how the flux-difference splitting coefficient A from the interface $x_{j-1/2-i}$ contributes to the flux difference at the interface $x_{j-1/2}$, which is $|i|$ cells away. This is illustrated in Figure 2.1b.

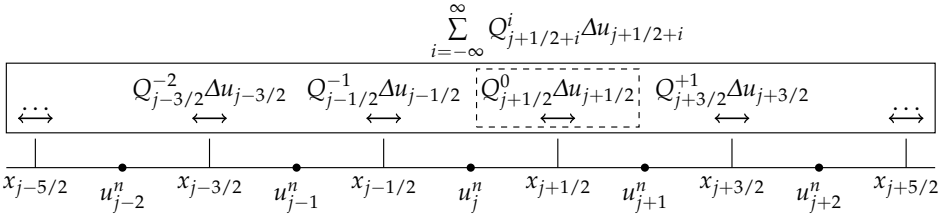

(a) Numerical viscosity form

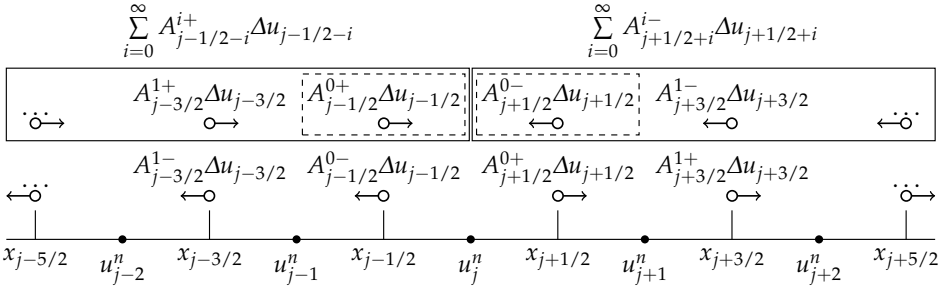

(b) Flux-difference splitting form

Figure 2.1.: Updating of u_j: domain of dependence of standard (dashed boxes) and LTS methods (full boxes) in numerical viscosity and flux-difference splitting forms.

The coefficients with the superscript 0 correspond to the standard methods (2.31) and (2.36).

Remark 2. We note that the absolute cell interface position has a meaning

only with respect to a particular cell, for instance x_j in the examples above. In order to make our definitions of Q and A more general, and to simplify the notation, we will suppress the absolute cell interface index. Then, our definition of Q and A tells us how the numerical viscosity (or flux-difference splitting) coefficient from an *arbitrary* interface contributes to the numerical flux function (or flux difference) at the interface that is $|i|$ cells away.

Lindqvist et al. [91] determined the partial viscosity coefficients of the LTS-Roe scheme:

$$Q^0_{\text{Roe}} = |\lambda|, \tag{2.62a}$$

$$Q^{\mp i}_{\text{Roe}} = 2\max\left(0, \pm\lambda - i\frac{\Delta x}{\Delta t}\right) \quad \text{for} \quad i > 0, \tag{2.62b}$$

the LTS-Godunov scheme:

$$Q^i_{\text{God}} = \begin{cases} 2\frac{\left(f(u)+iu\frac{\Delta x}{\Delta t}\right)_{j+1} - \mathcal{M}_{j+1/2}\left(f(u)+iu\frac{\Delta x}{\Delta t}\right)}{u_{j+1}-u_j} & \text{for} \quad i < 0, \\ \frac{f_j + f_{j+1} - 2\mathcal{M}_{j+1/2}(f(u))}{u_{j+1}-u_j} & \text{for} \quad i = 0, \\ 2\frac{\left(f(u)+iu\frac{\Delta x}{\Delta t}\right)_{j} - \mathcal{M}_{j+1/2}\left(f(u)+iu\frac{\Delta x}{\Delta t}\right)}{u_{j+1}-u_j} & \text{for} \quad i > 0, \end{cases} \tag{2.63}$$

and the LTS-Lax-Friedrichs scheme:

$$Q^0_{\text{LxF}} = k\frac{\Delta x}{\Delta t}, \tag{2.64a}$$

$$Q^{\mp i}_{\text{LxF}} = \frac{k-i}{k}\left(\pm\lambda + k\frac{\Delta x}{\Delta t}\right) \quad \text{for} \quad i > 0. \tag{2.64b}$$

Lindqvist et al. [91] also determined the flux-difference splitting coefficients of the LTS-Roe scheme:

$$A^{i\pm}_{\text{Roe}} = \pm\max\left(0, \min\left(\pm\lambda - i\frac{\Delta x}{\Delta t}, \frac{\Delta x}{\Delta t}\right)\right), \tag{2.65}$$

and the LTS-Godunov scheme:

$$\begin{aligned} A^{i+}_{\text{God},j-1/2-i} = \frac{1}{\Delta u_{j-1/2-i}}\Bigg(&\mathcal{M}_{j-1/2-i}\left(f(u) - (i+1)\,u\frac{\Delta x}{\Delta t}\right) \\ &-\mathcal{M}_{j-1/2-i}\left(f(u) - iu\frac{\Delta x}{\Delta t}\right) + u_{j-i}\frac{\Delta x}{\Delta t}\Bigg), \end{aligned} \tag{2.66a}$$

$$A^{i-}_{\mathrm{God},j+1/2+i} = \frac{1}{\Delta u_{j+1/2+i}} \left(\mathcal{M}_{j+1/2+i} \left(f(u) + iu\frac{\Delta x}{\Delta t} \right) \right.$$
$$\left. - \mathcal{M}_{j+1/2+i} \left(f(u) + (i+1)\, u\frac{\Delta x}{\Delta t} \right) + u_{j+i}\frac{\Delta x}{\Delta t} \right), \qquad (2.66b)$$

while Bore [10] determined them for the LTS-Lax-Friedrichs scheme:

$$A^{i\pm}_{\mathrm{LxF}} = \frac{1}{2k} \left(\lambda \pm k\frac{\Delta x}{\Delta t} \right). \qquad (2.67)$$

We note that for $k = 1$, (2.59) and (2.60) reduce to (2.29) and (2.35), respectively. Lindqvist et al. [91] also showed that there is a one-to-one mapping between the numerical viscosity and the flux-difference splitting coefficients:

Lemma 1 (Lindqvist et al. [91])**.** *For a given local multi-point scheme, there is a one-to-one mapping between the coefficients A of* (2.60) *and the coefficients Q of* (2.59) *as follows:*

$$A^{0\pm} = \frac{1}{2} \left(\lambda \pm Q^0 \mp Q^{\mp 1} \right), \qquad (2.68a)$$
$$A^{i\pm} = \pm\frac{1}{2} \left(Q^{\mp i} - Q^{\mp(i+1)} \right), \quad i \in \{1, \ldots, k-1\}, \qquad (2.68b)$$

and:

$$Q^i = \begin{cases} 2\sum_{p=-i}^{\infty} A^{p+} & \text{for} \quad i < 0, \\ \sum_{p=0}^{\infty} \left(A^{p+} - A^{p-} \right) & \text{for} \quad i = 0, \\ -2\sum_{p=i}^{\infty} A^{p-} & \text{for} \quad i > 0. \end{cases} \qquad (2.69)$$

We will denote the methods (2.62)–(2.64) and (2.65)–(2.67) as LTS *one-parameter* methods. Namely, even though the numerical flux function (2.59) may depend on more than one numerical viscosity coefficient Q, these methods are natural extensions of the standard one-parameter methods.

2.2.5. Convergence and entropy stability

Convergence

The Lax-Wendroff theorem from section 2.2.2 also applies to LTS methods. The conservation form is ensured by writing the LTS methods in the form

(2.59), while the consistency of the LTS-Godunov, LTS-Roe and LTS-Lax-Friedrichs schemes can be shown by using modified equation. The first-order accurate LTS method gives a second-order accurate approximation to the equation (see [91]):

$$u_t + f(u)_x = \frac{1}{2}\frac{\Delta x^2}{\Delta t}\left[\left(\sum_{i=1-k}^{k-1}\frac{\Delta t}{\Delta x}\bar{Q}^i - c^2\right)u_x\right]_x. \tag{2.70}$$

By using any Q from (2.62)–(2.64) in (2.70), by keeping $c = \text{const.}$ and by passing $\Delta x \to 0$ we recover the scalar conservation law (2.1).

The notion of TVD stability was generalized for multi-point schemes by Jameson and Lax [65, 66] (see also Lindqvist et al. [91]):

Lemma 2. *A multi-point conservative scheme in the form* (2.59) *is unconditionally TVD if and only if:*

$$2\left(\Delta x/\Delta t\right) - 2Q^0_{j+1/2} + Q^{-1}_{j+1/2} + Q^1_{j+1/2} \geq 0, \tag{2.71a}$$

$$Q^0_{j+1/2} - 2Q^{\pm 1}_{j+1/2} + Q^{\pm 2}_{j+1/2} \mp \lambda_{j+1/2} \geq 0, \tag{2.71b}$$

$$Q^{\pm i}_{j+1/2} - 2Q^{\pm(i+1)}_{j+1/2} + Q^{\pm(i+2)}_{j+1/2} \geq 0, \quad \forall\, i \geq 1, \quad \forall\, j. \tag{2.71c}$$

LeVeque [80] showed that the LTS-Godunov scheme is TVD, while Lindqvist et al. [91] showed that the LTS-Roe and LTS-Lax-Friedrichs schemes are also TVD. Further, the property that the Roe and Lax-Friedrichs schemes are the least and most diffusive possible TVD schemes also holds in the LTS framework, where the coefficients of the LTS-Roe and the LTS-Lax-Friedrichs schemes are the least and the most diffusive coefficients possible, respectively.

Entropy stability

Entropy stability of LTS methods is less understood than that of standard methods. In one of the papers on the LTS-Godunov method, LeVeque conjectured that the LTS-Godunov method converges to the entropy solution *provided the correct entropy solution is used for each Riemann problem* [80]. However, rigorous proof turned out to be very difficult to obtain and to this day it remains an open question.

Contributions to this matter have been made by Wang and Warnecke [144, 145] in the nineteen nineties, where they proved that the LTS-Godunov and LTS-Glimm schemes are entropy stable for $\bar{C} \leq 2$ if the flux function is

monotone, and for an arbitrary Courant number if the initial data is monotone. Later, Wang et al. [146] proved entropy stability of the LTS-Godunov method for any Courant number for some additional types of initial data. An example of monotone, hence entropy stable LTS method is an LTS version of Lax-Friedrichs scheme studied by Tang and Warnecke [133]. In section 3.3, we will show that the LTS-Lax-Friedrichs scheme of Lindqvist et al. [91] is entropy stable by showing it is monotone. An interesting result related to this matter is a monotone, entropy stable LTS-Engquist-Osher scheme by Brenier [12]. Therein, author considers averaged multivalued solutions, and the LTS-Engquist-Osher scheme is deduced from the transport-collapse operator.[6,7]

Since the numerical viscosity coefficients of some LTS methods were given only recently by Lindquist et al. [91], we are not familiar with analysis of entropy stability along the lines of work by Osher [110] and Tadmor [127] where the numerical viscosity coefficients Q are compared to the numerical viscosity coefficient of the Godunov scheme. One difficulty that immediately arises is that in LTS methods, the numerical diffusion in the numerical flux function (2.59) is not uniquely determined by a single Q. This leads to a possibility that different combinations of Q may result in the same overall amount of numerical diffusion.

The recent paper by Lindqvist et al. [91] addressed question of entropy stability by studying modified equation, an approach which we will employ in section 3.2. In [91], modified equation and numerical experiments are used to demonstrate that the LTS-Roe is not entropy stable. This is expected, since it is an extension of the standard Roe scheme. Further, it is shown that the LTS-Roe scheme leads to an entropy violation even more often than the standard Roe scheme. This observation has been reported by other authors as well. We will return to this point in section 3.2 where we will discuss entropy stability of LTS methods in more detail.

[6] Brenier's framework is quite different than the one considered in this thesis, and it remains to be explored how to compare it to the entropy violating LTS-Engquist-Osher scheme we will derive in chapter 3.

[7] An important point arising here is that LTS extensions of standard methods are not unique. This will be addressed in section 3.1.4.

2.3. Finite volume methods for systems of conservation laws

We consider systems of equations (2.13) and apply the integration procedure which we used in section 2.2 to go from the scalar conservation law (2.1) to the numerical method in conservation form (2.28). This results in conservation form:

$$\mathbf{U}_j^{n+1} = \mathbf{U}_j - \frac{\Delta t}{\Delta x}\left(\mathbf{F}_{j+1/2} - \mathbf{F}_{j-1/2}\right), \tag{2.72}$$

with the numerical flux function defined as:

$$\mathbf{F}_{j+1/2} = \frac{1}{2}\left(\mathbf{F}_j + \mathbf{F}_{j+1}\right) - \frac{1}{2}\sum_{i=-\infty}^{\infty} \mathbf{Q}_{j+1/2+i}^{i} \Delta \mathbf{U}_{j+1/2+i}, \tag{2.73}$$

where the partial numerical viscosity coefficients $\mathbf{Q}_{j+1/2+i}$ are now matrices. The corresponding flux-difference splitting form is:

$$\mathbf{U}_j^{n+1} = \mathbf{U}_j - \frac{\Delta t}{\Delta x}\sum_{i=0}^{\infty}\left(\mathbf{A}_{j-1/2-i}^{i+} \Delta \mathbf{U}_{j-1/2-i} + \mathbf{A}_{j+1/2+i}^{i-} \Delta \mathbf{U}_{j+1/2+i}\right), \tag{2.74}$$

where the flux-difference splitting coefficients $\mathbf{A}_{j+1/2\mp i}^{i\pm}$ are now matrices.

We observe that (2.73) and (2.74) are simply expressions (2.59) and (2.60) generalized to systems of equations, where we note that we immediately used generalized LTS expressions because these naturally contain the expressions for standard methods.

In order to generalize the ideas developed for scalar conservation laws in section 2.2 to systems of conservation laws, we follow the standard approach which consists of linearizing the problem (2.13) and then applying the theory developed for the scalar conservation laws to each characteristic field. Consider the Roe scheme [120] where the numerical viscosity matrix is given as:

$$\mathbf{Q}_{\text{Roe}} = |\hat{\mathbf{A}}|, \tag{2.75}$$

where $\hat{\mathbf{A}}$ is the Roe matrix [120] satisfying following conditions:

- $\hat{\mathbf{A}}$ is diagonalizable with real eigenvalues, i.e. it is hyperbolic;
- if $\mathbf{U}_j, \mathbf{U}_{j+1} \to \mathbf{U}$, then $\hat{\mathbf{A}}\left(\mathbf{U}_j, \mathbf{U}_{j+1}\right) = \mathbf{A}\left(\mathbf{U}\right)$, i.e. it is consistent with the original conservation law;

- $\hat{\mathbf{A}}\left(\mathbf{U}_j, \mathbf{U}_{j+1}\right)\left(\mathbf{U}_{j+1} - \mathbf{U}_j\right) = \mathbf{F}_{j+1} - \mathbf{F}_j$.

We then diagonalize the numerical viscosity matrix $\mathbf{Q}^i$ and the flux-difference splitting matrices $\mathbf{A}^{i\pm}$ with the eigenvectors of the Roe matrix as:

$$\mathbf{Q}^i_{j+1/2} = \left(\hat{\mathbf{R}}\boldsymbol{\Omega}^i\hat{\mathbf{R}}^{-1}\right)_{j+1/2}, \tag{2.76a}$$

$$\mathbf{A}^{i\pm}_{j+1/2} = \left(\hat{\mathbf{R}}\boldsymbol{\Lambda}^{i\pm}\hat{\mathbf{R}}^{-1}\right)_{j+1/2}, \tag{2.76b}$$

where $\boldsymbol{\Omega}$ and $\boldsymbol{\Lambda}$ are diagonal matrices of eigenvalues:

$$\boldsymbol{\Omega} = \operatorname{diag}\left(\omega_1, \ldots, \omega_N\right), \tag{2.77a}$$

$$\boldsymbol{\Lambda} = \operatorname{diag}\left(\lambda_1, \ldots, \lambda_N\right). \tag{2.77b}$$

Lindqvist et al. [91] determined the eigenvalues for the LTS-Roe scheme in the numerical viscosity form:

$$\omega^0_{\text{Roe}} = |\lambda|, \tag{2.78a}$$

$$\omega^{\mp i}_{\text{Roe}} = 2\max\left(0, \pm\lambda - i\frac{\Delta x}{\Delta t}\right) \quad \text{for} \quad i > 0, \tag{2.78b}$$

and the flux-difference splitting form:

$$\lambda^{i\pm}_{\text{Roe}} = \pm\max\left(0, \min\left(\pm\lambda - i\frac{\Delta x}{\Delta t}, \frac{\Delta x}{\Delta t}\right)\right). \tag{2.79}$$

They also obtained the eigenvalues for the LTS-Lax-Friedrichs scheme in the numerical viscosity form:

$$\omega^0_{\text{LxF}} = k\frac{\Delta x}{\Delta t}, \tag{2.80a}$$

$$\omega^{\mp i}_{\text{LxF}} = \frac{k-i}{k}\left(\pm\lambda + k\frac{\Delta x}{\Delta t}\right) \quad \text{for} \quad i > 0, \tag{2.80b}$$

while Bore [10] provided them for the flux-difference splitting form:

$$\lambda^{i\pm}_{\text{LxF}} = \frac{1}{2k}\left(\lambda \pm k\frac{\Delta x}{\Delta t}\right), \tag{2.81}$$

where we note that the operations above are applied in each characteristic field.

2.3.1. Convergence and entropy stability

Even though the Lax-Wendroff theorem also holds for systems of equations [84], it is in general not possible to prove convergence of numerical methods for systems of conservation laws. In fact, a proof of convergence for any finite volume method for a general system of hyperbolic conservation laws *remains an outstanding open problem*, see Bressan [13]. Situation is better when it comes to entropy stability, and it is possible to prove entropy stability of certain methods, for instance Godunov method [85], HLLE method [33] and HLLC method with wave velocity estimates according to Bouchut [11]. If these methods converge, we can be confident that they converge to the entropy solution.

An important contribution to the questions of convergence and entropy stability is the book by Bouchut [11], where preservation of invariant domains and existence of entropy inequalities are used as stability criteria. Therein, preservation of invariant domains is used to ensure positivity preservation, while existence of entropy inequalities *ensures the computation of admissible discontinuities, and at the same time it provides a global stability, by the property that a quantity measuring the global size of the data should not increase*, see Bouchut [11]. Our investigations of LTS methods for systems of equations will be based on comparison with standard, more established methods and on using well studied test cases. At best, we will give heuristic arguments and conjecture on properties of the methods.

There is much pleasure to be gained from useless knowledge.

Bertrand Russell

3 LTS-HLL-type schemes

This chapter presents the main results of this thesis. These results have been already described in 1.3 *Goals and thesis outline*, but we repeat them to give the structure of the chapter:

- In section 3.1 we develop the framework of the LTS-HLL-type schemes, and we develop LTS-HLL(C) schemes.
- In section 3.2 we investigate entropy stability of the LTS methods by using the modified equation analysis.
- In section 3.3 we investigate monotonicity and positivity preservation of the LTS methods.

3.1. Constructing the LTS-HLL and LTS-HLLC schemes

The HLL (Harten–Lax–van Leer) solver was proposed by Harten et al. [53] as an example of a very simple and inexpensive approximate Riemann solver for systems of hyperbolic conservation laws. In the original paper, the HLL scheme assumes a two-wave structure of the solution and constructs the approximate Riemann solver by using estimates of the velocities for the slowest and fastest waves. The choice of these estimates plays a decisive role for the properties of the scheme. Namely, by an appropriate

choice of the wave velocity estimates it is possible to tune the amount of numerical diffusion, recover some existing numerical methods and achieve an entropy stable and a positivity preserving scheme.

The choice of wave velocity estimates has been studied for instance by Davis [29], Einfeldt and co-workers [33, 34], Toro et al. [139], Batten et al. [6], Bouchut [11], Pelanti [114] and LeVeque and Pelanti [85]. In particular, the choice of wave velocities according to Einfeldt [33] became very popular because it yields an entropy stable and a positivity preserving scheme, known as the HLLE scheme. However, simplicity of the HLL scheme is owing to the fact that it is an *incomplete* Riemann solver. Namely, by assuming a two-wave structure of the solution, the HLL scheme imposes a single intermediate state across the Riemann fan. Because of this, the HLL scheme may poorly resolve certain waves in systems where solution structure consists of more than two waves. Einfeldt [33], Linde [89] and Park [112] introduced modifications of the HLL scheme in which the resolution of intermediate waves is improved. For the Euler equations, Toro et al. [139] proposed the HLLC (HLL–Contact) solver in which the contact discontinuity is reconstructed by assuming a three-wave structure of the solution.

As stated above, the original HLL scheme assumes a two-wave structure of the solution and it was originally intended as a solver for systems of equations. Later developments of the HLL scheme continued to work along these lines, and the same applies to the HLLC scheme which was designed as a solver for the Euler equations. We followed this same approach in our paper [P2] where we used the HLL and HLLC schemes for the system of conservation laws as the starting point.

Herein, we adopt a slightly different approach and interpret the HLL scheme as a method for scalar conservation laws. We define the HLL-type schemes, a class of standard *two-parameter* methods that also includes the one-parameter methods (2.31) and (2.36) considered in chapter 2. The new framework can be written in both numerical viscosity (2.29) and flux-difference splitting form (2.35). By introducing notion of *waves* [84], we can also write the new scheme in *wave propagation* form, which will provide a new insight into the TVD condition. Further, by interpreting the HLL scheme as a scheme for a scalar conservation law we are able to rigorously study its convergence and entropy stability.

The extension to the LTS-HLL scheme is made as in the previous chapter, following the work of Lindqvist et al. [91]. We define a class of LTS two-parameter methods, which allows us to obtain LTS extensions of

some standard one-parameter methods in a very simple way. Lastly, the extension to systems of equations is done as earlier by a classical field-by-field decomposition into characteristic variables.

A number of ideas that will be used in this section have been recognized and used by different authors, for instance Harten and Hyman [52], LeVeque [83, 84], Bouchut [11], Pelanti [114] and Einfeldt [33]. Our framework naturally incorporates these ideas as will be described in more detail below.

3.1.1. Standard HLL scheme for scalar conservation laws

Once again, we are interested in solving the scalar conservation law (2.1):

$$u_t + f(u)_x = 0. \tag{3.1}$$

In the previous chapter we solved (3.1) by using standard one-parameter methods written in the numerical viscosity (2.29) and flux-difference splitting (2.35) form. Herein, our first goal is to establish the HLL scheme.

We start by retaining the basic assumption of HLL-type schemes and assume a two-wave structure of the solution. This leads to a simplest possible two-wave Riemann solver:

$$\widetilde{u}_{j+1/2}(x/t) = \begin{cases} u_j & \text{if} \quad x < S_{\mathrm{L},j+1/2}t, \\ u^{\mathrm{HLL}}_{j+1/2} & \text{if} \quad S_{\mathrm{L},j+1/2}t < x < S_{\mathrm{R},j+1/2}t, \\ u_{j+1} & \text{if} \quad x > S_{\mathrm{R},j+1/2}t, \end{cases} \tag{3.2}$$

where $S_{\mathrm{L},j+1/2}$ and $S_{\mathrm{R},j+1/2}$ are wave velocity estimates (that are to be determined later on), while $u^{\mathrm{HLL}}_{j+1/2}$ is the intermediate state such that the Riemann solver (3.2) is consistent with the integral form of the conservation law (3.1):

$$u^{\mathrm{HLL}}_{j+1/2} = \frac{S_{\mathrm{R}}u_{j+1} - S_{\mathrm{L}}u_j + f_j - f_{j+1}}{S_{\mathrm{R}} - S_{\mathrm{L}}}, \tag{3.3}$$

where we suppressed the interface index on S_{L} and S_{R} because the interface index is given on the left-hand side. We refer to Toro [138, p. 319] for step by step derivation of (3.3). By using (3.2) in (2.26) we may write the HLL scheme in the conservation form (2.28) with the numerical flux function:

$$F^{\mathrm{HLL}}_{j+1/2} = \frac{S^+_{\mathrm{R}}f_j - S^-_{\mathrm{L}}f_{j+1} + S^-_{\mathrm{L}}S^+_{\mathrm{R}}\left(u_{j+1} - u_j\right)}{S^+_{\mathrm{R}} - S^-_{\mathrm{L}}}, \tag{3.4}$$

where $S^+ = \max(0, S)$ and $S^- = \min(0, S)$. Further, by equalizing (3.4) with (2.29) we can find that the numerical viscosity coefficient is:

$$Q_{\mathrm{HLL},j+1/2} = \frac{|S_\mathrm{R}|\,(\lambda - S_\mathrm{L}) + |S_\mathrm{L}|\,(S_\mathrm{R} - \lambda)}{S_\mathrm{R} - S_\mathrm{L}}. \tag{3.5}$$

Similarly, the flux-difference splitting coefficients are:

$$A^+_{\mathrm{HLL},j+1/2} = \frac{S^+_\mathrm{R}\,(\lambda - S_\mathrm{L}) + S^+_\mathrm{L}\,(S_\mathrm{R} - \lambda)}{S_\mathrm{R} - S_\mathrm{L}}, \tag{3.6a}$$

$$A^-_{\mathrm{HLL},j+1/2} = \frac{S^-_\mathrm{R}\,(\lambda - S_\mathrm{L}) + S^-_\mathrm{L}\,(S_\mathrm{R} - \lambda)}{S_\mathrm{R} - S_\mathrm{L}}, \tag{3.6b}$$

where we recall that λ was defined in (2.32).

Therefore, the HLL scheme is a class of standard *two-parameter* methods, where the NV and FDS coefficients depend on free parameters S_L and S_R. We can show that this class contains all standard one-parameter methods described by (2.31) and (2.36).

Lemma 3. *Consider a standard one-parameter conservative scheme written in the numerical viscosity form* (2.29)*, which is uniquely determined by the numerical viscosity coefficient Q_S. By defining S_L and S_R in the HLL scheme* (3.5) *as:*

$$S_\mathrm{L} = -Q_S, \quad S_\mathrm{R} = Q_S, \tag{3.7}$$

the numerical viscosity coefficient of the HLL scheme becomes:

$$Q_{HLL} = Q_S. \tag{3.8}$$

Proof. Use (3.7) in (3.5).[1] □

We have the equivalent results for the flux-difference splitting form:

Lemma 4. *Consider a standard one-parameter conservative scheme written in the flux-difference splitting form* (2.35)*, which is uniquely determined by the flux-difference coefficients $A^\pm_S$. By defining S_L and S_R in the HLL scheme* (3.6) *as:*

$$S_\mathrm{L} = A^-_S - A^+_S, \quad S_\mathrm{R} = A^+_S - A^-_S, \tag{3.9}$$

the flux-difference splitting coefficients of the HLL scheme become:

$$A^\pm_{HLL} = A^\pm_S. \tag{3.10}$$

[1] We note that this is not completely original results and that it was observed already by Davis [29] for the Rusanov and Lax-Friedrichs schemes as applied to the system of equations, and by Toro et al. [139] – "Other obvious choices reproduce star fluxes $\mathbf{F}^*_{j+1/2}$ associated with familiar schemes."

Proof. Use (3.9) in (3.6). □

We note that (3.7) and (3.9) are equivalent, due to relation (2.37).

We described standard one-parameter methods as a special case of standard two-parameter methods consisting of two waves. This has a very natural geometrical interpretation. Namely, even though solution of the Riemann problem for the scalar conservation law with strictly convex (or concave) flux function consists of either a shock or a rarefaction wave (see (2.9) and (2.11)), most of schemes in flux-difference splitting form (2.36) solve the Riemann problem by splitting a discontinuity into left- and right-going contribution that updates the cell to the left and right, respectively. However, there is a subtle difference in a way the flux-difference splitting and the HLL-type scheme split the Riemann problem, which we now describe.

Figure 3.1a shows a geometrical interpretation of the flux-difference splitting form (2.35), where $A^-\Delta u$ corresponds to the left-going, and $A^+\Delta u$ to the right-going contribution, respectively. Figure 3.1b shows the HLL-type scheme where $S_\mathrm{L}\mathcal{W}^1$ corresponds to the left-going, and $S_\mathrm{R}\mathcal{W}^2$ to the right-going contribution, respectively. The name *wave* formulation follows from the fact that the HLL-type scheme splits the discontinuity into two waves separated by the intermediate state u^HLL. These waves are then transported with the corresponding velocities S_L and S_R.

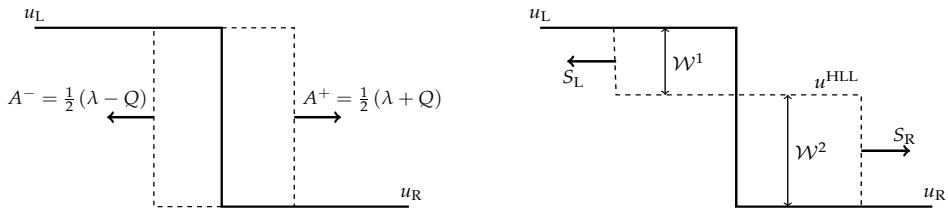

(a) Flux-difference splitting

(b) Wave formulation

Figure 3.1.: Geometrical interpretation of how different numerical forms split the discontinuity.

Since the HLL-type scheme consists of two waves, we can write the updating formula for u_j^{n+1} in the wave propagation form (see [85, p. 80]):

$$u_j^{n+1} = u_j - \frac{\Delta t}{\Delta x}\left(\sum_{p=1}^{2} S_{j-1/2}^{p,+}\mathcal{W}_{j-1/2}^{p} + \sum_{p=1}^{2} S_{j+1/2}^{p,-}\mathcal{W}_{j+1/2}^{p}\right), \tag{3.11}$$

where we introduce the notation $S^{p,+} = \max(0, S^p)$, $S^{p,-} = \min(0, S^p)$, and we define the wave velocities:

$$S^1_{j+1/2} = S_{\mathrm{L},j+1/2}, \quad S^2_{j+1/2} = S_{\mathrm{R},j+1/2}, \tag{3.12}$$

and the waves:

$$\mathcal{W}^1_{j+1/2} = u^{\mathrm{HLL}}_{j+1/2} - u_j, \quad \mathcal{W}^2_{j+1/2} = u_{j+1} - u^{\mathrm{HLL}}_{j+1/2}. \tag{3.13}$$

For standard, one-parameter methods it is easy to show that:

$$\begin{aligned} A^-_{\mathrm{S},j+1/2}\Delta u_{j+1/2} =& \frac{1}{2}\left(\lambda_{j+1/2} - Q_{\mathrm{S},j+1/2}\right)\Delta u_{j+1/2} \\ =& S_{\mathrm{L},j+1/2}\left(u^{\mathrm{HLL}}_{j+1/2} - u_j\right) = \sum_{p=1}^{2} S^{p,-}_{j+1/2}\mathcal{W}^p_{j+1/2}, \end{aligned} \tag{3.14}$$

$$\begin{aligned} A^+_{\mathrm{S},j+1/2}\Delta u_{j+1/2} =& \frac{1}{2}\left(\lambda_{j+1/2} + Q_{\mathrm{S},j+1/2}\right)\Delta u_{j+1/2} \\ =& S_{\mathrm{R},j+1/2}\left(u_{j+1} - u^{\mathrm{HLL}}_{j+1/2}\right) = \sum_{p=1}^{2} S^{p,+}_{j+1/2}\mathcal{W}^p_{j+1/2}. \end{aligned} \tag{3.15}$$

This new framework provides a new insight into some properties of one-parameter methods. For standard-one parameter methods, (3.11) becomes:

$$u^{n+1}_j = u_j - \frac{\Delta t}{\Delta x}\left(Q_{\mathrm{S},j-1/2}\left(u_j - u^{\mathrm{HLL}}_{j-1/2}\right) - Q_{\mathrm{S},j+1/2}\left(u^{\mathrm{HLL}}_{j+1/2} - u_j\right)\right), \tag{3.16}$$

where by using (3.7) in (3.3) we have that an intermediate state of a one-parameter method is:

$$u^{\mathrm{HLL(1)}}_{j+1/2} = \frac{1}{2}\left(u_j + u_{j+1}\right) - \frac{1}{2}\frac{\lambda_{j+1/2}}{Q_{\mathrm{S},j+1/2}}\left(u_{j+1} - u_j\right). \tag{3.17}$$

By looking at fig. 3.1 we heuristically argue that the intermediate state of the one-parameter method should lie between the left and right state:

$$u^{\mathrm{HLL(1)}}_{j+1/2} \in \left[\min\left(u_j, u_{j+1}\right), \max\left(u_j, u_{j+1}\right)\right]. \tag{3.18}$$

By enforcing this condition we find it is satisfied for:

$$\left|\lambda_{j+1/2}\right| \leq Q_{\mathrm{S},j+1/2}, \quad \forall\, j, \tag{3.19}$$

which we recognize as the lower bound of the TVD condition (2.44). We can see that in the wave propagation form, the upper bound of TVD condition limits how far can waves travel, while the lower bound limits the magnitude of the waves. We can show that (3.19) implies (3.18) by rewriting (3.18) as:

$$u_j \geq u_{j+1/2}^{\text{HLL(1)}} \geq u_{j+1} \quad \text{if} \quad u_j \geq u_{j+1}, \tag{3.20}$$

$$u_j \leq u_{j+1/2}^{\text{HLL(1)}} \leq u_{j+1} \quad \text{if} \quad u_j \leq u_{j+1}. \tag{3.21}$$

We suppress the interface indices and observe that when $u_j \geq u_{j+1}$, the left inequality can be rewritten as:

$$\frac{1}{2}\left(1 - \frac{\lambda}{Q_{\text{S}}}\right)\left(u_{j+1} - u_j\right) \leq 0. \tag{3.22}$$

Since $u_{j+1} - u_j \leq 0$, we require that:

$$1 - \frac{\lambda}{Q_{\text{S}}} \geq 0. \tag{3.23}$$

For $\lambda > 0$, we obtain that:

$$Q_{\text{S}} \geq |\lambda|, \tag{3.24}$$

while for $\lambda < 0$ we obtain:

$$1 + \frac{|\lambda|}{Q_{\text{S}}} \geq 0, \tag{3.25}$$

which is satisfied for any $Q_{\text{S}} \geq 0$. The remaining cases are done in the same way.

We can make several observation by considering $u_{j+1/2}^{\text{HLL(1)}}$, eq. (3.17). The Roe scheme in flux-difference splitting form consists of a single discontinuity traveling either to the left or right, i.e. either $A_{\text{Roe}}^{-} = 0$ or $A_{\text{Roe}}^{+} = 0$. The wave propagation form consists of two waves traveling to the left and right, but it can be shown that by using Q_{Roe} in (3.17) we obtain that either $u_{j+1/2}^{\text{HLL}} = u_j$ or $u_{j+1/2}^{\text{HLL}} = u_{j+1}$, hence one of the waves $\mathcal{W}$ is equal to zero. This fits into the discussion above, since the Roe scheme is precisely the lower limit of the TVD condition.

Next, for the Lax-Wendroff scheme, $Q_{\text{L-W}} = \lambda^2 \Delta t / \Delta x$, we obtain:

$$u_{j+1/2}^{\text{HLL-LW}} = \frac{1}{2}\left(u_j + u_{j+1}\right) - \frac{1}{2}\frac{1}{\lambda}\frac{\Delta x}{\Delta t}\left(u_{j+1} - u_j\right), \tag{3.26}$$

and the intermediate state is outside $\mathcal{R}$, except when $|\lambda| = \Delta x/\Delta t$.[2]

Further, in the case of transonic shock or transonic rarefaction when $\lambda = 0$, the Roe and Lax-Wendroff schemes do not have well defined intermediate state, since term λ/Q_S in (3.17) becomes $0/0$ and $\Delta x/0$, respectively.

Finally, we know that for the central scheme $Q_C = 0$. By using this in (3.3) the fraction on the right-hand side explodes, which explains why the scheme is unstable.

3.1.2. Convergence and entropy stability

We are now interested in convergence and entropy stability of the HLL-type scheme. As in previous chapter, we start by considering convergence to a weak solution along the lines of the Lax-Wendroff theorem. Then, we obtain stronger conditions to ensure convergence to the entropy solution.

Convergence

The question of conservation was already discussed and we do not repeat it here. Consistency may be shown as earlier, by using the modified equation:

Lemma 5 (Prebeg [P1])**.** *The HLL scheme with the numerical viscosity coefficient* (3.5) *is consistent with the scalar conservation law:*

$$u_t + f(u)_x = 0. \tag{3.27}$$

Proof. Standard first-order methods give a second-order accurate approximation to the equation:

$$u_t + f(u)_x = \frac{1}{2}\frac{\Delta x^2}{\Delta t}\left[\left(\frac{\Delta t}{\Delta x}\bar{Q} - c^2\right)u_x\right]_x. \tag{3.28}$$

By using (3.5) in (3.28) we obtain that the HLL scheme gives a second-order accurate approximation to the equation:

$$u_t + f(u)_x = \frac{1}{2}\frac{\Delta x^2}{\Delta t}\left[D_{\mathrm{HLL}}u_x\right]_x, \tag{3.29}$$

[2]Second-order accurate schemes are often achieved by using the *wave limiters* which, as the name suggests, limit the magnitude of the waves $\mathcal{W}$. Author conjectures that TVD wave limiters are precisely those that ensure that, at the discontinuities, the intermediate state lies within $\mathcal{R}$.

where:

$$D_{\mathrm{HLL}} = \frac{c - c_{\mathrm{L}}}{c_{\mathrm{R}} - c_{\mathrm{L}}} \left(|c_{\mathrm{R}}| - c_{\mathrm{R}}^2 \right) + \frac{c_{\mathrm{R}} - c}{c_{\mathrm{R}} - c_{\mathrm{L}}} \left(|c_{\mathrm{L}}| - c_{\mathrm{L}}^2 \right) + \left(c - c_{\mathrm{L}} \right) \left(c_{\mathrm{R}} - c \right), \tag{3.30}$$

where $c_{\mathrm{L}} = S_{\mathrm{L}} \Delta t / \Delta x$ and $c_{\mathrm{R}} = S_{\mathrm{R}} \Delta t / \Delta x$. By keeping $c = \text{const.}$ and passing $\Delta x \to 0$ we recover the scalar conservation law (3.27). □

Next, we obtain conditions for the TVD stability:

Lemma 6. *The HLL scheme with the numerical viscosity coefficient* (3.5) *is TVD if:*

$$-\frac{\Delta x}{\Delta t} \leq S_{\mathrm{L},j+1/2} \leq \lambda_{j+1/2} \leq S_{\mathrm{R},j+1/2} \leq \frac{\Delta x}{\Delta t}, \quad \forall\, j. \tag{3.31}$$

Proof. We suppress the interface indices and recall that a standard conservative scheme is unconditionally TVD if and only if:

$$|\lambda| \leq Q \leq \frac{\Delta x}{\Delta t}, \tag{3.32}$$

where for Q_{HLL} we require the following:

$$|\lambda| \leq \frac{|S_{\mathrm{R}}| \left(\lambda - S_{\mathrm{L}} \right) + |S_{\mathrm{L}}| \left(S_{\mathrm{R}} - \lambda \right)}{S_{\mathrm{R}} - S_{\mathrm{L}}} \leq \frac{\Delta x}{\Delta t}. \tag{3.33}$$

The upper bound in (3.33) can be rewritten as:

$$\left(\lambda - S_{\mathrm{L}} \right) \left(|S_{\mathrm{R}}| - \frac{\Delta x}{\Delta t} \right) + \left(S_{\mathrm{R}} - \lambda \right) \left(|S_{\mathrm{L}}| - \frac{\Delta x}{\Delta t} \right) \leq 0, \tag{3.34}$$

which is always satisfied when the outer inequalities in (3.31) hold. The lower bound in (3.33) can be rewritten as:

$$\left(\lambda - S_{\mathrm{L}} \right) \left(|S_{\mathrm{R}}| - |\lambda| \right) + \left(S_{\mathrm{R}} - \lambda \right) \left(|S_{\mathrm{L}}| - |\lambda| \right) \geq 0, \tag{3.35}$$

which is always satisfied when the inner inequalities in (3.31) hold. □

Entropy stability

The TVD stability result above does not tell us if the scheme converges to the unique entropy-satisfying weak solution of the scalar conservation law. We can show that a scheme is entropy stable by using entropy functions, by showing that it is an E-scheme or by showing that it is monotone.

Herein, we will use entropy functions to show that the HLL scheme with the choice of the wave velocities according to Einfeldt [33]:

$$S_{\mathrm{L}} = \min\left(\lambda_{j+1/2}, f'(u_j)\right), \tag{3.36a}$$

$$S_{\mathrm{R}} = \max\left(\lambda_{j+1/2}, f'(u_{j+1})\right), \tag{3.36b}$$

is entropy stable.[3] Our proof closely follows the proof by Pelanti et al. [114, p. 12] (see also [52, 42]).

We consider the discrete Riemann problem (2.8) for the scalar conservation law (3.1) with a convex flux function $f(u)$. If the solution to the Riemann problem is supposed to be a shock (2.9), the HLLE scheme yields $S_{\mathrm{L}} = S_{\mathrm{R}} = \lambda$, and it can be shown that in the limit when $S_{\mathrm{L}}, S_{\mathrm{R}} \to \lambda$, the HLLE scheme becomes the Roe scheme and the solution is:

$$\widetilde{u}(x/t) = \begin{cases} u_{\mathrm{L}} & \text{if} \quad x < \lambda t, \\ u_{\mathrm{R}} & \text{if} \quad x > \lambda t. \end{cases} \tag{3.37}$$

If the solution is supposed to be a rarefaction (2.11), the HLLE scheme yields $S_{\mathrm{L}} = f'(u_j)$ and $S_{\mathrm{R}} = f'(u_{j+1})$, and the solution is:

$$\widetilde{u}(x/t) = \begin{cases} u_{\mathrm{L}} & \text{if} \quad x < f'(u_{\mathrm{L}})t, \\ u^{\mathrm{HLL}} & \text{if} \quad f'(u_{\mathrm{L}})t < x < f'(u_{\mathrm{R}})t, \\ u_{\mathrm{R}} & \text{if} \quad x > f'(u_{\mathrm{R}})t. \end{cases} \tag{3.38}$$

If the rarefaction is a *transonic* rarefaction, i.e. $f'(u_{\mathrm{L}}) < 0 < f'(u_{\mathrm{R}})$, certain schemes (such as the Roe scheme) may lead to an entropy violation. If the HLLE scheme is entropy stable, the solution (3.38) must satisfy the integral form of the entropy condition (2.5):

$$\int_0^{\Delta t} \int_{-\frac{\Delta x}{2}}^{\frac{\Delta x}{2}} \left[\eta(u)_t + \psi(u)_x\right] \mathrm{d}x\mathrm{d}t \leq 0. \tag{3.39}$$

[3] In Einfeldt's paper [33], the HLLE scheme is developed for the Euler equations. We will denote the choice (3.36) as the scalar HLLE because it is equivalent to applying the original Einfeldt's choice to the scalar conservation law.

By using $u = \widetilde{u}(x/t)$ and integrating (3.39) we obtain:

$$\int_{-\frac{\Delta x}{2}}^{\frac{\Delta x}{2}} \eta(\widetilde{u}(x/\Delta t))\mathrm{d}x \leq \frac{\Delta x}{2}\left(\eta(u_{\mathrm{L}}) + \eta(u_{\mathrm{R}})\right) - \Delta t\left(\psi(u_{\mathrm{R}}) - \psi(u_{\mathrm{L}})\right). \quad (3.40)$$

Since (3.38) consists of piecewise constant data, the left-hand side is:

$$\begin{aligned}\int_{-\frac{\Delta x}{2}}^{\frac{\Delta x}{2}} \eta(\widetilde{u}(x/\Delta t))\mathrm{d}x = \eta(u^{\mathrm{HLL}})\left(S_{\mathrm{R}}\Delta t - S_{\mathrm{L}}\Delta t\right) \\ + \eta(u_{\mathrm{L}})\left(S_{\mathrm{L}}\Delta t + \frac{\Delta x}{2}\right) + \eta(u_{\mathrm{R}})\left(\frac{\Delta x}{2} - S_{\mathrm{R}}\Delta t\right). \quad (3.41)\end{aligned}$$

The outer bounds enclosing u^{HLL} in (3.38) are physical signal velocities that also appear in the exact solution (2.11), so we know from the conservation principle that u^{HLL} is equal to the integral of the exact solution $u^{\mathrm{E}}(x/t)$ from $f'(u_{\mathrm{L}})\Delta t$ to $f'(u_{\mathrm{R}})\Delta t$:

$$u^{\mathrm{HLL}} = \frac{1}{\Delta t\left(S_{\mathrm{R}} - S_{\mathrm{L}}\right)} \int_{S_{\mathrm{L}}\Delta t}^{S_{\mathrm{R}}\Delta t} u^{E}(x/\Delta t)\mathrm{d}x, \quad (3.42)$$

where we used that $S_{\mathrm{L}} = f'(u_{\mathrm{L}})$ and $S_{\mathrm{R}} = f'(u_{\mathrm{R}})$ are the outer bounds of the exact solution (2.11). By using Jensen's inequality we have that:

$$\eta(u^{\mathrm{HLL}}) \leq \frac{1}{\Delta t\left(S_{\mathrm{R}} - S_{\mathrm{L}}\right)} \int_{S_{\mathrm{L}}t}^{S_{\mathrm{R}}t} \eta(u^{\mathrm{E}}(x/\Delta t))\mathrm{d}x. \quad (3.43)$$

By using (3.43) in (3.41) we obtain:

$$\begin{aligned}\int_{-\frac{\Delta x}{2}}^{\frac{\Delta x}{2}} \eta(\widetilde{u}(x/\Delta t))\mathrm{d}x \leq \int_{S_{\mathrm{L}}\Delta t}^{S_{\mathrm{R}}\Delta t} \eta(u^{\mathrm{E}}(x/\Delta t))\mathrm{d}x \\ + \eta(u_{\mathrm{L}})\left(S_{\mathrm{L}}t + \frac{\Delta x}{2}\right) + \eta(u_{\mathrm{R}})\left(\frac{\Delta x}{2} - S_{\mathrm{R}}\Delta t\right), \quad (3.44)\end{aligned}$$

where the right-hand side is the exact solution:

$$\begin{aligned}\int_{-\frac{\Delta x}{2}}^{\frac{\Delta x}{2}} \eta(\widetilde{u}(x/\Delta t))\mathrm{d}x \leq \int_{-\frac{\Delta x}{2}}^{\frac{\Delta x}{2}} \eta(u^{\mathrm{E}}(x/\Delta t))\mathrm{d}x \\ \leq \frac{\Delta x}{2}\left(\eta(u_{\mathrm{L}}) + \eta(u_{\mathrm{R}})\right) - \Delta t\left(\psi(u_{\mathrm{R}}) - \psi(u_{\mathrm{L}})\right), \quad (3.45)\end{aligned}$$

where the last inequality follows from the fact that the exact solution satisfies the entropy inequality. Hence, we showed that the HLLE scheme is entropy stable, provided that the TVD condition (3.31) is satisfied.

3.1.3. LTS-HLL scheme for scalar conservation laws

In addition to the numerical viscosity and the flux-difference splitting form, we recall that it was also possible to write the updating formula of a standard method in terms of the solutions to the neighboring Riemann problems (see (2.26)):

$$u_j^{n+1} = \frac{1}{\Delta x}\int_0^{\frac{\Delta x}{2}} \widetilde{u}_{j-1/2}\left(x/\Delta t\right) \mathrm{d}x + \frac{1}{\Delta x}\int_{-\frac{\Delta x}{2}}^{0} \widetilde{u}_{j+1/2}\left(x/\Delta t\right) \mathrm{d}x, \tag{3.46}$$

where $\widetilde{u}_{j-1/2}(x/t)$ is the approximate solution to the local Riemann problem at the cell interface $x_{j-1/2}$. Since in LTS method the value of u_j^{n+1} may depend on more than three cells, it might also depend on more than two Riemann problems. Following LeVeque [81] (see also Lindqvist et al. [91]) we may write the general updating formula of LTS method in terms of solutions to all Riemann problems in the domain of dependence:

$$u_j^{n+1} = \frac{\Delta t}{\Delta x}\sum_{i=-\infty}^{\infty}\int_{(i-1)\frac{\Delta x}{\Delta t}}^{i\frac{\Delta x}{\Delta t}} \widetilde{u}_{j+1/2-i}\mathrm{d}\xi_i - \sum_{l=-\infty}^{\infty} u_l, \tag{3.47}$$

where $\widetilde{u}_{j+1/2-i}$ is the solution to the Riemann problem at $x_{j+1/2-i}$ and:

$$\xi_i = \frac{x - x_{j+1/2-i}}{t - t^n}. \tag{3.48}$$

We note that (3.47) reduces to (3.46) when $\bar{C} \leq 1$.

To obtain the numerical viscosity and flux-difference splitting coefficients of the LTS-HLL scheme, we follow our paper [P2] and use (3.2) in (3.47) to determine the flux-difference splitting coefficients, and then use the formula (2.69) to directly obtain the numerical viscosity coefficients. For a slightly different approach, which includes geometrical consideration and more heuristic arguments we also refer to our paper [P2], where as the starting point we used HLL(C) schemes for systems of equations.

Proposition 1 (Prebeg et al. [P2])**.** *The LTS-HLL scheme can be written in the flux-difference splitting form* (2.60) *with coefficients:*

$$\begin{aligned} A_{HLL}^{i\pm} = &\pm \frac{\lambda - S_{\mathrm{L}}}{S_{\mathrm{R}} - S_{\mathrm{L}}} \max\left(0, \min\left(\pm S_{\mathrm{R}} - i\frac{\Delta x}{\Delta t}, \frac{\Delta x}{\Delta t}\right)\right) \\ &\pm \frac{S_{\mathrm{R}} - \lambda}{S_{\mathrm{R}} - S_{\mathrm{L}}} \max\left(0, \min\left(\pm S_{\mathrm{L}} - i\frac{\Delta x}{\Delta t}, \frac{\Delta x}{\Delta t}\right)\right). \end{aligned} \tag{3.49}$$

Proof. The HLL Riemann solver (3.2) can be written as:

$$\widetilde{u}_{j+1/2}(\zeta) = u_j + H(\zeta - S_{\mathrm{L}})\left(u^{\mathrm{HLL}}_{j+1/2} - u_j\right) + H(\zeta - S_{\mathrm{R}})\left(u_{j+1} - u^{\mathrm{HLL}}_{j+1/2}\right) \tag{3.50a}$$

$$= u_{j+1} - H(S_{\mathrm{L}} - \zeta)\left(u^{\mathrm{HLL}}_{j+1/2} - u_j\right) - H(S_{\mathrm{R}} - \zeta)\left(u_{j+1} - u^{\mathrm{HLL}}_{j+1/2}\right), \tag{3.50b}$$

where H is the Heaviside function. By using (3.3) we can rewrite this as:

$$\widetilde{u}_{j+1/2}(\zeta) = u_j + \left(\frac{H(\zeta - S_{\mathrm{L}})}{S_{\mathrm{R}} - S_{\mathrm{L}}}(S_{\mathrm{R}} - \lambda) + \frac{H(\zeta - S_{\mathrm{R}})}{S_{\mathrm{R}} - S_{\mathrm{L}}}(\lambda - S_{\mathrm{L}})\right)(u_{j+1} - u_j) \tag{3.51a}$$

$$= u_{j+1} - \left(\frac{H(S_{\mathrm{L}} - \zeta)}{S_{\mathrm{R}} - S_{\mathrm{L}}}(S_{\mathrm{R}} - \lambda) + \frac{H(S_{\mathrm{R}} - \zeta)}{S_{\mathrm{R}} - S_{\mathrm{L}}}(\lambda - S_{\mathrm{L}})\right)(u_{j+1} - u_j). \tag{3.51b}$$

We then use (3.51a) in (3.47) and note that for $i \leq 0$ we can write:

$$\int_{(i-1)\frac{\Delta x}{\Delta t}}^{i\frac{\Delta x}{\Delta t}} \widetilde{u}_{j+1/2-i}(\zeta_i)\mathrm{d}\zeta_i = \frac{\Delta x}{\Delta t}u_{j-i} - A^{(-i)-}_{j+1/2-i}\left(u_{j+1-i} - u_{j-i}\right), \tag{3.52}$$

where A^{i-} is the flux-difference splitting coefficient:

$$A^{i-}_{\mathrm{HLL}} = \frac{\lambda - S_{\mathrm{L}}}{S_{\mathrm{R}} - S_{\mathrm{L}}}\min\left(0, \max\left(S_{\mathrm{R}} + i\frac{\Delta x}{\Delta t}, -\frac{\Delta x}{\Delta t}\right)\right) + \frac{S_{\mathrm{R}} - \lambda}{S_{\mathrm{R}} - S_{\mathrm{L}}}\min\left(0, \max\left(S_{\mathrm{L}} + i\frac{\Delta x}{\Delta t}, -\frac{\Delta x}{\Delta t}\right)\right). \tag{3.53}$$

Similarly, we use (3.51b) in (3.47) and note that for $i \geq 1$ we can write:

$$\int_{(i-1)\frac{\Delta x}{\Delta t}}^{i\frac{\Delta x}{\Delta t}} \widetilde{u}_{j+1/2-i}(\zeta_i)\mathrm{d}\zeta_i = \frac{\Delta x}{\Delta t}u_{j+1-i} - A^{(i-1)+}_{j+1/2-i}\left(u_{j+1-i} - u_{j-i}\right), \tag{3.54}$$

where A^{i+} is the flux-difference splitting coefficient:

$$A^{i+}_{\mathrm{HLL}} = \frac{\lambda - S_{\mathrm{L}}}{S_{\mathrm{R}} - S_{\mathrm{L}}}\max\left(0, \min\left(S_{\mathrm{R}} - i\frac{\Delta x}{\Delta t}, \frac{\Delta x}{\Delta t}\right)\right) + \frac{S_{\mathrm{R}} - \lambda}{S_{\mathrm{R}} - S_{\mathrm{L}}}\max\left(0, \min\left(S_{\mathrm{L}} - i\frac{\Delta x}{\Delta t}, \frac{\Delta x}{\Delta t}\right)\right). \tag{3.55}$$

Substituting (3.52) and (3.54) into (3.47) we recover the LTS method in the flux-difference splitting form (2.60). □

Proposition 2 (Prebeg et al. [P2])**.** *The LTS-HLL scheme can be written in the numerical viscosity form* (2.59) *with coefficients:*

$$Q^0_{HLL} = \frac{|S_\mathrm{R}|\,(\lambda - S_\mathrm{L}) + |S_\mathrm{L}|\,(S_\mathrm{R} - \lambda)}{S_\mathrm{R} - S_\mathrm{L}}, \tag{3.56a}$$

$$\begin{aligned} Q^{\mp i}_{HLL} &= 2\frac{\lambda - S_\mathrm{L}}{S_\mathrm{R} - S_\mathrm{L}} \max\left(0, \pm S_\mathrm{R} - i\frac{\Delta x}{\Delta t}\right) \\ &\quad + 2\frac{S_\mathrm{R} - \lambda}{S_\mathrm{R} - S_\mathrm{L}} \max\left(0, \pm S_\mathrm{L} - i\frac{\Delta x}{\Delta t}\right) \quad \textit{for} \quad i > 0. \end{aligned} \tag{3.56b}$$

Proof. Use (3.49) in (2.69) to recover (3.56). □

In addition to NV and FDS form, we may also write the LTS-HLL scheme in the wave propagation form (3.11):

$$u_j^{n+1} = u_j - \frac{\Delta t}{\Delta x} \sum_{i=0}^{\infty} \left(\sum_{p=1}^{2} S^{p,i+}_{j-1/2-i} \mathcal{W}^p_{j-1/2-i} + \sum_{p=1}^{2} S^{p,i-}_{j+1/2+i} \mathcal{W}^p_{j+1/2+i} \right), \tag{3.57}$$

where we recall that $S^1 = S_\mathrm{L}$ and $S^2 = S_\mathrm{R}$ (eq. (3.12)). The wave velocities (3.12) are modified as:

$$S^{p,i\pm} = \pm \max\left(0, \min\left(\pm S^p - i\frac{\Delta x}{\Delta t}, \frac{\Delta x}{\Delta t}\right)\right). \tag{3.58}$$

We recall that the interface indices on A, Q and S^p have been suppressed, and we refer to remark 2 (p. 25) for explanation of the notation.

3.1.4. A class of LTS one-parameter methods

In Lemmas 3 and 4 we showed that the standard one-parameter methods (2.31) and (2.36) can be deduced from the HLL-type scheme by appropriate choice of S_L and S_R. This motivated the question if we can obtain LTS one-parameter methods from the the LTS-HLL-type scheme by appropriate choice of S_L and S_R.

We begin with the LTS-Roe and LTS-Lax-Friedrichs schemes because we already have their NV and FDS coefficients. We may recover the LTS-Roe scheme in the NV (2.62) and FDS (2.65) form by using:

$$S_\mathrm{L} = -Q_\mathrm{Roe}, \quad S_\mathrm{R} = Q_\mathrm{Roe}, \tag{3.59}$$

in the LTS-HLL-type scheme in the NV (3.56) and FDS (3.49) form, respectively. In order to obtain the LTS-Lax-Friedrichs scheme in the NV (2.64) and FDS (2.67) form, we must use:

$$S_{\mathrm{L}} = -kQ_{\mathrm{LxF}}, \quad S_{\mathrm{R}} = kQ_{\mathrm{LxF}}, \tag{3.60}$$

in the LTS-HLL-type scheme in the NV (3.56) and FDS (3.49) form, respectively. This illuminates an important point related to the Lax-Friedrichs scheme. The numerical viscosity coefficient of the standard Lax-Friedrichs scheme (2.31b) was defined as:

$$Q_{\mathrm{LxF}} = \Delta x/\Delta t, \tag{3.61}$$

while the partial numerical viscosity coefficient of the LTS-Lax-Friedrichs scheme (2.64) associated with $i = 0$ was defined as:

$$Q^0_{\text{LTS-LxF}} = k\Delta x/\Delta t. \tag{3.62}$$

In order to obtain the LTS-Lax-Friedrichs scheme (2.64) from the LTS-HLL-type scheme (3.56), we must use (3.62). We can now see that in the standard Lax-Friedrichs scheme (3.61) the coefficient $k = 1$ is implicitly assumed, and that the numerical viscosity coefficient of the standard method in fact reads $Q_{\mathrm{LxF}} = k\Delta x/\Delta t$.

Having obtained the LTS-Roe and LTS-Lax-Friedrichs schemes by following the approach used for standard methods (see Lemmas 3 and 4), we establish equivalent results for other LTS methods.

Proposition 3. *Consider a first-order accurate, LTS one-parameter conservative scheme written in the numerical viscosity form* (2.59)*, which is uniquely determined by the partial numerical viscosity coefficients Q^i_S. By defining S_{L} and S_{R} in the LTS-HLL-type scheme* (3.56) *as:*

$$S_{\mathrm{L}} = -Q_S, \quad S_{\mathrm{R}} = Q_S, \tag{3.63}$$

the numerical viscosity coefficients of the HLL-type scheme become:

$$Q^0_{HLL} = Q_S, \tag{3.64a}$$

$$\begin{aligned} Q^{\mp i}_{HLL} = {} & \frac{\lambda - Q_S}{Q_S} \max\left(0, \pm Q_S - i\frac{\Delta x}{\Delta t}\right) \\ & + \frac{Q_S - \lambda}{Q_S} \max\left(0, \mp Q_S - i\frac{\Delta x}{\Delta t}\right) \quad \textit{for} \quad i > 0. \end{aligned} \tag{3.64b}$$

Proof. Use (3.63) in (3.56) to obtain (3.64). □

Proposition 4. *Consider a first-order accurate, LTS one-parameter conservative scheme written in the flux-difference splitting form* (2.60)*, which is uniquely determined by the flux-difference splitting coefficients* $A_S^{i\pm}$*. By defining* S_{L} *and* S_{R} *in the LTS-HLL-type scheme* (3.56) *as:*

$$S_{\mathrm{L}} = A_S^- - A_S^+ = -Q_S, \quad S_{\mathrm{R}} = A_S^+ - A_S^- = Q_S, \tag{3.65}$$

the flux-difference splitting coefficients of the HLL-type scheme become:

$$\begin{aligned} A_S^{i\pm} = &\pm \frac{\lambda + Q_S}{2Q_S} \max\left(0, \min\left(\pm Q_S - i\frac{\Delta x}{\Delta t}, \frac{\Delta x}{\Delta t}\right)\right) \\ &\pm \frac{Q_S - \lambda}{2Q_S} \max\left(0, \min\left(\mp Q_S - i\frac{\Delta x}{\Delta t}, \frac{\Delta x}{\Delta t}\right)\right). \end{aligned} \tag{3.66}$$

Proof. Use (3.65) is (3.49) to obtain (3.66). □

We obtained a framework of LTS two-parameter methods that contains already existing LTS-Roe and LTS-Lax-Friedrichs schemes, and allows us to directly obtain an LTS extension of any first-order accurate standard one-parameter method. We note that an LTS extension of standard method is not unique. In our framework, what makes an LTS method an extension of a standard method is the fact that they are based on the same NV (or FDS) coefficients, and that the LTS method reduces to the standard method for $\bar{C} \leq 1$. Newly developed LTS extensions include:

- *LTS-Engquist-Osher:* Framework established above provides an LTS extension of the Engquist-Osher scheme. In the next section, we will show that our LTS-Engquist-Osher scheme is not entropy stable. On the other hand, Brenier [12] developed a monotone (hence entropy stable) LTS-Engquist-Osher scheme. Unfortunately, we do not know NV or FDS coefficients of the LTS-Engquist-Osher scheme by Brenier so at the moment we cannot compare these two.

- *LTS-Godunov:* Using $S_{\mathrm{L}} = -Q_{\mathrm{God}}$ and $S_{\mathrm{R}} = Q_{\mathrm{God}}$ does not recover the LTS-Godunov scheme of Lindqvist et al. [91]. In our framework, every scheme can be interpreted as the two-wave Riemann solver (3.2), and that also applies to our LTS-Godunov scheme when the solution is supposed to be a rarefaction. On the other hand, the LTS-Godunov scheme of Lindqvist et al. [91] splits a rarefaction into as many waves necessary to resolve it exactly (to projection error) on the given grid.

- *LTS-Lax-Wendroff:* Propositions 3 and 4 are stated for first-order accurate schemes. A straightforward LTS extension of the Lax-Wendroff scheme seems to be unstable. This issue is currently being investigated, and as a possible cause of failure we note that for standard methods we have:

$$c^2 \leq |c| \leq 1 \quad \rightarrow \quad Q_{\text{L-W}} \leq Q_{\text{Roe}} \leq Q_{\text{LxF}}. \tag{3.67}$$

  However, for LTS methods with an arbitrary Courant number, the numerical viscosity coefficient of the Lax-Wendroff scheme may exceed both Q_{Roe} and Q_{LxF}.

3.1.5. Convergence and entropy stability

Convergence

All considerations regarding the convergence of existing LTS methods (see section 2.2.5) also apply to LTS-HLL-type schemes. Namely, following the Lax-Wendroff theorem we are able to show that LTS-HLL-type methods with certain restrictions on the wave velocity estimates S_{L} and S_{R} converge to a weak solution.

The question of conservation was already discussed and we do not repeat it here. Consistency may be shown as earlier, by using the modified equation:

Lemma 7 (Prebeg [P1])**.** *The LTS-HLL scheme with the numerical viscosity coefficient* (3.56) *is consistent with the scalar conservation law:*

$$u_t + f(u)_x = 0. \tag{3.68}$$

Proof. First-order methods give a second-order accurate approximation to the equation:

$$u_t + f(u)_x = \frac{1}{2}\frac{\Delta x^2}{\Delta t}\left[\left(\sum_{i=1-k}^{k-1}\frac{\Delta t}{\Delta x}\bar{Q}^i - c^2\right)u_x\right]_x. \tag{3.69}$$

By using (3.56) in (3.69) we obtain that the LTS-HLL scheme gives a second-order accurate approximation to the equation:

$$u_t + f(u)_x = \frac{1}{2}\frac{\Delta x^2}{\Delta t}\left[D_{\text{LTS-HLL}}u_x\right]_x, \tag{3.70}$$

where:

$$
\begin{aligned}
D_{\text{LTS-HLL}} = & \frac{c - c_{\mathrm{L}}}{c_{\mathrm{R}} - c_{\mathrm{L}}} \left(\lceil |c_{\mathrm{R}}| \rceil - |c_{\mathrm{R}}| \right) \left(1 + |c_{\mathrm{R}}| - \lceil |c_{\mathrm{R}}| \rceil \right) \\
& + \frac{c_{\mathrm{R}} - c}{c_{\mathrm{R}} - c_{\mathrm{L}}} \left(\lceil |c_{\mathrm{L}}| \rceil - |c_{\mathrm{L}}| \right) \left(1 + |c_{\mathrm{L}}| - \lceil |c_{\mathrm{L}}| \rceil \right) \\
& + \left(c - c_{\mathrm{L}} \right) \left(c_{\mathrm{R}} - c \right), \qquad (3.71)
\end{aligned}
$$

where $c_{\mathrm{L}} = S_{\mathrm{L}} \Delta t / \Delta x$, $c_{\mathrm{R}} = S_{\mathrm{R}} \Delta t / \Delta x$, and $\lceil c \rceil = \min\{ n \in \mathbb{Z} \,|\, n \geq c \}$ is a ceiling function. By keeping $c = \text{const.}$ and passing $\Delta x \to 0$ we recover the scalar conservation law (3.68). □

To show TVD stability we use the TVD conditions for the LTS method in terms of the numerical viscosity coefficients, see (2.71).

Lemma 8. *The LTS-HLL scheme with the numerical viscosity coefficients* (3.56) *is TVD if:*

$$
S_{\mathrm{L},j+1/2} \leq \lambda_{j+1/2} \leq S_{\mathrm{R},j+1/2}, \quad \forall\, j. \qquad (3.72)
$$

Proof. We suppress the interface indices and note that by substituting (3.56) in (2.71a)–(2.71c) the TVD conditions become:

$$
\begin{aligned}
& (\lambda - S_{\mathrm{L}}) \left(\frac{\Delta x}{\Delta t} - \min \left(|S_{\mathrm{R}}|, \frac{\Delta x}{\Delta t} \right) \right) \\
& + (S_{\mathrm{R}} - \lambda) \left(\frac{\Delta x}{\Delta t} - \min \left(|S_{\mathrm{L}}|, \frac{\Delta x}{\Delta t} \right) \right) \geq 0, \qquad (3.73a) \\
& (\lambda - S_{\mathrm{L}}) \max \left(0, \min \left(\pm 2 S_{\mathrm{R}}, 4 \frac{\Delta x}{\Delta t} \mp 2 S_{\mathrm{R}} \right) \right) \\
& + (S_{\mathrm{R}} - \lambda) \max \left(0, \min \left(\pm 2 S_{\mathrm{L}}, 4 \frac{\Delta x}{\Delta t} \mp 2 S_{\mathrm{L}} \right) \right) \geq 0, \qquad (3.73b) \\
& (\lambda - S_{\mathrm{L}}) \max \left(0, \min \left(\pm S_{\mathrm{R}} - i \frac{\Delta x}{\Delta t}, \mp S_{\mathrm{R}} + i \frac{\Delta x}{\Delta t} + 2 \right) \right) \\
& + (S_{\mathrm{R}} - \lambda) \max \left(0, \min \left(\pm S_{\mathrm{L}} - i \frac{\Delta x}{\Delta t}, \mp S_{\mathrm{L}} + i \frac{\Delta x}{\Delta t} + 2 \right) \right) \geq 0 \quad \forall \quad i \geq 1, \\
& \qquad (3.73c)
\end{aligned}
$$

which are always satisfied under the condition (3.72). □

Entropy stability

The discussion on entropy stability of existing LTS methods from section 2.2.5 also applies here. We note that in general, the class of TVD LTS-HLL-type schemes is not entropy stable, because this class includes the entropy violating LTS-Roe scheme. We will address the question of entropy stability in LTS methods in section 3.2 by using the modified equation analysis.

3.1.6. LTS-HLL(C) schemes for systems of conservation laws

The LTS-HLL-type schemes can be extended to systems of equations following the same way the already existing LTS methods have been extended to systems of equations, see section 2.3. A slightly different approach to obtain the LTS-HLL scheme for systems of equations is given in our paper [P2], where we start with the standard HLL(C) schemes for systems of equations and extend them to the LTS framework. Our paper [P2] also includes analysis of numerical diffusion in the LTS-HLL scheme for the Euler equations, and numerical results for both LTS-HLL(C) schemes applied to the Euler equations.

Up to now, we did not explicitly present the HLLC and the LTS-HLLC schemes. This is due to the fact that we did not develop a scalar counterpart of the HLLC scheme, and because the HLLC scheme does not naturally fit into the NV and FDS form. Nevertheless, an LTS-HLLC scheme in a conservation form can be obtained in a relatively straightforward manner and we refer to our papers [P1, P2] for more details.

Herein, we show that both LTS-HLL(C) schemes for systems of equations can be also written in the wave propagation form. This can be done by combining elements of wave propagation form and the HLLC scheme, as is done for instance by Pelanti and Shyue [115]. We skip technical details and give a final result.

An LTS scheme for scalar conservation law in the wave propagation form (3.57) can be extended to systems of equations as:

$$\mathbf{U}_j^{n+1} = \mathbf{U}_j - \frac{\Delta t}{\Delta x} \sum_{i=0}^{\infty} \left(\sum_{p=1}^{m} S_{j-1/2-i}^{p,i+} \mathcal{W}_{j-1/2-i}^{p} + \sum_{p=1}^{m} S_{j+1/2+i}^{p,i-} \mathcal{W}_{j+1/2+i}^{p} \right), \tag{3.74}$$

where for the HLL scheme $m = 2$, and the wave velocities are:

$$S^1 = S, \quad S^2 = S_{\mathrm{R}}, \tag{3.75}$$

while the waves are:

$$\mathcal{W}^1_{j-1/2} = \mathbf{U}^{\mathrm{HLL}}_{j-1/2} - \mathbf{U}_{j-1}, \tag{3.76a}$$

$$\mathcal{W}^2_{j-1/2} = \mathbf{U}_{j} - \mathbf{U}^{\mathrm{HLL}}_{j-1/2}, \tag{3.76b}$$

where $\mathbf{U}^{\mathrm{HLL}}_{j-1/2}$ is determined following the same principles as for the intermediate state in case of scalar conservation law (3.3). For the HLLC scheme applied to one-dimensional Euler equations $m = 3$, and the wave velocities are:

$$S^1 = S_{\mathrm{L}}, \quad S^2 = S_{\mathrm{C}}, \quad S^3 = S_{\mathrm{R}}, \tag{3.77}$$

while the waves are:

$$\mathcal{W}^1_{j-1/2} = \mathbf{U}^{\mathrm{HLLC}}_{\mathrm{L},j-1/2} - \mathbf{U}_{j-1}, \tag{3.78a}$$

$$\mathcal{W}^2_{j-1/2} = \mathbf{U}^{\mathrm{HLLC}}_{\mathrm{R},j-1/2} - \mathbf{U}^{\mathrm{HLLC}}_{\mathrm{L},j-1/2}, \tag{3.78b}$$

$$\mathcal{W}^3_{j-1/2} = \mathbf{U}^{\mathrm{HLLC}}_{j} - \mathbf{U}^{\mathrm{HLLC}}_{\mathrm{R},j-1/2}, \tag{3.78c}$$

where the definition of the contact wave velocity S_{C} and the intermediate states $\mathbf{U}^{\mathrm{HLLC}}_{\mathrm{L,R},j-1/2}$ can be found in our papers [P1, P2] and in paper by Toro et al. [139] and the book by Toro [138], from where we adopted them. All velocities are modified in the same manner as:

$$S^{i\pm}_{\mathrm{L,C,R}} = \pm \max\left(0, \min\left(\pm S_{\mathrm{L,C,R}} - i\frac{\Delta x}{\Delta t}, \frac{\Delta x}{\Delta t}\right)\right). \tag{3.79}$$

3.1.7. Choice of the wave velocity estimates S_{L} and S_{R}

We now address the question on how to choose the wave velocity estimates S_{L} and S_{R}. This question was left open in the original paper where the HLL scheme was introduced [53], and was addressed by a number of authors in the coming years, see beginning of section 3.1. Herein, we outline some of velocity choices as applied to systems of equations, and we note that all of these also apply to the HLLC scheme and to the LTS extensions of the HLL(C) schemes.

We have already seen that for the scalar conservation laws, we can recover standard one-parameter methods from the standard HLL-type framework by an appropriate choice of S_{L} and S_{R}. In addition, we constructed genuinely two-parameter HLLE scheme. For systems of conservation laws, we can exactly deduce one-parameter methods from the HLL-type framework only for systems with two equations. If system of equations has more

than two equations, we can exactly deduce only those one-parameter methods which consist of two waves (such as the Lax-Friedrichs scheme), but not those schemes that consist of more than two waves (such as the Roe scheme).

For example, by defining:

$$S_{\mathrm{L},j+1/2} = -k\Delta x/\Delta t, \qquad S_{\mathrm{R},j+1/2} = k\Delta x/\Delta t, \tag{3.80}$$

we obtain the eigenvalues $(\omega^1, \ldots, \omega^N)$ and $(\lambda^1, \ldots, \lambda^N)$ corresponding to the Lax-Friedrichs scheme, and by defining:

$$S_{\mathrm{L},j+1/2} = -S_{\mathrm{R},j+1/2}, \qquad S_{\mathrm{R},j+1/2} = \max(|\lambda_j^1|, |\lambda_{j+1}^1|, |\lambda_j^N|, |\lambda_{j+1}^N|), \tag{3.81}$$

we obtain the eigenvalues $(\omega^1, \ldots, \omega^N)$ and $(\lambda^1, \ldots, \lambda^N)$ corresponding to the Rusanov scheme. We note that we will obtain genuine Lax-Friedrichs and Rusanov schemes independent of how many waves the system of equations has. By choosing:

$$S_{\mathrm{L},j+1/2} = \lambda^1_{\mathrm{Roe},j+1/2}, \qquad S_{\mathrm{R},j+1/2} = \lambda^N_{\mathrm{Roe},j+1/2}, \tag{3.82}$$

we obtain the eigenvalues (ω^1, ω^N) and (λ^1, λ^N) corresponding to the Roe scheme. The choice (3.82) identically reduces to the Roe scheme only for systems with two waves. For standard methods, the above was observed already by Davis [29] and Einfeldt [33].

Some other choices are given as:

$$\begin{aligned} S_{\mathrm{L},j+1/2} &= \lambda_j^1 \\ S_{\mathrm{R},j+1/2} &= \lambda_{j+1}^N \end{aligned} \qquad \text{Davis \#1 [29].} \tag{3.83}$$

$$\begin{aligned} S_{\mathrm{L},j+1/2} &= \min\left(\lambda_j^1, \lambda_{j+1}^1\right) \\ S_{\mathrm{R},j+1/2} &= \max\left(\lambda_j^N, \lambda_{j+1}^N\right) \end{aligned} \qquad \text{Davis \#2 [29].} \tag{3.84}$$

$$\begin{aligned} S_{\mathrm{L},j+1/2} &= \min\left(\lambda_j^1, \lambda_{j+1/2}^1\right) \\ S_{\mathrm{R},j+1/2} &= \max\left(\lambda_{j+1/2}^N, \lambda_{j+1}^N\right) \end{aligned} \qquad \text{Einfeldt [33].} \tag{3.85}$$

More complicated choices constructed for the Euler equations can be found in Toro et al. [139] and Bouchut [11], where Bouchut developed a special choice of S_{L} and S_{R} in order to handle vacuum in the Euler equations.

The choice of the wave velocities according to Einfeldt [33] is very popular among the standard methods, because it yields an entropy stable and a positivity preserving scheme [34]. Among the choices (3.83)–(3.85) and those found in Toro et al. [139], Einfeldt's choice (3.85) was also found to yield the very best results when used in LTS-HLL(C) schemes. These observations are based on our experience, and more rigorous comparison may be fruitful.

The LTS-HLLE scheme for systems of equations seems to inherit the HLLE scheme property of being entropy stable, but does not inherit the HLLE scheme property of being positivity preserving. The former will be addressed in the next section 3.2 *Entropy stability* and it is a topic of our conference paper [P1], while the latter will be addressed in section 3.3 *Positivity preservation* and it is a topic of our journal paper [P4].

3.2. Entropy stability

Earlier in the thesis (sections 2.2.5 and 3.1.5), we have seen that the tools commonly used to prove entropy stability of standard methods are not readily available for LTS methods. Therein, we postponed the discussion on entropy stability in LTS methods, and now we finally address it by using modified equation. We begin this section with a word of caution:

> *"Modified equations have been a commonly used tool in the study of difference schemes. Because of the lack of any theoretical foundation, this use has been accompanied by constant difficulties and results derived from modified equations have sometimes been regarded with apprehension. As a result, a situation arises where authors either disregard entirely the technique or have an unjustified faith in its scope."*
>
> Griffiths and Sanz-Serna [47]

We are hoping to avoid both of these pitfalls, and to use modified equation while being fully aware that it is based on certain assumptions that prevent us from using it as a tool to rigorously prove entropy stability. With this in mind we proceed to use modified equation analysis to conjecture about the entropy stability of the LTS-HLL-type schemes.

We start by outlining how entropy violation happens in standard methods following the *numerical viscosity* interpretation [84]. We then move to LTS methods, and present new difficulties that arise in LTS framework and different ways how this is handled in the existing literature. By following

the modified equation analysis by Lindqvist et al. [91], we illustrate the mechanism behind the entropy violation in the LTS-Roe scheme. Then, we show how is it avoided in some LTS-HLL-type schemes.

Part of discussion in this section closely follows our conference paper [P1]. The major difference is that here we focus on scalar conservation laws, while in the paper we consider the Euler equations.

3.2.1. Entropy violation

Entropy violation is most commonly associated and discussed as it appears in the Roe scheme [120]. Therefore, we focus on the Roe scheme and start by following the numerical viscosity interpretation of the entropy violation as found in the book by LeVeque [84].

The numerical flux function of the Roe scheme can be written as:

$$F^{\text{Roe}}_{j+1/2} = \frac{1}{2}\left(f_j + f_{j+1}\right) - \frac{1}{2}\left|\lambda_{j+1/2}\right|\left(u_{j+1} - u_j\right), \tag{3.86}$$

where we recall that $\lambda_{j+1/2}$ was defined in (2.32). In the case of a transonic rarefaction, $f'(u_j) < 0 < f'(u_{j+1})$, the shock speed may be very close to zero, corresponding to no viscosity. We define the interface Courant number $C_{j+1/2} = \lambda_{j+1/2}\Delta t/\Delta x$ and note that if:

$$C_{j+1/2} = 0, \tag{3.87}$$

we might obtain an entropy violation, because in case of a transonic rarefaction the exact solution is supposed to be a rarefaction wave (2.11), while the Roe scheme will treat it as a stationary shock with the velocity $\lambda_{j+1/2} = 0$. For the standard methods, these situations are well understood and we refer to [84] and references therein for more detailed discussions.

For the LTS-Roe scheme, most of authors observed that it leads to entropy violations more often than the standard Roe scheme [79, 81, 117, 99, 148, 91, 90]. Lindqvist et al. [91] showed that such LTS-related entropy violation may appear when:

$$C_{j+1/2} = -i, \quad \forall\, i \in \mathbb{Z}. \tag{3.88}$$

In earlier papers on LTS methods, this issue is solved by manually splitting the rarefaction wave into several expansion shocks [79, 81, 117, 99, 148] or by varying the time step [90, 91]. We now show how this issue is automatically avoided in the LTS-HLLE and LTS-Rusanov schemes.

3.2.2. Modified equation analysis

For the standard one-parameter method we may gain insight into the numerical viscosity of the method by looking at the numerical flux function and the corresponding numerical viscosity coefficient Q. However, for LTS methods the numerical flux function contains multiple numerical viscosity coefficients, so it is more convenient to work with the modified equation.

Earlier on (sections 2.2.5 and 3.1.5) we have seen that a first-order LTS methods give a second-order accurate approximation to the equation:

$$u_t + f(u)_x = \frac{1}{2}\frac{\Delta x^2}{\Delta t}\left[Du_x\right]_x, \tag{3.89}$$

where the inherent numerical diffusion was already introduced for standard schemes (2.48):

$$D = \sum_{i=1-k}^{k-1} \frac{\Delta t}{\Delta x}\bar{Q}^i - c^2. \tag{3.90}$$

Lindqvist et al. [91] determined the inherent numerical diffusion of the LTS-Roe and LTS-Lax-Friedrichs schemes:

$$D_{\text{LTS-Roe}} = \left(\lceil |c| \rceil - |c|\right)\left(1 + |c| - \lceil |c| \rceil\right), \tag{3.91}$$

$$D_{\text{LTS-LxF}} = k^2 - c^2. \tag{3.92}$$

In our conference paper [P1] we determined it for the LTS-HLL scheme:

$$\begin{aligned} D_{\text{LTS-HLL}} = {} & \frac{c - c_{\text{L}}}{c_{\text{R}} - c_{\text{L}}}\left(\lceil |c_{\text{R}}| \rceil - |c_{\text{R}}|\right)\left(1 + |c_{\text{R}}| - \lceil |c_{\text{R}}| \rceil\right) \\ & + \frac{c_{\text{R}} - c}{c_{\text{R}} - c_{\text{L}}}\left(\lceil |c_{\text{L}}| \rceil - |c_{\text{L}}|\right)\left(1 + |c_{\text{L}}| - \lceil |c_{\text{L}}| \rceil\right) \\ & + \left(c - c_{\text{L}}\right)\left(c_{\text{R}} - c\right), \end{aligned} \tag{3.93}$$

where we recall that we defined $c_{\text{L}} = S_{\text{L}}\Delta t/\Delta x$, $c_{\text{R}} = S_{\text{R}}\Delta t/\Delta x$ and $c = f'(u)\Delta t/\Delta x$, where $\lceil c \rceil = \min\{n \in \mathbb{Z} \mid n \geq c\}$ is the ceiling function.

We can observe that the inherent numerical diffusion of the LTS-Roe scheme (3.91) vanishes when the condition (3.88) is satisfied, leading to no diffusion being introduced by the method. If the exact solution is a rarefaction wave, this will lead to an entropy violation. This does not happen in the LTS-HLLE scheme:

Proposition 5 (Prebeg [P1])**.** *If the exact solution of the Riemann problem is a rarefaction wave, i.e.:*

$$f'(u_j) < \lambda_{j+1/2} < f'(u_{j+1}), \tag{3.94}$$

the inherent numerical diffusion of the LTS-HLLE scheme satisfies:

$$D_{\text{LTS-HLLE}} > 0. \tag{3.95}$$

Proof. In the HLLE scheme, the wave velocity estimates are:

$$S_{\text{L}} = \min\left(\lambda_{j+1/2}, f'(u_j)\right), \tag{3.96a}$$
$$S_{\text{R}} = \max\left(\lambda_{j+1/2}, f'(u_{j+1})\right). \tag{3.96b}$$

If (3.94) holds, then (3.96) yields:

$$S_{\text{L}} = f'(u_j) < \lambda_{j+1/2} < S_{\text{R}} = f'(u_{j+1}). \tag{3.97}$$

By using these in (3.93) we observe that:

$$D_{\text{LTS-HLLE}} \geq (c - c_{\text{L}})\,(c_{\text{R}} - c) > 0. \tag{3.98}$$

□

We can see that if the solution to the Riemann problem is a rarefaction wave, the LTS-HLLE scheme always introduces a certain amount of numerical diffusion. This is due to the fact that the HLLE scheme splits each discontinuity into two waves, and it is in fact entropy stable. We recall that LeVeque conjectured that the LTS-Godunov method converges to the unique entropy solution if we use the entropy solution for each Riemann problem [80] (see also page 27 of this thesis). This conjecture holds for any Riemann solver that itself satisfies the entropy condition, so we conjecture that the LTS-HLLE scheme converges to the entropy solution, because we use the entropy stable solution for each Riemann problem.

3.2.3. A class of one-parameter modified equations

Following the reasoning we used to deduce standard one-parameter methods from the HLL-type scheme (Lemmas 3 and 4), and to deduce LTS one-parameter methods from the LTS-HLL-type scheme (Propositions 3 and 4), we establish the equivalent result for the modified equations.

Proposition 6. *A first-order accurate, LTS one-parameter conservative scheme written in the numerical viscosity form* (2.59)*, which is uniquely determined by the partial numerical viscosity coefficients Q_S^i, gives a second-order accurate approximation to the equation:*

$$u_t + f(u)_x = \frac{1}{2}\frac{\Delta x^2}{\Delta t}\left[D_S u_x\right]_x, \tag{3.99}$$

where the inherent numerical diffusion is:

$$D_S = c_S\left(2\lceil c_S\rceil - 1\right) + \lceil c_S\rceil\left(1 - \lceil c_S\rceil\right) - c^2, \tag{3.100}$$

with $c_S = Q_S\Delta t/\Delta x$.

Proof. The derivation of the modified equation for the LTS-HLL-type scheme (3.93) makes no assumptions on the choice of S_L and S_R. Hence, we may define $S_\mathrm{L} = -Q_\mathrm{S}$ and $S_\mathrm{R} = Q_\mathrm{S}$ in (3.93), which then reduces to (3.100). □

For $c_\mathrm{S} = c$ and for $c_\mathrm{S} = k$, this reduces to the modified equations of the LTS-Roe (3.91) and LTS-Lax-Friedrichs schemes (3.92), respectively. Following Proposition 5, we can show the same result for the LTS-Rusanov scheme.

Proposition 7. *If the exact solution of the Riemann problem is a rarefaction wave, i.e.:*

$$f'(u_j) < \lambda_{j+1/2} < f'(u_{j+1}), \tag{3.101}$$

the inherent numerical diffusion of the LTS-Rusanov scheme satisfies:

$$D_{\text{LTS-Rus}} > 0. \tag{3.102}$$

Proof. With the Rusanov scheme, the numerical viscosity coefficient is:

$$Q_\mathrm{Rus} = \max\left(|\lambda_j|, |\lambda_{j+1}|\right) = \max\left(|f'(u_j)|, |f'(u_{j+1})|\right). \tag{3.103}$$

If (3.101) holds, then using (3.103) in (3.100) and rewriting yields:

$$D_{\text{LTS-Rus}} = \left(\lceil|c_\mathrm{Rus}|\rceil - |c_\mathrm{Rus}|\right)\left(1 + |c_\mathrm{Rus}| - \lceil|c_\mathrm{Rus}|\rceil\right) + c_\mathrm{Rus}^2 - c^2, \tag{3.104}$$

where $c_\mathrm{Rus} = Q_\mathrm{Rus}\Delta t/\Delta x$. The first term has the same form as the LTS-Roe scheme (3.91):

$$\left(\lceil|c_\mathrm{Rus}|\rceil - |c_\mathrm{Rus}|\right)\left(1 + |c_\mathrm{Rus}| - \lceil|c_\mathrm{Rus}|\rceil\right) \geq 0, \tag{3.105}$$

and since $c_{\text{Rus}} > c$, the second term is:

$$c_{\text{Rus}}^2 - c^2 > 0. \tag{3.106}$$

Hence we have that:

$$D_{\text{LTS-Rus}} > 0. \tag{3.107}$$

□

We may also make certain observations about our LTS extensions of other one-parameter methods mentioned on page 48:

- *LTS-Godunov:* NV coefficient of the standard Godunov scheme differs from the NV coefficient of the standard Roe scheme only in the case of a transonic rarefaction. This property also holds for the LTS-Godunov scheme introduced in this thesis and the LTS-Roe scheme. This means that the LTS-Godunov scheme successfully resolves the transonic rarefaction, but it fails in the same manner as the Roe scheme when the condition (3.88) holds.

- *LTS-Engquist-Osher:* The argument applied for the LTS-Godunov scheme also applies for the LTS-Engquist-Osher scheme.

- *LTS-Lax-Wendroff:* By choosing $c_{\text{S}} = c^2$, (3.100) yields:

  $$D_{\text{LTS-L-W}} = 2c^2\lceil c^2 \rceil - 2c^2 + \lceil c^2 \rceil - \lceil c^2 \rceil^2, \tag{3.108}$$

  which vanished only for $c \leq 1$. Hence, our LTS-Lax-Wendroff scheme is not second-order accurate.

We summarize our observations regarding the entropy stability of LTS methods in the Table 3.1.

Table 3.1.: Entropy stability of different methods: standard and LTS (conjectured[4])

	Roe	LxF	Rus	E-O	God	HLLE
Standard	no	yes	yes	yes	yes	yes
LTS	no	yes	yes	no	no	yes

[4]The LTS-Lax-Friedrichs scheme is proved to be entropy stable by proving it is monotone. This will be shown in next section.

We consider the inviscid Burgers' equation and two Riemann problems:

$$u(x,0) = \begin{cases} 0 & \text{if} \quad x < 0, \\ 1 & \text{if} \quad x > 0. \end{cases} \tag{3.109a}$$

$$u(x,0) = \begin{cases} -1 & \text{if} \quad x < 0, \\ 2 & \text{if} \quad x > 0. \end{cases} \tag{3.109b}$$

Figure 3.2 shows the numerical solution to the Riemann problem (3.109a) with different LTS methods with $\bar{C} = 5$ on two different grids on the interval $x \in [-1, 1.5]$. In Figure 3.2a we see that the LTS-Lax-Friedrichs, LTS-Rusanov and LTS-HLLE successfully resolve the rarefaction, while the LTS-Roe, LTS-Engquist-Osher and LTS-Godunov all lead to the same pattern of entropy violation. This is expected, because for the initial data (3.109a) these three schemes are identical. In Figure 3.2a, the LTS-Lax-Friedrichs scheme leads to a step-like pattern solution, but this is not an entropy violation but a consequence of the fact that the LTS-Lax-Friedrichs scheme splits the discontinuity into two waves, while we only did 8 time steps. Figure 3.2b shows that as we refine the grid, the LTS-Lax-Friedrichs scheme converges to the exact solution.

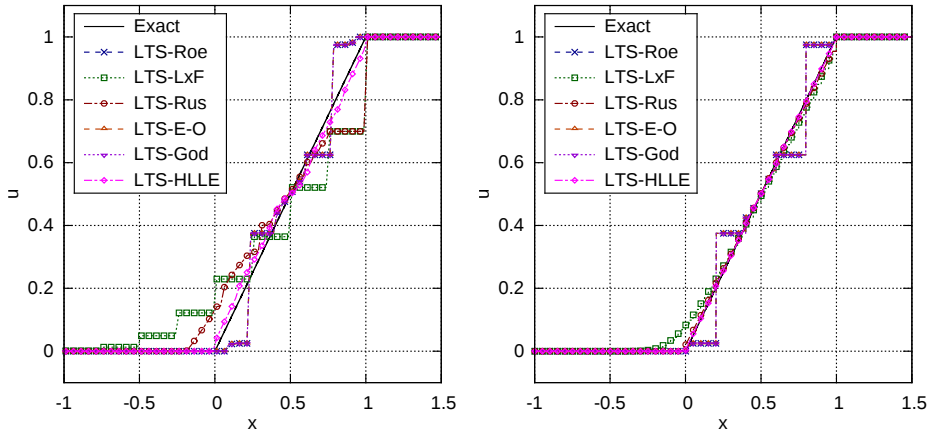

(a) 100 cells, $\Delta t = 0.125$, 8 time steps

(b) 1000 cells, $\Delta t = 0.0125$, 80 time steps

Figure 3.2.: Comparison of different LTS methods at $\bar{C} = 5$ for the Riemann problem (3.109a)

We now consider a transonic rarefaction. Figure 3.3 shows the numerical solution to the Riemann problem (3.109b) with different LTS methods with $\bar{C} = 5$ on two different grids on the interval $x \in [-2.5, 2.5]$. In Figure 3.3a we see that the LTS-Lax-Friedrichs, LTS-Rusanov and LTS-HLLE successfully resolve the rarefaction. The LTS-Roe, LTS-Engquist-Osher and LTS-Godunov schemes lead to an entropy violation, but this time in a different manner. The entropy violation in LTS-Roe scheme is a combination of two types of entropy violations – the standard Roe scheme entropy violation (3.87) (at transonic rarefaction) and the LTS-Roe scheme entropy violation (3.88). The LTS-Godunov and LTS-Engquist-Osher schemes successfully resolve the entropy violation related to the transonic rarefaction, but they do not resolve the LTS entropy violation.

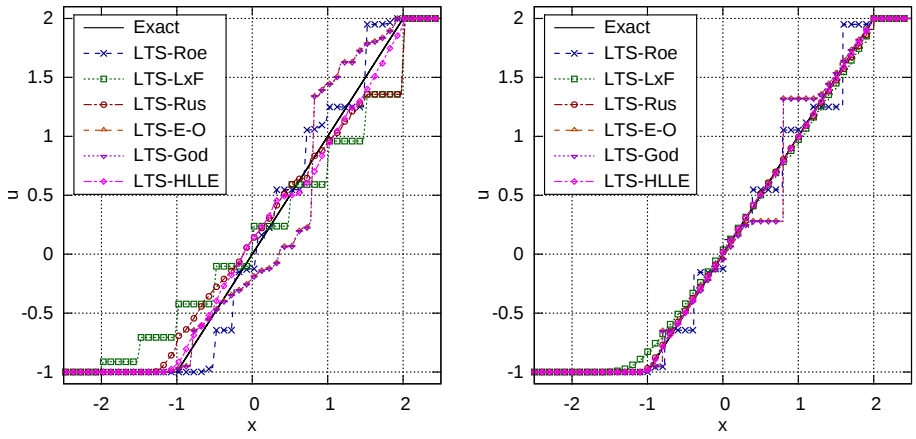

(a) 100 cells, $\Delta t = 0.125$, 8 time steps

(b) 1000 cells, $\Delta t = 0.0125$, 80 time steps

Figure 3.3.: Comparison of different LTS methods at $\bar{C} = 5$ for the Riemann problem (3.109b)

We can see that the conjectures from Table 3.1 are in agreement with the numerical experiments. A number of numerical experiments for the LTS-HLLE scheme applied to systems of equations implies the same. We refer to Nygaard [108] for the shallow water equations, and to our papers [P1, P2, P4] for the Euler equations.

3.3. Positivity preservation

In the previous two sections 3.1 and 3.2 we presented results on the construction of LTS-HLL-type schemes and the entropy violation by some of them. These results are related to our papers [P1, P2], but we presented them in detail because we focused on scalar conservation laws, while our papers [P1, P2] focused on the Euler equations.

In this section we present our results on monotonicity and positivity preservation in LTS methods, with a focus on the positivity preserving property of LTS methods for the Euler equations. The content of this section very closely follows our paper [P4], and this section is more a summary than a presentation of its own. The main results in [P4] are:

- a set of conditions on the numerical flux function of an LTS method that guarantees that the method is monotone;
- a proof that the LTS-Lax-Friedrichs scheme of Lindqvist et al. [91] for scalar conservation laws is monotone;
- a proof that the LTS-HLLE scheme is not positivity preserving, unlike its standard counterpart the HLLE scheme;
- a proof that the LTS-Lax-Friedrichs scheme of Lindqvist et al. [91] for systems of conservation laws is positivity preserving for one-dimensional Euler equations.

3.3.1. Monotonicity

The question of monotonicity was introduced earlier in section 2.1.1 where we considered mathematical properties of scalar conservation laws. Therein, a class of monotone schemes was introduced because they possess two very attractive properties:

- Monotone schemes satisfy the discrete version of the strict maximum principle (2.7). Let us define:

$$m = \min_j(u_j^0), \quad M = \max_j(u_j^0), \tag{3.110}$$

then the monotone scheme guarantees that:

$$u_j^n \in [m, M] \quad \forall \quad j, n. \tag{3.111}$$

- Monotone schemes are E-schemes, hence they converge to the entropy solution.

Unfortunately, monotone schemes have a third, less attractive property – they are at best first-order accurate [110]. Further, even though they cannot introduce new extrema, monotone LTS methods can produce oscillatory solutions, as was shown by Tang and Warnecke [133]. Nevertheless, monotone schemes are an essential tool in development of numerical methods and their understanding is important for many aspects of numerical modeling. The monotone scheme is defined as:

Definition 2 (Harten et al. [54], Trangenstein [142])**.** *An explicit numerical method:*

$$u_j^{n+1} = \mathcal{H}(u_{j-k}, \ldots, u_{j+k}; \Delta x, \Delta t), \tag{3.112}$$

is monotone if and only if it preserves inequalities between sets of numerical results:

$$\forall\, u_j^n, \forall\, v_j^n \quad \text{if} \quad \forall\, j \quad u_j^n \leq v_j^n, \tag{3.113}$$

then $\forall\, j$*:*

$$u_j^{n+1} = \mathcal{H}(u_{j-k}, \ldots, u_{j+k}; \Delta x, \Delta t) \leq \mathcal{H}(v_{j-k}, \ldots, v_{j+k}; \Delta x, \Delta t) = v_j^{n+1}. \tag{3.114}$$

We can determine if the method is monotone by the following result:

Lemma 9 (Trangenstein [142])**.** *Suppose that:*

$$u_j^{n+1} = \mathcal{H}(u_{j-k}, \ldots, u_{j+k}; \Delta x, \Delta t), \tag{3.115}$$

is a monotone scheme and that it is differentiable in each of its u_l *arguments for* $j - k \leq l \leq j + k$*. Then:*

$$\frac{\partial \mathcal{H}}{\partial u_l} \geq 0, \quad \forall \quad j - k \leq l \leq j + k. \tag{3.116}$$

Conversely, if:

$$\frac{\partial \mathcal{H}}{\partial u_l} \geq 0, \quad \forall \quad j - k \leq l \leq j + k, \tag{3.117}$$

then (3.115) *is a monotone scheme.*

A standard numerical method is monotone if the numerical flux function $F(u_j, u_{j+1})$ is non-decreasing in its first argument, non-increasing in its second argument and the CFL condition (2.54) holds.

The first result in our paper [P4] is the set of conditions on the numerical flux function of an LTS method that ensures that the method is monotone. The conditions are given in Proposition 1 of paper [P4], which also includes the proof. In addition, by using Lemma 9 we prove that the LTS-Lax-Friedrichs scheme of Lindqvist et al. [91] is monotone.

3.3.2. Positivity preservation

When we consider systems of equations, it may be unreasonable to require that a certain conserved variable remains bounded between its initial values at all time. However, it is often natural to require that some variables remain bounded in some specific sense, such as for example the positivity of density and internal energy in the Euler equations or positivity of water depth in the shallow water equations. We will denote such density and internal energy as physically real. If the scheme satisfies:

$$\rho_j^n > 0, \quad \forall\, j, n, \tag{3.118}$$

as well as the positivity of other variables of interest, we say that the scheme is positivity preserving.

Definition 3 (Einfeldt et al. [34])**.** *A class of schemes that always generates physically real solutions from physically real data is denoted as positivity preserving schemes.*

Condition (3.118) is so natural that it is somewhat surprising (and disappointing) that many popular schemes do not guarantee positivity preservation. Namely, certain generally well-behaved schemes may completely fail for certain types of initial data, and the question of positivity preservation is an ongoing field of research. Notable results include the paper by Einfeldt et al. [34], where it is shown that the Godunov and HLLE schemes are positivity preserving, while the Roe scheme is not, the paper by Batten et al. [6] where they showed that the HLLC [139] scheme is positivity preserving with an appropriate choice of wave velocity estimates, the work by Perthame and Shu [116] where they established a general framework to achieve high-order positivity preserving methods for the Euler equations in one and two dimensions, and the book by Bouchut [11] where the conditions on the wave velocities estimates are determined so that the HLLC

scheme can also handle vacuum. Areas of interest include the Euler equations (Calgaro et al. [14], Hu et al. [61], Li et al. [87], Zhang and Shu [150, 151, 152]), shallow water equations [121, 71, 147, 3], magnetohydrodynamics [4, 67, 40], multiphase flows (Chen and Shu [18]), unstructured meshes (Berthon [8]) and flux-vector splitting methods (Gressier et al. [46]), to name just a few. These papers consider standard methods and mostly tackle issues with positivity preserving that arise in high-order methods.

We considered the positivity preservation in LTS methods. The positivity preservation in the LTS-Roe scheme has been addressed by Morales-Hernández and co-workers [99, 100], where they considered the shallow water equations with source terms, and suggested to handle loss of positivity by reducing the Courant number when the loss of positivity is likely to happen. We took a slightly different direction and focused on the loss of positivity in the LTS-HLLE scheme, and on increasing the robustness of the LTS-HLLE scheme by adding numerical diffusion. We outline our two main results below.

We considered the classical result by Einfeldt et al. [34]:

Lemma 10 (Einfeldt et al. [34])**.** *An approximate Riemann solver leads to a positively conservative scheme if and only if all the states generated are physically real.*

An example of such Riemann solver is the HLLE scheme, and the generated states in question are intermediate states appearing across the Riemann fan. Our first result related to positivity preservation is showing that physically real intermediate states are a necessary, but not a sufficient condition for positivity preservation in the LTS methods. We did this by considering the LTS-HLLE scheme, for which all intermediate states are physically real, and showing that it is not positivity preserving for the Euler equations (see paper [P4]).

Our second result is the proof that the LTS-Lax-Friedrichs scheme of Lindqvist et al. [91] is positivity preserving for the Euler equations. Our proof closely follows the proof by Zhang and Shu [150] where they showed that the standard Lax-Friedrichs scheme is positivity preserving for the Euler equations. We follow their proof and generalize it to hold under the relaxed CFL condition (2.58) (see paper [P4], Proposition 3).

In order to make the LTS-HLLE scheme more robust, we defined the wave velocity estimates as a convex combination:

$$S_{\mathrm{L}} = (1-\beta)\, S_{\mathrm{L}}^{\mathrm{E}} + \beta S_{\mathrm{L}}^{\mathrm{LxF}}, \qquad S_{\mathrm{R}} = (1-\beta)\, S_{\mathrm{R}}^{\mathrm{E}} + \beta S_{\mathrm{R}}^{\mathrm{LxF}}, \tag{3.119}$$

where $S^{\mathrm{E}}_{\mathrm{L,R}}$ are the wave velocity estimates according to Einfeldt (3.85), and $S^{\mathrm{LxF}}_{\mathrm{L,R}}$ are the wave velocity estimates corresponding to the Lax-Friedrichs scheme (3.80). This approach reduced oscillations, and provided an increase in robustness in a sense that we could use the scheme defined by (3.119) for Courant numbers at which the LTS-HLLE scheme would lose positivity. However, such a straightforward increase in numerical diffusion across all cells and all time steps also led to a decrease in accuracy. We believe that this can be improved by selectively introducing numerical diffusion only when it is necessary to preserve positivity. That way positivity would be ensured, while the solution would be kept as sharp as possible. Numerical results obtained with the LTS-HLLE scheme and LTS-HLLEβ (3.119) schemes can be found in our paper [P4], where we applied them to the one-dimensional Euler equations and considered double rarefaction, LeBlanc's shock tube and the Sedov blast-wave as test cases.

Truth is much too complicated to allow anything but approximations.

John von Neumann

4 Multiphase flow modeling

This chapter presents the application of the LTS-Roe scheme to one-dimensional two-fluid model and the contribution to treatment of boundary conditions and source terms in LTS framework.

4.1. Mathematical modeling of two-phase flow

In the previous sections we studied single phase flow which can be completely described by the Navier–Stokes equations (for viscous flows) and the Euler equations (for inviscid flows). In particular, we focused on one-dimensional scalar conservation laws and the Euler equations.

However, in practical applications most of the fluid flows are multiphase and/or multicomponent in their nature. In a world of unlimited computational resources, these flows could be modeled by applying the Navier–Stokes equation locally to the domain where a certain fluid is present, and by direct modeling of the interfaces between different phases. However, the present computing capabilities are not even close to that goal, and at the moment they do not seem to be achievable in any foreseen future:

"For example, turbulence or three-dimensional hydrodynamics, those are problems that can eat up an arbitrary capacity on any computer we're ever likely to see. So you have to be clever."

Bernie Alder

Being clever consists of using simplified models of the Navier–Stokes equations and/or by developing more accurate and more efficient numerical methods. There exist a great variety of simplified models for multiphase flow modeling, and they all boil down to finding the optimal balance between ensuring that the mathematical model possesses a capability to describe all the physics we are interested in, while at the same time keeping the model simple enough to be able to numerically solve it in a reasonable time.

One of the most commonly used simplifications is *averaging*, where the flow parameters are averaged either over time, space or ensemble. A vast body of literature has been written on this topic, and we point out to books by Drew and Passman [31], Ishii and Hibiki [64] and Städtke [125] and literature therein for a comprehensive overview of the topic. Much of the progress in both mathematical and numerical modeling of multiphase flows was driven by demands of nuclear and petroleum industries, where notable softwares include CATHARE [5] and RELAP5 [15] for safety analysis of nuclear reactors, and LedaFlow [26], OLGA [7], PeTra [72] and TACITE [113] for oil & gas industry. Herein, we do not study these models.

Instead, we focus on a very simple two-fluid model and use it to illustrate some of the major difficulties encountered in multiphase flow modeling.

4.1.1. Two-fluid model

We consider a one-dimensional isentropic equal-pressure two-fluid model without energy equation in which we solve separate evolution equations for mass and momentum of two fluids:

$$\partial_t(\alpha_g\rho_g) + \partial_x(\alpha_g\rho_g v_g) = 0, \tag{4.1a}$$

$$\partial_t(\alpha_l\rho_l) + \partial_x(\alpha_l\rho_l v_l) = 0, \tag{4.1b}$$

$$\partial_t(\alpha_g\rho_g v_g) + \partial_x(\alpha_g\rho_g v_g^2 + (p - p^i)\alpha_g) + \alpha_g\partial_x p^i = Q_g, \tag{4.1c}$$

$$\partial_t(\alpha_l\rho_l v_l) + \partial_x(\alpha_l\rho_v v_l^2 + (p - p^i)\alpha_l) + \alpha_l\partial_x p^i = Q_l, \tag{4.1d}$$

where ρ, α, v, Q are the density, volume fraction, velocity and the source term with corresponding phase indices g, l for the gas and liquid phase,

respectively. The pressure p denotes a common pressure of both phases, while the pressure p^i denotes the pressure at the interface between gas and liquid. For more details and closure relations we refer to the paper by Evje and Flåtten [37] from where this model was adopted.

This and similar models have been studied by a number of authors [141, 23, 22, 37, 30, 103] since it is one of the most simple two-fluid model that contains many of the difficulties that distinguish it from single phase hyperbolic systems such as the Euler equations.

Systems of equations such as (4.1) can be written as:

$$\mathbf{U}_t + \mathbf{F}(\mathbf{U})_x + \mathbf{B}(\mathbf{U})\mathbf{W}(\mathbf{U})_x = \mathbf{Q}(\mathbf{U}), \tag{4.2}$$

where $\mathbf{U}$ is a vector of evolved variables, $\mathbf{F}(\mathbf{U})$ is a flux function, $\mathbf{B}(\mathbf{U})\mathbf{W}(\mathbf{U})_x$ represents non-conservative transport terms and $\mathbf{Q}(\mathbf{U})$ is a vector of source terms. We may observe that already this very simple two-fluid model possesses two difficulties that were not present in the Euler equations:

- *non-conservative terms:* The presence of non-conservative terms in this (and many other) two-fluid models presents a difficulty when it comes to the numerical modeling, because it is not possible to write the left-hand side of (4.2) in conservation form. Hence, we cannot rely on the Lax-Wendroff theorem when considering convergence, and we do not possess a flux function that completely describes the evolution of the left-hand side, which prevents us from fully exploiting advantages of numerical methods based on the numerical viscosity form.

  This has been a long standing challenge both for mathematical theory and numerical modeling. The pioneering work on the mathematical theory of non-conservative products goes back to Vol'pert [143], while notable papers include the works of Dal Maso et al. [25], Hou and LeFloch [60], Parés [111] and Castro et al. [17]. From the numerical modeling viewpoint, we mention the papers by Toumi and co-workers [140, 141], Castro and Toro [16], Dumbser et al. [32], Munkejord et al. [104] and Flåtten and Morin [39].

  We outline the approach we used to treat the non-conservative terms in section 4.2 where we discuss numerical modeling of (4.2).

- *source terms:* In the system of equations (4.1) the source terms appear only in the momentum equations modeling the effect of gravity. In

more general case described by (4.2) source terms may appear in all equations and they may account for a variety of physical phenomena. For example, in a two-phase flow modeling the source terms are used to model the *relaxation processes* that account for transfer processes between two phases. These processes include transfer of heat, mass and volume due to differences in temperature, chemical potential and pressure, see Lund [94] for a comprehensive analysis of the relaxation models. Further modeling difficulties may appear if the source terms are *stiff*, or if the system of equations is close to steady-state. The latter difficulties gave rise to a a class of *well-balanced* schemes. We refer to LeVeque [84] and Bouchut [11] for an overview of these difficulties and further reading.

Herein, we wish to stress that these concepts (relaxation terms, stiff source terms, well-balanced schemes) are still an active area of research and there are numerous unresolved problems even for standard methods. Hence, we are still a long way from having an established theory how source terms should be treated in LTS methods. A pioneering work on this topic has been done by Morales-Hernández, Murillo, García-Navarro and co-workers [105, 99, 101, 100, 102] where they studied the source terms in the shallow water equations. In addition to these two difficulties that can be immediately seen from (4.2), there are several other challenges that may appear in practical applications (for both single and multiphase flows):

- *boundary conditions:* The treatment of boundary conditions is still a challenging topic and an active field of research even for standard numerical methods. Definition of boundary conditions in LTS methods is further complicated by the fact that we need to define additional ghost points at the boundaries. In addition, the presence of source terms leads to further difficulties due to a very delicate effect of the source terms at the boundaries of the domain when we use LTS methods. The question of boundary conditions in LTS methods has been addressed by LeVeque [82] and Morales-Hernández and co-workers [105, 99, 101, 100, 102]. The treatment of boundary conditions in LTS methods is the topic of our conference and journal papers [P5] and [P3], respectively. We outline how we approached these difficulties in section 4.2.

- *positivity preservation:* In section 3.3 we studied difficulties related to positivity preservation in the Euler equations. The presence of two (or

more) fluids and source terms, and their complex interaction poses an even greater challenge for the capability of method to preserve positivity, especially when we extend the method to LTS framework.

- *stability of standard methods:* The CFL condition is only a necessary condition for stability of standard methods. Indeed, for most homogeneous one-dimensional systems of hyperbolic conservation laws, most standard schemes will be stable up to a Courant number of unity. However, in more complex flows it is very often the case that the actual upper bound of the Courant number is less than unity, and running a simulation requires us to use a lower Courant number than one might expect.

  Such difficulties were, for example, reported by Pelanti and Shyue [115] where the six-equation two-phase model was studied. Therein, these difficulties are attributed to the stiffness of the source terms. In practice, there is a variety of reasons why the actual CFL bound can be reduced. The difficulty for our interests is that if the nature of the model prevents even standard methods from reaching the standard Courant number, it remains an open question how we can apply LTS methods to such problems.

Remark 3. We note that chronologically, the content of chapter 4 was the first thing done at the beginning of the PhD project. Unfortunately, the fact that the LTS-Roe scheme is not positivity preserving became a serious obstacle for more complicated models (this is not surprise, since the standard Roe scheme is not positivity preserving itself). The difficulty with positivity preservation was one of the main reasons that motivated us to study the HLL(C) schemes which are known to be positivity preserving. However, severe problems with positivity preservation of the LTS-HLL(C) schemes were observed for five-equation models of Allaire et al. [1] and Murrone and Guillard [106]. We then opted to study the issues with the positivity preservation by using simpler models such as the Euler equations.

4.2. Numerical modeling of two-phase flow

Herein, we outline the approach we used to numerically solve the two-fluid model (4.1). For more general numerical methods for multiphase flow modeling we refer to the literature outlined in previous section.

The system of equations (4.2) can be written in quasilinear form as:

$$\mathbf{U}_t + \mathbf{A}(\mathbf{U})\mathbf{U}_x = \mathbf{Q}(\mathbf{U}), \tag{4.3}$$

where:

$$\mathbf{A}(\mathbf{U}) = \frac{\partial \mathbf{F}(\mathbf{U})}{\partial \mathbf{U}} + \mathbf{B}(\mathbf{U})\frac{\partial \mathbf{W}(\mathbf{U})}{\partial \mathbf{U}}. \tag{4.4}$$

We then solve the system of equations (4.3) with the explicit Euler method in time and the LTS-Roe scheme in flux-difference splitting form in space:

$$\mathbf{U}_j^{n+1} = \mathbf{U}_j - \frac{\Delta t}{\Delta x}\sum_{i=0}^{\infty}\left(\hat{\mathbf{A}}^{i+}_{j-1/2-i}\Delta\mathbf{U}_{j-1/2-i} + \hat{\mathbf{A}}^{i-}_{j+1/2+i}\Delta\mathbf{U}_{j+1/2+i}\right) + \Delta t\mathbf{Q}(\mathbf{U}), \tag{4.5}$$

where we left the source term $\mathbf{Q}(\mathbf{U})$ undiscretized for now. We note that for this system, the treatment of the non-conservative term was straightforward, and its effect was simply incorporated into the coefficient matrix $\mathbf{A}$, eq. (4.4), as it was done by Evje and Flåtten [37].

The major findings of our papers [P3, P5] are related to treatment of boundary conditions and source terms with the method (4.5). Herein, we outline the main results on these.

4.2.1. Treatment of the boundary conditions

In standard methods the value of $\mathbf{U}_j^{n+1}$ at the new time step depends only on the value at three cells in the previous time step:

$$\mathbf{U}_j^{n+1} = \mathbf{U}\left(\mathbf{U}_{j-1}^n, \mathbf{U}_j^n, \mathbf{U}_{j+1}^n\right). \tag{4.6}$$

For the first cell in the domain, this implies that:

$$\mathbf{U}_1^{n+1} = \mathbf{U}\left(\mathbf{U}_{\mathrm{LBC}}^n, \mathbf{U}_1^n, \mathbf{U}_2^n\right), \tag{4.7}$$

where $\mathbf{U}_{\mathrm{LBC}}$ is the value of $\mathbf{U}$ in the left boundary cell. Hence, the treatment of the boundaries in the standard methods requires us to define a single ghost cell at each boundary. In the LTS methods the value at the new time step depends on up to k cells at the previous time step:

$$\mathbf{U}_j^{n+1} = \mathbf{U}\left(\ldots, \mathbf{U}_{j-2}^n, \mathbf{U}_{j-1}^n, \mathbf{U}_j^n, \mathbf{U}_{j+1}^n, \mathbf{U}_{j+2}^n, \ldots\right), \tag{4.8}$$

which implies that we may need to provide more than one ghost cell at the boundary:

$$\mathbf{U}_1^{n+1} = \mathbf{U}\left(\ldots, \mathbf{U}_{-1}^n, \mathbf{U}_{\mathrm{LBC}}^n, \mathbf{U}_1^n, \mathbf{U}_2^n, \mathbf{U}_3^n, \ldots\right). \tag{4.9}$$

We proposed two ways how to define these additional boundary cells:

- *Extrapolated boundary conditions (EBC):* All additional boundary cells are equal to the original boundary cell:

$$\mathbf{U}_j^n = \mathbf{U}_{\mathrm{LBC}}^n \quad \forall \quad j < \mathrm{LBC}, \tag{4.10a}$$

$$\mathbf{U}_j^n = \mathbf{U}_{\mathrm{RBC}}^n \quad \forall \quad j > \mathrm{RBC}, \tag{4.10b}$$

  where the value of the the primary boundary cells at x_{LBC} and x_{RBC} may be defined in a number of ways, for example by extrapolation of the characteristic [38] or primitive variables. The difficulties observed with the LTS method are somewhat independent of the way we define $\mathbf{U}_{\mathrm{LBC}}$ and $\mathbf{U}_{\mathrm{RBC}}$, and in our papers [P3, P5] we used primitive variable extrapolation.

- *Steady-state boundary conditions (SSBC):* We solve the steady-state version of (4.3) to obtain the slopes of the evolved variables $\mathbf{U}$ due to the effect of the source term $\mathbf{Q}(\mathbf{U})$:

$$\mathbf{U}_x = \mathbf{A}(\mathbf{U})^{-1}\mathbf{Q}(\mathbf{U}). \tag{4.11}$$

  The discrete version of (4.11) allows us to determine the change of the evolved variables $\mathbf{U}$ at the boundaries as:

$$\delta_x \mathbf{U}_{\mathrm{L}} = \left(\mathbf{A}(\mathbf{U}_{\mathrm{LBC}})\right)^{-1} \mathbf{Q}(\mathbf{U}_{\mathrm{LBC}}), \tag{4.12a}$$

$$\delta_x \mathbf{U}_{\mathrm{R}} = \left(\mathbf{A}(\mathbf{U}_{\mathrm{RBC}})\right)^{-1} \mathbf{Q}(\mathbf{U}_{\mathrm{RBC}}). \tag{4.12b}$$

  We then use these to replace (4.10) by:

$$\mathbf{U}_j^n = \mathbf{U}_{\mathrm{LBC}}^n + (j - \mathrm{LBC})\Delta x \delta_x \mathbf{U}_{\mathrm{L}} \quad \forall \quad j \in [\mathrm{LBC} - M, \ldots, \mathrm{LBC}], \tag{4.13a}$$

$$\mathbf{U}_j^n = \mathbf{U}_{\mathrm{RBC}}^n + (j - \mathrm{RBC})\Delta x \delta_x \mathbf{U}_{\mathrm{R}} \quad \forall \quad j \in [\mathrm{RBC}, \ldots, \mathrm{RBC} + M], \tag{4.13b}$$

  where $M = \lceil \bar{C} \rceil$.

SSBC led to an increase in accuracy, especially on coarser grids. However, SSBC requires additional computational work since one has to resolve the eigenstructure in newly defined cells. A more thorough analysis and comparison between solutions obtained with EBC ans SSBC can be found in our papers [P3, P5].

4.2.2. Treatment of the source terms

We investigated two ways to treat the source term in (4.5):

- *Explicit Euler treatment:* The source term is approximated directly as:

$$\Delta t\mathbf{Q}(\mathbf{U}) = \Delta t\mathbf{Q}(\mathbf{U}_j). \tag{4.14}$$

  This approach gave acceptable results only if the LTS-Roe scheme was applied only on the acoustic waves. If the Courant number associated with the phase waves was increased above the standard CFL condition, severe oscillations appeared in the volume fraction and velocity profiles.

- *Split treatment:* In this approach we followed the work by Morales-Hernández and co-workers [105, 99, 101, 100, 102], but generalized in slightly different direction more suitable for implementation in flux-difference splitting framework.

  The source term is approximated in an upwind manner, where the contributions from the source terms are evaluated at the interfaces:

$$\Delta t\mathbf{Q}(\mathbf{U}) = \frac{\Delta t}{\Delta x}\sum_{i=0}^{\infty}\left(\tilde{\mathbf{A}}^{i+}_{j-1/2-i}\mathbf{S}_{j-1/2-i} + \tilde{\mathbf{A}}^{i-}_{j+1/2+i}\mathbf{S}_{j+1/2+i}\right), \tag{4.15}$$

  where for the definition of $\tilde{\mathbf{A}}$ and $\mathbf{S}$ we refer to our paper [P3]. This approach resulted in notable improvement of accuracy compared to the simpler approach (4.14) and allowed us to use the Courant number up to $\bar{C} \approx 2.4$ for phase waves. However, it did not yield an unconditionally stable scheme, and further increase of the Courant number gave rise to oscillations. In addition, split treatment is clearly more computationally expensive than the explicit Euler treatment.

A scientific approach means knowing what one knows and what one doesn't. Absolute or complete knowledge is unscientific.

Karl Jaspers

5 Conclusions and outlook

5.1. Conclusions

We developed and investigated Large Time Step HLL-type finite volume methods for hyperbolic conservation laws. Our major contributions are presented in chapters 3 and 4 and they can be summarized as follows:

- Section 3.1: We developed the LTS-HLL-type schemes.
- Section 3.2: We investigated entropy stability of LTS methods by using the modified equation analysis.
- Section 3.3: We investigated monotonicity and positivity preservation of LTS methods.
- Chapter 4: We investigated the treatment of boundary conditions and source terms in LTS methods.

In section 3.1 we interpreted the HLL scheme as a numerical scheme for scalar conservation laws. We developed a two-parameter HLL-type schemes, and determined the TVD conditions on the wave velocity estimates. We showed that the HLLE scheme is consistent, TVD and entropy stable, i.e. it converges to the entropy solution. We then developed the LTS-HLL-type schemes. We described these new schemes in the numerical

viscosity, flux-difference splitting and wave propagation form, and we determined the TVD conditions on the wave velocity estimates. We showed that the LTS-HLLE scheme is consistent and TVD. However, a rigorous proof of entropy stability remains unresolved.

This new class of schemes provided greater flexibility in constructing new schemes because it has two free parameters, while at the same time it allows us to simply deduce LTS extensions of standard one-parameter methods, such as the Roe, Lax-Friedrichs, Rusanov, Godunov and Engquist-Osher schemes. Working along the lines of the approach above, we extended the standard HLL and HLLC schemes for systems of conservation laws to the LTS-HLL(C) schemes.

In section 3.2 we investigated the question of entropy stability by using the modified equation analysis. First, we used the modified equation to quantify the amount of numerical diffusion in the LTS-HLL-type schemes. We performed numerical experiments to gain better insight into how entropy violations happen in LTS methods, and to conjecture how are they avoided in certain LTS-HLL-type schemes. In particular, we conjecture that the LTS-HLLE and LTS-Rusanov schemes are entropy stable. Numerical results for both scalar conservation laws and the Euler equations are in agreement with theoretical results obtained with the modified equation analysis.

In section 3.3 we investigated questions of monotonicity and positivity preservation. First, we determined the monotonicity conditions on the numerical flux function of an LTS method, and we showed that the LTS-Lax-Friedrichs scheme is monotone. Then, we moved to systems of equations and showed that the positivity preserving conditions in LTS methods are stronger than in standard methods. For some special cases of initial data, we described how loss of positivity preserving occurs in the LTS-HLLE scheme, we showed that the LTS-Lax-Friedrichs scheme is positivity preserving, and we numerical demonstrated that robustness of the LTS-HLLE scheme can be increased by adding numerical diffusion.

Lastly, in chapter 4 we applied the LTS-Roe scheme to a one-dimensional two-fluid model and focused on the difficulties related to the boundary conditions and the source terms. We proposed a new way to define the boundary conditions in the LTS framework, and we handled the source terms by following Morales-Hernández and co-workers [105, 99, 101, 100, 102]. It is shown that the accuracy of the solution can be greatly improved by appropriate treatment of boundary conditions and source terms.

5.2. Future outlook

Large Time Step methods have been around for more than thirty years, but they never really became a part of the mainstream in the finite volume methods/hyperbolic conservation laws community. Nevertheless, there seems to be an unfailing appeal in their increased stability and explicitness, and it seems that throughout their history there was always someone trying to exploit their full potential.

I am not convinced that my humble contributions will change this trend. But in case time proves me wrong, and for those who will be interested in further exploring LTS methods I will consider some possible directions and possibilities.

- *Numerical diffusion:* The majority of the numerical investigations performed by us and other authors suggest that most errors in LTS methods appear in form of oscillations around shocks and contact discontinuities. These errors can be reduced by introducing numerical diffusion, as it was successfully done by Lindqvist et al. [91], Solberg [124] and Nygaard [108]. Therein, the amount of the numerical diffusion being added is partially automated and partially tuned manually. We showed that manually adding numerical diffusion increases the robustness of LTS methods. Any LTS method aiming for generality and robustness will need to have a sophisticated and fully automatized mechanism to add numerical diffusion.

  One idea on how to do this might be along the lines of how higher order TVD methods are designed: use second-order scheme where the data is smooth, and reduce it to a first-order schemes around discontinuities. We believe that is possible to construct an LTS method which will automatically introduce appropriate amount of numerical diffusion around discontinuities or when loss of positivity is likely to happen.

- *Computational efficiency and convergence rates:* Even though the computational efficiency is one of the most attractive features of LTS methods, it was not the main objective of our investigations. However, any strong argument in favor of LTS methods must be supported by evidence of increased computational efficiency.

  Our preliminary investigations suggest that the decrease in computational time is greatest immediately after going from $\bar{C} = 1 \rightarrow \bar{C} = 2$.

A further increase in Courant number yielded smaller and smaller gains in computational time (see for instance our papers [P3, P2, P5]). This suggests that in terms of computational time, it might be optimal to use a relatively small Courant number. A better criterion for choosing the Courant number would be computational efficiency, which was also investigated in our papers [P3, P2]. Therein, computational efficiency and convergence rates are studied, and it is observed that LTS methods generally have higher convergence rates than their first-order counterparts. We note that our numerical codes were build to be simple and modular, and we believe that by optimizing the code we could further improve the gains in computational time and computational efficiency.

Since a significant increase in Courant number leads to oscillations and inevitable decrease in accuracy, it might not be fruitful to push the Courant number above a single digit numbers. Another attractive feature of keeping the Courant number relatively low is that it might result in increased computational efficiency while applying the LTS method only on acoustic waves, which brings us to the next point.

- *Low Mach number flows:* LTS methods might be an attractive candidate for low Mach number flows, where it would be possible to use very high Courant numbers for the acoustic waves, and standard methods for the slow waves. We obtained some preliminary results in this direction in our paper [P3], where we considered the water faucet test case. Therein, slow waves are not strongly affected by acoustic waves and it was possible to use an LTS method for the acoustic waves in a straightforward way, which led to a notable decrease in computational time and increase in accuracy of slow waves.

Bibliography

[1] G. Allaire, S. Clerc, and S. Kokh. "A Five-Equation Model for the Simulation of Interfaces between Compressible Fluids". *J. Comput. Phys.* 181.2 (2002), pp. 577–616.

[2] V. R. Ambati and O. Bokhove. "Space–Time Discontinuous Galerkin Discretization of Rotating Shallow Water Equations". *J. Comput. Phys.* 225.2 (2007), pp. 1233–1261.

[3] E. Audusse and M.-O. Bristeau. "A Well-Balanced Positivity Preserving Second-Order Scheme for Shallow Water Flows on Unstructured Meshes". *J. Comput. Phys.* 206.1 (2005), pp. 311–333.

[4] S. D. Balsara and D. Spicer. "Maintaining Pressure Positivity in Magnetohydrodynamic Simulations". *J. Comput. Phys.* 148.1 (1999), pp. 133–148.

[5] F. Barre and M. Bernard. "The CATHARE Code Strategy and Assessment". *Nucl. Eng. Des.* 124.3 (1990), pp. 257–284.

[6] P. Batten, N. Clarke, C. Lambert, and D. M. Causon. "On the Choice of Wavespeeds for the HLLC Riemann Solver". *SIAM J. Sci. Comput.* 18.6 (1997), pp. 1553–1570.

[7] K. H. Bendiksen, D. Maines, R. Moe, and S. Nuland. "The Dynamic Two-Fluid Model OLGA: Theory and Application". *SPE Prod. Eng.* 6.2 (1991), pp. 171–180.

[8] C. Berthon. "Robustness of MUSCL Schemes for 2D Unstructured Meshes". *J. Comput. Phys.* 218.2 (2006), pp. 495–509.

[9] C. Berthon, P. Charrier, and B. Dubroca. "An HLLC Scheme to Solve the M_1 Model of Radiative Transfer in Two Space Dimensions". *J. Sci. Comput.* 31.3 (2007), pp. 347–389.

[10] S. L. Bore. "High-Resolution Large Time-Step Schemes for Hyperbolic Conservation Laws". MA thesis. Norwegian University of Science and Technology: Dept. of Energy and Process Engineering, 2015. URL: http://hdl.handle.net/11250/2352144.

[11] F. Bouchut. *Nonlinear Stability of Finite Volume Methods for Hyperbolic Conservation Laws*. 1st ed. Frontiers in Mathematics. Birkhäuser Basel, 2004.

[12] Y. Brenier. "Averaged Multivalued Solutions for Scalar Conservation Laws". *SIAM J. Numer. Anal.* 21.6 (1984), pp. 1013–1037.

[13] A. Bressan. "Open Questions in the Theory of One Dimensional Hyperbolic Conservation Laws". In: *Nonlinear Conservation Laws and Applications*. Ed. by A. Bressan, G.-Q. G. Chen, M. Lewicka, and Wang. D. Boston, MA: Springer US, 2011, pp. 1–22.

[14] C. Calgaro, E. Creusé, T. Goudon, and Y. Penel. "Positivity-Preserving Schemes for Euler Equations: Sharp and Practical CFL Conditions". *J. Comput. Phys.* 234 (2013), pp. 417–438.

[15] K. E. Carlson, R. A. Riemke, S. Z. Rouhani, R. W. Shumway, and W. L. Weaver. *RELAP5/MOD3 Code Manual Volume I: Code Structure, System Models and Solutions Methods*. INEL Report, NUREG/CR-5535 (EGG-2596). 1990.

[16] C. E. Castro and E. F. Toro. "A Riemann Solver and Upwind Methods for a Two-Phase Flow Model in Non-Conservative Form". *Int. J. Numer. Meth. Fluids* 50.3 (2006), pp. 275–307.

[17] M. J. Castro, P. G. LeFloch, M. L. Muñoz Ruiz, and C. Parés. "Why Many Theories of Shock Waves are Necessary: Convergence Error in Formally Path-Consistent Schemes". *J. Comput. Phys.* 227.17 (2008), pp. 8107–8129.

[18] J. Cheng and C.-W. Shu. "Positivity-Preserving Lagrangian Scheme for Multi-Material Compressible Flow". *J. Comput. Phys.* 257.A (2014), pp. 143–168.

[19] A. Chertock, S. Cui, A. Kurganov, and T. Wu. "Well-Balanced Positivity Preserving Central-Upwind Scheme for Shallow Water System with Friction Term". *Int. J. Numer. Meth. Fluids* 78.6 (2015), pp. 355–383.

[20] L. Corrias, M. Falcone, and R. Natalini. “On a Class of Large Time-Step Schemes for Conservation Laws”. In: *Nonlinear Hyperbolic Problems: Theoretical, Applied, and Computational Aspects: Proceedings of the Fourth International Conference on Hyperbolic Problems*. Ed. by A. Donato and F. Oliveri. Notes on Numerical Fluid Mechanics. Taormina, Italy: Vieweg+Teubner Verlag, 1993, pp. 159–170.

[21] L. Corrias, M. Falcone, and R. Natalini. “Numerical Schemes for Conservation Laws via Hamilton-Jacobi Equations”. *Math. Comp.* 64.210 (1995), pp. 555–580.

[22] J. Cortes. “On the Construction of Upwind Schemes for Non-Equilibrium Transient Two-Phase Flows”. *Comput. Fluids* 31.2 (2002), pp. 159–182.

[23] J. Cortes, A. Debussche, and I. Toumi. “A Density Perturbation Method to Study the Eigenstructure of Two-Phase Flow Equation Systems”. *J. Comput. Phys.* 147.2 (1998), pp. 463–484.

[24] C. M. Dafermos. *Hyperbolic Conservation Laws in Continuum Physics*. 3rd ed. Vol. 325. Grundlehren der mathematischen Wissenschaften. Springer-Verlag Berlin Heidelberg, 2010.

[25] G. Dal Maso, P. G. LeFloch, and F. Murat. “Definition and Weak Stability of Nonconservative Products”. *J. Math. Pures Appl.* 74.6 (1995), pp. 483–548.

[26] T. J. Danielson, K. M. Bansal, B. Djoric, E.-D. Duret, S. Johansen, and Ø. Hellan. “Testing and Qualification of a New Multiphase Flow Simulator”. In: *Offshore Technology Conference, Houston, Texas, USA, 2–5 May*. 2011.

[27] F. Daude and P. Galon. “On the Computation of the Baer–Nunziato Model Using ALE Formulation with HLL- and HLLC-type Solvers Towards Fluid–Structure Interactions”. *J. Comput. Phys.* 304 (2016), pp. 189–230.

[28] F. Daude, P. Galon, Z. Gao, and E. Blaud. “Numerical Experiments Using a HLLC-type Scheme With ALE Formulation for Compressible Two-Phase Flows Five-Equation Models With Phase Transition”. *Comput. Fluids* 94 (2014), pp. 112–138.

[29] S. F. Davis. “Simplified Second-Order Godunov-Type Methods”. *SIAM J. Sci. Stat. Comput.* 9.3 (1988), pp. 445–473.

[30] F. De Vuyst. “Stable and Accurate Hybrid Finite Volume Methods Based on Pure Convexity Arguments for Hyperbolic Systems of Conservation Law”. *J. Comput. Phys.* 193.2 (2004), pp. 426–468.

[31] D. A. Drew and S. L. Passman. *Theory of Multicomponent Fluids*. Vol. 135. Applied Mathematical Sciences. Springer, New York, NY, 1999.

[32] M. Dumbser, A. Hidalgo, M. Castro, C. Parés, and E. F. Toro. “FORCE Schemes on Unstructured Meshes II: Non-Conservative Hyperbolic Systems”. *Comput. Meth. Appl. Mech. Eng.* 199.9–12 (2010), pp. 625–647.

[33] B. Einfeldt. “On Godunov-Type Methods for Gas Dynamics”. *SIAM J. Numer. Anal.* 25.2 (1988), pp. 294–318.

[34] B. Einfeldt, C.-D. Munz, P. L. Roe, and B. Sjögreen. “On Godunov-Type Methods near Low Densities”. *J. Comput. Phys.* 92.2 (1991), pp. 273–295.

[35] R. C. Elliot and Chaudhry M. H. “A Wave Propagation Model for Two-Dimensional Dam-Break Flows”. *J. Hydraul. Res.* 30.4 (1992), pp. 467–483.

[36] B. Engquist and S. Osher. “One-Sided Difference Approximations for Nonlinear Conservation Laws”. *Math. Comp.* 36.154 (1981), pp. 321–351.

[37] S. Evje and T. Flåtten. “Hybrid Flux-Splitting Schemes for a Common Two-Fluid Model”. *J. Comput. Phys.* 192.1 (2003), pp. 175–210.

[38] K. K. Fjelde and K. H. Karlsen. “High-Resolution Hybrid Primitive–Conservative Upwind Schemes for the Drift Flux Model”. *Comput. Fluids* 31.3 (2002), pp. 335–367.

[39] T. Flåtten and A. Morin. “On Interface Transfer Terms in Two-Fluid Models”. *Int. J. Multiph. Flow* 45 (2012), pp. 24–29.

[40] G. Gallice. “Positive and Entropy Stable Godunov-type Schemes for Gas Dynamics and MHD Equations in Lagrangian or Eulerian Coordinates”. *Numer. Math.* 94.4 (2003), pp. 673–713.

[41] P. García-Navarro and A. Priestley. “A Conservative and Shape-Preserving Semi-Lagrangian Method for the Solution of the Shallow Water Equations”. *Int. J. Numer. Meth. Fluids* 18.3 (1994), pp. 273–294.

[42] E. Godlewski and P.-A. Raviart. *Numerical Approximation of Hyperbolic Systems of Conservation Laws*. 2nd ed. Vol. 118. Applied Mathematical Sciences. Springer New York, 1996.

[43] S. K. Godunov. "A Finite Difference For Numerical Calculation of Discontinuous Solutions of the Equations of Hydrodynamics". *Mat. Sb.* 89.3 (1959). (In Russian), pp. 271–306.

[44] D. E. Goldberg and E. Benjamin Wylie. "Characteristics Method Using Time-Line Interpolations". *J. Hydraul. Eng.* 109.5 (1983), pp. 670–683.

[45] J. A. Greenberg and W. J. Rider. "A Quantitative Comparison of Numerical Methods for the Compressible Euler Equations: Fifth-Order WENO and Piecewise-Linear Godunov". *J. Comput. Phys.* 196.1 (2004), pp. 259–281.

[46] J. Gressier, P. Villedieu, and Moschetta J.-M. "Positivity of Flux Vector Splitting Schemes". *J. Comput. Phys.* 155.1 (1999), pp. 199–220.

[47] D. F. Griffiths and J. M. Sanz-Serna. "On the Scope of the Method of Modified Equations". *SIAM J. Sci. Stat. Comput.* 7.3 (1986), pp. 994–1008.

[48] V. Guinot. "An Unconditionally Stable, Explicit Godunov Scheme for Systems of Conservation Laws". *Int. J. Numer. Meth. Fluids* 38.6 (2002), pp. 567–588.

[49] V. Guinot. "The Time-Line Interpolation Method for Large-Time-Step Godunov-Type Schemes". *J. Comput. Phys.* 177.2 (2002), pp. 394–417.

[50] A. Harten. "High Resolution Schemes for Hyperbolic Conservation Laws". *J. Comput. Phys.* 49.3 (1983), pp. 357–393.

[51] A. Harten. "On a Large Time–Step High Resolution Scheme". *Math. Comp.* 46.174 (1986), pp. 379–399.

[52] A. Harten and J. M. Hyman. "Self Adjusting Grid Methods for One-Dimensional Hyperbolic Conservation Laws". *J. Comput. Phys.* 50.2 (1983), pp. 235–269.

[53] A. Harten, P. D. Lax, and B. van Leer. "On Upstream Differencing and Godunov-Type Schemes for Hyperbolic Conservation Laws". *SIAM Rev.* 25.1 (1983), pp. 35–61.

[54] A. Harten, J. M. Hyman, Lax. P. D., and B. Keyfitz. “On Finite-Difference Approximations and Entropy Conditions for Shocks”. *Comm. Pure and Appl. Math.* 29.3 (1976), pp. 297–322.

[55] C. Helzel and G. Warnecke. “Unconditionally Stable Explicit Schemes for the Approximation of Conservation Laws”. In: *Ergodic Theory, Analysis, and Efficient Simulation of Dynamical Systems*. Ed. by B. Fiedler. Berlin, Heidelberg: Springer Berlin Heidelberg, 2001, pp. 775–804.

[56] H. Holden, L. Holden, and R. Høegh-Krohn. “A Numerical Method for First Order Nonlinear Scalar Conservation Laws in One-Dimension”. *Comput. Math. Appl.* 15.6–8 (1988), pp. 595–602.

[57] H. Holden, L. Knut-Andreas, and N. H. Risebro. “An Unconditionally Stable Method for the Euler Equations”. *J. Comput. Phys.* 150.1 (1999), pp. 76–96.

[58] H. Holden and N. H. Risebro. “A Method of Fractional Steps for Scalar Conservation Laws Without the CFL Condition”. *Math. Comp.* 60.201 (1993), pp. 221–232.

[59] V. Honkkila and P. Janhunen. “HLLC Solver for Ideal Relativistic MHD”. *J. Comput. Phys.* 223.2 (2007), pp. 643–656.

[60] T. Y. Hou and P. G. LeFloch. “Why Nonconservative Schemes Converge to Wrong Solutions: Error Analysis”. *Math. Comp.* 62.206 (1994), pp. 497–530.

[61] X. Y. Hu, N. A. Adams, and C.-W. Shu. “Positivity-Preserving Method for High-Order Conservative Schemes Solving Compressible Euler Equations”. *J. Comput. Phys.* 242 (2013), pp. 169–180.

[62] J. Huang, J. Wang, and G. Warnecke. “Error Bounds for the Large Time Step Glimm Scheme Applied to Scalar Conservation Laws”. *Numer. Math.* 91.1 (2002), pp. 13–34.

[63] M. Hussain, I. Haq, and N. Fatima. “Efficient and Accurate Scheme for Hyperbolic Conservation Laws”. *Int. J. Math. Model. Meth. Appl. Sci.* 9.504–511 (2015), pp. 504–511.

[64] M. Ishii and T. Hibiki. *Thermo-Fluid Dynamics of Two-Phase Flow*. 2nd ed. Springer-Verlag New York, 2011.

[65] A. Jameson and P. D. Lax. “Conditions for the Construction of Multi-Point Total Variationl Diminishing Difference Schemes”. *Appl. Numer. Math.* 2.3–5 (1986), pp. 335–345.

[66] A. Jameson and P. D. Lax. “Corrigendum: ”Conditions for the Construction of Multi-Point Total Variation Diminishing Difference Schemes””. *Appl. Numer. Math.* 3.3 (1987), p. 289.

[67] P. Janhunen. “A Positive Conservative Method for Magnetohydrodynamics Based on HLL and Roe Methods”. *J. Comput. Phys.* 160.2 (2000), pp. 649–661.

[68] R. Klein. “Semi-Implicit Extension of a Godunov-type Scheme Based on Low Mach Number Asymptotics I: One-Dimensional Flow”. *J. Comput. Phys.* 121.2 (1995), pp. 213–237.

[69] C. Klingenberg, W. Schmidt, and K. Waagan. “Numerical Comparison of Riemann Solvers for Astrophysical Hydrodynamics”. *J. Comput. Phys.* 227.1 (2007), pp. 12–35.

[70] S. N. Kružkov. “First Order Quasilinear Equations in Several Independent Variables”. *Math. USSR Sb.* 10.2 (1970), pp. 217–243.

[71] A. Kurganov and G. Petrova. “A Second-Order Well-Balanced Positivity Preserving Central-Upwind Scheme for the Saint-Venant System”. *Commun. Math. Sci.* 5.1 (2007), pp. 133–160.

[72] M. Larsen, E. Hustvedt, P. Hedne, and T. Straume. “PeTra: A Novel Computer Code for Simulation of Slug Flow”. In: *SPE Annual Technical Conference and Exhibition, SPE 38851*. Society of Petroleum Engineers, 1997.

[73] P. Lax. *Hyperbolic Systems of Conservation Laws and the Mathematical Theory of Shock Waves*. Society for Industrial and Applied Mathematics, 1972.

[74] P. Lax and B. Wendroff. “Systems of Conservation Laws”. *Comm. Pure and Appl. Math.* 13.2 (1960), pp. 217–237.

[75] M. Lentine, J. T. Grétarsson, and R. Fedkiw. “An Unconditionally Stable Fully Conservative Semi-Lagrangian Method”. *J. Comput. Phys.* 230.8 (2011), pp. 2857–2879.

[76] B. P. Leonard. “Note on the von Neumann Stability of Explicit One-Dimensional Advection Schemes”. *Comput. Methods Appl. Mech. Engrg.* 118.1–2 (1994), pp. 29–46.

[77] B. P. Leonard, A. P. Lock, and M. K. MacVean. “The NIRVANA Scheme Applied to One-Dimensional Advection”. *Int. J. Num. Meth. Heat Fluid Flow* 5.4 (1995), pp. 341–377.

[78] B. P. Leonard, A. P. Lock, and M. K. MacVean. “Conservative Explicit Unrestricted-Time-Step Multidimensional Constancy-Preserving Advection Schemes”. *Mon. Weather Rev.* 124.11 (1996), pp. 2588–2606.

[79] R. J. LeVeque. “Large Time Step Shock-Capturing Techniques for Scalar Conservation Laws”. *SIAM J. Numer. Anal.* 19.6 (1982), pp. 1091–1109.

[80] R. J. LeVeque. “Convergence of a Large Time Step Generalization of Godunov’s Method for Conservation Laws”. *Comm. Pure Appl. Math.* 37.4 (1984), pp. 463–477.

[81] R. J. LeVeque. “A Large Time Step Generalization of Godunov’s Method for Systems of Conservation Laws”. *SIAM J. Numer. Anal.* 22.6 (1985), pp. 1051–1073.

[82] R. J. LeVeque. “High Resolution Finite Volume Methods on Arbitrary Grids via Wave Propagation”. *J. Comput. Phys.* 78.1 (1988), pp. 36–63.

[83] R. J. LeVeque. *Numerical Methods for Conservation Laws*. 2nd ed. Lectures in Mathematics. ETH Zürich. Birkhäuser Basel, 1992.

[84] R. J. LeVeque. *Finite Volume Methods for Hyperbolic Problems*. 1st ed. Cambridge Texts in Applied Mathematics (Book 31). Cambridge University Press, 2002.

[85] R. J. LeVeque and M. Pelanti. “A Class of Approximate Riemann Solvers and Their Relation to Relaxation Schemes”. *J. Comput. Phys.* 172.2 (2001), pp. 572–591.

[86] R. J. LeVeque and K.-M. Shyue. “One-Dimensional Front Tracking Based on High Resolution Wave Propagation Methods”. *SIAM J. Sci. Comput.* 16.2 (1995), pp. 348–377.

[87] P. Li, W.-S. Don, C. Wang, and Z. Gao. “High Order Positivity- and Bound-Preserving Hybrid Compact-WENO Finite Difference Scheme for the Compressible Euler Equations”. *J. Sci. Comput.* (2017), pp. 1–27.

[88] S. Li. “An HLLC Riemann Solver for Magneto-Hydrodynamics”. *J. Comput. Phys.* 230.1 (2005), pp. 344–357.

[89] T. Linde. “A Practical, General-Purpose, Two-state HLL Riemann Solver for Hyperbolic Conservation Laws”. *Int. J. Numer. Meth. Fluids* 40.3–4 (2002), pp. 391–402.

[90] S. Lindqvist and H. Lund. "A Large Time Step Roe Scheme Applied to Two-Phase Flow". In: *VII European Congress on Computational Methods in Applied Sciences and Engineering*. Ed. by M. Papadrakakis, V. Papadopoulos, G. Stefanou, and V. Plevris. ECCOMAS. Crete Island, Greece, 2016.

[91] S. Lindqvist, P. Aursand, T. Flåtten, and A. A. Solberg. "Large Time Step TVD Schemes for Hyperbolic Conservation Laws". *SIAM J. Numer. Anal.* 54.5 (2016), pp. 2775–2798.

[92] H. Lochon, F. Daude, P. Galon, and J.-M Hérard. "HLLC-type Riemann Solver with Approximated Two-Phase Contact for the Computation of the Baer–Nunziato Two-Fluid Model". *J. Comput. Phys.* 326 (2016), pp. 733–762.

[93] B. J. Lucier. "Error Bounds for the Methods of Glimm, Godunov and LeVeque". *SIAM J. Numer. Anal.* 22.6 (1985), pp. 1074–1081.

[94] H. Lund. "Relaxation Models for Two-Phase Flow With Applications to CO_2 Transport". PhD thesis. Norwegian University of Science and Technology, 2013.

[95] N. N. Makwana and A. Chatterjee. "Fast Solution of Time Domain Maxwell's Equations Using Large Time Steps". In: *2015 IEEE International Conference on Computational Electromagnetics (ICCEM 2015)*. Hong Kong, China: Institute of Electrical and Electronics Engineers (IEEE), 2015, pp. 330–332.

[96] E. A. Meese and S. T. Johansen. "A Simulation Concept for Generic Simulation of Multi-Material Flow Using Staggered Cartesian Grids". In: *Progress in Applied CFD – CFD2017*. Ed. by J. E. Olsen and S. T. Johansen. Trondheim, Norway: SINTEF Academic Press, 2017, pp. 253–263.

[97] A. Mignone and G. Bodo. "An HLLC Riemann Solver for Relativistic Flows – II. Magnetohydrodynamics". *Mon. Not. R. Astron. Soc* 368.3 (2006), pp. 1040–1054.

[98] T. Miyoshi and K. Kusano. "A Multi-State HLL Approximate Riemann Solver for Ideal Magnetohydrodynamics". *J. Comput. Phys.* 208.1 (2005), pp. 315–344.

[99] M. Morales-Hernández, P. García-Navarro, and J. Murillo. "A Large Time Step 1D Upwind Explicit Scheme (CFL>1): Application to Shallow Water Equations". *J. Comput. Phys.* 231.19 (2012), pp. 6532–6557.

[100] M. Morales-Hernández, M. E. Hubbard, and P. García-Navarro. "A 2D Extension of a Large Time Step Explicit Scheme (CFL>1) for Unsteady Problems with Wet/Dry Boundaries". *J. Comput. Phys.* 263 (2014), pp. 303–327.

[101] M. Morales-Hernández, J. Murillo, P. García-Navarro, and J. Burguete. "A Large Time Step Upwind Scheme for the Shallow Water Equations With Source Terms". In: *Numerical Methods for Hyperbolic Equations*. Ed. by Elena Vázquez Cendón, Arthuro Hidalgo, P. García-Navarro, and Luis Cea. CRC Press, 2012, pp. 141–148.

[102] M. Morales-Hernández, A. Lacasta, J. Murillo, and P. García-Navarro. "A Large Time Step Explicit Scheme (CFL>1) on Unstructured Grids for 2D Conservation Laws: Application to the Homogeneous Shallow Water Equations". *Appl. Math. Model.* 47 (2017), pp. 294–317.

[103] S. T. Munkejord. "Comparison of Roe-type Methods for Solving the Two-Fluid Model with and Without Pressure Relaxation". *Comput. Fluids* 36.6 (2007), pp. 1061–1080.

[104] S. T. Munkejord, S. Evje, and T. Flåtten. "A MUSTA Scheme for a Nonconservative Two-Fluid Model". *SIAM. J. Sci. Comput.* 31.4 (2009), pp. 2587–2622.

[105] J. Murillo, P. García-Navarro, P. Brufau, and J. Burguete. "Extension of an Explicit Finite Volume Method to Large Time Steps (CFL>1): Application to Shallow Water Flows". *Int. J. Numer. Meth. Fluids* 50.1 (2006), pp. 63–102.

[106] A. Murrone and H. Guillard. "A Five Equation Reduced Model for Compressible Two Phase Flow Problems". *J. Comput. Phys.* 202.2 (2005), pp. 664–698.

[107] M. R. Norman, D. R. Nair, and F. H. M. Semazzi. "A Low Communication and Large Time Step Explicit Finite-Volume Solver for Non-Hydrostatic Atmospheric Dynamics". *J. Comput. Phys.* 230.4 (2011), pp. 1567–1584.

[108] R. Nygaard. “Large Time Step Methods for Hyperbolic Partial Differential Equations”. MA thesis. Norwegian University of Science and Technology: Dept. of Energy and Process Engineering, 2017. URL: http://hdl.handle.net/11250/2454922.

[109] O. A. Oleinik. “Discontinuous Solutions of Non-Linear Differential Equations”. *Amer. Math. Soc. Transl. Ser. 2* 26 (1957), pp. 95–172.

[110] S. Osher. “Riemann Solvers, the Entropy Condition, and Difference Approximations”. *SIAM J. Numer. Anal.* 21.2 (1984), pp. 217–235.

[111] C. Parés. “Numerical Methods for Nonconservative Hyperbolic Systems: a Theoretical Framework”. *SIAM J. Numer. Anal.* 44.1 (2006), pp. 300–321.

[112] S. H. Park and J. H. Kwon. “On the Dissipation Mechanism of Godunov-type Schemes”. *J. Comput. Phys.* 188.2 (2003), pp. 524–542.

[113] C. L. Pauchon and H. Dhulesia. “TACITE: A Transient Tool for Multiphase Pipeline and Well Simulation”. In: *SPE Annual Technical Conference and Exhibition, 25-28 September, New Orleans, Louisiana*. 1994.

[114] M. Pelanti, L. Quartapelle, and L. Vigevano. *A Review of Entropy Fixes as Applied to Roes Linearization*. Teaching material of the Aerospace and Aeronautics Department of Politecnico di Milano. 2001. URL: http://services.aero.polimi.it/~quartape/bacheca/materiale_didattico/ef_JCP.pdf.

[115] M. Pelanti and K.-M. Shyue. “A Mixture-Energy-Consistent Six-Equation Two-Phase Numerical Model for Fluids with Interfaces, Cavitation and Evaporation Waves”. *J. Comput. Phys.* 259 (2014), pp. 331–357.

[116] B. Perthame and C.-W. Shu. “On Positivity Preserving Finite Volume Schemes For Euler Equations”. *Numer. Math.* 73.1 (1996), pp. 119–130.

[117] Z. Qian and C.-H. Lee. “A Class of Large Time Step Godunov Schemes for Hyperbolic Conservation Laws and Applications”. *J. Comput. Phys.* 230.19 (2011), pp. 7418–7440.

[118] Z. Qian and C.-H. Lee. “On Large Time Step TVD Scheme for Hyperbolic Conservation Laws and Its Efficiency Evaluation”. *J. Comput. Phys.* 231.21 (2012), pp. 7415–7430.

[119] J.-M. Qiu and C.-W. Shu. “Convergence of Godunov-type Schemes for Scalar Conservation Laws under Large Time Steps”. *SIAM J. Numer. Anal.* 46.5 (2008), pp. 2211–2237.

[120] P. Roe. “Approximate Riemann Solvers, Parameter Vectors, and Difference Schemes”. *J. Comput. Phys.* 43.2 (1981), pp. 357–372.

[121] H. Shirkhani, A. Mohammadian, O. Seidou, and A. Kurganov. “A Well-Balanced Positivity-Preserving Central-Upwind Scheme for Shallow Water Equations on Unstructured Quadrilateral Grids”. *Comput. Fluids* 121 (2016), pp. 25–40.

[122] C.-W. Shu. “High Order ENO and WENO Schemes for Computational Fluid Dynamics”. In: *High-Order Methods for Computational Physics*. Ed. by T. J. Barth and H. Deconinck. Berlin, Heidelberg: Springer Berlin Heidelberg, 1999, pp. 439–582.

[123] N. F. Siddiqui, M. Hussain, and M. M. Baig. “To Study Large Time Step High Resolution Low Dissipative Schemes for Hyperbolic Conservation Laws”. *J. Appl. Fluid. Mech.* 9.4 (2016), pp. 2073–2081.

[124] A. A. Solberg. “Large Time Step Explicit Schemes for Partial Differential Evolution Equations”. MA thesis. Norwegian University of Science and Technology: Dept. of Energy and Process Engineering, 2016. URL: `http://hdl.handle.net/11250/2409951`.

[125] H. Städtke. *Gasdynamic Aspects of Two-Phase Flow*. 1st ed. Wiley-VCH Verlag GmbH & Co. KGaA, 2006.

[126] A. Staniforth and J. Côté. “Semi-Lagrangian Integration Schemes for Atmospheric Models—A Review”. *Mon. Weather Rev.* 119.9 (1991), pp. 2206–2223.

[127] E. Tadmor. “Numerical Viscosity and the Entropy Condition for Conservative Difference Schemes”. *Math. Comp* 43.168 (1984), pp. 369–381.

[128] E. Tadmor. “The Large-Time Behavior of the Scalar, Genuinely Nonlinear Lax-Friedrichs Scheme”. *Math. Comp* 43.168 (1984), pp. 353–368.

[129] E. Tadmor. “A Minimum Entropy Principle in the Gas Dynamics Equations”. *Appl. Numer. Math.* 2.3–5 (1986), pp. 211–219.

[130] E. Tadmor. “Entropy Functions for Symmetric Systems of Conservation Laws”. *J. Math. Anal. Appl.* 122.2 (1987), pp. 355–359.

[131] E. Tadmor. “Entropy Stability Theory for Difference Approximations of Nonlinear Conservation Laws and Related Time-Dependent Problems”. *Acta Numerica* 12 (2003), pp. 451–512.

[132] E. Tadmor. “Entropy Stable Schemes”. In: *Handbook of Numerical Methods for Hyperbolic Problems*. Ed. by R. Abgrall and C.-W. Shu. Handbook of Numerical Analysis. North Holland, 2016. Chap. 18, pp. 467–493.

[133] H. Tang and G. Warnecke. “A Note on (2K+1)-point Conservative Monotone Schemes”. *ESAIM Math. Model. Numer. Anal.* 38.2 (2004), pp. 345–357.

[134] K. Tang, A. Beccantini, and C. Corre. “Combining Discrete Equations Method and Upwind Downwind-Controlled Splitting for Non-Reacting and Reacting Two-Fluid Computations: One Dimensional Case”. *Comput. Fluids* 93 (2014), pp. 74–90.

[135] R.J. Thompson and T. Moeller. “A Discontinuous Wave-in-Cell Numerical Scheme for Hyperbolic Conservation Laws”. *J. Comput. Phys.* 299 (2015), pp. 404–428.

[136] B. Tian, E. F. Toro, and C. E. Castro. “A Path-Conservative Method for a Five-Equation Model of Two-Phase Flow with an HLLC-type Riemann Solver”. *Comput. Fluids* 46.1 (2011), pp. 122–132.

[137] S. A. Tokareva and E. F. Toro. “HLLC-type Riemann Solver for Baer–Nunziato Equations of Compressible Two-Phase Flow”. *J. Comput. Phys.* 229.10 (2010), pp. 3573–3604.

[138] E. F. Toro. *Riemann Solvers and Numerical Methods for Fluid Dynamics*. 3rd ed. Springer-Verlag Berlin Heidelberg, 2009.

[139] E. F. Toro, M. Spruce, and W. Speares. “Restoration of the Contact Surface in the HLL-Riemann Solver”. *Shock Waves* 4.1 (1994), pp. 25–34.

[140] I. Toumi. “A Weak Formulation of Roe’s Approximate Riemann Solver”. *J. Comput. Phys.* 102.2 (1992), pp. 360–373.

[141] I. Toumi and A. Kumbaro. “An Approximate Linearized Riemann Solver for a Two-Fluid Model”. *J. Comput. Phys.* 124.2 (1996), pp. 286–300.

[142] J. A. Trangenstein. *Numerical Solution of Hyperbolic Partial Differential Equations*. Cambridge University Press, 2009.

[143] A. I. Vol'pert. "The Spaces BV and Quasilinear Equations". *Math. Sb.* 73(115).2 (1967). In Russian, pp. 255–302.

[144] J. Wang and G. Warnecke. "On Entropy Consistency of Large Time Step Schemes I. The Godunov and Glimm Schemes". *SIAM J. Numer. Anal.* 30.5 (1993), pp. 1229–1251.

[145] J. Wang and G. Warnecke. "On Entropy Consistency of Large Time Step Schemes II. Approximate Riemann Solvers". *SIAM J. Numer. Anal.* 30.5 (1993), pp. 1252–1267.

[146] J. Wang, H. Wen, and T. Zhou. "On Large Time Step Godunov Scheme for Hyperbolic Conservation Laws". *Comm. Math. Sci.* 2.3 (2004), pp. 477–495.

[147] Y. Xing, X. Zhang, and C.-W. Shu. "Positivity-Preserving High Order Well-Balanced Discontinuous Galerkin Methods for the Shallow Water Equations". *Adv. Water Resour.* 33.12 (2010), pp. 1476–1493.

[148] R. Xu, D. Zhong, B. Wu, X. Fu, and R. Miao. "A Large Time Step Godunov Scheme for Free-Surface Shallow Water Equations". *Chinese Sci. Bull.* 59.21 (2014), pp. 2534–2540.

[149] G.-S. Yeom and K.-S. Chang. "Two-Dimensional Two-Fluid Two-Phase Flow Simulation Using an Approximate Jacobian Matrix for HLL Scheme". *Numer. Heat Tran. B* 56.5 (2010), pp. 372–392.

[150] X. Zhang and C.-W. Shu. "On Positivity-Preserving High Order Discontinuous Galerkin Schemes for Compressible Euler Equations on Rectangular Meshes". *J. Comput. Phys.* 229.23 (2010), pp. 8918–8934.

[151] X. Zhang and C.-W. Shu. "Maximum-Principle-Satisfying and Positivity-Preserving High-Order Schemes for Conservation Laws: Survey and New Developments". *Proc. Math. Phys. Eng. Sci.* 467.2134 (2011), pp. 2752–2776.

[152] X. Zhang and C.-W. Shu. "Positivity-Preserving High Order Finite Difference WENO Schemes for Compressible Euler Equations". *J. Comput. Phys.* 231.5 (2012), pp. 2245–2258.

Copying extensively from one source is plagiarism; copying extensively from several is research.

Anonymous

A
Research papers

My publications

[P1] M. Prebeg. "Numerical Viscosity in Large Time Step HLL-type Schemes". In: *Proceedings of the Sixteenth International Conference on Hyperbolic Problems, HYP2016*. Ed. by C. Klingenberg and M. Westdickenberg. Accepted for publication. Aachen, Germany, 2017.

[P2] M. Prebeg, T. Flåtten, and B. Müller. "Large Time Step HLL and HLLC schemes" (2017). Submitted.

[P3] M. Prebeg, T. Flåtten, and B. Müller. "Large Time Step Roe Scheme for a Common 1D Two-Fluid Model". *Appl. Math. Model.* 44 (2017), pp. 124–142.

[P4] M. Prebeg, T. Flåtten, and B. Müller. "Monotonicity and Positivity Preservation in Large Time Step Methods" (2017). Preprint.

[P5] M. Prebeg, T. Flåtten, and B. Müller. "Boundary and Source Term Treatment in the Large Time Step Method for a Common Two-Fluid Model". In: *Proceedings of the 11th International Conference on CFD in the Minerals and Process Industries*. Ed. by C. B. Solnordal, P. Liovic, G. W. Delaney, S. J. Cummins, M. P. Schwarz, and P. J. Witt. Melbourne, Australia, 2015.

My contributions to manuscripts:

All manuscripts were written by me. Flåtten proposed the *Steady-state boundary conditions* (SSBC) used in papers [P5, P3], and determined the flux-difference splitting coefficients of the LTS-HLL scheme [P2, Proposition 2], and TVD conditions for the LTS-HLL scheme [P2, Proposition 5]. Flåtten contributed to all articles by discussing the manuscripts and reported results. Müller contributed to all articles by discussing the manuscripts and reported results.

Journal paper 1 (P3)

Large Time Step Roe scheme for a common 1D two-fluid model

Marin Prebeg, Tore Flåtten and Bernhard Müller

Applied Mathematical Modelling, Vol. 44, pp. 124–142, 2017.

Large Time Step Roe scheme for a common 1D two-fluid model

Marin Prebeg[a], Tore Flåtten[b], Bernhard Müller[a]

[a]*Department of Energy and Process Engineering, Norwegian University of Science and Technology, Kolbjørn Hejes vei 2, Trondheim, Norway*
[b]*SINTEF Materials and Chemistry, Oil and Gas Process Technology, S. P. Andersens veg 15 B, Trondheim, Norway*

Abstract

We present the Large Time Step (LTS) extension of the Roe scheme and apply it to a standard two-fluid model. Herein, LTS denotes a class of explicit methods that are not limited by the CFL (Courant–Friedrichs–Lewy) condition, allowing us to use very large time steps compared to standard explicit methods. The LTS method was originally developed in the nineteen eighties (LeVeque, 1985), where the Godunov scheme was extended to the LTS Godunov scheme. In the present work, the relaxation of the CFL condition is achieved by increasing the domain of dependence. This might lead to difficulties when it comes to boundary and source terms treatment. We address and discuss these difficulties and propose different ways to treat them. For a shock tube test case, where there are neither source terms nor difficulties associated with the boundaries, the method increases both accuracy and efficiency. For a water faucet test case that includes a source term, the method increases the efficiency, while the accuracy strongly depends on the appropriate treatment of boundary conditions and source terms.

Keywords: Large Time Step method, Roe scheme, Two-fluid model, Boundary treatment, Source term

1. Introduction

In this paper, we are interested in the numerical simulation of one dimensional two-phase flow. To that end, we use a one dimensional, equal-pressure two-fluid model studied by many authors [1, 2, 3, 4, 5, 6]. This and other similar models are in widespread use for the simulation of two-phase flow, and they have been used successfully in many applications by the oil & gas [7, 8] and nuclear industry [9]. In practical applications one usually has to make a compromise between accuracy and efficiency. The balance between these requirements is, among other things, strongly affected by the numerical time integration method, where the main division is made between explicit and implicit time integration methods. As is well known, explicit methods are associated with higher accuracy and simpler implementation, but their efficiency and stability are limited by the CFL (Courant–Friedrichs–Lewy) condition. Implicit methods are not limited by the CFL condition and may be very efficient, but they are associated with a number of different difficulties, most important being the excessive diffusion and difficult parallelization. In this paper we study a class of explicit methods that are not limited by the CFL condition, thereby allowing us to use time steps much larger than usually associated with explicit methods. Such methods are knows as the Large Time Step (LTS) methods and they have been first introduced in the nineteen eighties by LeVeque [10, 11, 12]. Therein, the Godunov scheme was extended to the LTS Godunov scheme and applied to scalar conservation laws and the Euler equations.

In his work, LeVeque treats each discontinuity as a wave and allows waves from each Riemann problem to travel more than one cell during a single time step, allowing for interaction between the waves. These interactions are assumed to be linear, i.e. the waves are passing through each other without change in speed or strength [12]. From the way LeVeque's LTS method is defined, it uses a Lagrangian point of view by tracking where the characteristics are going. Through the years, these ideas have been recognized and used by many authors. Here, we address the most recent contributions, without attempting to provide a complete and comprehensive overview.

Murillo, Morales-Hernández and co-workers [13, 14, 15, 16] applied the LTS Roe scheme to the one and two dimensional shallow water equations and focused on the treatment of source terms and boundary conditions. Xu et al. [17] applied the LTS Godunov scheme to the shallow water equations. Qian and Lee [18] applied the LTS Godunov scheme to the three dimensional Euler equations by using a dimensional splitting approach. Tang et al. [19] applied the LTS Godunov scheme to high speed combustion waves. Makwana and Chatterjee [20] applied the LTS Godunov scheme to the Maxwell's equations, and Lindqvist and Lund [21] applied the LTS Roe scheme to two-phase flow and focused on accuracy and computational efficiency. Lindqvist et al. [22] also studied more theoretical properties of the LTS methods and how they fit into the TVD setting. Therein, the LTS method of LeVeque is defined in the numerical viscosity and flux difference splitting framework, a perspective more coinciding with the Eulerian point of view. It is shown that these formulations are mathematically equivalent to the original formulation by LeVeque [12].

Herein, we use the LTS method of LeVeque in the form presented by Lindqvist et al. [22] and apply it to the one dimensional non-conservative two-fluid model. In [22], the relaxation of the CFL condition is achieved by extending the domain of dependence. This leads to difficulties when it comes to the treatment of boundary conditions and source terms. These issues are the central topic of this paper. For the homogeneous system, the LTS Roe scheme shows promising results when applied to test cases where no complex wave interactions occur at the boundaries, as will be illustrated by the numerical example of the shock tube. However, "interesting" boundaries and/or source terms require special treatment. In the present paper we will illustrate difficulties related to the boundary conditions and source terms as separate challenges, using the classical water faucet test case as an example. First, we will discuss the definition of the boundary conditions in the LTS Roe scheme. Namely, the presence of source terms may lead to a distinct pattern of numerical errors being generated in the vicinity of the boundary. We will show how boundary conditions can be modified to reduce these errors and improve the accuracy of the solution. Second, the presence of source terms in the LTS Roe scheme may lead to numerical errors being generated elsewhere in the domain as well. We will discuss how these errors are generated and show that the most simple, straightforward treatment of source terms is not well suited for the LTS method. To resolve this, we will discretize the source term by formulating a slight modification to the approach presented by Murillo and García-Navarro [23]. The separate treatment of the difficulties related to the boundary conditions and source terms will be justified in sections 4 and 5, where we will show that the numerical errors being generated in the vicinity of the boundary and elsewhere in the domain are caused by distinct but related mechanisms.

This paper is structured as follows: in section 2, we present the two-fluid model we use. In section 3, we present the numerical method and outline the standard Roe and LTS Roe schemes. Sections 4 and 5 discuss boundary and source term treatments, respectively, with corresponding numerical investigations. Section 6 discusses accuracy and computational performance, and section 7 closes with conclusions.

2. Mathematical model

We are considering a one dimensional isentropic equal-pressure two-fluid model [1, 2, 3, 4, 5, 6] without energy equation, where we solve separate evolution equations for mass and momentum of two fluids:

$$\partial_t(\alpha_g\rho_g) + \partial_x(\alpha_g\rho_g v_g) = 0, \tag{2.1}$$

$$\partial_t(\alpha_l\rho_l) + \partial_x(\alpha_l\rho_l v_l) = 0, \tag{2.2}$$

$$\partial_t(\alpha_g\rho_g v_g) + \partial_x(\rho_g\alpha_g v_g^2 + (p - p^i)\alpha_g) + \alpha_g\partial_x p^i = Q_g, \tag{2.3}$$

$$\partial_t(\alpha_l\rho_l v_l) + \partial_x(\rho_l\alpha_l v_l^2 + (p - p^i)\alpha_l) + \alpha_l\partial_x p^i = Q_l, \tag{2.4}$$

where ρ, α, v, Q are the density, volume fraction, velocity and the source term with corresponding phase indices g, l for the gas and liquid phase, respectively. The pressure p denotes a common pressure of both phases, while the pressure p^i denotes the pressure at the interface between gas and liquid.

In this basic model, several physical effects that would be present for a number of engineering applications have been neglected. For numerical studies, this practice has been followed by many authors [1, 2, 3, 4, 5, 6] and a thorough discussion of its justification can be found in the book of Städtke [24].

In this respect, we would like to emphasize that a number of practical applications would require viscous terms [25], i.e. terms involving second-order spatial derivatives, to be naturally incorporated into our framework. Such terms would typically render the model parabolic, and would be physically important for problems involving for instance thermal conduction or wax deposition. As demonstrated in [22], our numerical Large Time Step framework naturally includes numerical diffusion. This was exploited by Solberg [26] who proposed a concrete extension of the LTS framework to systems containing viscous terms.

2.1. Quasilinear form

The Eqs. (2.1)–(2.4) can be written in a quasilinear form as:

$$\partial_t\mathbf{U} + \mathbf{A}(\mathbf{U})\partial_x\mathbf{U} = \mathbf{Q}(\mathbf{U}), \tag{2.5}$$

where the vector of evolved variables $\mathbf{U}$ and the vector of source terms $\mathbf{Q}$ are defined as:

$$\mathbf{U} = \left[\rho_g\alpha_g, \rho_l\alpha_l, \rho_g\alpha_g v_g, \rho_l\alpha_l v_l\right]^{\mathrm{T}}, \tag{2.6}$$

$$\mathbf{Q}(\mathbf{U}) = \left[0, 0, Q_g, Q_l\right]^{\mathrm{T}}, \tag{2.7}$$

and the coefficient matrix $\mathbf{A}$ is defined as in [3]:

$$\mathbf{A}(\mathbf{U}) = \begin{bmatrix} 0 & 0 & 1 & 0 \\ 0 & 0 & 0 & 1 \\ \kappa\left(\rho_l\alpha_g + \Delta p\alpha_l\frac{\partial\rho_l}{\partial p}\right) - v_g^2 & \kappa\left(\rho_g\alpha_g - \Delta p\alpha_g\frac{\partial\rho_g}{\partial p}\right) & 2v_g & 0 \\ \kappa\left(\rho_l\alpha_l - \Delta p\alpha_l\frac{\partial\rho_l}{\partial p}\right) & \kappa\left(\rho_g\alpha_l + \Delta p\alpha_g\frac{\partial\rho_g}{\partial p}\right) - v_l^2 & 0 & 2v_l \end{bmatrix}, \tag{2.8}$$

where κ is defined as:

$$\kappa = \frac{1}{\frac{\partial\rho_g}{\partial p}\alpha_g\rho_l + \frac{\partial\rho_l}{\partial p}\alpha_l\rho_g}, \tag{2.9}$$

and the interface pressure term Δp is defined as:

$$\Delta p = p - p^i = \delta \frac{\alpha_g \alpha_l \rho_g \rho_l}{\rho_g \alpha_l + \rho_l \alpha_g} \left(v_g - v_l\right)^2, \tag{2.10}$$

with $\delta = 1.2$. The interface pressure term Δp ensures that the system remains hyperbolic for physically realistic states. For the cases we consider in this paper the system will always remain hyperbolic, i.e. the coefficient matrix $\mathbf{A}$ will have 4 real and distinct eigenvalues and thus linearly independent eigenvectors. Physically, these eigenvalues correspond to fast pressure waves and slow interface (volume fraction) waves. Although it is possible to derive the analytical expressions for eigenvalues and eigenvectors, these expressions are too complicated to be of practical value. Some useful approximations may be obtained through perturbation techniques [2, 3, 5]:

- *pressure waves:*

$$\lambda^{\mathrm{p}} \approx \frac{\rho_g \alpha_l v_l + \rho_l \alpha_g v_g}{\rho_g \alpha_l + \rho_l \alpha_g} \pm \sqrt{\frac{\rho_g \alpha_l + \rho_l \alpha_g}{\rho_g \alpha_l \partial_p \rho_l + \rho_l \alpha_g \partial_p \rho_g}}, \tag{2.11}$$

- *interface waves:*

$$\lambda^{\mathrm{i}} \approx \frac{\rho_g \alpha_l v_g + \rho_l \alpha_g v_l}{\rho_g \alpha_l + \rho_l \alpha_g} \pm \frac{\sqrt{\Delta p(\rho_g \alpha_l + \rho_l \alpha_g) - \rho_g \rho_l \alpha_g \alpha_l (v_g - v_l)^2}}{\rho_g \alpha_l + \rho_l \alpha_g}. \tag{2.12}$$

These expressions may become inaccurate if the relative velocity becomes too large. In the following, we will not use the approximations (2.11) and (2.12). Instead we will calculate the eigenstructure numerically for increased accuracy.

2.2. Closure relations and thermodynamic submodel

The model is closed by a basic relation between volume fractions and by an equation of state for each phase k:

$$\alpha_g + \alpha_l = 1, \qquad \rho_k = \rho_{k,0} + \frac{p - p_{k,0}}{a_k^2}, \tag{2.13}$$

where the speed of sound a is defined as $a_k^2 = \partial p / \partial \rho_k$. The parameters are $p_{l,0} = 10^5$ Pa, $p_{g,0} = 0$, $\rho_{l,0} = 1000$ kg/m^3, $\rho_{g,0} = 0$, $a_l = 10^3$ m/s and $a_g = \sqrt{10^5}$ m/s. The assumption of equal phase pressures, $p_g = p_l = p$, allows us to write (2.13) in terms of conserved variables:

$$\frac{u_1}{\rho_g(p)} + \frac{u_2}{\rho_l(p)} = 1 \qquad \rightarrow \qquad p = p(u_1, u_2), \tag{2.14}$$

where $u_1 = \rho_g \alpha_g$ and $u_2 = \rho_l \alpha_l$ are elements of the vector of evolved variables $\mathbf{U}$, Eq. (2.6). For details on closure relations and interface pressure modeling we refer to the papers [3, 27].

3. Numerical model

We start by discretizing the homogeneous version of (2.5) by the explicit Euler method in time and a Roe scheme in space:

$$\mathbf{U}_j^{n+1} = \mathbf{U}_j^n - \frac{\Delta t}{\Delta x} \left(\hat{\mathbf{A}}^+_{j-1/2} \Delta \mathbf{U}^n_{j-1/2} + \hat{\mathbf{A}}^-_{j+1/2} \Delta \mathbf{U}^n_{j+1/2} \right), \tag{3.1}$$

where $\mathbf{U}_j^n$ is a discrete approximation of the cell average of $\mathbf{U}$ in the cell with center at x_j and at the time level n, and $\hat{\mathbf{A}}^{\pm}_{j\mp1/2}\Delta\mathbf{U}_{j\mp1/2}$ are flux differences at the cell interfaces $x_{j\mp1/2}$, where we introduce $\Delta\mathbf{U}_{j+1/2} = \mathbf{U}_{j+1} - \mathbf{U}_j$. For more convenient notation, here and throughout the paper, we assume that the absence of a time index implies the time level n.

Herein, the fundamental component is the construction of a Roe matrix $\hat{\mathbf{A}}$, originally proposed for the Euler equations [28]. We are discussing the non-conservative system modeling two-phase flow and we construct the Roe matrix $\hat{\mathbf{A}}$ following the approach found in [5, 3]. Once the Roe matrix $\hat{\mathbf{A}}$ is defined, the positive and negative parts of $\hat{\mathbf{A}}$ are defined through its eigenvalues:

$$\hat{\mathbf{A}}^{\pm} = \hat{\mathbf{R}}\hat{\mathbf{\Lambda}}^{\pm}\hat{\mathbf{R}}^{-1}, \tag{3.2}$$

where $\hat{\mathbf{R}}$ is the matrix of right eigenvectors and $\hat{\mathbf{\Lambda}}$ is the diagonal matrix of eigenvalues with the eigenvalues defined as:

$$\lambda^+ = \max(0, \lambda), \qquad \lambda^- = \min(0, \lambda). \tag{3.3}$$

A known limitation of this scheme is that the time step must satisfy the constraint $C \leq 1$, where C is the Courant number:

$$C = \max_j |\lambda_j| \frac{\Delta t}{\Delta x}. \tag{3.4}$$

In the following, we will describe an extension of the Roe scheme that is not limited by this condition.

3.1. Large Time Step Roe scheme

To extend the standard Roe scheme to the LTS Roe scheme we use the ideas developed by LeVeque [12] and approach used by Lindqvist et al. [22]. We start by recalling that the standard Roe scheme is a three-point scheme:

$$\mathbf{U}_j^{n+1} = \mathbf{U}\left(\mathbf{U}_{j-1}^n, \mathbf{U}_j^n, \mathbf{U}_{j+1}^n\right). \tag{3.5}$$

In the standard Roe scheme this property is ensured by the CFL condition (3.4), which requires that no wave can travel more than one cell during a single time step. As a consequence, the $\mathbf{U}_j^{n+1}$ in the (3.1) is updated only by the flux differences at the cell interfaces $x_{j-1/2}$ and $x_{j+1/2}$, see Figure 1. However, if we increase the time step Δt, the particular wave may travel more than one cell during a single time step. To take this into the account we increase the domain of dependence. Therefore, the value in a particular cell may depend on more than three cells:

$$\mathbf{U}_j^{n+1} = \mathbf{U}\left(..., \mathbf{U}_{j-2}^n, \mathbf{U}_{j-1}^n, \mathbf{U}_j^n, \mathbf{U}_{j+1}^n, \mathbf{U}_{j+2}^n, ...\right), \tag{3.6}$$

where the particular size of the domain of dependence depends on the local Courant number. Since the information from the domain of dependence with which we update cell state $\mathbf{U}_j^{n+1}$ is delivered in terms of flux differences through the cell faces, we reformulate the flux differences to include all flux differences in the domain of dependence. Hence we modify the flux differences in (3.1) to obtain the LTS extension of the Roe scheme:

$$\mathbf{U}_j^{n+1} = \mathbf{U}_j^n - \frac{\Delta t}{\Delta x}\left(\sum_{i=0}^{\infty} \hat{\mathbf{A}}^{i+}_{j-1/2-i}\Delta\mathbf{U}_{j-1/2-i} + \sum_{i=0}^{\infty} \hat{\mathbf{A}}^{i-}_{j+1/2+i}\Delta\mathbf{U}_{j+1/2+i}\right). \tag{3.7}$$

The matrices $\hat{\mathbf{A}}^{i\pm}$ are defined as:

$$\hat{\mathbf{A}}^{i\pm} = \hat{\mathbf{R}}\hat{\mathbf{\Lambda}}^{i\pm}\hat{\mathbf{R}}^{-1}, \tag{3.8}$$

with the eigenvalues defined as in [22]:

$$\lambda^{i\pm} = \pm\max\left(0, \min\left(\pm\lambda - i\frac{\Delta x}{\Delta t}, \frac{\Delta x}{\Delta t}\right)\right). \tag{3.9}$$

The superscripts $i+$ and $i-$ in (3.8) denote the parts of the Roe matrix $\hat{\mathbf{A}}$ defined by the positive $(i+)$ and the negative $(i-)$ wave speeds λ^{i+} and λ^{i-} at the cell interface located i cells to the left $(i+)$ and to the right $(i-)$ of the cell interface associated with $i = 0$, i.e. $x_{j+1/2}$. Herein, flux differences associated with $\hat{\mathbf{A}}^{i+}$ and $\hat{\mathbf{A}}^{i-}$ are traveling to the right and left, respectively.

We assume that these flux differences, i.e. the waves they describe are moving independently of each other, i.e. all the interactions between the waves are linear. Figure 1 shows the flux differences that update the cell $\mathbf{U}_j$ in the standard and LTS Roe scheme. We note that even though we allow more waves to pass through the particular interface, the different waves need to travel a different distance before they start "passing" through the relevant interface. This fact is taken into the account by the modification of the eigenvalues in (3.9). Also, we note that the infinite sums in (3.7) will only contain a finite number of nonzero terms, because the term $\lambda - i\frac{\Delta x}{\Delta t}$ becomes negative, and the term $\lambda + i\frac{\Delta x}{\Delta t}$ becomes positive in (3.9) for sufficiently large i. The reader is referred to [22] for a more extensive explanation of the LTS method.

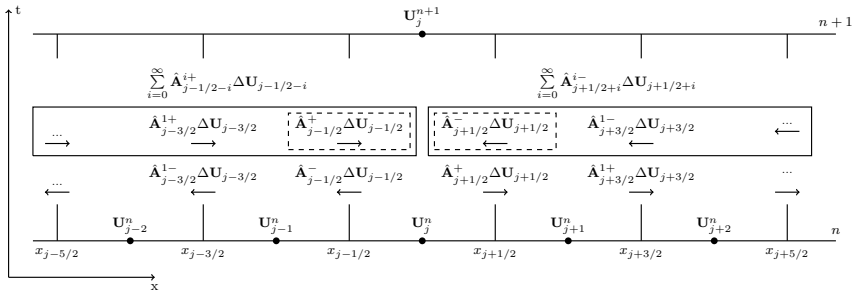

Figure 1: Updating of $\mathbf{U}_j$: domain of dependence and flux differences in standard Roe (dashed boxes) and LTS Roe scheme (full boxes)

4. Boundary conditions

We now discuss how to incorporate boundary conditions into the LTS scheme (3.7). Boundary conditions may be divided into two main categories [14]: *closed*, in which no information is allowed to cross the boundary, and *open*, in which information travels across the boundaries along the waves inherent in the equations, as described for instance in [29].

Herein, the direction of information flow is determined by the sign of the eigenvalues of the matrix $\mathbf{A}$ given by (2.8), with positive eigenvalues corresponding to flow along the positive x-direction. Hence, the number of imposed boundary conditions must correspond to the number of inflowing characteristics at the given boundary.

For the purposes of this paper, we will assume that the flow is subsonic. In that case we have at least one incoming and one outgoing characteristic at each boundary, i.e. one of the pressure

eigenvalues (2.11) will be positive and one will be negative. Then, at each boundary, we are left with 3 different scenarios according to the sign of the interface eigenvalues (2.12):

- No interface eigenvalue represents inflow: 1 boundary condition must be imposed;
- one interface eigenvalue represents inflow: 2 boundary conditions must be imposed;
- both interface eigenvalues represent inflow: 3 boundary conditions must be imposed.

In this paper, we will present a method general enough to handle all these cases. We will however limit ourselves to *constant* boundary conditions, i.e. we consider only cases where both the imposed boundary conditions and the signs of the boundary eigenvalues do not vary in time. This allows us to focus on a main difficulty in the LTS setting (3.7): how to naturally incorporate boundary cells into the increased domain of dependence.

For the first cell in the domain, the standard Roe scheme stencil (3.5) implies:

$$\mathbf{U}_1^{n+1} = \mathbf{U}\left(\mathbf{U}_{\mathrm{LBC}}^n, \mathbf{U}_1^n, \mathbf{U}_2^n\right), \tag{4.1}$$

with $\mathbf{U}_{\mathrm{LBC}}$ being $\mathbf{U}$ in the left boundary cell, where the value at the boundary is typically prescribed for the problem. Clearly, this leads to a difficulty when it comes to the definition of numerical boundary conditions in the LTS method. If we assume that $\mathbf{U}_j$ in (3.6) is the first cell in the domain, then the LTS Roe scheme stencil (3.6) implies:

$$\mathbf{U}_1^{n+1} = \mathbf{U}\left(..., \mathbf{U}_{-1}^n, \mathbf{U}_{\mathrm{LBC}}^n, \mathbf{U}_1^n, \mathbf{U}_2^n, \mathbf{U}_3^n, ...\right). \tag{4.2}$$

Here, we do not have the cell values associated with $\mathbf{U}_{j-1}^n$, $\mathbf{U}_{j-2}^n$, etc. We now suggest two different ways to define these boundary cells.

4.1. Extrapolated boundary conditions

Assume that we apply a Courant number $C > 0$, i.e. we will need $M = \mathrm{ceil}(C)$ numerical ghost cells at each boundary to directly apply the LTS Roe scheme, where $\mathrm{ceil}(C)$ is the smallest integer that is larger or equal to C. The straightforward way to provide these additional cells is to simply extrapolate the values of the original boundary cell. In this way, all additional cells in the boundary zone will have the same values as the original boundary cell:

$$\mathbf{U}_j^n = \mathbf{U}_{\mathrm{LBC}}^n \quad \forall \quad j < \mathrm{LBC}, \tag{4.3}$$

$$\mathbf{U}_j^n = \mathbf{U}_{\mathrm{RBC}}^n \quad \forall \quad j > \mathrm{RBC}, \tag{4.4}$$

where LBC and RBC denote the indices of the left and right boundary cells, respectively. Assuming N cells in the interior domain, we will use the convention that $\mathrm{LBC} = 0$ and $\mathrm{RBC} = N + 1$. We will refer to this formulation as EBC, i.e. extrapolated boundary conditions. If there are no source terms present in the computational domain and the boundary conditions are constant in time this approach will be very effective, and very accurate results may be obtained, as will be shown for the shock tube example.

Next, we are interested how appropriate this definition is when there are source terms present. If we assume constant boundary conditions, the assumption of locally uniform data corresponds to a valid steady state solution in the absence of source terms. Consequently, the application of (4.3) and (4.4) may be viewed as follows:

- Calculate $\mathbf{U}_{\mathrm{LBC}}$ and $\mathbf{U}_{\mathrm{RBC}}$ by some boundary scheme.
- Solve the steady state and homogeneous version of the problem (2.5):

$$\mathbf{A}\,\mathrm{d}_x\mathbf{U} = 0, \tag{4.5}$$

  in an artifical domain extended at the boundaries (the solution is simply $\mathbf{U} = \text{const.}$)
- Transport the solution from this artificial domain into the actual computational domain through the LTS method.

Comparing the steady state form of (2.5) to (4.5), we see that under this point of view the EBC approach assumes there is no effect of the source terms in the boundary cells. Applying a Courant number $C > 1$, we will then see this manifest itself as a discontinuity in the numerical solution, propagating C cells per time step away from the boundary. Clearly, this is a numerical artifact due to the fact that we allow information to travel more than one cell during a single time step, without being affected by the source term. Herein, there are a number of ways of constructing the values of the primary boundary cells at x_{LBC} and x_{RBC}, for instance by extrapolation of the characteristic [30] or primitive variables. However, regardless of our choice of updating $\mathbf{U}_{\mathrm{LBC}}$ and $\mathbf{U}_{\mathrm{RBC}}$, we are left with a central problem associated with the EBC as given by (4.3) and (4.4) in the presence of source terms. We observe that this problem is somewhat independent of the choice of extrapolation variables, and we focus on primitive variable extrapolation for the purposes of this paper.

4.2. Steady state boundary condition

To overcome the problem discussed above, we replace (4.5) by the steady state form of (2.5):

$$\mathbf{A}\,\mathrm{d}_x\mathbf{U} = \mathbf{Q}(\mathbf{U}). \tag{4.6}$$

Assuming that the eigenvalues of $\mathbf{A}$ are nonzero, we obtain:

$$\mathrm{d}_x\mathbf{U} = (\mathbf{A}(\mathbf{U}))^{-1}\,\mathbf{Q}(\mathbf{U}). \tag{4.7}$$

Now, by discretizing this equation at the left and the right boundary cells we obtain the slopes $\delta_x\mathbf{U}_{\mathrm{L}}$ and $\delta_x\mathbf{U}_{\mathrm{R}}$ (left and right, respectively) as:

$$\delta_x\mathbf{U}_{\mathrm{L}} = (\mathbf{A}(\mathbf{U}_{\mathrm{LBC}}))^{-1}\,\mathbf{Q}(\mathbf{U}_{\mathrm{LBC}}), \qquad \delta_x\mathbf{U}_{\mathrm{R}} = (\mathbf{A}(\mathbf{U}_{\mathrm{RBC}}))^{-1}\,\mathbf{Q}(\mathbf{U}_{\mathrm{RBC}}), \tag{4.8}$$

which we then use to formulate the additional boundary cells as:

$$\mathbf{U}_j^n = \mathbf{U}_{\mathrm{LBC}}^n + (j - \mathrm{LBC})\Delta x\delta_x\mathbf{U}_{\mathrm{L}}, \quad \forall \quad j \in [\mathrm{LBC} - M, \ldots, \mathrm{LBC}], \tag{4.9}$$

at the left boundary zone and:

$$\mathbf{U}_j^n = \mathbf{U}_{\mathrm{RBC}}^n + (j - \mathrm{RBC})\Delta x\delta_x\mathbf{U}_{\mathrm{R}}, \quad \forall \quad j \in [\mathrm{RBC}, \ldots, \mathrm{RBC} + M], \tag{4.10}$$

at the right boundary zone. These equations then replace (4.3) and (4.4). We will refer to this formulation as SSBC, i.e. steady state boundary conditions.

Remark 1: *We note that in practice, this approach must be handled with caution. Namely, using* (4.9) *and* (4.10) *may result in negative values of the conserved variables. This will be further addressed in section 5.*

4.3. Numerical example

To illustrate how the presence of a source term causes an error close to the boundary and to show the advantage of using the SSBC we consider a linear advection with a source term:

$$\partial_t u + a\partial_x u = q(u), \qquad a = 1, \tag{4.11}$$

with initial data and source term defined as:

$$u(x,0) = 1, \qquad q(u) = -0.1u. \tag{4.12}$$

For the problem (4.11) to be well-posed we need a boundary condition at the left boundary. We choose $u(0,t) = 1$. The Eq. (4.11) is solved by the explicit Euler method in time, the LTS upwind scheme in space and an explicit treatment of the source term:

$$u_j^{n+1} = u_j^n - \frac{\Delta t}{\Delta x}\left(\sum_{i=0}^{\infty} a^{i+}_{j-1/2-i}\Delta u_{j-1/2-i} + \sum_{i=0}^{\infty} a^{i-}_{j+1/2+i}\Delta u_{j+1/2+i}\right) + \Delta t q_j(u_j^n), \tag{4.13}$$

where we note that (4.13) is (3.7) applied to the scalar problem (4.11) including the source term. We set $\Delta x = 1$ and evaluate the solution at time $t = 3$. Figure 2a shows the solution obtained with the non–LTS upwind scheme ($\Delta t = 1 \Rightarrow C = 1$, 3 time steps). Next, we consider the solution obtained with the LTS upwind scheme ($\Delta t = 3 \Rightarrow C = 3$, 1 time step) and EBC, see Figure 2b. It can be seen that the EBC approach neglects the effect of the source term during a single LTS step, and then applies the source term only at the end of the LTS step. In addition, the effect of the source term is magnified, since it multiplies Δt and Δt is larger in the LTS method. To fix this issue, we use the SSBC and reconstruct the boundary zone according to (4.6) – (4.10), see Figure 2c.

Here we note that this pattern of error generation in the presence of source term is not limited only to the vicinity of the boundaries. Similar pattern may appear whenever we transport a discontinuity since the LTS method neglects the effect of the source term on the Riemann problem during a single LTS step. In addition, similar mechanism may arise if there are no source terms, but strong nonlinear effects. In that case, the LTS method neglects the nonlinear interactions during a single LTS step, leading to errors that exhibit similar behavior, i.e. transport of sections of constant data unaffected by nonlinear interactions. In section 5 we will discuss errors caused by the source term elsewhere in the domain.

Remark 2: *It should be noted that the discretization* (4.13) *is stable for our illustrative example, but for arbitrary initial data stability may be lost due to interaction between the source and transport terms.*

To demonstrate the performance of the LTS Roe scheme and boundary treatments we consider two test cases. The numerical solutions are obtained by (3.7) and explicit treatment of the source term:

$$\mathbf{U}_j^{n+1} = \mathbf{U}_j - \frac{\Delta t}{\Delta x}\left(\sum_{i=0}^{\infty} \hat{\mathbf{A}}^{i+}_{j-1/2-i}\Delta\mathbf{U}_{j-1/2-i} + \sum_{i=0}^{\infty} \hat{\mathbf{A}}^{i-}_{j+1/2+i}\Delta\mathbf{U}_{j+1/2+i}\right) + \Delta t\mathbf{Q}_j. \tag{4.14}$$

In all the numerical investigations considered below, the time step Δt is fixed and determined at the beginning of the calculation, based on the Courant number we want to use and prior knowledge of the largest eigenvalue that will appear during the computation:

$$\Delta t = \frac{C\Delta x}{\max\limits_{j,n}|\lambda_j^n|}. \tag{4.15}$$

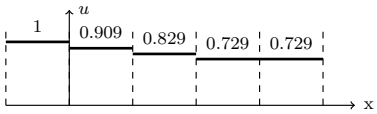

(a) Standard (non–LTS) upwind scheme with $C = 1$

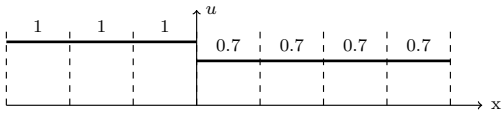

(b) LTS–upwind scheme with $C = 3$ and EBC

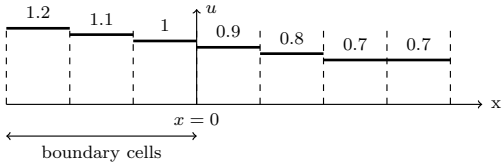

(c) LTS–upwind scheme with $C = 3$ and SSBC

Figure 2: Numerical solution for problem (4.11) after $t = 3$

4.4. Shock tube results

We first consider a shock tube problem studied by Cortes et al. [2] and Evje and Flåtten [3]. The tube has a length of 100 m and initial data with a discontinuity at $x = 50$ m. The initial data on the left and the right of the discontinuity are:

$$\mathbf{V}(x,0) = \left[p, \alpha_l, v_g, v_l\right]^{\mathrm{T}} = \begin{cases} [265000\ \text{Pa}, 0.71, 65\ \text{m/s}, 1\ \text{m/s}] & \text{if } x < 50; \\ [265000\ \text{Pa}, 0.7, 50\ \text{m/s}, 1\ \text{m/s}] & \text{if } x > 50. \end{cases} \tag{4.16}$$

The solution is evaluated at the time $t = 0.1$s. Boundary conditions are obtained by simple extrapolation (EBC), because the waves will not reach the boundaries, therefore no special treatment of the boundaries is required. The numerical solution is obtained with (4.14), and we note that for the shock tube test case $\mathbf{Q}_j^n = 0$. The reference solution is obtained by the Roe scheme with superbee wave limiter on a grid with 12 000 cells and $\Delta t = 2.1815 \cdot 10^{-5}$ s, corresponding to $C \approx 1$.

Figure 3 shows the comparison between the standard and LTS Roe scheme at Courant number $C \approx 5$ and $C \approx 39$ on the grid with 100 cells. It can be seen that the LTS Roe scheme with $C \approx 5$ resolves the left going shock with higher accuracy than non–LTS Roe scheme. The LTS Roe scheme with $C \approx 39$ achieves even higher accuracy. However, one can note that LTS Roe scheme leads to slight overshoots and undershoots which can be best seen in pressure and liquid velocity profiles. Similar oscillations have been observed previously for the Euler equations [22, 18], and are due to the assumption of linear wave interactions. Regardless of these oscillations one should note that the solution obtained with the LTS Roe scheme took only 8 and 1 time steps (ts), respectively, making it more efficient than the standard Roe scheme that took 39 time steps.

We also investigate the convergence of the LTS Roe scheme for different grids and Courant numbers, see Table 1. We can observe that the accuracy increases as we refine the grid and that

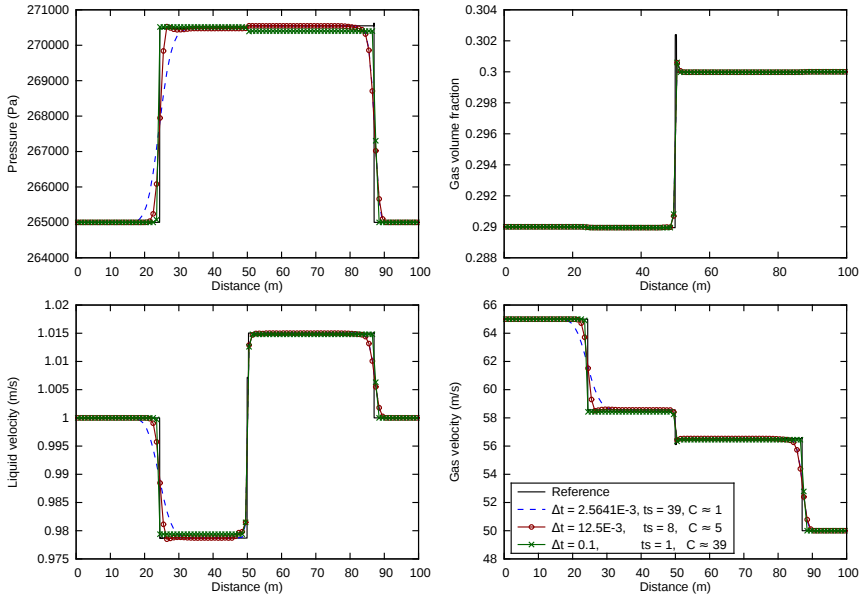

Figure 3: Comparison between standard and LTS Roe scheme on the grid with 100 cells for shock tube problem (4.16)

Table 1: 1-norm error estimate $\mathcal{E}$ ($\times 10^3$ Pa) and convergence rates $\mathcal{L}$ for pressure for shock tube problem (4.16)

	Roe		Roe + superbee		LTS Roe		LTS Roe		LTS Roe	
$\frac{\Delta t}{\Delta x}$	$2.6 \cdot 10^{-3}$ ($C \approx 1$)		$2.6 \cdot 10^{-3}$ ($C \approx 1$)		$1.25 \cdot 10^{-2}$ ($C \approx 5$)		$2.5 \cdot 10^{-2}$ ($C \approx 10$)		0.1 ($C \approx 39$)	
n	$\mathcal{E}_n$	$\mathcal{L}_n$	$\mathcal{E}_n$	$\mathcal{L}_n$	$\mathcal{E}_n$	$\mathcal{L}_n$	$\mathcal{E}_n$	$\mathcal{L}_n$	$\mathcal{E}_n$	$\mathcal{L}_n$
100	15.5	–	4.12	–	8.27	–	6.41	–	11.2	–
200	11.1	0.482	2.58	0.676	6.31	0.390	4.85	0.401	6.54	0.777
400	7.16	0.633	1.04	1.311	4.01	0.654	2.84	0.775	3.25	1.009
800	4.90	0.546	0.52	0.986	2.64	0.605	1.75	0.700	1.59	1.031

in most cases the convergence rate increases as we increase the Courant number. A similar trend is observed for the velocity profiles, while the accuracy and convergence of the volume fraction are somewhat ambiguous due to the presence of the spike, see Figure 3.

4.5. Water faucet results

As a second test case we consider the classical water faucet problem proposed by Ransom [31]. The problem consists of a vertical pipe 12 meters long with initial data:

$$\mathbf{V}(x,0) = \left[p, \alpha_l, v_g, v_l\right]^{\mathrm{T}} = \left[10^5 \text{ Pa}, 0.8, 0 \text{ m/s}, 10 \text{ m/s}\right]. \tag{4.17}$$

The water in the pipe is accelerated due to the effect of gravity which we define as a source term in (2.5):

$$\mathbf{Q}(\mathbf{U}) = [0, 0, g\rho_g\alpha_g, g\rho_l\alpha_l]^{\mathrm{T}}, \tag{4.18}$$

where $g = 9.81$ m/s^2. The solution is computed at time $t = 0.6$ s. In addition, the following boundary conditions are given:

$$\begin{aligned} &\text{Inlet:} \quad \alpha_l = 0.8, \quad v_l = 10 \text{ m/s}, \quad v_g = 0 \text{ m/s}, \\ &\text{Outlet:} \quad p = 10^5 \text{ Pa}. \end{aligned}$$

The remaining values required to determine the evolved variables at the boundary cells are extrapolated from the computational domain, which yields the following set of values at the boundaries:

$$\mathbf{B}^n_{\mathrm{LBC}} = \begin{bmatrix} p \\ \alpha_l \\ v_g \\ v_l \end{bmatrix}^n_{\mathrm{LBC}} = \begin{bmatrix} p^n_1 \\ 0.8 \\ 0 \\ 10 \text{ m/s} \end{bmatrix}, \quad \mathbf{B}^n_{\mathrm{RBC}} = \begin{bmatrix} p \\ \alpha_l \\ v_g \\ v_l \end{bmatrix}^n_{\mathrm{RBC}} = \begin{bmatrix} 10^5 \text{ Pa} \\ (\alpha_l)^n_N \\ (v_g)^n_N \\ (v_l)^n_N \end{bmatrix}. \tag{4.19}$$

The analytical solution for the liquid volume fraction and liquid velocity can be found in [3]. The reference solution for the remaining variables is obtained by the standard Roe scheme with superbee wave limiter on a grid with 12 000 cells and $\Delta t = 2.9154 \cdot 10^{-6}$ s, corresponding to $C \approx 1$.

4.5.1. Effect of time step

Figure 4 shows the comparison between the standard and the LTS Roe scheme with different time steps and different implementations of the boundary conditions on the grid with 100 cells.

It can be seen that the pressure solution obtained with SSBC is smoother and larger than the solution obtained with EBC for corresponding time steps, especially for larger time steps. That is expected regarding smoothness, since the boundaries defined with SSBC introduce a smaller error and provide a smoother transition between the boundary zone and the rest of the domain.

The accuracy of the gas volume fraction and liquid velocity increase as we increase the Courant number. This is because the larger time step Δt leads to a smaller number of time steps, which reduces the numerical diffusion introduced each time we average a cell state, i.e. in each time step. However, the error in the gas velocity near the outlet gets larger for larger Courant numbers. We note that the Courant numbers corresponding to the interface waves are smaller than one for all cases. More rigorous insight into the relation between time step and numerical diffusion can be gained through the modified equation analysis, see for instance Harten et al. [32].

4.5.2. Effect of grid refinement

We also compare the effect of grid refinement starting with a grid of 100 cells and a time step $\Delta t = 0.0017$ s, which corresponds to $C \approx 5$. For each refined grid we keep the Courant number constant, i.e. the ratio $\Delta t/\Delta x = 0.0146 = \text{const.}$, see Figure 5. We again note that the SSBC provides smoother and larger pressure profiles than EBC. However, this effect becomes less significant as the grid is refined. This is expected, since the number of boundary cells remains constant as the total number of grid cells is increased. Hence their relative influence becomes smaller. Nevertheless, practical simulations are often performed on coarse grids due to computational efficiency constraints. Here the results may be sensitive to the different treatments

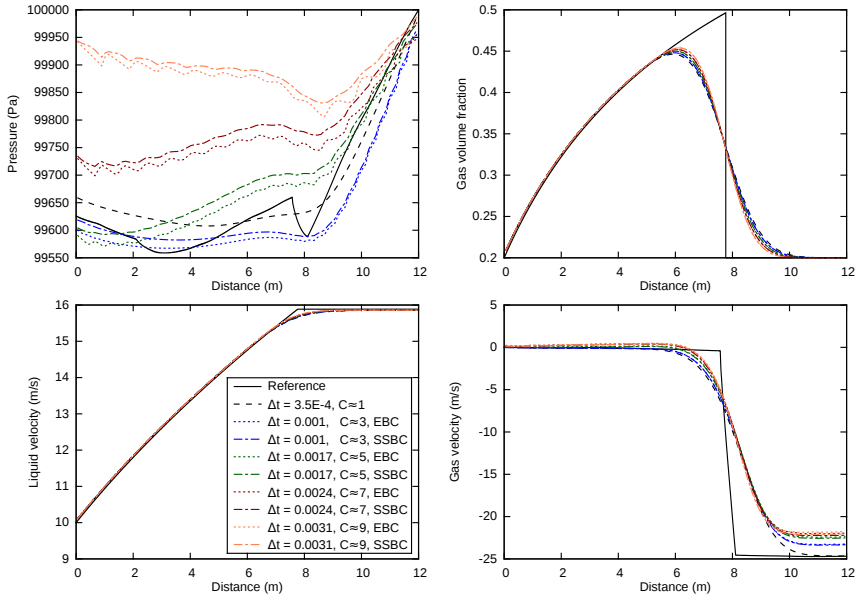

Figure 4: Effect of increasing the time step for different treatments of boundary conditions on the grid with 100 cells for water faucet problem (4.17)

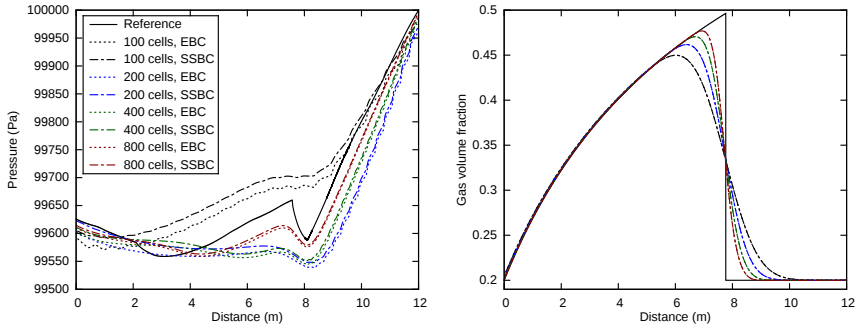

Figure 5: Effect of grid refinement for different treatments of boundary conditions with $\Delta t/\Delta x$ = const., (C ≈ 5) for water faucet problem (4.17)

of the boundary conditions presented here. Figure 5 indicates that both with EBC and SSBC, the LTS Roe scheme converges to the exact solution as the grid is refined. A similar trend is observed for the velocities.

To confirm that, we again investigate the convergence of the LTS Roe scheme for different grids and Courant numbers, see Table 2. We can observe that both accuracy and convergence

rate tend to increase as we increase the Courant number and refine the grid. A similar trend is observed for the pressure and velocity profiles.

Table 2: 1-norm error estimate $\mathcal{E}$ ($\times 10^{-2}$) and convergence rates $\mathcal{L}$ for volume fraction for water faucet problem (4.17)

	Roe		Roe + superbee		LTS Roe		LTS Roe		LTS Roe	
$\frac{\Delta t}{\Delta x}$	$2.9 \cdot 10^{-3}$ ($C \approx 1$)		$2.9 \cdot 10^{-3}$ ($C \approx 1$)		$1.46 \cdot 10^{-2}$ ($C \approx 5$)		$2.91 \cdot 10^{-2}$ ($C \approx 10$)		$5.81 \cdot 10^{-2}$ ($C \approx 20$)	
n	$\mathcal{E}_n$	$\mathcal{L}_n$	$\mathcal{E}_n$	$\mathcal{L}_n$	$\mathcal{E}_n$	$\mathcal{L}_n$	$\mathcal{E}_n$	$\mathcal{L}_n$	$\mathcal{E}_n$	$\mathcal{L}_n$
100	20.99	–	1.55	–	18.76	–	15.64	–	7.12	–
200	13.82	0.603	0.85	0.867	12.26	0.614	10.05	0.637	4.01	0.827
400	8.87	0.641	0.50	0.751	7.78	0.655	6.26	0.683	2.10	0.932
800	5.50	0.689	0.28	0.847	4.76	0.707	3.75	0.741	1.10	0.934

5. Source terms

Until now, we applied the explicit Euler method for time integration of the source term $\mathbf{Q}$, cf. Eq. (4.14). That way, the accuracy of solutions for volume fractions and phase velocities were increased at the cost of the accuracy of the pressure profile. The oscillations in the pressure profile did not affect the volume fraction profiles, because interface waves are not strongly affected by the pressure waves, cf. see the results in section 4.5. Further, the pressure waves are not strongly affected by gravity. For the water faucet example this is an acceptable approach as long as we apply the LTS method only to the pressure waves, i.e. the Courant numbers corresponding to interface waves (2.12) are less or equal to one at all times:

$$C^{\mathrm{i}} = \frac{\Delta t}{\Delta x} \max_{j,n} \left| \left(\lambda^{\mathrm{i}}\right)_j^n \right| \leq 1, \tag{5.1}$$

where C^{i} are interface Courant numbers and λ^{i} are the interface eigenvalues (2.12). We note that the eigenvalues associated with the interface waves (2.12) could be further approximated by assuming $\rho_g/\rho_l \approx 0$ for which we would obtain that both interface waves are $\lambda^i \approx v_l$. For the water faucet case considered here this assumption is also justified by numerical investigations.

However, if the source term is discretized with the explicit Euler method, and interface Courant number is increased beyond the standard CFL condition, severe oscillations will appear in the volume fraction and velocity profiles, regardless of how we define additional boundary cells. This suggest that if we want to use the LTS discretization for interface waves we need a more refined treatment of the source term.

In the literature, two improvements to the straightforward Euler discretization of the source term are commonly applied [33]:

- *Operator splitting* [34], which is based on solving the hyperbolic system $\partial_t \mathbf{U} + \mathbf{A}(\mathbf{U})\partial_x \mathbf{U} = 0$ alternately with the ODE $\mathrm{d}\mathbf{U} = \mathbf{Q}(\mathbf{U})$ to approximate the solution to the full problem (2.5).
- *Flux modification* [35], which is based on modifying the numerical flux at the cell interfaces to take into account the effect of the source term during the time step.

LeVeque [36] notes that operator splitting methods may cause difficulties when the system is close to a steady state solution, i.e. when the flux gradients are balanced with the source terms. Schemes that correctly balance the source volume integral with the flux surface integral are

denoted as *well-balanced* schemes, and are most conveniently formulated in the flux modification setting.

In this paper, we will follow the flux modification approach, starting by considering a scalar conservation law. Then, we provide the natural extension to the LTS Roe scheme and the system of equations. We follow the work of Murillo and García-Navarro [23], which again is based on ideas introduced by Bermúdez and Vázquez-Cendón [35]. We will end up formulating a slightly modified discretization.

5.1. Scalar conservation law with source term

We are considering a scalar conservation law with source term in the form:

$$\partial_t u + \partial_x f(u) = q(u), \tag{5.2}$$

with initial data corresponding to the Riemann problem:

$$u(x,0) = \begin{cases} u_\mathrm{L} & \text{if } x < 0; \\ u_\mathrm{R} & \text{if } x > 0. \end{cases} \tag{5.3}$$

We can also write (5.2) in quasilinear form as:

$$\partial_t u + \lambda \partial_x u = q(u), \qquad \lambda = \mathrm{d}_u f(u). \tag{5.4}$$

The Riemann problem (5.3) can be solved exactly by integrating (5.2) over the control volume $[x_\mathrm{L}, x_\mathrm{R}] \times [0, T]$ such that:

$$|\lambda_\mathrm{RP} T| < |x_\mathrm{L}|, |x_\mathrm{R}|, \qquad x_\mathrm{L} < 0 < x_\mathrm{R}, \tag{5.5}$$

where λ_RP is wave speed corresponding to Riemann problem (5.3) determined by the Rankine–Hugoniot condition. By integrating (5.2) in space and time we obtain:

$$\int_{x_\mathrm{L}}^{x_\mathrm{R}} u(x,T)\,\mathrm{d}x = u_\mathrm{R} x_\mathrm{R} - u_\mathrm{L} x_\mathrm{L} + T\left(f(u_\mathrm{L}) - f(u_\mathrm{R})\right) + \int_0^T \int_{x_\mathrm{L}}^{x_\mathrm{R}} q(u)\,\mathrm{d}x\,\mathrm{d}t. \tag{5.6}$$

As a discrete analogue to the above, we consider the local Riemann problem with piecewise initial data:

$$u(x,0) = \begin{cases} u_j & \text{if } x < 0; \\ u_{j+1} & \text{if } x > 0. \end{cases} \tag{5.7}$$

By integrating the local Riemann problem over the corresponding discrete control volume $[-\frac{\Delta x}{2}, \frac{\Delta x}{2}] \times [0, T]$ we obtain:

$$\int_{-\frac{\Delta x}{2}}^{\frac{\Delta x}{2}} u(x,T)\,\mathrm{d}x = \frac{\Delta x}{2}\left(u_{j+1} + u_j\right) + T\left(f(u_j) - f(u_{j+1})\right) + T s_{j+1/2}, \tag{5.8}$$

where we expressed the source term as:

$$T s_{j+1/2} = \int_0^T \int_{x_\mathrm{L}}^{x_\mathrm{R}} q_{j+1/2}\,\mathrm{d}x\,\mathrm{d}t. \tag{5.9}$$

As for now, we will leave the specific ways to evaluate the source term $q_{j+1/2}$ at the interface aside and return to it later, when we consider system of equations, cf. section 5.4. Since we

are considering a scalar conservation law, the Riemann problem (5.7) consists of only one wave traveling either to the right (if $\lambda_{j+1/2} > 0$) or to the left (if $\lambda_{j+1/2} < 0$). If the wave speed $\lambda_{j+1/2}$ is positive, the value of u^+_{j+1} corresponding to the right going wave can be calculated from (5.8) as:

$$\int_{-\frac{\Delta x}{2}}^{0} u(x,T)\,\mathrm{d}x + \int_{0}^{\lambda_{j+1/2}T} u^+(x,T)\,\mathrm{d}x + \int_{\lambda_{j+1/2}T}^{\frac{\Delta x}{2}} u(x,T)\,\mathrm{d}x = \frac{\Delta x}{2}\left(u_{j+1}+u_j\right) + T\left(f(u_j)-f(u_{j+1})\right) + T s_{j+1/2}. \tag{5.10}$$

By using the Rankine–Hugoniot condition:

$$f(u_{j+1}) - f(u_j) = \lambda_{j+1/2}\left(u_{j+1}-u_j\right), \tag{5.11}$$

on the right hand side of (5.10) and the fact that the integrands on the left hand side of (5.10) are equal to u_j, u^+_{j+1} and u_{j+1}, respectively, (5.10) yields:

$$u^+_{j+1} = u_j + \frac{s_{j+1/2}}{\lambda_{j+1/2}}, \tag{5.12}$$

where u^+_{j+1} denotes the state that travels to the right of the Riemann problem, into the cell with center at x_{j+1}. If the wave speed $\lambda_{j+1/2}$ is negative, the corresponding u^-_j is:

$$u^-_j = u_{j+1} - \frac{s_{j+1/2}}{\lambda_{j+1/2}}, \tag{5.13}$$

where u^-_j denotes the state that travels to the left of the Riemann problem, into the cell with center at x_j. Therefore, an arbitrary cell state u_j can be seen as being updated by information from neighboring Riemann problems:

$$u^{n+1}_j \Delta x = u_j \Delta x + (u^+_j - u_j)\lambda^+_{j-1/2}\Delta t - (u^-_j - u_j)\lambda^-_{j+1/2}\Delta t, \tag{5.14}$$

where we recall that $\lambda^\pm$ was defined according to (3.3). By inserting (5.12) and (5.13) into the (5.14) we have:

$$u^{n+1}_j = u^n_j - \frac{\Delta t}{\Delta x}\left(\lambda^+_{j-1/2}\Delta u_{j-1/2} + \lambda^-_{j+1/2}\Delta u_{j+1/2}\right) + \frac{\Delta t}{\Delta x}\left(s^+_{j-1/2} + s^-_{j+1/2}\right), \tag{5.15}$$

with $s^+_{j-1/2}$ and $s^-_{j+1/2}$ defined as:

$$s^+_{j-1/2} = \frac{\lambda^+_{j-1/2}}{\lambda_{j-1/2}} s_{j-1/2}, \qquad s^-_{j+1/2} = \frac{\lambda^-_{j+1/2}}{\lambda_{j+1/2}} s_{j+1/2}. \tag{5.16}$$

We will denote this type of source term discretization as the *split* source discretization, as opposed to *unsplit* explicit Euler discretization. We note that the quotient of eigenvalues in the (5.16) is either zero or one, i.e. the source terms in (5.16) are either zero or $s_{j-1/2}$ or $s_{j+1/2}$, respectively.

Note that, as in the original formulations [35, 23], the expressions (5.16) are not defined if a cell interface eigenvalue is zero. In this case, a convention would be needed to uniquely define the splitting of the source term. As this situation will not arise for any of our test cases, the description (5.16) will be sufficient for our present purposes.

In [23], Murillo and García-Navarro obtain the equivalent of finite volume method (5.15) as:

$$u_j^{n+1} = u_j^n - \frac{\Delta t}{\Delta x}\left(\lambda^+_{j-1/2}\theta_{j-1/2}\Delta u_{j-1/2} + \lambda^-_{j+1/2}\theta_{j+1/2}\Delta u_{j+1/2}\right), \tag{5.17}$$

with $\theta_{j+1/2}$:

$$\theta_{j+1/2} = 1 - \frac{s_{j+1/2}}{\lambda_{j+1/2}(u_{j+1} - u_j)}. \tag{5.18}$$

Although (5.15) and (5.17) are mathematically equivalent, (5.17) suffers from a drawback that source term yields no effect if the initial data is uniform. Since the initial data in the water faucet problem is uniform, it is necessary to use the approach corresponding to (5.15).

Remark 3: *In [23], Murillo and García-Navarro further discuss the effect of source term on the time step Δt and the effect it might have on the positivity preserving property of the scheme. Here, we do not discuss that matter because the water faucet test case, as discussed here, does not contain issues related to loss of positivity.*

5.2. Extension into the LTS framework

In this subsection, we are interested in generalizing this new discretization of the source term into the LTS framework. We start by observing that for a homogeneous problem, (5.15) is the scalar formulation of the flux difference splitting form (3.1). In section 3, the discretization (3.1) was extended into the LTS framework by extending the domain of dependence, i.e. by taking into the account more flux differences, cf. section 3.1. The procedure may be summarized as:

- Take into the account flux difference contributions from all interfaces in the domain of dependence;
- modify the wave speeds associated with flux differences according to (3.9).

By applying these steps, the homogeneous version of (5.15) can be extended into the LTS framework as:

$$u_j^{n+1} = u_j^n - \frac{\Delta t}{\Delta x}\left(\sum_{i=0}^{\infty}\lambda^{i+}_{j-1/2-i}\Delta u_{j-1/2-i} + \sum_{i=0}^{\infty}\lambda^{i-}_{j+1/2+i}\Delta u_{j+1/2+i}\right). \tag{5.19}$$

Based on this, we argue that the same reasoning may be applied on the source term contributions in the (5.15):

- Take into the account source effect contributions from all interfaces in the domain of dependence;
- modify the wave speeds associated with source contribution according to (3.9).

Hence, we obtain the LTS extension of (5.15) as:

$$\begin{aligned} u_j^{n+1} = u_j^n &- \frac{\Delta t}{\Delta x}\left(\sum_{i=0}^{\infty}\lambda^{i+}_{j-1/2-i}\Delta u_{j-1/2-i} + \sum_{i=0}^{\infty}\lambda^{i-}_{j+1/2+i}\Delta u_{j+1/2+i}\right) \\ &+ \frac{\Delta t}{\Delta x}\left(\sum_{i=0}^{\infty}\frac{\lambda^{i+}_{j-1/2-i}}{\lambda_{j-1/2-i}}s_{j-1/2-i} + \sum_{i=0}^{\infty}\frac{\lambda^{i-}_{j+1/2+i}}{\lambda_{j+1/2+i}}s_{j+1/2+i}\right). \end{aligned} \tag{5.20}$$

That way we take into account source effects that are delivered from all interfaces in the domain of dependence, and we ensure that the source terms further away from the cell we are updating contribute less than those closer. We note that in fractions of eigenvalues associated with source terms in (5.20), we modify only the eigenvalue in the numerator. Due to that, the quotient of eigenvalues is not either zero or one anymore, but may gradually decrease from one to zero as we are moving further away from the interface.

5.3. Generalization to system of equations

We are now interested in generalizing (5.20) to systems of equations. We start by generalizing the non-LTS (5.15), and then proceed to generalize (5.20). For homogeneous problem, we already observed that (5.15) is the scalar formulation of the flux difference splitting form (3.1). Hence, we look for the generalization of (5.15) in the form:

$$\mathbf{U}_j^{n+1} = \mathbf{U}_j^n - \frac{\Delta t}{\Delta x}\left(\hat{\mathbf{A}}^+_{j-1/2}\Delta\mathbf{U}_{j-1/2} + \hat{\mathbf{A}}^-_{j+1/2}\Delta\mathbf{U}_{j+1/2}\right) + \frac{\Delta t}{\Delta x}\left(\mathbf{S}^+_{j-1/2} + \mathbf{S}^-_{j+1/2}\right), \tag{5.21}$$

where $\mathbf{S}^{\pm}_{j+1/2}$ will be the system equivalent to $s^{\pm}_{j+1/2}$ in the (5.16). To see how (5.15) generalizes to system of equations, we recall the way the Roe scheme [28] is constructed, but note that for our investigations we consider the Roe matrix $\hat{\mathbf{A}}$ defined for two-fluid model, cf. section 3. We consider the system of equations (2.5) and linearize:

$$\partial_t\mathbf{U} + \hat{\mathbf{A}}_{j+1/2}\partial_x\mathbf{U} = \mathbf{Q}_{j+1/2}, \tag{5.22}$$

where $\mathbf{Q}_{j+1/2}$ is a vector of source terms evaluated at the interface $x_{j+1/2}$. Different ways on how to construct this vector will be addressed in section 5.4. Then, we solve this linearized problem exactly by considering the individual Riemann problem for (5.22) with:

$$\mathbf{U}(x,0) = \begin{cases} \mathbf{U}_j & \text{if } x < 0; \\ \mathbf{U}_{j+1} & \text{if } x > 0. \end{cases} \tag{5.23}$$

We start by multiplying (5.22) by $\hat{\mathbf{R}}^{-1}$, where $\hat{\mathbf{R}}^{-1}$ is the right eigenvector matrix of $\hat{\mathbf{A}} = \hat{\mathbf{A}}_{j+1/2}$:

$$\hat{\mathbf{R}}^{-1}\partial_t\mathbf{U} + \hat{\mathbf{R}}^{-1}\hat{\mathbf{A}}\hat{\mathbf{R}}\hat{\mathbf{R}}^{-1}\partial_x\mathbf{U} = \hat{\mathbf{R}}^{-1}\mathbf{Q}_{j+1/2}, \tag{5.24}$$

to obtain:

$$\partial_t\mathbf{W} + \hat{\mathbf{\Lambda}}\partial_x\mathbf{W} = \mathbf{\Omega}_{j+1/2}, \tag{5.25}$$

where $\mathbf{W} = \hat{\mathbf{R}}^{-1}\mathbf{U}$ is the vector of characteristic variables, $\hat{\mathbf{\Lambda}}$ is the diagonal matrix of eigenvalues, and $\mathbf{\Omega}_{j+1/2} = \hat{\mathbf{R}}^{-1}\mathbf{Q}_{j+1/2}$ is the vector of characteristic source terms. This way we decoupled the system (5.22) into linear advection equations. Then we solve each of these equations according to the theory we presented for scalar conservation laws, section 5.1. Therefore, for each characteristic variable w^p of vector $\mathbf{W}$ we have equation equivalent to (5.15):

$$\begin{aligned}(w^p)_j^{n+1} = (w^p)_j^n &- \frac{\Delta t}{\Delta x}\left((\lambda^p)^+_{j-1/2}\Delta w^p_{j-1/2} + (\lambda^p)^-_{j+1/2}\Delta w^p_{j+1/2}\right) \\ &+ \frac{\Delta t}{\Delta x}\left((s^p)^+_{j-1/2} + (s^p)^-_{j+1/2}\right) \quad \forall p,\end{aligned} \tag{5.26}$$

where s^p is p-th component of vector $\mathbf{S}$. We note that $\mathbf{S}$ is obtained by integrating components of $\mathbf{\Omega}$ as done with $q_{j+1/2}$ in (5.9):

$$T\mathbf{S}_{j+1/2} = \int_0^T \int_{x_\mathrm{L}}^{x_\mathrm{R}} \mathbf{\Omega}_{j+1/2}\,\mathrm{d}x\,\mathrm{d}t. \tag{5.27}$$

Following LeVeque [36], the flux difference terms in Eq. (3.1) may be defined as:

$$\hat{\mathbf{A}}^{\pm}\Delta\mathbf{U}_{j+1/2} = \hat{\mathbf{R}}\hat{\mathbf{\Lambda}}^{\pm}\hat{\mathbf{R}}^{-1}\Delta\mathbf{U}_{j+1/2} = \sum_{p=1}^{m} (\lambda^p)^{\pm}\, r^p \Delta w^p_{j+1/2}. \tag{5.28}$$

Similarly, we argue that the *split* source term can be defined as:

$$\mathbf{S}^{\pm}_{j+1/2} = \hat{\mathbf{R}}\hat{\mathbf{\Lambda}}^{\pm}\hat{\mathbf{\Lambda}}^{-1}\hat{\mathbf{R}}^{-1}\mathbf{S}_{j+1/2} = \sum_{p=1}^{m} \frac{(\lambda^p)^{\pm}}{\lambda^p} r^p s^p_{j+1/2}. \tag{5.29}$$

Therefore we have that:

$$\mathbf{S}^{\pm}_{j+1/2} = \tilde{\mathbf{A}}^{\pm}_{j+1/2}\mathbf{S}_{j+1/2}, \tag{5.30}$$

where we introduced:

$$\tilde{\mathbf{A}}^{\pm} = \hat{\mathbf{R}}\tilde{\mathbf{\Lambda}}^{\pm}\hat{\mathbf{R}}^{-1}, \tag{5.31}$$

$$\tilde{\mathbf{\Lambda}}^{\pm} = \hat{\mathbf{\Lambda}}^{\pm}\hat{\mathbf{\Lambda}}^{-1}. \tag{5.32}$$

Here we point out that (5.30) is system equivalent of (5.16), where term $\tilde{\mathbf{A}}^{\pm}_{j+1/2}$ in (5.30) corresponds to the quotients of eigenvalues in (5.16). Here, just as in the (5.16), the diagonal elements of matrix $\tilde{\mathbf{\Lambda}}^{\pm}$ in (5.32) take the values of either zero or one.

Once we have established the relation between (5.15) and (5.21), we are left with the task of establishing the LTS framework for (5.21). Recall that in section 3 we extended (3.1) to the LTS framework (3.7) by extending the domain of dependence. The same idea was applied in extending the scalar conservation law with source term (5.15) to the LTS framework (5.20). Following that idea, we propose the LTS discretization of the source terms (5.30) in Eq. (5.21) as:

$$\mathbf{S}^{+}_{j+1/2} = \tilde{\mathbf{A}}^{+}_{j+1/2}\mathbf{S}_{j+1/2} \longrightarrow \sum_{i=0}^{\infty} \tilde{\mathbf{A}}^{i+}_{j+1/2-i}\mathbf{S}_{j+1/2-i}, \tag{5.33}$$

$$\mathbf{S}^{-}_{j+1/2} = \tilde{\mathbf{A}}^{-}_{j+1/2}\mathbf{S}_{j+1/2} \longrightarrow \sum_{i=0}^{\infty} \tilde{\mathbf{A}}^{i-}_{j+1/2+i}\mathbf{S}_{j+1/2+i}, \tag{5.34}$$

with:

$$\tilde{\mathbf{A}}^{i\pm} = \hat{\mathbf{R}}\tilde{\mathbf{\Lambda}}^{i\pm}\hat{\mathbf{R}}^{-1}, \tag{5.35}$$

$$\tilde{\mathbf{\Lambda}}^{i\pm} = \hat{\mathbf{\Lambda}}^{i\pm}\hat{\mathbf{\Lambda}}^{-1}. \tag{5.36}$$

The modification of eigenvalues in (5.36) has the same role as with the flux difference contributions – source terms coming from interfaces further away from relevant interface are contributing less than the source terms closer to the relevant interface, due to the fact that they have to travel a certain distance before they start passing through the relevant interface. Here, we note that the diagonal elements of matrix $\tilde{\mathbf{\Lambda}}^{i\pm}$ in (5.36) are not either zero or one, respectively, but may instead gradually decrease towards zero.

5.4. On the choice of average for $\mathbf{Q}_{j+1/2}$

Herein we propose two different ways on how to approximate the source term $\mathbf{Q}_{j+1/2}$ in (5.22) at the cell interface. As a first choice we propose the arithmetic average of $\mathbf{Q}$ in neighboring cells, i.e. a *central* discretization:

$$\mathbf{Q}_{j+1/2} = \frac{1}{2}\left(\mathbf{Q}_j + \mathbf{Q}_{j+1}\right). \tag{5.37}$$

An alternative choice is to take into the account the physics of the particular problem. This may be done by considering the signs of the eigenvalues and defining:

$$\mathbf{Q}_{j+1/2} = \tilde{\mathbf{A}}^{-}_{j+1/2}\mathbf{Q}_j + \tilde{\mathbf{A}}^{+}_{j+1/2}\mathbf{Q}_{j+1}, \tag{5.38}$$

which will be denoted as *upwind* discretization of the source term. We note that $\tilde{\mathbf{A}}^{\pm}_{j+1/2}$ was defined in (5.31).

5.5. Water faucet results

Herein, we once again consider the water faucet test case from section 4.5 and use the same initial data, boundary conditions and means of obtaining the reference solution.

In this section we are interested in increasing the global Courant number so that even the interface Courant number (5.1) exceeds the standard CFL limit. Table 3 shows several global Courant numbers estimated on prior knowledge of the largest wave speeds and the corresponding largest interface Courant numbers C^{i} at starting and end time.

Table 3: Global Courant numbers C with time steps Δt and largest interface Courant number C^{i} on grid with 100 cells

Global C	Δt in s	C^{i} ($t = 0$)	C^{i} ($t = 0.6$ s)
≈ 1	3.4985×10^{-4}	0.030	0.049
≈ 10	0.0035	0.300	0.490
≈ 30	0.0103	0.879	1.444
≈ 49	0.0171	1.459	2.398

5.5.1. Treatment of boundary conditions for very large Courant numbers

At the moment, it remains ambiguous what is the optimal way to apply SSBC approach (cf. section 4) when we use very large Courant numbers. Namely, we wish to apply SSBC to as many boundary cells as possible to reduce the oscillations in the pressure. At the same time, applying (4.9) and (4.10) directly may lead to negative values of the conserved variables. We observed that if interface Courant number (5.1) is higher than one, using EBC will lead to oscillations in volume fraction as well. The error will develop in a similar manner as the error in the pressure profile discussed in section 4, i.e. there will be a step-like pattern in the volume fraction profile. Since in this section we are interested in volume fraction profiles we apply SSBC to just enough cells to ensure that we apply the SSBC to the interface waves. Regardless of how we define the remaining cells, their treatment will affect only the pressure waves and at the moment these waves are not the focus of our interest. Therefore, we used:

- Left boundary: by examining the Table 3 and noting that the domain of dependence of interface waves consists of at most three upwind cells, we used the SSBC approach for five boundary cells at the left boundary.

- Right boundary: at the right boundary we applied SSBC on all the boundary cells because it did not cause any of the conserved variables to become negative.

A more rigorous and more general framework on how to properly apply SSBC in the LTS Roe scheme is being currently investigated.

Remark 4: *As discussed above, using EBC when the interface Courant number is larger than one leads to a step-like error in the volume fraction. We found that this error is independent of how we treat the source term, i.e. it yields the same error for both unsplit and split discretization of the source term and it is not affected by the choice of average for* $\mathbf{Q}_{j+1/2}$*. This justifies our simplification to treat errors caused by the source terms in the vicinity of the boundaries and the errors caused by the treatment of source terms elsewhere in the domain as independent problems.*

5.5.2. Comparison between different discretizations of source term at Courant number $C \approx 30$

Figure 6 shows the comparison of results for the water faucet problem solved by standard Roe scheme, standard Roe scheme with superbee limiter and three different discretizations of the source term for global Courant number $C \approx 30$, all on the grid with 100 cells. The pressure

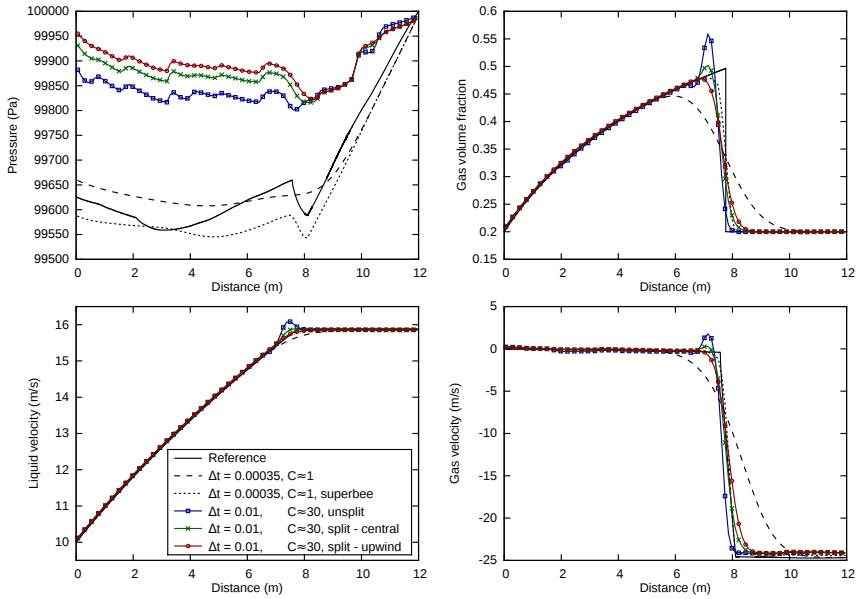

Figure 6: Effect of source term treatment at $C = 30$ on grid with 100 cells for for water faucet problem (4.17)

profiles associated with the LTS method show strong oscillations which are due to the very large global Courant number and somewhat ambiguous treatment of boundary conditions that may affect the accuracy of the pressure waves, see section 5.5.1. In addition, these pressure profiles seem to stabilize themselves at a values slightly lower than the prescribed outlet pressure (10^5 Pa). Regardless of that, the volume fraction waves were not affected by the oscillations of the pressure, and therefore we do not focus on these errors.

In the plot for the volume fraction, we may see that the standard *unsplit* treatment leads to a very large error in the volume fraction on the upstream side of the contact discontinuity, while the corresponding *split* discretizations yield much better solution. The best solution is obtained by using the *upwind* approximation for the source term (5.38). This hierarchy is expected, and may be explained in a following way. First, we note that the error manifests itself as an increase in gas volume fraction. Second, we recall that the source term in (2.5) and the corresponding discretization in (5.21) are positive. The source term is given by the (4.18), where gravity g is constant, while the changes in volume fractions dominate the changes in densities. When we update cell $\mathbf{U}_j$, and we treat the source term with *unsplit* approach, we simply multiply the strength of the source term at that cell by time step Δt. We may observe that this is not true, because what actually enters the cell is coming from the upstream direction, and upstream of the contact discontinuity the volume fraction is smaller than in the cell at x_j. Hence, this approach overestimates the amount of gas phase. Following the same reasoning, we may see why central discretization yields a better solution. The central discretization (5.37) of the split source term uses the volume fractions, i.e. the source terms from upstream interfaces, where value at each interface is determined according to (5.37). This approach uses smaller values of volume fraction, and these values give much better results, but they still overestimate the source strength in the cell at x_j. Upwind discretization (5.38) uses even smaller values of the volume fraction than the central discretization, and does not lead to too large accumulation of the volume fraction in the cell at x_j. We may observe that the accuracy of the best solution obtained with the LTS Roe scheme is much closer to the high resolution Roe scheme than to the standard Roe scheme.

The same hierarchy of the solutions is observed for the liquid and gas velocity profiles. We note that for the gas velocity profile all LTS Roe schemes results seem to stabilize around a slightly too big outlet velocity at the right boundary.

5.5.3. Comparison between different discretizations of source term at Courant number $C \approx 49$

Next we further increase the Courant number and compare different choices of average for $\mathbf{Q}_{j+1/2}$ with *split* discretization of the source term, Figure 7.

For Courant number $C \approx 49$ the accuracy of pressure profiles is further decreased. In addition, the pressure profiles corresponding to Courant number $C \approx 49$ stabilize themselves at different values than before, but still not at the prescribed outlet pressure (10^5 Pa). Once again, we do not focus on these errors, because we concluded that they do not significantly affect the volume fractions and the velocity profiles.

For the volume fractions, further increase of the Courant number leads to further increase in the error upstream of the contact discontinuity. At $C \approx 49$, only the *split* discretization of the source term with upwind average for $\mathbf{Q}_{j+1/2}$ gives reasonably good solutions, although if we further increase the Courant number or the simulation time this error keeps increasing. Similar trend is observed for the velocities. Therefore, even though our new approach significantly improves the solution compared to the explicit treatment of the source term, it does not guarantee an unconditionally stable treatment of the source term.

Remark 5: *Herein, we note that the error in the volume fraction upstream of the contact discontinuity is independent of the way we treat boundary conditions, i.e. it is the same for the EBC and SSBC. This is in agreement with remark 4.*

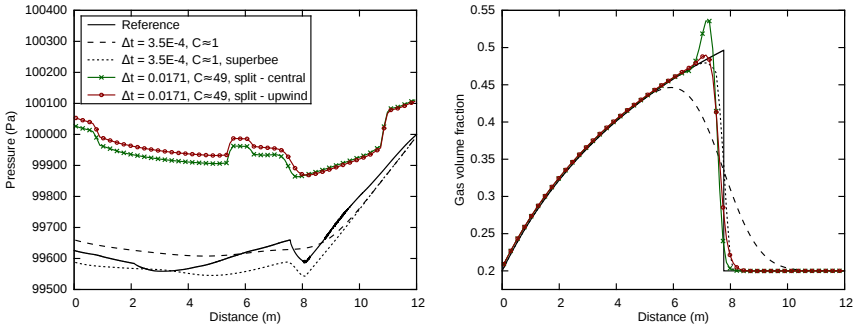

Figure 7: Effect of source term treatment at $C = 49$ on grid with 100 cells for for water faucet problem (4.17)

6. Computational performance

Through the paper, it was repeatedly stated that the LTS Roe scheme is more efficient than the standard Roe scheme. Herein, we investigate the computational efficiency of the LTS Roe scheme by examining the relationship between the computational time and the 1-norm of the error for different grids and Courant numbers, Fig. 8.

For the shock tube problem (4.16) (Fig. 8a) we used the EBC treatment of the boundary conditions. For the water faucet problem (4.17) (Fig. 8b) we used the SSBC treatment of the boundary conditions as described in section 5.5.1 and upwind treatment of the source term with the average (5.38). The CPU times are obtained with the MATLAB tic–toc function averaged over several simulations. We observe that:

- For all the cases, the LTS Roe scheme is more accurate than the standard Roe scheme;
- at each grid size, the increase of Courant number leads to an increase of the efficiency;
- for the shock tube problem (4.16) (Fig. 8a) the optimal Courant number depends on the grid size. The convergence rate indicates that as we refine the grid, the solution obtained with the highest Courant number will achieve the highest accuracy.

We note that these results are dependent on numerical implementation of the method and the features of the studied problems. However, similar results were independently obtained by Lindqvist and Lund [21].

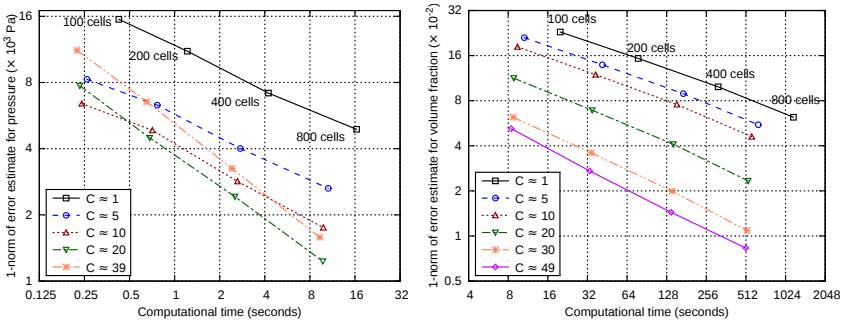

(a) Shock tube problem (4.16) (b) Water faucet problem (4.17)

Figure 8: 1–norm error estimate $\mathcal{E}$ vs. computational time on grids with 100, 200, 400 and 800 cells

7. Conclusions

We extended the standard Roe scheme to the LTS Roe scheme and showed that the two-fluid model can be solved with an explicit method not limited by the CFL condition. We applied the LTS Roe scheme to two test cases, shock tube and water faucet, and focused on the difficulties related to the treatment of boundary conditions and source terms.

The LTS Roe scheme performed very well for the shock tube test case, where there are neither source terms nor difficulties associated with boundary conditions. For the water faucet test case, applying the LTS Roe scheme with the most simple treatment of boundary conditions and source terms led to two distinct, but related, patterns of error generation. The first error is associated with the effect of the source term in the vicinity of the boundary. It is highly dependent on the definition of the boundary cells, and it was shown that this error can be reduced by imposing the steady state boundary conditions (SSBC). In particular, the SSBC approach reduced the oscillations and led to smoother profiles of all variables affected by this error. The second error is associated with the effect of the source term in general, and it is highly dependent on the discretization of the source term. This error was especially important when the interface Courant numbers were increased above one, since it caused severe oscillations in the volume fractions and velocities. It was shown that an appropriate *split* discretization of the source term allows us to use interface Courant numbers up to up to $C^{\mathrm{i}} \approx 2.4$, which corresponds to global Courant number $C \approx 49$. However, the oscillations associated with the pressure profile remained, and got even worse as we increased the Courant number. Reducing the oscillations caused by the source term in the vicinity of the boundaries by introducing SSBC treatment of the boundary conditions and reducing the oscillations in volume fractions and velocities caused by the source term elsewhere in the domain by introducing the *split* discretization of the source term are the main contributions of this paper.

Finally, it was shown that the LTS Roe scheme is more efficient than the standard Roe scheme for all the cases investigated in this paper. Further, the convergence analysis suggests that increasing the Courant number increases the convergence rate. The optimal choice of the Courant number remains to be determined for each particular problem.

The proposed method shows promising potential, especially in the following cases. First, for the problems where there are no source terms and where complex wave dynamics is not

happening close at the boundaries. Second, in problems with a large number of grid cells where the number of additional ghost cells introduced by the LTS method is relatively small compared to the number of grid cells in the domain. And last, in problems where the velocities of the phases are much smaller than the pressure wave speeds and we are not interested in maximum accuracy of the pressure field compared to the accuracy required for volume fractions and velocities.

We believe that the interface Courant number can be further increased by more appropriate treatment of the source term. First, errors observed in Figure 6 led to an erroneous overshoots in velocities, and for our investigations we used fixed time step determined at the beginning of the simulation. Hence, adaptive time stepping procedure may be more appropriate for situations when the LTS method may cause overshoots in velocity. Second, the *split* discretization of the source term, although more successful than standard discretization of the source term, does not take into the account effect of the source term during single LTS steps. These effects may be taken into consideration by investigating the discretization of the source term in direction of well-balanced schemes or some completely new approach, for example by taking into the account the modification of the wave speeds by the source term. As for now, these investigations remain outside the scope of this paper.

Acknowledgments

This paper is an extension of a conference paper [37] that was presented at the Eleventh International Conference on CFD in the Minerals and Process Industries (CFD2015), and was nominated for invitation into the CFD2015 Special Issue of Applied Mathematical Modelling based on its designation as a high-quality paper of relevance to the modelling of fluids-based systems.

The authors were supported by the Research Council of Norway (234126/30) through the SIMCOFLOW project. We are grateful to our colleagues Sigbjørn Løland Bore, Stein Tore Johansen, Ernst Meese and Marica Pelanti for fruitful discussions.

References

[1] J. Cortes, On the construction of upwind schemes for non-equilibrium transient two-phase flows, Comput. Fluids 31 (2) (2002) 159–182.

[2] J. Cortes, A. Debussche, I. Tuomi, A Density Perturbation Method to Study the Eigenstructure of Two-Phase Flow Equation Systems, J. Comput. Phys. 147 (2) (1998) 463–484.

[3] S. Evje, T. Flåtten, Hybrid flux-splitting schemes for a common two-fluid model, J. Comput. Phys. 192 (1) (2003) 175–210.

[4] S. T. Munkejord, Comparison of Roe-type methods for solving the two-fluid model with and without pressure relaxation, Comput. Fluids 36 (6) (2007) 1061–1080.

[5] I. Toumi, A. Kumbaro, An Approximate Linearized Riemann Solver for a Two-Fluid Model, J. Comput. Phys. 124 (2) (1996) 286–300.

[6] F. De Vuyst, Stable and accurate hybrid finite volume methods based on pure convexity arguments for hyperbolic systems of conservation law, J. Comput. Phys. 193 (2) (2004) 426–468.

[7] M. Larsen, E. Hustvedt, P. Hedne, T. Straume, PeTra: A Novel Computer Code for Simulation of Slug Flow, in: SPE Annual Technical Conference and Exhibition, 5-8 October, San Antonio, Texas, Society of Petroleum Engineers, 1997, SPE 38841.

[8] K. Bendiksen, D. Maines, R. Moe, S. Nuland, The Dynamic Two-Fluid Model OLGA: Theory and Application, SPE Prod. Eng. 6 (2) (1991) 171–180.

[9] F. Barre, M. Bernard, The CATHARE code strategy and assessment, Nucl. Eng. Des. 124 (3) (1990) 257–284.

[10] R. J. LeVeque, Large Time Step Shock-Capturing Techniques for Scalar Conservation Laws, SIAM J. Numer. Anal. 19 (6) (1982) 1091–1109.

[11] R. J. LeVeque, Convergence of a Large Time Step Generalization of Godunov's Method for Conservation Laws, Comm. Pure Appl. Math. 37 (4) (1984) 463–477.
[12] R. J. LeVeque, A large Time Step Generalization of Godunov's Method for Systems of Conservation Laws, SIAM J. Numer. Anal. 22 (6) (1985) 1051–1073.
[13] J. Murillo, P. García-Navarro, P. Brufau, J. Burguete, Extension of an explicit finite volume method to large time steps (CFL>1): application to shallow water flows, Int. J. Numer. Meth. Fluids 50 (1) (2006) 63–102.
[14] M. Morales-Hernández, P. García-Navarro, J. Murillo, A large time step 1D upwind explicit scheme (CFL>1): Application to shallow water equations, J. Comput. Phys. 231 (19) (2012) 6532–6557.
[15] M. Morales-Hernández, J. Murillo, P. García-Navarro, J. Burguete, A large time step upwind scheme for the shallow water equations with source terms, in: E. Vázquez Cendón, A. Hidalgo, P. García-Navarro, L. Cea (Eds.), Numerical Methods for Hyperbolic Equations, CRC Press, 2012, pp. 141–148.
[16] M. Morales-Hernández, M. Hubbard, P. García-Navarro, A 2D extension of a Large Time Step explicit scheme (CFL>1) for unsteady problems with wet/dry boundaries, J. Comput. Phys. 263 (2014) 303–327.
[17] R. Xu, D. Zhong, B. Wu, X. Fu, R. Miao, A large time step Godunov scheme for free-surface shallow water equations, Chinese Sci. Bull. 59 (21) (2014) 2534–2540.
[18] Z. Qian, C.-H. Lee, A class of large time step Godunov schemes for hyperbolic conservation laws and applications, J. Comput. Phys. 230 (19) (2011) 7418–7440.
[19] K. Tang, A. Beccantini, C. Corre, Combining Discrete Equations Method and upwind downwind-controlled splitting for non-reacting and reacting two-fluid computations: One dimensional case, Comput. Fluids 93.
[20] N. N. Makawana, A. Chatterjee, Fast Solution of Time Domain Maxwell's Equations Using Large Time Steps, in: 2015 IEEE International Conference on Computational Electromagnetics (ICCEM), 2-5 February, Hong Kong, Institute of Electrical and Electronics Engineers (IEEE), 2015, pp. 330–332.
[21] S. Lindqvist, H. Lund, A Large Time Step Roe scheme scheme applied to two-phase flow, in: M. Papadrakakis, V. Papadopoulos, G. Stefanou, V. Pleveris (Eds.), VII European Congress on Computational Methods in Applied Sciences and Engineering, 5-10 June, Crete Island, Greece, 2016.
[22] S. Lindqvist, P. Aursand, T. Flåtten, A. Solberg, Large Time Step TVD schemes for Hyperbolic Conservation Laws, SIAM J. Numer. Anal. 54 (5) (2016) 2775–2798.
[23] J. Murillo, P. García-Navarro, Weak solutions for partial differential equations with source terms: Application to the shallow water equations, J. Comput. Phys. 229 (11) (2010) 4327–4368.
[24] H. Städtke, Gasdynamic Aspects of Two-Phase Flow, Wiley-VCH, 2006.
[25] H. Holmås, T. Sira, M. Nordsveen, H. P. Langtangen, R. Schulkes, Analysis of a 1D incompressible two-fluid model including artificial diffusion, IMA J. Appl. Math. 73 (4) (2008) 651–667.
[26] A. A. Solberg, Large Time Step explicit schemes for partial differential evolution equations, Master's thesis, Dept. of Energy and Process Engineering, Norwegian University of Science and Technology (2016).
URL `http://hdl.handle.net/11250/2409951`
[27] T. Flåtten, A. Morin, On interface transfer terms in two-fluid models, Int. J. Multiph. Flow 45 (2012) 24–29.
[28] P. Roe, Approximate Riemann solvers, parameter vectors, and difference schemes, J. Comput. Phys. 43 (2) (1981) 357–372.
[29] S. T. Munkejord, Partially-reflection boundary conditions for transient two-phase flow, Commun. Numer. Meth. Engng. 22.
[30] K. Fjelde, K. Karlsen, High-resolution hybrid primitive-conservative upwind schemes for the drift flux model, Comput. Fluids 31 (3) (2002) 335–367.
[31] V. Ransom, Numerical benchmark tests, Multiphase Sci. Tech. 3 (1–4) (1987) 465–473.
[32] A. Harten, J. M. Hyman, P. D. Lax, B. Keyfitz, On Finite-Difference Approximations and Entropy Conditions for Shocks, Comm. Pure Appl. Math. 29 (3) (1976) 297–322.
[33] H. Lund, F. Müller, B. Müller, P. Jenny, Rankine–Hugoniot–Riemann solver for steady multidimensional conservation laws with source terms, Comput. Fluids 101 (2014) 1–14.
[34] R. J. LeVeque, Balancing Source Terms and Flux Gradients in High-Resolution Godunov Methods: The Quasi-Steady Wave-Propagation Algorithm, J. Comput. Phys. 146 (1) (1998) 346–365.
[35] A. Bermúdez, M. E. Vázquez-Cendón, Upwind methods for hyperbolic conservation laws with source terms, Comput. Fluids 23 (8) (1994) 1049–1071.
[36] R. J. LeVeque, Finite Volume Methods for Hyperbolic Problems, Cambridge University Press, 2002.
[37] M. Prebeg, T. Flåtten, B. Müller, Boundary and source term treatment in the Large Time Step method for a common two-fluid model, in: C. B. Solnordal, P. Liovic, G. W. Delaney, S. J. Cummins, M. P. Schwarz, P. Witt (Eds.), The 11th International Conference on CFD in the Minerals and Process Industries, 7-9 December, Melbourne, Australia, 2015.

Journal paper 2 (P2)

Large Time Step HLL and HLLC schemes

Marin Prebeg, Tore Flåtten and Bernhard Müller

Submitted for publication to ESAIM: Mathematical Modelling and Numerical Analysis, 2017.

Mathematical Modelling and Numerical Analysis Will be set by the publisher
Modélisation Mathématique et Analyse Numérique

LARGE TIME STEP HLL AND HLLC SCHEMES *

Marin Prebeg[1], Tore Flåtten[2] and Bernhard Müller[1]

Abstract. We present Large Time Step (LTS) extensions of the Harten-Lax-van Leer (HLL) and Harten-Lax-van Leer-Contact (HLLC) schemes. Herein, LTS denotes a class of explicit methods stable for Courant numbers greater than one. The original LTS method [R. J. LeVeque, *SIAM J. Numer. Anal.*, 22 (1985), pp. 1051–1073] was constructed as an extension of the Godunov scheme, and successive versions have been developed in the framework of Roe's approximate Riemann solver. In this paper, we formulate the LTS extension of the HLL and HLLC schemes in conservation form. We provide explicit expressions for the flux-difference splitting coefficients and the numerical viscosity coefficients of the LTS-HLL scheme. We apply the new schemes to the one-dimensional Euler equations and compare them to their non-LTS counterparts. As test cases, we consider the classical Sod shock tube problem and the Woodward-Colella blast-wave problem. We numerically demonstrate that for the right choice of wave velocity estimates both schemes calculate entropy satisfying solutions.

1991 Mathematics Subject Classification. 65M99, 35L65, 65Y20.

The dates will be set by the publisher.

1. Introduction

We consider the hyperbolic system of conservation laws:

$$\mathbf{U}_t + \mathbf{F}(\mathbf{U})_x = 0, \tag{1.1a}$$

$$\mathbf{U}(x,0) = \mathbf{U}_0(x), \tag{1.1b}$$

where $\mathbf{U} \in \mathbb{R}^N$ is the vector of conserved variables, $\mathbf{F}(\mathbf{U})$ is the flux function and $\mathbf{U}_0$ is the initial data. We are interested in solving (1.1) with an explicit finite volume method not limited by the CFL (Courant-Friedrichs-Lewy) condition.

A class of such methods has been proposed by LeVeque in a series of papers [13, 14, 15] in the 1980s. Therein, the Godunov scheme was extended to the LTS-Godunov scheme and applied to the Euler equations. The CFL condition is relaxed by allowing the waves from each Riemann problem to travel more than one cell during a single time step. Each wave is treated as a discontinuity, and the interactions between the waves are assumed to be linear. Through the years this idea has been used by a number of authors. For the shallow water equations, Murillo, Morales-Hernández and co-workers [27, 23, 25, 24, 26] applied the LTS-Roe scheme

Keywords and phrases: Large Time Step, HLL, HLLC, Euler equations, Riemann solver

* *The authors were supported by the Research Council of Norway (234126/30) through the SIMCOFLOW project.*

[1] Department of Energy and Process Engineering, Norwegian University of Science and Technology, Kolbjørn Hejes vei 2, NO-7491 Trondheim, Norway; e-mail: marin.prebeg@ntnu.no, marin.prebeg@gmail.com & bernhard.muller@ntnu.no

[2] SINTEF Materials and Chemistry, P. O. Box 4760 Sluppen, NO-7465 Trondheim, Norway; e-mail: toref@math.uio.no

and Xu et al. [41] applied the LTS-Godunov scheme. Further applications of the LTS-Godunov scheme include the 3D Euler equations by Qian and Lee [31], high speed combustion waves by Tang et al. [35], and Maxwell's equations by Makwana and Chatterjee [21]. Lindqvist and Lund [18] and Prebeg et al. [30] applied the LTS-Roe scheme to two-phase flow models. Lindqvist et al. [19] also studied the TVD properties of LTS methods and showed that the LTS-Roe scheme and the LTS-Lax-Friedrichs scheme are the least and most diffusive TVD LTS methods, respectively. All the methods discussed above share the feature of starting from a Godunov or Roe-type Riemann solver and extending it to the LTS framework. The goal of this paper is to establish a more general platform for LTS extensions of approximate Riemann solvers. In particular, we will construct the natural LTS extensions of the HLL and HLLC schemes, and quantify their level of numerical diffusion.

The original HLL scheme, proposed by Harten, Lax and van Leer [9] in the 1980s, assumes a two-wave structure of the solution and constructs the approximate Riemann solver by using estimates of the velocities of the slowest and the fastest waves. The choice for these velocity estimates has been studied for instance by Davis [4], Einfeldt and co-workers [5, 6] and Batten et al. [1]. The original HLL solver may poorly resolve certain physics in systems where the solution structure consists of more than two waves. For the Euler equations, Toro et al. [39] proposed the HLLC solver in which the contact discontinuity is reconstructed by assuming a three-wave structure of the solution. Today, HLL and HLLC solvers are widely used in a number of different fields, such as multiphase flow modeling [42, 37, 36, 28, 3, 2, 20] and magnetohydrodynamics [12, 22].

In this paper, we show how LeVeque's approach [15] may be directly used to derive LTS extensions of the HLL and HLLC schemes, denoted as LTS-HLL and LTS-HLLC, respectively. In section 2 we present our basic model and numerical framework. In section 3 we present the standard HLL scheme and extend it to the LTS framework. In particular, we write the scheme in numerical viscosity and flux-difference splitting form. Section 4 presents the LTS extension of the HLLC scheme. In section 5, we study in more detail the numerical diffusion of the LTS-HLL scheme. We provide a direct proof that the numerical viscosity coefficients satisfy the TVD property without any restriction on the time step. We also prove that for subsonic flows, the numerical diffusion for the contact wave increases monotonically with the time step. This is in contrast with previously investigated LTS methods [15, 23, 19], where the numerical diffusion will typically attain local minima for integer Courant numbers. In section 6 we present numerical investigations for the one-dimensional Euler equations. The resulting LTS-HLL(C) schemes are seen to improve the efficiency of standard HLL(C) schemes while also providing improved robustness compared to previously studied LTS methods. In section 7 we close with conclusions.

2. Preliminaries

2.1. Problem outline

As a special example of (1.1) we consider the Euler equations where the vector of conserved variables $\mathbf{U}$ and the flux function $\mathbf{F}(\mathbf{U})$ are defined as:

$$\mathbf{U} = \begin{pmatrix} \rho \\ \rho u \\ E \end{pmatrix}, \qquad \mathbf{F}(\mathbf{U}) = \begin{pmatrix} \rho u \\ \rho u^2 + p \\ u(E+p) \end{pmatrix}, \tag{2.1}$$

where ρ, u, E, p denote the density, velocity, total energy density and pressure, respectively. The system is closed by the relation for the total energy density, $E = \rho e + \rho u^2/2$, and an equation of state for perfect gas, $e = p/(\rho(\gamma - 1))$. Throughout the paper we will use $\gamma = 1.4$ for air. Alternatively, we can write (1.1) in a quasilinear form as:

$$\mathbf{U}_t + \mathbf{A}(\mathbf{U})\mathbf{U}_x = 0, \qquad \mathbf{A}(\mathbf{U}) = \partial\mathbf{F}(\mathbf{U})/\partial\mathbf{U}. \tag{2.2}$$

We assume that the system of equations (2.2) is hyperbolic, i.e. the Jacobian matrix $\mathbf{A}$ has real eigenvalues and linearly independent eigenvectors. The eigenvalues of the Euler system (2.1) are:

$$\lambda_1 = u - a, \quad \lambda_2 = u, \quad \lambda_3 = u + a, \tag{2.3}$$

where a is the speed of sound.

2.2. Numerical methods

We discretize (1.1) by the explicit Euler method in time and the finite volume method in space:

$$\mathbf{U}_j^{n+1} = \mathbf{U}_j^n - \frac{\Delta t}{\Delta x}\left(\mathbf{F}_{j+1/2}^n - \mathbf{F}_{j-1/2}^n\right), \tag{2.4}$$

where $\mathbf{U}_j^n$ is a piecewise constant approximation of $\mathbf{U}$ in the cell with center at x_j at time level n and $\mathbf{F}_{j+1/2}^n$ is a numerical approximation of the flux function at the cell interface $x_{j+1/2}$ at time level n.

2.2.1. *Standard 3-point methods*

In the case that the numerical flux depends only on the neighboring cell values, we can with no loss of generality write the scheme in the numerical viscosity form [7, 34]:

$$\mathbf{F}_{j+1/2}^n = \mathbf{F}\left(\mathbf{U}_j^n, \mathbf{U}_{j+1}^n\right) = \frac{1}{2}\left(\mathbf{F}_j^n + \mathbf{F}_{j+1}^n\right) - \frac{1}{2}\mathbf{Q}_{j+1/2}^n\left(\mathbf{U}_{j+1}^n - \mathbf{U}_j^n\right), \tag{2.5}$$

where $\mathbf{F}_j^n = \mathbf{F}\left(\mathbf{U}_j^n\right)$ and $\mathbf{Q}_{j+1/2}^n$ is the numerical viscosity matrix. To simplify the notation, the time level n will be implicitly assumed in the absence of a temporal index. The choice of the numerical viscosity matrix $\mathbf{Q}$ determines the finite volume method we use, i.e. for the Lax-Friedrichs scheme $\mathbf{Q}_{\text{LxF}} = \text{diag}(\Delta x/\Delta t)$, and for the Roe scheme $\mathbf{Q}_{\text{Roe}} = |\hat{\mathbf{A}}|$ where $\hat{\mathbf{A}}$ is the Roe matrix [32]. $\hat{\mathbf{A}}$ can be diagonalized as:

$$\hat{\mathbf{A}} = \hat{\mathbf{R}}\hat{\mathbf{\Lambda}}\hat{\mathbf{R}}^{-1}, \tag{2.6}$$

where $\hat{\mathbf{R}}$ is the matrix of right eigenvectors and $\hat{\mathbf{\Lambda}} = \text{diag}(\lambda_1, \ldots, \lambda_N)$ is the matrix of eigenvalues. We note that in the Lax-Friedrichs and the Roe schemes, the numerical viscosity matrix $\mathbf{Q}$ acts independently on each characteristic field. In that case, $\mathbf{Q}$ can be diagonalized as:

$$\mathbf{Q} = \hat{\mathbf{R}}\mathbf{\Omega}\hat{\mathbf{R}}^{-1}, \tag{2.7}$$

where $\mathbf{\Omega} = \text{diag}(\omega_1, \ldots, \omega_N)$ is the matrix of eigenvalues of $\mathbf{Q}$, and $\mathbf{Q}$ and $\hat{\mathbf{A}}$ have the same eigenvectors. The numerical viscosity matrices of the Lax-Friedrichs and the Roe scheme are then obtained by:

$$\mathbf{\Omega}_{\text{LxF}} = \frac{\Delta x}{\Delta t}\mathbf{I}, \quad \mathbf{\Omega}_{\text{Roe}} = |\hat{\mathbf{\Lambda}}|. \tag{2.8}$$

An alternative way to discretize (1.1) is with the flux-difference splitting:

$$\mathbf{U}_j^{n+1} = \mathbf{U}_j^n - \frac{\Delta t}{\Delta x}\left(\hat{\mathbf{A}}_{j-1/2}^+\left(\mathbf{U}_j^n - \mathbf{U}_{j-1}^n\right) + \hat{\mathbf{A}}_{j+1/2}^-\left(\mathbf{U}_{j+1}^n - \mathbf{U}_j^n\right)\right), \tag{2.9}$$

where $\hat{\mathbf{A}}^\pm$ represent a splitting of the Roe matrix (2.6) according to:

$$\hat{\mathbf{A}}^\pm = \hat{\mathbf{R}}\hat{\mathbf{\Lambda}}^\pm\hat{\mathbf{R}}^{-1}. \tag{2.10}$$

Herein, $\hat{\mathbf{\Lambda}}^\pm$ are obtained by transforming each diagonal entry of $\hat{\mathbf{\Lambda}}$:

$$\lambda_{\text{LxF}}^\pm = \frac{1}{2}\left(\lambda \pm \frac{\Delta x}{\Delta t}\right), \quad \lambda_{\text{Roe}}^\pm = \pm\max(0, \pm\lambda). \tag{2.11}$$

For 3-point methods, the size of the time step in discretizations (2.5) and (2.9) is limited by the CFL condition:

$$C = \max_{p,x} |\lambda_p(x,t)| \frac{\Delta t}{\Delta x} \leq 1, \tag{2.12}$$

where λ_p are the eigenvalues of the Jacobian matrix $\mathbf{A}$ in (2.2). In this paper, we consider explicit methods that are not limited by the constraint (2.12).

2.2.2. *Large Time Step methods*

The natural LTS extension of the numerical viscosity formulation (2.5) is (see [19]):

$$\mathbf{F}_{j+1/2} = \frac{1}{2}\left(\mathbf{F}_j + \mathbf{F}_{j+1}\right) - \frac{1}{2}\sum_{i=-\infty}^{\infty} \mathbf{Q}^i_{j+1/2+i} \Delta \mathbf{U}_{j+1/2+i}, \tag{2.13}$$

and the natural LTS extension of the flux-difference splitting formulation (2.9) is (see [19]):

$$\mathbf{U}_j^{n+1} = \mathbf{U}_j - \frac{\Delta t}{\Delta x}\sum_{i=0}^{\infty}\left(\hat{\mathbf{A}}^{i+}_{j-1/2-i}\Delta \mathbf{U}_{j-1/2-i} + \hat{\mathbf{A}}^{i-}_{j+1/2+i}\Delta \mathbf{U}_{j+1/2+i}\right), \tag{2.14}$$

where we introduced the notation $\Delta \mathbf{U}_{j+1/2} = \mathbf{U}_{j+1} - \mathbf{U}_j$. We note that (2.13) differs from [19] in a sense that we scale $\mathbf{Q}^i$ with $\Delta x/\Delta t$. Herein, the upper indices denote the relative cell interface position. These will be further clarified in section 3.2. Lindqvist et al. [19] provided the partial viscosity coefficients $\mathbf{Q}^i$ and the flux-difference splitting coefficients $\hat{\mathbf{A}}^{i\pm}$ for the LTS-Godunov, LTS-Roe and LTS-Lax-Friedrichs schemes. For the LTS-Roe scheme [19], the partial viscosity coefficients are defined through the eigenvalues of $\mathbf{Q}^i$:

$$\mathbf{Q}^i_{j+1/2} = \left(\hat{\mathbf{R}}\mathbf{\Omega}^i\hat{\mathbf{R}}^{-1}\right)_{j+1/2}, \tag{2.15}$$

where the eigenvalues are defined as:

$$\omega^0_{\text{Roe}} = |\lambda|, \tag{2.16a}$$

$$\omega^{\mp i}_{\text{Roe}} = 2\max\left(0, \pm\lambda - i\frac{\Delta x}{\Delta t}\right), \quad \text{for } i > 0, \tag{2.16b}$$

and the flux-difference splitting coefficients are defined through the eigenvalues of $\hat{\mathbf{A}}^{i\pm}$:

$$\hat{\mathbf{A}}^{i\pm}_{j+1/2} = \left(\hat{\mathbf{R}}\hat{\mathbf{\Lambda}}^{i\pm}\hat{\mathbf{R}}^{-1}\right)_{j+1/2}, \tag{2.17}$$

where the eigenvalues are defined as:

$$\lambda^{i\pm}_{\text{Roe}} = \pm\max\left(0, \min\left(\pm\lambda - i\frac{\Delta x}{\Delta t}, \frac{\Delta x}{\Delta t}\right)\right). \tag{2.18}$$

In the following section we determine these coefficients for the LTS-HLL scheme.

3. LTS-HLL scheme

We start by presenting the standard HLL scheme of Harten et al. [9]. Then we formulate the natural LTS extension of the HLL scheme and provide explicit expressions for the flux-difference splitting and the numerical viscosity coefficients.

3.1. **The standard HLL scheme**

We consider the cell interface Riemann problem:

$$\mathbf{U}(x,0) = \begin{cases} \mathbf{U}_j & \text{if} \quad x < 0, \\ \mathbf{U}_{j+1} & \text{if} \quad x > 0. \end{cases} \tag{3.1}$$

The original HLL scheme by Harten et al. [9] solves the Riemann problem approximately by assuming a single state between the left and right states:

$$\widetilde{\mathbf{U}}(x/t) = \begin{cases} \mathbf{U}_j & \text{if} \quad x < S_{\mathrm{L}} t, \\ \mathbf{U}^{\mathrm{HLL}}_{j+1/2} & \text{if} \quad S_{\mathrm{L}} t < x < S_{\mathrm{R}} t, \\ \mathbf{U}_{j+1} & \text{if} \quad x > S_{\mathrm{R}} t, \end{cases} \tag{3.2}$$

where S_{L} and S_{R} are approximations of the smallest and the largest wave velocities at the interface $x_{j+1/2}$. As for now, we leave these unspecified and return to them in section 6. The intermediate state $\mathbf{U}^{\mathrm{HLL}}_{j+1/2}$ is defined such that the Riemann solver is consistent with the integral form of the conservation law (1.1), see [9, 5]:

$$\mathbf{U}^{\mathrm{HLL}}_{j+1/2} = \frac{S_{\mathrm{R}}\mathbf{U}_{j+1} - S_{\mathrm{L}}\mathbf{U}_j + \mathbf{F}_j - \mathbf{F}_{j+1}}{S_{\mathrm{R}} - S_{\mathrm{L}}}. \tag{3.3}$$

Next, we use $\mathbf{U}^{\mathrm{HLL}}_{j+1/2}$ to determine the flux function $\mathbf{F}_{j+1/2}$. This is defined as:

$$\mathbf{F}_{j+1/2} = \begin{cases} \mathbf{F}_j & \text{if} \quad 0 < S_{\mathrm{L}}, \\ \mathbf{F}^{\mathrm{HLL}}_{j+1/2} & \text{if} \quad S_{\mathrm{L}} < 0 < S_{\mathrm{R}}, \\ \mathbf{F}_{j+1} & \text{if} \quad 0 > S_{\mathrm{R}}. \end{cases} \tag{3.4}$$

In the interesting case, $S_{\mathrm{L}} < 0 < S_{\mathrm{R}}$, the flux function has the form [38]:

$$\mathbf{F}^{\mathrm{HLL}}_{j+1/2} = \mathbf{F}_j + S_{\mathrm{L}}\left(\mathbf{U}^{\mathrm{HLL}}_{j+1/2} - \mathbf{U}_j\right), \tag{3.5}$$

$$\mathbf{F}^{\mathrm{HLL}}_{j+1/2} = \mathbf{F}_{j+1} + S_{\mathrm{R}}\left(\mathbf{U}^{\mathrm{HLL}}_{j+1/2} - \mathbf{U}_{j+1}\right). \tag{3.6}$$

These two equations are equivalent and by using (3.3) in any of them we obtain:

$$\mathbf{F}^{\mathrm{HLL}}_{j+1/2} = \frac{S_{\mathrm{R}}\mathbf{F}_j - S_{\mathrm{L}}\mathbf{F}_{j+1} + S_{\mathrm{L}}S_{\mathrm{R}}\left(\mathbf{U}_{j+1} - \mathbf{U}_j\right)}{S_{\mathrm{R}} - S_{\mathrm{L}}}. \tag{3.7}$$

Further, the equations (3.4) and (3.7) can be written more compactly as:

$$\mathbf{F}_{j+1/2} = \frac{S^+_{\mathrm{R}}\mathbf{F}_j - S^-_{\mathrm{L}}\mathbf{F}_{j+1} + S^-_{\mathrm{L}}S^+_{\mathrm{R}}\left(\mathbf{U}_{j+1} - \mathbf{U}_j\right)}{S^+_{\mathrm{R}} - S^-_{\mathrm{L}}}, \tag{3.8}$$

where $S^-_{\mathrm{L}} = \min(S_{\mathrm{L}}, 0)$ and $S^+_{\mathrm{R}} = \max(S_{\mathrm{R}}, 0)$. Equation (3.8) is then used in (2.4). For more information and more detailed derivation we refer to [9, 4, 5, 1, 38]. Einfeldt [5] showed that the numerical flux (3.8) can be recovered from the numerical viscosity framework (2.5) by setting:

$$\mathbf{Q}_{\mathrm{HLL}} = \frac{S^+_{\mathrm{R}} + S^-_{\mathrm{L}}}{S^+_{\mathrm{R}} - S^-_{\mathrm{L}}}\hat{\mathbf{A}} - 2\frac{S^-_{\mathrm{L}}S^+_{\mathrm{R}}}{S^+_{\mathrm{R}} - S^-_{\mathrm{L}}}\mathbf{I}. \tag{3.9}$$

Following the framework introduced in (2.8), we define the HLL scheme through the diagonal entries of $\mathbf{\Omega}$ as:

$$\omega_{\text{HLL}} = \frac{S_{\text{R}}^{+}(\lambda - S_{\text{L}}^{-}) - S_{\text{L}}^{-}(S_{\text{R}}^{+} - \lambda)}{S_{\text{R}}^{+} - S_{\text{L}}^{-}} = \frac{|S_{\text{R}}|\,(\lambda - S_{\text{L}}) + |S_{\text{L}}|\,(S_{\text{R}} - \lambda)}{S_{\text{R}} - S_{\text{L}}}. \tag{3.10}$$

The HLL scheme can also be written in the flux-difference splitting framework (2.11) by modifying the diagonal entries of $\hat{\mathbf{\Lambda}}^{\pm}$ as:

$$\lambda_{\text{HLL}}^{+} = \frac{\lambda - S_{\text{L}}^{-}}{S_{\text{R}}^{+} - S_{\text{L}}^{-}} S_{\text{R}}^{+} = \frac{\lambda - S_{\text{L}}}{S_{\text{R}} - S_{\text{L}}} S_{\text{R}}^{+} + \frac{S_{\text{R}} - \lambda}{S_{\text{R}} - S_{\text{L}}} S_{\text{L}}^{+}, \tag{3.11}$$

$$\lambda_{\text{HLL}}^{-} = \frac{S_{\text{R}}^{+} - \lambda}{S_{\text{R}}^{+} - S_{\text{L}}^{-}} S_{\text{L}}^{-} = \frac{\lambda - S_{\text{L}}}{S_{\text{R}} - S_{\text{L}}} S_{\text{R}}^{-} + \frac{S_{\text{R}} - \lambda}{S_{\text{R}} - S_{\text{L}}} S_{\text{L}}^{-}. \tag{3.12}$$

3.2. **The LTS-HLL scheme**

We want to construct the LTS extension of the numerical flux function (3.8). Consider the Figure 1a and the Riemann problem at the interface $x_{j+1/2}$. First, we consider the wave structure when $C \leq 1$, denoted in Figure 1b as $\Delta t^{\text{non-LTS}}$. In this case, the Riemann problem at $x_{j+1/2}$ is completely defined by $\mathbf{U}_j, \mathbf{U}_{j+1}$ and velocities $S_{\text{L},j+1/2}$ and $S_{\text{R},j+1/2}$ being emitted from the interface $x_{j+1/2}$, see (3.2)–(3.8). Next, we consider the case when $C > 1$, denoted in Figure 1b as Δt^{LTS}. For this case, the wave emitted from the interface $x_{j-1/2}$ and associated with velocity $S_{\text{R},j-1/2}$ passes through the interface $x_{j+1/2}$.

This wave violates the CFL condition (2.12) since we allowed the wave to travel more than one cell during a single time step. However, we may relax the CFL condition (2.12) if we modify (3.8) by taking into account this additional contribution. We start by assuming that the interactions between the waves are linear and we note that:

- The flux function (3.8) at the interface $x_{j+1/2}$ is increased by the contribution from the *jump 2* moving to the right with the velocity $S_{\text{R},j-1/2}$.
- The contribution from the *jump 2* does not start passing through the interface $x_{j+1/2}$ immediately, i.e. it has to travel through the cell x_j before it starts to pass through the interface $x_{j+1/2}$.

Based on this, we modify (3.8) as:

$$\mathbf{F}_{j+1/2}^{\text{LTS-HLL}} = \mathbf{F}_{j+1/2}^{0} + S_{\text{R},j-1/2}^{-1}\left(\mathbf{U}_{j-1/2}^{\text{HLL}} - \mathbf{U}_j\right), \tag{3.13}$$

where we denoted (3.8) as $\mathbf{F}_{j+1/2}^{0}$, and:

$$S_{\text{R},j-1/2}^{-1} = S_{\text{R},j-1/2} - \frac{\Delta x}{\Delta t}. \tag{3.14}$$

The purpose of this modification is to take into the account the fact that the wave has to travel one cell before it starts contributing to the flux function (3.13). In the general case, we allow for an arbitrarily large time step size Δt, therefore allowing the waves to travel several cells during a single time step. In addition, we note that each interface may emit waves where each of the local wave speeds S_{L} and S_{R} may be either negative, zero or positive. Therefore, the general formula for the flux function of the LTS-HLL scheme has the form:

$$\mathbf{F}_{j+1/2}^{\text{LTS-HLL}} = \mathbf{F}_{j+1/2}^{0} + \sum_{i=1}^{\infty} \mathbf{F}_{j+1/2-i}^{-i} + \sum_{i=1}^{\infty} \mathbf{F}_{j+1/2+i}^{+i}, \tag{3.15}$$

where the additional terms under the sum signs represent the information reaching the interface $x_{j+1/2}$ from neighboring Riemann problems on the left and on the right, respectively. The newly introduced terms in (3.15)

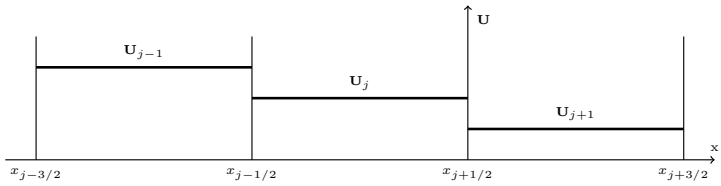

(A) Riemann problems at $x_{j-1/2}$ and $x_{j+1/2}$

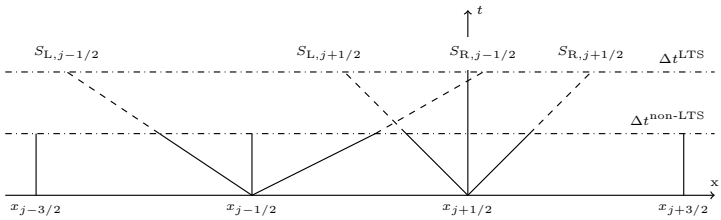

(B) Characteristics with slopes $\mathrm{d}x(t)/\mathrm{d}t = S_{\mathrm{L,R}}$ at $x_{j\mp1/2}$

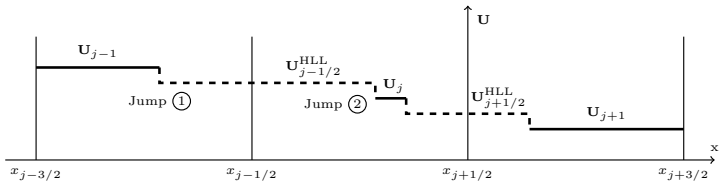

(C) Approximate solutions of Riemann problems at $x_{j\mp1/2}$ with HLL scheme

FIGURE 1. Wave structure in the LTS-HLL scheme

are:

$$\mathbf{F}^{-i}_{j+1/2-i} = S^{-i}_{\mathrm{R},j+1/2-i}\left(\mathbf{U}^{\mathrm{HLL}}_{j+1/2-i} - \mathbf{U}_{j+1-i}\right) + S^{-i}_{\mathrm{L},j+1/2-i}\left(\mathbf{U}_{j-i} - \mathbf{U}^{\mathrm{HLL}}_{j+1/2-i}\right), \tag{3.16}$$

$$\mathbf{F}^{+i}_{j+1/2+i} = S^{+i}_{\mathrm{L},j+1/2+i}\left(\mathbf{U}^{\mathrm{HLL}}_{j+1/2+i} - \mathbf{U}_{j+i}\right) + S^{+i}_{\mathrm{R},j+1/2+i}\left(\mathbf{U}_{j+1+i} - \mathbf{U}^{\mathrm{HLL}}_{j+1/2+i}\right), \tag{3.17}$$

where the modified wave velocities are:

$$S^{-i}_{[\mathrm{L,R}],j+1/2-i} = \max\left(S_{[\mathrm{L,R}],j+1/2-i} - i\frac{\Delta x}{\Delta t}, 0\right), \tag{3.18a}$$

$$S^{+i}_{[\mathrm{L,R}],j+1/2+i} = \min\left(S_{[\mathrm{L,R}],j+1/2+i} + i\frac{\Delta x}{\Delta t}, 0\right). \tag{3.18b}$$

Equation (3.15) is then used in (2.4).

3.2.1. *The LTS-HLL scheme in numerical viscosity form*

We can now write the LTS-HLL scheme in the numerical viscosity form (2.13).

Proposition 1. *Given the Roe matrix:*

$$\hat{\mathbf{A}}_{j+1/2} = \left(\hat{\mathbf{R}}\hat{\mathbf{\Lambda}}\hat{\mathbf{R}}^{-1}\right)_{j+1/2} \quad \forall j, \tag{3.19}$$

where $\hat{\mathbf{\Lambda}}$ *is the diagonal matrix of eigenvalues, the LTS-HLL scheme defined by* (3.13)–(3.18) *can be written in the numerical viscosity form* (2.13) *with coefficients:*

$$\mathbf{Q}^i_{j+1/2} = \left(\hat{\mathbf{R}}\mathbf{\Omega}^i\hat{\mathbf{R}}^{-1}\right)_{j+1/2}, \tag{3.20}$$

where $\mathbf{\Omega}^i(\hat{\mathbf{\Lambda}}, S_{\mathrm{L}}, S_{\mathrm{R}})$ *is the diagonal matrix with entries given by:*

$$\omega^0_{HLL} = \frac{|S_{\mathrm{R}}|\,(\lambda - S_{\mathrm{L}}) + |S_{\mathrm{L}}|\,(S_{\mathrm{R}} - \lambda)}{S_{\mathrm{R}} - S_{\mathrm{L}}}, \tag{3.21a}$$

$$\omega^{\mp i}_{HLL} = 2\frac{\lambda - S_{\mathrm{L}}}{S_{\mathrm{R}} - S_{\mathrm{L}}}\max\left(0, \pm S_{\mathrm{R}} - i\frac{\Delta x}{\Delta t}\right) + 2\frac{S_{\mathrm{R}} - \lambda}{S_{\mathrm{R}} - S_{\mathrm{L}}}\max\left(0, \pm S_{\mathrm{L}} - i\frac{\Delta x}{\Delta t}\right) \quad \textit{for} \quad i > 0. \tag{3.21b}$$

Proof. The coefficient $\mathbf{Q}^0$ has already been determined by (3.9). We obtain the coefficients $\mathbf{Q}^i$ for $i \neq 0$ by equalizing (2.13) and (3.15), while using the Roe condition [32]:

$$\hat{\mathbf{A}}_{j+1/2}\,(\mathbf{U}_{j+1} - \mathbf{U}_j) = \mathbf{F}(\mathbf{U}_{j+1}) - \mathbf{F}(\mathbf{U}_j). \tag{3.22}$$

□

We point out the similarity of the LTS-HLL partial viscosity coefficients (3.21) to the partial viscosity coefficients of the LTS-Roe scheme (2.16).

3.2.2. *The LTS-HLL scheme in flux-difference splitting form*

We have built the LTS-HLL scheme by heuristic arguments as an extension of the standard HLL scheme, following LeVeque's general approach of treating all wave interactions as linear [15]. We now derive the flux-difference splitting formulation in a more formal way, starting with LeVeque's general updating formula [15]:

$$\mathbf{U}^{n+1}_j = \frac{\Delta t}{\Delta x}\sum_{i=-\infty}^{\infty}\int_{(i-1)\frac{\Delta x}{\Delta t}}^{i\frac{\Delta x}{\Delta t}} \widetilde{\mathbf{U}}_{j+1/2-i}(\zeta_i)\,\mathrm{d}\zeta_i - \sum_{\ell=-\infty}^{\infty}\mathbf{U}_\ell, \tag{3.23}$$

where $\widetilde{\mathbf{U}}_{j+1/2-i}(\zeta_i)$ is the solution to the Riemann problem at $x_{j+1/2-i}$. Herein:

$$\zeta_i = \frac{x - x_{j+1/2-i}}{t - t^n}. \tag{3.24}$$

Proposition 2. *Given the Roe matrix:*

$$\hat{\mathbf{A}}_{j+1/2} = \left(\hat{\mathbf{R}}\hat{\mathbf{\Lambda}}\hat{\mathbf{R}}^{-1}\right)_{j+1/2} \quad \forall j, \tag{3.25}$$

where $\hat{\mathbf{\Lambda}}$ *is the diagonal matrix of eigenvalues, the LTS-HLL scheme can be written in the flux-difference splitting form* (2.14) *with coefficients:*

$$\hat{\mathbf{A}}^{i\pm}_{j+1/2} = \left(\hat{\mathbf{R}}\hat{\mathbf{\Lambda}}^{i\pm}\hat{\mathbf{R}}^{-1}\right)_{j+1/2}, \tag{3.26}$$

where $\hat{\mathbf{\Lambda}}^{i\pm}(\hat{\mathbf{\Lambda}}, S_{\mathrm{L}}, S_{\mathrm{R}})$ *is the diagonal matrix with entries given by:*

$$\lambda^{i\pm}_{HLL} = \pm\frac{\lambda - S_{\mathrm{L}}}{S_{\mathrm{R}} - S_{\mathrm{L}}}\max\left(0, \min\left(\pm S_{\mathrm{R}} - i\frac{\Delta x}{\Delta t}, \frac{\Delta x}{\Delta t}\right)\right) \pm \frac{S_{\mathrm{R}} - \lambda}{S_{\mathrm{R}} - S_{\mathrm{L}}}\max\left(0, \min\left(\pm S_{\mathrm{L}} - i\frac{\Delta x}{\Delta t}, \frac{\Delta x}{\Delta t}\right)\right). \quad (3.27)$$

Proof. The HLL Riemann solver (3.2) can be written as:

$$\widetilde{\mathbf{U}}_{j+1/2}(\zeta) = \mathbf{U}_j + H(\zeta - S_{\mathrm{L}})\left(\mathbf{U}^{\mathrm{HLL}}_{j+1/2} - \mathbf{U}_j\right) + H(\zeta - S_{\mathrm{R}})\left(\mathbf{U}_{j+1} - \mathbf{U}^{\mathrm{HLL}}_{j+1/2}\right) \quad (3.28a)$$

$$= \mathbf{U}_{j+1} - H(S_{\mathrm{L}} - \zeta)\left(\mathbf{U}^{\mathrm{HLL}}_{j+1/2} - \mathbf{U}_j\right) - H(S_{\mathrm{R}} - \zeta)\left(\mathbf{U}_{j+1} - \mathbf{U}^{\mathrm{HLL}}_{j+1/2}\right), \quad (3.28b)$$

where H is the Heaviside function. Using (3.3) we can rewrite this as:

$$\widetilde{\mathbf{U}}_{j+1/2}(\zeta) = \mathbf{U}_j + \left(\frac{H(\zeta - S_{\mathrm{L}})}{S_{\mathrm{R}} - S_{\mathrm{L}}}(\mathbf{S}_{\mathrm{R}} - \hat{\mathbf{A}}) + \frac{H(\zeta - S_{\mathrm{R}})}{S_{\mathrm{R}} - S_{\mathrm{L}}}(\hat{\mathbf{A}} - \mathbf{S}_{\mathrm{L}})\right)(\mathbf{U}_{j+1} - \mathbf{U}_j) \quad (3.29a)$$

$$= \mathbf{U}_{j+1} - \left(\frac{H(S_{\mathrm{L}} - \zeta)}{S_{\mathrm{R}} - S_{\mathrm{L}}}(\mathbf{S}_{\mathrm{R}} - \hat{\mathbf{A}}) + \frac{H(S_{\mathrm{R}} - \zeta)}{S_{\mathrm{R}} - S_{\mathrm{L}}}(\hat{\mathbf{A}} - \mathbf{S}_{\mathrm{L}})\right)(\mathbf{U}_{j+1} - \mathbf{U}_j), \quad (3.29b)$$

where $\mathbf{S}_{\mathrm{L}} = S_{\mathrm{L}}\mathbf{I}$ and $\mathbf{S}_{\mathrm{R}} = S_{\mathrm{R}}\mathbf{I}$. We then use (3.29a) in (3.23) and note that for $i \leq 0$ we can write:

$$\int_{(i-1)\frac{\Delta x}{\Delta t}}^{i\frac{\Delta x}{\Delta t}} \widetilde{\mathbf{U}}_{j+1/2-i}(\zeta_i)\,\mathrm{d}\zeta_i = \frac{\Delta x}{\Delta t}\mathbf{U}_{j-i} - \hat{\mathbf{A}}^{(-i)-}_{j+1/2-i}\left(\mathbf{U}_{j+1-i} - \mathbf{U}_{j-i}\right), \quad (3.30)$$

where:

$$\hat{\mathbf{A}}^{i-} = \hat{\mathbf{R}}\hat{\mathbf{\Lambda}}^{i-}\hat{\mathbf{R}}^{-1}, \quad (3.31)$$

and $\hat{\mathbf{\Lambda}}^{i-}$ is the diagonal matrix with values:

$$\lambda^{i-} = \frac{\lambda - S_{\mathrm{L}}}{S_{\mathrm{R}} - S_{\mathrm{L}}}\min\left(0, \max\left(S_{\mathrm{R}} + i\frac{\Delta x}{\Delta t}, -\frac{\Delta x}{\Delta t}\right)\right) + \frac{S_{\mathrm{R}} - \lambda}{S_{\mathrm{R}} - S_{\mathrm{L}}}\min\left(0, \max\left(S_{\mathrm{L}} + i\frac{\Delta x}{\Delta t}, -\frac{\Delta x}{\Delta t}\right)\right). \quad (3.32)$$

Similarly, we use (3.29b) in (3.23) and note that for $i \geq 1$ we can write:

$$\int_{(i-1)\frac{\Delta x}{\Delta t}}^{i\frac{\Delta x}{\Delta t}} \widetilde{\mathbf{U}}_{j+1/2-i}(\zeta_i)\,\mathrm{d}\zeta_i = \frac{\Delta x}{\Delta t}\mathbf{U}_{j+1-i} - \hat{\mathbf{A}}^{(i-1)+}_{j+1/2-i}\left(\mathbf{U}_{j+1-i} - \mathbf{U}_{j-i}\right), \quad (3.33)$$

where:

$$\hat{\mathbf{A}}^{i+} = \hat{\mathbf{R}}\hat{\mathbf{\Lambda}}^{i+}\hat{\mathbf{R}}^{-1}, \quad (3.34)$$

and $\hat{\mathbf{\Lambda}}^{i+}$ is the diagonal matrix with values:

$$\lambda^{i+} = \frac{\lambda - S_{\mathrm{L}}}{S_{\mathrm{R}} - S_{\mathrm{L}}}\max\left(0, \min\left(S_{\mathrm{R}} - i\frac{\Delta x}{\Delta t}, \frac{\Delta x}{\Delta t}\right)\right) + \frac{S_{\mathrm{R}} - \lambda}{S_{\mathrm{R}} - S_{\mathrm{L}}}\max\left(0, \min\left(S_{\mathrm{L}} - i\frac{\Delta x}{\Delta t}, \frac{\Delta x}{\Delta t}\right)\right). \quad (3.35)$$

Substituting (3.30) and (3.33) into (3.23) we recover the LTS flux-difference splitting equation (2.14). □

We point out the similarity of the LTS-HLL flux-difference splitting coefficients (3.27) to the flux-difference splitting coefficients of the LTS-Roe scheme (2.18).

Proposition 3. *The flux-difference splitting formulation* (3.26)–(3.27) *and the numerical viscosity formulation* (3.20)–(3.21) *are equivalent.*

Proof. Lindqvist et al. [19] derived the following one-to-one mapping between the numerical viscosity and flux-difference splitting coefficients:

$$\mathbf{A}^{0\pm} = \frac{1}{2}\left(\mathbf{A} \pm \mathbf{Q}^{0} \mp \mathbf{Q}^{\mp 1}\right), \quad \mathbf{A}^{i\pm} = \pm\frac{1}{2}\left(\mathbf{Q}^{\mp i} - \mathbf{Q}^{\mp(i+1)}\right). \tag{3.36}$$

By using(3.20)–(3.21) in (3.36) we obtain (3.26)–(3.27). □

4. LTS-HLLC scheme

In this section we propose a direct extension from the HLLC scheme to the LTS-HLLC scheme, following the approaches from section 3.

4.1. **Standard HLLC scheme**

We recall that the standard HLL scheme assumes a two wave structure of the solution with a single, uniform state $\mathbf{U}^{\mathrm{HLL}}$ between the waves. This is a correct assumption for hyperbolic systems consisting of only two equations (such as the one-dimensional shallow water equations). However, for the Euler equations this assumption leads to neglecting the contact discontinuity. The approach to recover the missing contact discontinuity was first presented by Toro et al. [39]. Herein, we outline an approach to reconstruct the missing wave following the approach described by Toro in [38].

The standard HLLC scheme is given in the form similar to the HLL scheme defined by equations (3.2) and (3.4), but with the state $\mathbf{U}^{\mathrm{HLL}}$ being split into two states separated by a contact discontinuity:

$$\widetilde{\mathbf{U}}(x/t) = \begin{cases} \mathbf{U}_j & \text{if} \quad x < S_{\mathrm{L}}t, \\ \mathbf{U}_{\mathrm{L}}^{\mathrm{HLLC}} & \text{if} \quad S_{\mathrm{L}}t < x < S_{\mathrm{C}}t, \\ \mathbf{U}_{\mathrm{R}}^{\mathrm{HLLC}} & \text{if} \quad S_{\mathrm{C}}t < x < S_{\mathrm{R}}t, \\ \mathbf{U}_{j+1} & \text{if} \quad x > S_{\mathrm{R}}t. \end{cases} \tag{4.1}$$

Based on this, the numerical flux function is defined as:

$$\mathbf{F}_{j+1/2} = \begin{cases} \mathbf{F}_j & \text{if} \quad 0 < S_{\mathrm{L}}, \\ \mathbf{F}_{\mathrm{L},j+1/2}^{\mathrm{HLLC}} & \text{if} \quad S_{\mathrm{L}} < 0 < S_{\mathrm{C}}, \\ \mathbf{F}_{\mathrm{R},j+1/2}^{\mathrm{HLLC}} & \text{if} \quad S_{\mathrm{C}} < 0 < S_{\mathrm{R}}, \\ \mathbf{F}_{j+1} & \text{if} \quad 0 > S_{\mathrm{R}}. \end{cases} \tag{4.2}$$

In the interesting case, $S_{\mathrm{L}} < 0 < S_{\mathrm{R}}$, the numerical flux function has the form:

$$\mathbf{F}_{\mathrm{L},j+1/2}^{\mathrm{HLLC}} = \mathbf{F}_j + S_{\mathrm{L}}\left(\mathbf{U}_{\mathrm{L},j+1/2}^{\mathrm{HLLC}} - \mathbf{U}_j\right), \tag{4.3}$$

$$\mathbf{F}_{\mathrm{R},j+1/2}^{\mathrm{HLLC}} = \mathbf{F}_{j+1} + S_{\mathrm{R}}\left(\mathbf{U}_{\mathrm{R},j+1/2}^{\mathrm{HLLC}} - \mathbf{U}_{j+1}\right), \tag{4.4}$$

where the intermediate states are determined according to [38]:

$$\mathbf{U}_{\mathrm{K}}^{\mathrm{HLLC}} = \rho_{\mathrm{K}}\left(\frac{S_{\mathrm{K}} - u_{\mathrm{K}}}{S_{\mathrm{K}} - S_{\mathrm{C}}}\right)\begin{bmatrix} 1 \\ S_{\mathrm{C}} \\ \frac{E_{\mathrm{K}}}{\rho_{\mathrm{K}}} + (S_{\mathrm{C}} - u_{\mathrm{K}})\left(S_{\mathrm{C}} + \frac{p_{\mathrm{K}}}{\rho_{\mathrm{K}}(S_{\mathrm{K}} - u_{\mathrm{K}})}\right) \end{bmatrix}, \tag{4.5}$$

where index K denotes left (L) or right (R) state in (4.1). The contact discontinuity velocity is given by [38]:

$$S_{\mathrm{C}} = \frac{p_{\mathrm{R}} - p_{\mathrm{L}} + \rho_{\mathrm{L}} u_{\mathrm{L}}(S_{\mathrm{L}} - u_{\mathrm{L}}) - \rho_{\mathrm{R}} u_{\mathrm{R}}(S_{\mathrm{R}} - u_{\mathrm{R}})}{\rho_{\mathrm{L}}(S_{\mathrm{L}} - u_{\mathrm{L}}) - \rho_{\mathrm{R}}(S_{\mathrm{R}} - u_{\mathrm{R}})}. \tag{4.6}$$

For details on the derivation of these formulae we refer to the book by Toro [38].

4.2. **LTS-HLLC scheme**

Following the approaches of section 3, we obtain the following expression for the numerical flux to be used in (2.4):

Proposition 4. *The numerical flux of the LTS-HLLC scheme* (4.2) *is:*

$$\mathbf{F}^{LTS\text{-}HLLC}_{j+1/2} = \mathbf{F}^{0}_{j+1/2} + \sum_{i=1}^{\infty} \mathbf{F}^{-i}_{j+1/2-i} + \sum_{i=1}^{\infty} \mathbf{F}^{+i}_{j+1/2+i}, \tag{4.7}$$

where $\mathbf{F}^{0}_{j+1/2}$ *is the standard HLLC flux given by* (4.2)*, and the additional terms are:*

$$\begin{aligned}
\mathbf{F}^{-i}_{j+1/2-i} &= S^{-i}_{R,j+1/2-i}\left(\mathbf{U}^{HLLC}_{R,j+1/2-i} - \mathbf{U}_{j+1-i}\right) \\
&\quad + S^{-i}_{C,j+1/2-i}\left(\mathbf{U}^{HLLC}_{L,j+1/2-i} - \mathbf{U}^{HLLC}_{R,j+1/2-i}\right) \\
&\quad + S^{-i}_{L,j+1/2-i}\left(\mathbf{U}_{j-i} - \mathbf{U}^{HLLC}_{L,j+1/2-i}\right), \qquad (4.8) \\
\mathbf{F}^{+i}_{j+1/2+i} &= S^{+i}_{L,j+1/2+i}\left(\mathbf{U}^{HLLC}_{L,j+1/2+i} - \mathbf{U}_{j+i}\right) \\
&\quad + S^{+i}_{C,j+1/2+i}\left(\mathbf{U}^{HLLC}_{R,j+1/2+i} - \mathbf{U}^{HLLC}_{L,j+1/2+i}\right) \\
&\quad + S^{+i}_{R,j+1/2+i}\left(\mathbf{U}_{j+1+i} - \mathbf{U}^{HLLC}_{R,j+1/2+i}\right). \qquad (4.9)
\end{aligned}$$

Herein, the modified velocities are:

$$S^{-i}_{[L,C,R],j+1/2-i} = \max\left(S_{[L,C,R],j+1/2-i} - i\frac{\Delta x}{\Delta t}, 0\right), \tag{4.10}$$

$$S^{+i}_{[L,C,R],j+1/2+i} = \min\left(S_{[L,C,R],j+1/2+i} + i\frac{\Delta x}{\Delta t}, 0\right). \tag{4.11}$$

Proof. The HLLC Riemann solver (4.1) can be written as:

$$\begin{aligned}
\widetilde{\mathbf{U}}_{j+1/2}(\zeta) = \mathbf{U}_j &+ H(\zeta - S_{\mathrm{L}})\left(\mathbf{U}^{\mathrm{HLLC}}_{\mathrm{L}} - \mathbf{U}_j\right) \\
&+ H(\zeta - S_{\mathrm{C}})\left(\mathbf{U}^{\mathrm{HLLC}}_{\mathrm{R}} - \mathbf{U}^{\mathrm{HLLC}}_{\mathrm{L}}\right) + H(\zeta - S_{\mathrm{R}})\left(\mathbf{U}_{j+1} - \mathbf{U}^{\mathrm{HLLC}}_{\mathrm{R}}\right), \qquad (4.12)
\end{aligned}$$

or equivalently:

$$\begin{aligned}
\widetilde{\mathbf{U}}_{j+1/2}(\zeta) = \mathbf{U}_{j+1} &- H(S_{\mathrm{L}} - \zeta)\left(\mathbf{U}^{\mathrm{HLLC}}_{\mathrm{L}} - \mathbf{U}_j\right) \\
&- H(S_{\mathrm{C}} - \zeta)\left(\mathbf{U}^{\mathrm{HLLC}}_{\mathrm{R}} - \mathbf{U}^{\mathrm{HLLC}}_{\mathrm{L}}\right) - H(S_{\mathrm{R}} - \zeta)\left(\mathbf{U}_{j+1} - \mathbf{U}^{\mathrm{HLLC}}_{\mathrm{R}}\right), \qquad (4.13)
\end{aligned}$$

where H is the Heaviside function and ζ is given by (3.24). We then use (4.12) in (3.23) and note that for $i \leq 0$ we can write:

$$\begin{aligned}\int_{(i-1)\frac{\Delta x}{\Delta t}}^{i\frac{\Delta x}{\Delta t}} \widetilde{\mathbf{U}}_{j+1/2-i}(\zeta_i)\,\mathrm{d}\zeta_i = \frac{\Delta x}{\Delta t}\mathbf{U}_{j-i} \\ + \left(\min\left(0, S_{\mathrm{L}} - (i-1)\frac{\Delta x}{\Delta t}\right) - \min\left(0, S_{\mathrm{L}} - i\frac{\Delta x}{\Delta t}\right)\right)\left(\mathbf{U}_{\mathrm{L}}^{\mathrm{HLLC}} - \mathbf{U}_{j-i}\right) \\ + \left(\min\left(0, S_{\mathrm{C}} - (i-1)\frac{\Delta x}{\Delta t}\right) - \min\left(0, S_{\mathrm{C}} - i\frac{\Delta x}{\Delta t}\right)\right)\left(\mathbf{U}_{\mathrm{R}}^{\mathrm{HLLC}} - \mathbf{U}_{\mathrm{L}}^{\mathrm{HLLC}}\right) \\ + \left(\min\left(0, S_{\mathrm{R}} - (i-1)\frac{\Delta x}{\Delta t}\right) - \min\left(0, S_{\mathrm{R}} - i\frac{\Delta x}{\Delta t}\right)\right)\left(\mathbf{U}_{j+1-i} - \mathbf{U}_{\mathrm{R}}^{\mathrm{HLLC}}\right). \quad (4.14)\end{aligned}$$

Similarly, we use (4.13) in (3.23) and note that for $i \geq 1$ we can write:

$$\begin{aligned}\int_{(i-1)\frac{\Delta x}{\Delta t}}^{i\frac{\Delta x}{\Delta t}} \widetilde{\mathbf{U}}_{j+1/2-i}(\zeta_i)\,\mathrm{d}\zeta_i = \frac{\Delta x}{\Delta t}\mathbf{U}_{j+1-i} \\ + \left(\max\left(0, S_{\mathrm{L}} - (i-1)\frac{\Delta x}{\Delta t}\right) - \max\left(0, S_{\mathrm{L}} - i\frac{\Delta x}{\Delta t}\right)\right)\left(\mathbf{U}_{\mathrm{L}}^{\mathrm{HLLC}} - \mathbf{U}_{j-i}\right) \\ + \left(\max\left(0, S_{\mathrm{C}} - (i-1)\frac{\Delta x}{\Delta t}\right) - \max\left(0, S_{\mathrm{C}} - i\frac{\Delta x}{\Delta t}\right)\right)\left(\mathbf{U}_{\mathrm{R}}^{\mathrm{HLLC}} - \mathbf{U}_{\mathrm{L}}^{\mathrm{HLLC}}\right) \\ + \left(\max\left(0, S_{\mathrm{R}} - (i-1)\frac{\Delta x}{\Delta t}\right) - \max\left(0, S_{\mathrm{R}} - i\frac{\Delta x}{\Delta t}\right)\right)\left(\mathbf{U}_{j+1-i} - \mathbf{U}_{\mathrm{R}}^{\mathrm{HLLC}}\right). \quad (4.15)\end{aligned}$$

Herein, the index $_{j+1/2-i}$ is implicitly assumed on the parameters $S_{[\mathrm{L,C,R}]}$ and $\mathbf{U}_{[\mathrm{L,R}]}^{\mathrm{HLLC}}$. Using (4.14) and (4.15) in (3.23) we can write the LTS-HLLC scheme as:

$$\mathbf{U}_j^{n+1} = \mathbf{U}_j^n - \frac{\Delta t}{\Delta x}\left(\mathbf{F}_{j+1/2}^{\text{LTS-HLLC}} - \mathbf{F}_{j-1/2}^{\text{LTS-HLLC}}\right). \quad (4.16)$$

□

We note that (4.8) and (4.9) are very similar to the corresponding numerical flux functions for the LTS-HLL scheme, (3.16) and (3.17), but with the addition of the middle wave associated with S_{C}.

5. TVD analysis and modified equation

We interpret the LTS-HLL scheme as a numerical method for the scalar conservation law and we show that the LTS-HLL scheme is TVD. Next, we employ the modified equation analysis and use the results of Lindqvist et al. [19] and Prebeg [29] to study the numerical diffusion of the LTS-HLL scheme.

5.1. **TVD analysis**

The original HLL scheme [9] and the HLLC scheme [39] have been constructed as approximate Riemann solvers for hyperbolic systems of conservation laws. However, we may interpret the standard HLL and the LTS-HLL scheme as a numerical method for scalar conservation laws with two input parameters S_{L} and S_{R}. This allows us to perform the TVD analysis of the scheme.

For the standard HLL scheme Einfeldt [5] showed that the HLL scheme satisfies the TVD-type condition if the eigenvalues ω_{HLL} of the numerical viscosity matrix $\mathbf{Q}_{\mathrm{HLL}}$ satisfy:

$$|\lambda_{p,\mathrm{Roe}}| \leq \omega_{p,\mathrm{HLL}}, \quad (5.1)$$

for each characteristic field p. The set of TVD conditions for LTS methods for scalar conservation laws was determined by Jameson and Lax [10, 11] (see also Lindqvist et al. [19]).

Lemma 1. *A multipoint conservative scheme in the form* (2.13) *is unconditionally TVD if and only if:*

$$2\left(\Delta x/\Delta t\right) - 2Q^{0}_{j+1/2} + Q^{-1}_{j+1/2} + Q^{1}_{j+1/2} \geq 0, \tag{5.2a}$$

$$Q^{0}_{j+1/2} - 2Q^{\pm 1}_{j+1/2} + Q^{\pm 2}_{j+1/2} \mp \lambda_{j+1/2} \geq 0, \tag{5.2b}$$

$$Q^{\pm i}_{j+1/2} - 2Q^{\pm(i+1)}_{j+1/2} + Q^{\pm(i+2)}_{j+1/2} \geq 0, \quad \forall \quad i \geq 1, \tag{5.2c}$$

for all j, where Q are the numerical viscosity coefficients.

By interpreting the numerical viscosity coefficients of the LTS-HLL scheme (3.21) as the numerical viscosity coefficients Q of the numerical method for the scalar conservation law we may show that:

Proposition 5. *The LTS-HLL scheme is TVD under the condition:*

$$S_{\mathrm{L}} \leq \lambda \leq S_{\mathrm{R}}. \tag{5.3}$$

Proof. By substituting (3.21) in (5.2a)–(5.2c) the TVD conditions become:

$$\begin{aligned}
&\left(\lambda - S_{\mathrm{L}}\right)\left(\frac{\Delta x}{\Delta t} - \min\left(\left|S_{\mathrm{R}}\right|, \frac{\Delta x}{\Delta t}\right)\right) \\
&+ \left(S_{\mathrm{R}} - \lambda\right)\left(\frac{\Delta x}{\Delta t} - \min\left(\left|S_{\mathrm{L}}\right|, \frac{\Delta x}{\Delta t}\right)\right) \geq 0,
\end{aligned} \tag{5.4a}$$

$$\begin{aligned}
&\left(\lambda - S_{\mathrm{L}}\right)\max\left(0, \min\left(\pm 2S_{\mathrm{R}}, 4\frac{\Delta x}{\Delta t} \mp 2S_{\mathrm{R}}\right)\right) \\
&+ \left(S_{\mathrm{R}} - \lambda\right)\max\left(0, \min\left(\pm 2S_{\mathrm{L}}, 4\frac{\Delta x}{\Delta t} \mp 2S_{\mathrm{L}}\right)\right) \geq 0,
\end{aligned} \tag{5.4b}$$

$$\begin{aligned}
&\left(\lambda - S_{\mathrm{L}}\right)\max\left(0, \min\left(\pm S_{\mathrm{R}} - i\frac{\Delta x}{\Delta t}, \mp S_{\mathrm{R}} + i\frac{\Delta x}{\Delta t} + 2\right)\right) \\
&+ \left(S_{\mathrm{R}} - \lambda\right)\max\left(0, \min\left(\pm S_{\mathrm{L}} - i\frac{\Delta x}{\Delta t}, \mp S_{\mathrm{L}} + i\frac{\Delta x}{\Delta t} + 2\right)\right) \geq 0, \quad \forall \quad i \geq 1,
\end{aligned} \tag{5.4c}$$

which are always satisfied under the condition (5.3). □

In the limit $\lambda = S_{\mathrm{L}} = S_{\mathrm{R}}$, we recover the LTS-Roe scheme which is well established to be TVD [15, 19].

5.2. **Modified equation analysis**

Once we have obtained the partial viscosity coefficients $\mathbf{Q}^i$, we may use them to compare the amount of the numerical diffusion between different schemes. One way of doing this is by employing the modified equation analysis.

Lindqvist et al. [19] showed that for the scalar conservation law the LTS scheme (2.13) and (2.14) gives a second-order accurate approximation to the equation:

$$u_t + f(u)_x = \frac{1}{2}\frac{\Delta x^2}{\Delta t}\left[\left(\sum_{i=1-k}^{k-1}\frac{\Delta t}{\Delta x}\bar{Q}^i - c^2\right)u_x\right]_x, \tag{5.5}$$

where $\bar{Q}^i = Q^i(u, \ldots, u)$ is the numerical viscosity coefficient of the $(2k+1)$-point scheme, and $c = f'(u)\Delta t/\Delta x$. We distinguish between the numerical diffusion inherent to the scheme:

$$D(u) = \sum_{i=1-k}^{k-1} \frac{\Delta t}{\Delta x} \bar{Q}^i - c^2, \tag{5.6}$$

and the total numerical diffusion ν:

$$\nu(u) = \frac{1}{2} \frac{\Delta x^2}{\Delta t} D(u). \tag{5.7}$$

Lindqvist et al. [19] determined $D(u)$ for the LTS-Roe and LTS-Lax-Friedrichs scheme as:

$$D_{\text{LTS-Roe}} = \left(\lceil |c| \rceil - |c|\right)\left(1 + |c| - \lceil |c| \rceil\right), \tag{5.8}$$

$$D_{\text{LTS-LxF}} = k^2 - c^2, \tag{5.9}$$

where $\lceil c \rceil = \min\{n \in \mathbb{Z} \,|\, n \geq c\}$ is the ceiling function. By using the numerical viscosity coefficients (3.21) in (5.6), Prebeg [29] determined $D(u)$ for the LTS-HLL scheme as:

$$\begin{aligned} D_{\text{LTS-HLL}} = &\frac{c - c_{\text{L}}}{c_{\text{R}} - c_{\text{L}}}\left(\lceil |c_{\text{R}}| \rceil - |c_{\text{R}}|\right)\left(1 + |c_{\text{R}}| - \lceil |c_{\text{R}}| \rceil\right) \\ &+ \frac{c_{\text{R}} - c}{c_{\text{R}} - c_{\text{L}}}\left(\lceil |c_{\text{L}}| \rceil - |c_{\text{L}}|\right)\left(1 + |c_{\text{L}}| - \lceil |c_{\text{L}}| \rceil\right) \\ &+ \left(c - c_{\text{L}}\right)\left(c_{\text{R}} - c\right), \end{aligned} \tag{5.10}$$

where $c_{\text{L}} = S_{\text{L}}\Delta t/\Delta x$ and $c_{\text{R}} = S_{\text{R}}\Delta t/\Delta x$. We use equations (5.8)–(5.10) to investigate the numerical diffusion of the LTS-Roe, LTS-Lax-Friedrichs and LTS-HLL schemes.

We consider the Euler equations and investigate the numerical diffusion at a Riemann problem with subsonic flow conditions and the Roe eigenvalues defined as:

$$\lambda_1 = -0.5, \quad \lambda_2 = 0.25, \quad \lambda_3 = 1. \tag{5.11}$$

Figure 2 shows D_p and ν_p for the p-th characteristic field as a function of the global Courant number $\bar{c}$. We use the global Courant number as an input variable and determine the time step from it as:

$$\Delta t_{\bar{c}} = \frac{\bar{c}\Delta x}{\max\left(|\lambda_1|, |\lambda_2|, |\lambda_3|\right)}. \tag{5.12}$$

Then the numerical diffusion D_p and ν_p are determined as functions of the local eigenvalue λ_p and the global time step size $\Delta t_{\bar{c}}$:

$$D_p = D\left(\lambda_p, \Delta t_{\bar{c}}, \Delta x\right), \quad \nu_p = \nu\left(\lambda_p, \Delta t_{\bar{c}}, \Delta x\right), \tag{5.13}$$

where we note that for the Figure 2 we use $S_{\text{L}} = \lambda_1$ and $S_{\text{R}} = \lambda_3$, and we assume that $\Delta x = 1$.

We observe that the area between LTS-Roe and LTS-Lax-Friedrichs curves (including the curves) is the TVD-type region. This follows from the result in [19] where it is shown that the LTS-Roe is the least diffusive and that the LTS-Lax-Friedrichs is the most diffusive TVD scheme. The range of numerical diffusion that can be achieved by the LTS-HLL scheme is hatched. Einfeldt [5] showed that for subsonic flow conditions, the standard HLL scheme can reproduce the full span of numerical diffusion between the Roe and Lax-Friedrichs schemes in the 1st and 3rd characteristic field corresponding to either shock or rarefaction. The amount of diffusion in 2nd characteristic field (contact discontinuity) is always higher than in the Roe scheme.

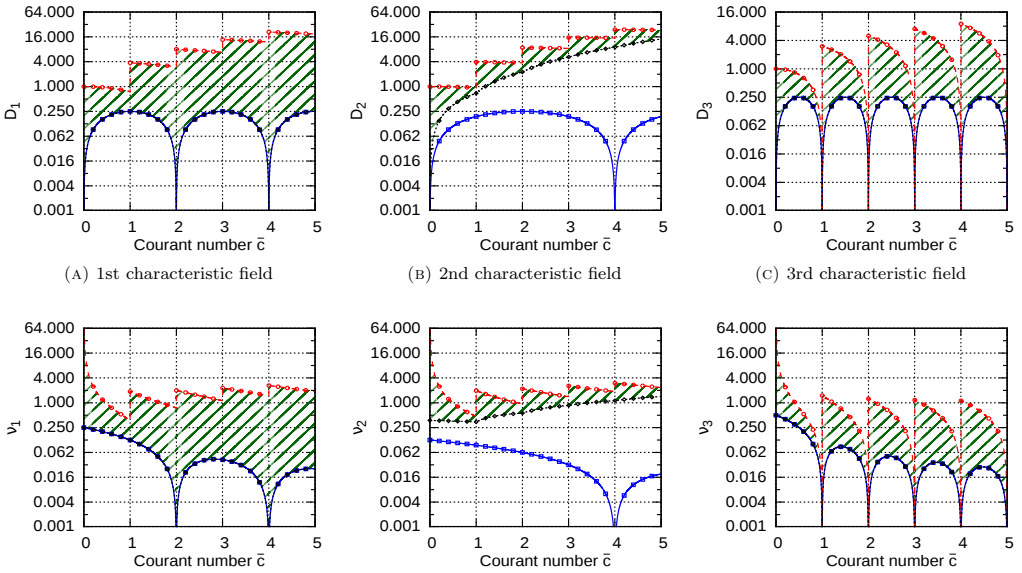

(A) 1st characteristic field (B) 2nd characteristic field (C) 3rd characteristic field

(D) 1st characteristic field (E) 2nd characteristic field (F) 3rd characteristic field

FIGURE 2. Numerical diffusion $D(u)$ and $\nu(u)$ in characteristic fields of the Euler equations for (5.11). LTS-Roe (blue-squares), LTS-Lax-Friedrichs (red-circles), LTS-HLL (black-diamonds). Hatched region (dark green-lines) is the range of numerical diffusion that can be achieved by the LTS-HLL scheme by varying S_{L} and S_{R}.

We may show that in the subsonic case, the numerical diffusion of the LTS-HLL scheme in the 2nd characteristic field is always bigger than the numerical diffusion of the LTS-Roe scheme and that it is always increasing with the time step.

Proposition 6. *The numerical diffusion of the LTS-HLL scheme in the 2nd characteristic field:*

$$D_{2,LTS\text{-}HLL} = \frac{c_2 - c_{\mathrm{L}}}{c_{\mathrm{R}} - c_{\mathrm{L}}} \mathcal{H}\left(|c_{\mathrm{R}}|\right) + \frac{c_{\mathrm{R}} - c_2}{c_{\mathrm{R}} - c_{\mathrm{L}}} \mathcal{H}\left(|c_{\mathrm{L}}|\right) + \left(c_2 - c_{\mathrm{L}}\right)\left(c_{\mathrm{R}} - c_2\right), \tag{5.14}$$

where we define:

$$c_{\mathrm{L}} = c_2 - \sigma, \quad c_{\mathrm{R}} = c_2 + \sigma, \tag{5.15}$$

with:

$$c_2 = \lambda_2 \frac{\Delta t}{\Delta x}, \quad \sigma = a \frac{\Delta t}{\Delta x}, \tag{5.16}$$

and where:

$$\mathcal{H}(|x|) = \lceil |x| \rceil + 2|x| \lceil |x| \rceil - |x| - |x|^2 - \lceil |x| \rceil^2, \tag{5.17}$$

and:

$$S_{\mathrm{L}} < 0 < |\lambda_2| < S_{\mathrm{R}}, \tag{5.18}$$

is a monotone function of the time step Δt.

Proof. By using (5.15), we can rewrite (5.14) as:

$$D_{2,\text{LTS-HLL}} = \frac{1}{2}\mathcal{H}\left(|c_\text{R}|\right) + \frac{1}{2}\mathcal{H}\left(|c_\text{L}|\right) + \sigma^2. \tag{5.19}$$

We introduce the dimensionless parameter z:

$$z = \frac{\Delta t_z}{\Delta t}, \tag{5.20}$$

and note that showing that (5.19) is a monotonically increasing function of Δt_z is equivalent to showing that:

$$D(z) = \frac{1}{2}\mathcal{H}\left(z\,|c_\text{R}|\right) + \frac{1}{2}\mathcal{H}\left(z\,|c_\text{L}|\right) + z^2\sigma^2, \tag{5.21}$$

is a monotonically increasing function of z. We note that $\mathcal{H}$ is a continuous function of x, hence $D(z)$ is also a continuous function of z. Therefore $D(z)$ is monotonically increasing if the first derivative is always positive. In other words, we need to show:

$$\frac{\mathrm{d}D(z)}{\mathrm{d}z} = |c_\text{R}|\left(\lceil z\,|c_\text{R}|\rceil - z\,|c_\text{R}|\right) + |c_\text{L}|\left(\lceil z\,|c_\text{L}|\rceil - z\,|c_\text{L}|\right) - \frac{1}{2}\left(|c_\text{L}| + |c_\text{R}|\right) + 2z\sigma^2 > 0 \quad \forall z > 0. \tag{5.22}$$

We define the maximum Courant number:

$$c_\text{max} = \max\left(|zc_\text{L}|, |zc_\text{R}|\right), \tag{5.23}$$

and consider the cases $c_\text{max} \leq 1$ and $c_\text{max} > 1$.

Case $c_\text{max} > 1$:

The first two terms in (5.22) are non-negative, so it is sufficient to show that:

$$-\frac{1}{2}\left(|c_\text{L}| + |c_\text{R}|\right) + 2z\sigma^2 > 0. \tag{5.24}$$

For subsonic flows we have that:

$$\frac{1}{2}\left(|c_\text{L}| + |c_\text{R}|\right) = \frac{1}{2}\left(c_\text{R} - c_\text{L}\right) = \sigma. \tag{5.25}$$

Hence (5.24) becomes:

$$z\sigma > \frac{1}{2}. \tag{5.26}$$

By using (5.16) we have that:

$$a\frac{\Delta t_z}{\Delta x} > \frac{1}{2}, \tag{5.27}$$

which always holds for subsonic flows when $c_\text{max} > 1$.

Case $c_\text{max} \leq 1$:

For $c_\text{max} \leq 1$ the equation (5.22) becomes:

$$\frac{\mathrm{d}D(z)}{\mathrm{d}z} = (c_2 + \sigma)(1 - zc_2 - z\sigma) - (c_2 - \sigma)(1 + zc_2 - z\sigma) - \sigma + 2z\sigma^2 > 0, \tag{5.28}$$

which simplifies to:

$$\frac{\mathrm{d}D(z)}{\mathrm{d}z} = \sigma - 2\left(c_2\right)^2 z > 0. \tag{5.29}$$

We have already proved that the expression is positive for $z > 1/(2\sigma)$, in the opposite case the lowest value of (5.29) is attained for:

$$z = \frac{1}{2\sigma}, \tag{5.30}$$

giving:

$$\frac{\mathrm{d}D(z)}{\mathrm{d}z} = \sigma - \frac{(c_2)^2}{\sigma} = \frac{1}{\sigma}(\sigma - c_2)(\sigma + c_2), \tag{5.31}$$

which is always positive for subsonic flows. □

6. Results

In this section we compare the new schemes with their non-LTS counterparts and the LTS-Roe scheme. Until now, we did not discuss how to choose the wave velocity estimates for S_L and S_R in the HLL and HLLC schemes and their LTS extensions. For our investigations, the choice of wave velocity estimates for S_L and S_R is made according to Einfeldt [5]:

$$S_{\mathrm{L},j+1/2} = \min\left(\lambda_1(\mathbf{U}_j), \lambda_1(\widehat{\mathbf{U}}_{j+1/2})\right), \tag{6.1a}$$

$$S_{\mathrm{R},j+1/2} = \max\left(\lambda_3(\widehat{\mathbf{U}}_{j+1/2}), \lambda_3(\mathbf{U}_{j+1})\right), \tag{6.1b}$$

where $\widehat{\mathbf{U}}$ denotes the Roe average of conserved variables. For the Euler equations, the eigenvalues are defined as $\lambda_1 = u - a$ and $\lambda_3 = u + a$, where u and a are the velocity and speed of sound, respectively. We note that the choice of wave velocity estimates is not a trivial matter and refer to Davis [4], Einfeldt [5] and Toro et al. [39] for detailed discussions about a number of different estimates and their properties. Herein, we choose (6.1) based on our own experience, where this choice yielded very good results, especially when it came to calculating entropy satisfying solutions. A more rigorous comparison between different wave velocity estimates in the LTS framework may be very fruitful, but at the moment it remains outside the scope of this paper.

In all the numerical experiments below, the input discretization parameters were the Courant number C and Δx. Then, the time step Δt was evaluated at each time step according to:

$$\Delta t = \frac{C\Delta x}{\max\limits_{p,x} |\lambda_p(x,t)|}, \tag{6.2}$$

where λ_p are the eigenvalues of the Jacobian matrix $\mathbf{A}$ in (2.2).

6.1. Sod shock tube

As a first test case we consider the classic Sod shock tube problem [33], with initial data $\mathbf{V}(x,0) = (\rho, u, p)^\mathrm{T}$:

$$\mathbf{V}(x,0) = \begin{cases} (1,0,1)^\mathrm{T} & \text{if} \quad x < 0, \\ (0.125,0,0.1)^\mathrm{T} & \text{if} \quad x > 0, \end{cases} \tag{6.3}$$

where the solution is evaluated at $t = 0.4$ on a grid with 100 cells. Figure 3 shows the results obtained with HLL(C) and LTS-HLL(C) schemes with $C = 1$ and $C = 3$. We observe that the LTS-HLL scheme (Figure 3a) increases the accuracy of the shock and the left going part of the rarefaction wave, while increasing the diffusion of the contact discontinuity. This is in agreement with the results from section 5.2 and it is due to the fact that the standard HLL scheme assumes a two wave structure of the solution and neglects the contact discontinuity, leading to excessive diffusion. Since the LTS-HLL scheme maintains the two wave assumption, it can be seen that the increase in the time step leads to further smearing of the contact discontinuity. The LTS-HLLC scheme (Figure 3b) also improves the accuracy of the shock and the rarefaction wave. In addition, the LTS-HLLC

scheme also improves the accuracy of the contact discontinuity, because the HLLC scheme resolves the wave missing in the HLL scheme. The velocity profiles show that the LTS-HLLC scheme produces more spurious oscillations than the LTS-HLL scheme.

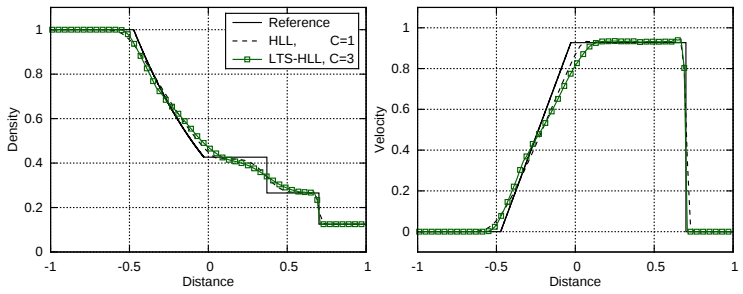

(A) Standard HLL and LTS-HLL scheme

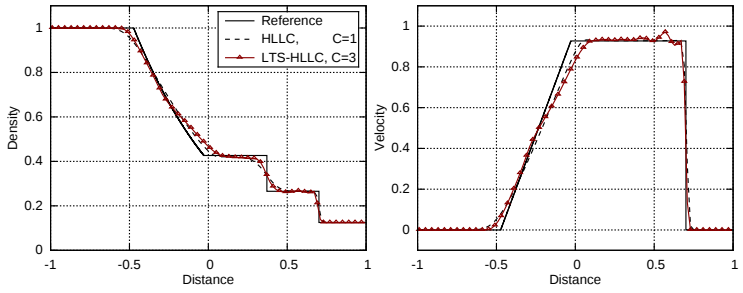

(B) Standard HLLC and LTS-HLLC scheme

FIGURE 3. Comparison between the standard HLL(C) and the LTS-HLL(C) schemes for the problem (6.3)

Next, we compare the performance of the LTS methods to each other. We consider the same test case and also include the results obtained with the LTS-Roe scheme [19]. Figure 4 shows that the LTS-Roe scheme produces spurious oscillations in both density and internal energy. Further, we observe that the LTS-Roe scheme violates the entropy condition, while both LTS-HLL and LTS-HLLC schemes produce entropy satisfying solutions. We note that for this test case, the standard Roe scheme does not lead to an entropy violation because there is no sonic point across the rarefaction wave. Lindqvist et al. [19] showed how the LTS-Roe scheme can lead to an entropy violation even if there is no sonic point across the rarefaction wave. Such an LTS-related entropy violation cannot be fixed with standard entropy fixes developed for the Roe scheme, but it can be fixed by splitting the rarefaction wave into several expansion shocks [13, 15, 31, 23, 41] or by varying the time step [18, 19]. Prebeg [29] showed that the LTS-HLL scheme with the wave velocity estimates (6.1) always produces entropy satisfying solutions.

Last, we investigate the computational times for the LTS-HLL(C) schemes at different Courant numbers and different grids, see Figure 5. We observe that for any grid, the CPU time decreases as we increase the Courant number. However, by looking at the CPU time required to reach the same error we observe that the HLL scheme tends to be more efficient than the LTS-HLL scheme, and that the LTS-HLLC scheme tends to be more efficient than the HLLC scheme.

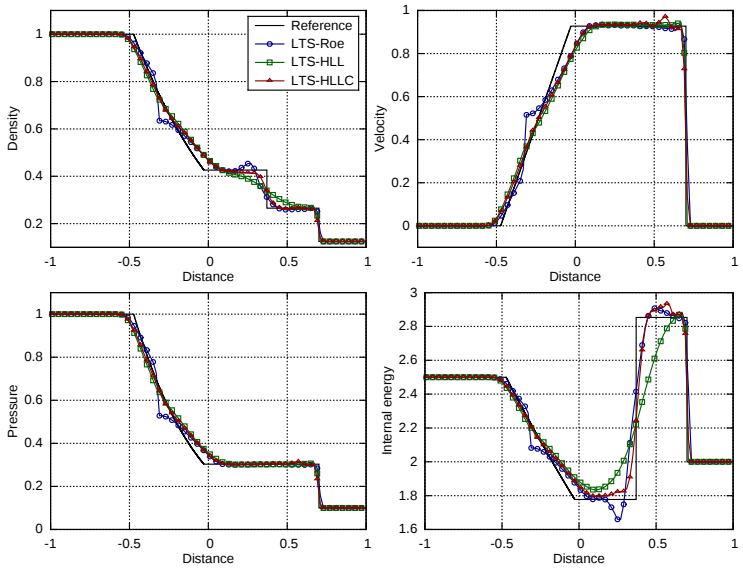

FIGURE 4. Comparison between different LTS schemes at $C = 3$ for problem (6.3)

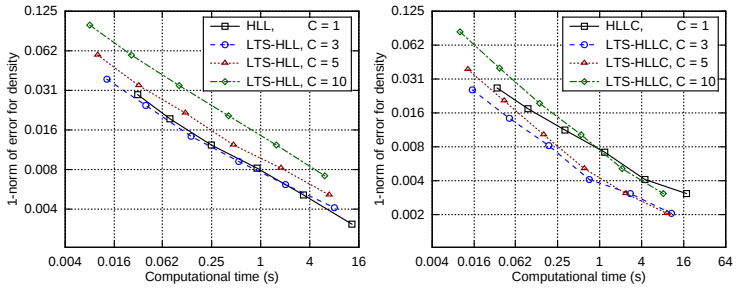

FIGURE 5. Computational time vs. error estimate $\mathcal{E}$ for density with the LTS-HLL(C) schemes for the problem (6.3) with 100, 200, 400, 800, 1600 and 3200 cells

Remark 1. The CPU times are obtained with the MATLAB tic-toc function and averaged over a number of simulations. The computational times in Figure 5 correspond to implementation in the framework (2.5) with the numerical flux functions evaluated with (3.15) for the LTS-HLL and (4.7) for the LTS-HLLC scheme. We note that for the LTS-HLL scheme the similar computational efficiency trends are observed for implementations in the numerical viscosity framework (2.13) with (3.21), and the flux-difference splitting framework (2.14) with (3.26). Similar computational efficiency trends were reported by Lindqvist and Lund [18] and Prebeg et al. [30].

6.2. **Woodward-Colella blast-wave problem**

We consider the Woodward-Colella blast-wave problem [40]. The initial data is given by uniform density $\rho(x,0) = 1$, uniform velocity $u(x,0) = 0$, and two discontinuities in the pressure:

$$p(x,0) = \begin{cases} 1000 & \text{if} \quad 0 < x < 0.1, \\ 0.01 & \text{if} \quad 0.1 < x < 0.9, \\ 100 & \text{if} \quad 0.9 < x < 1. \end{cases} \tag{6.4}$$

The solution is evaluated at $t = 0.038$ on a grid with 500 cells. The solution consists of contact discontinuities at $x = 0.6$, $x = 0.76$ and $x = 0.8$ and shock waves at $x = 0.65$ and $x = 0.87$, see [17]. The boundary walls at $x = 0$ and $x = 1$ are modeled as reflective boundary condition. The reference solution was obtained by the Roe scheme with the superbee wave limiter on the grid with 16000 cells.

Figure 6 shows the results obtained with the standard HLLC scheme at $C = 1$ and different LTS methods at $C = 5$. We observe that both LTS-Roe and LTS-HLLC schemes are more accurate than the standard HLLC scheme. Next, we observe that all schemes correctly capture the positions of both shocks and contact discontinuities. As expected, all schemes resolve the shocks much more accurately than the contact discontinuities, especially the LTS-HLL scheme which introduces very strong diffusion at the contact discontinuities.

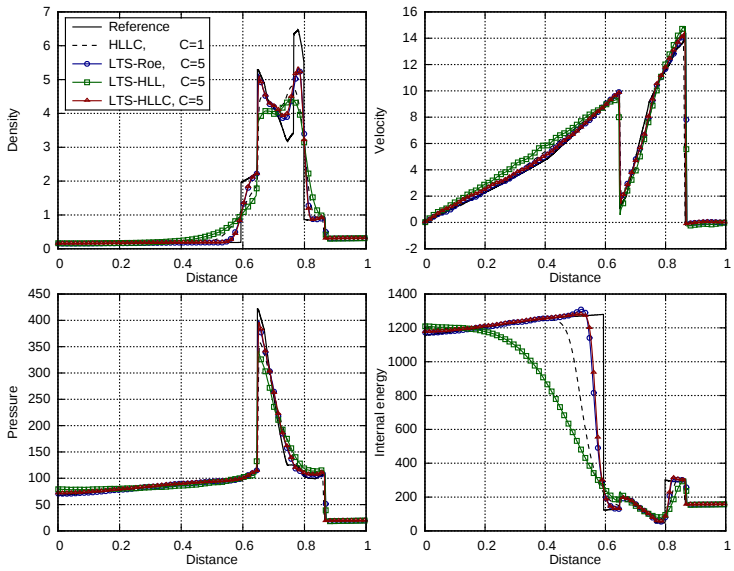

FIGURE 6. Comparison between the standard HLLC and different LTS methods for problem (6.4)

Last, we investigate the computational time for the LTS-HLL(C) schemes at different Courant numbers and different grids, see Figure 7. We observe that for any grid, the CPU time decreases as we increase the Courant number. For the LTS-HLL scheme, the optimal choice of the Courant number depends on the grid size. The LTS-HLLC scheme is always more efficient than the HLLC scheme. The observations made in Remark 1 also apply for Figure 7.

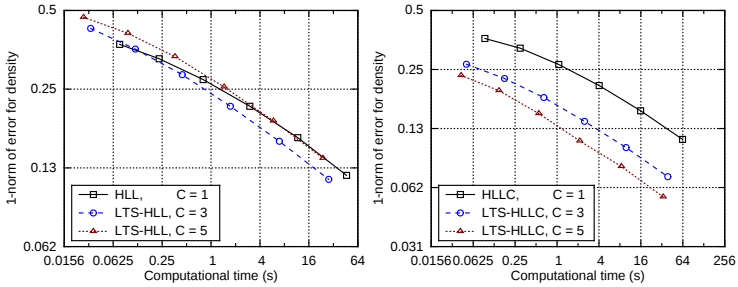

FIGURE 7. Computational time vs. error estimate $\mathcal{E}$ for density with the LTS-HLL(C) schemes for the problem (6.4) with 100, 200, 400, 800, 1600 and 3200 cells

7. Conclusions

Following LeVeque [15], previous works on Large Time Step (LTS) explicit methods have focused on the LTS-Roe and LTS-Godunov Riemann solvers. Aiming to achieve a more general platform for LTS methods, we have here formulated LTS versions of the HLL and HLLC approximate Riemann solvers. In particular, we have determined the explicit expressions for the flux-difference splitting coefficients and the numerical viscosity coefficients of the LTS-HLL scheme through our Propositions 2 and 3.

Through a modified equation analysis, we are able to precisely quantify the numerical diffusion associated with LTS approximate Riemann solvers. So far, the lack of a controlled mechanism for introducing stabilizing numerical diffusion has been a drawback for LTS methods [41]. In this respect, our Proposition 6 may be of interest, as it allows for interpreting S_{L} and S_{R} as parameters for smoothly controlling the numerical diffusion within the TVD region.

We applied the LTS-HLL(C) schemes to one-dimensional test cases for the Euler equations. At moderate Courant numbers the LTS-HLL scheme leads to increased accuracy of shocks and rarefaction waves compared to the standard HLL scheme. The stabilizing excessive diffusion on the contact wave is evident. For moderate Courant numbers, the LTS-HLLC scheme leads to an increased accuracy of shocks, rarefaction waves and contact discontinuities compared to the standard HLLC scheme. It also shows potential for increased robustness compared to the previously investigated LTS-Roe scheme [15, 19, 31]. We observe that for the Einfeldt's [5] choice of velocity estimates, both the LTS-HLL and LTS-HLLC schemes calculate entropy satisfying solutions. This is in agreement with a recent result by Prebeg [29] where the modified equation analysis was used to show that the LTS-HLL scheme with Einfeldt's choice of velocity estimates yields entropy satisfying solutions. This is a notable improvement compared to the existing LTS-Roe scheme for which entropy violations are observed for even more cases than with the standard Roe scheme [19, 31, 23]. For moderate Courant numbers, the LTS-HLLC scheme tends to be more efficient than the standard HLLC scheme in achieving a giving accuracy. For larger Courant numbers, both the LTS-HLL and LTS-HLLC schemes produced spurious oscillations and the accuracy decreased.

Further investigations are needed for robust higher order extensions of LTS methods, which were already considered by LeVeque [16] and Harten [8]. Moreover, conditions for preservation of positivity should be explored for LTS methods.

References

[1] P. Batten, N. Clarke, C. Lambert, and D. M. Causon. "On the Choice of Wavespeeds for the HLLC Riemann Solver". *SIAM J. Sci. Comput.* 18 (6) (1997), pp. 1553–1570.

[2] F. Daude and P. Galon. "On the Computation of the Baer–Nunziato Model Using ALE Formulation with HLL- and HLLC-Type Solvers Towards Fluid–Structure Interactions". *J. Comput. Phys.* 304 (2016), pp. 189–230.

[3] F. Daude, P. Galon, Z. Gao, and E. Blaud. "Numerical Experiments Using a HLLC-Type Scheme With ALE Formulation for Compressible Two-Phase Flows Five-Equation Models With Phase Transition". *Comput. Fluids* 94 (2014), pp. 112–138.

[4] S.F. Davis. "Simplified Second-Order Godunov-Type Methods". *SIAM J. Sci. Stat. Comput.* 9 (3) (1988), pp. 445–473.

[5] B. Einfeldt. "On Godunov-Type Methods for Gas Dynamics". *SIAM J. Numer. Anal.* 25 (2) (1988), pp. 294–318.

[6] B. Einfeldt, C.-D. Munz, P.L. Roe, and B. Sjögreen. "On Godunov-Type Methods near Low Densities". *J. Comput. Phys.* 92 (2) (1991), pp. 273–295.

[7] A. Harten. "High Resolution Schemes for Hyperbolic Conservation Laws". *J. Comput. Phys.* 49 (3) (1983), pp. 357–393.

[8] A. Harten. "On a Large Time–Step High Resolution Scheme". *Math. Comp.* 46 (174) (1986), pp. 379–399.

[9] A. Harten, P. D. Lax, and B. van Leer. "On Upstream Differencing and Godunov-Type Schemes for Hyperbolic Conservation Laws". *SIAM Rev.* 25 (1) (1983), pp. 35–61.

[10] A. Jameson and P. D. Lax. "Conditions for the Construction of Multi-Point Total Variation Diminishing Difference Schemes". *Appl. Numer. Math.* 2 (3–5) (1986), pp. 335–345.

[11] A. Jameson and P. D. Lax. "Corrigendum: Conditions for the Construction of Multi-Point Total Variation Diminishing Difference Schemes". *Appl. Numer. Math.* 3 (3) (1987), p. 289.

[12] P. Janhunen. "A Positive Conservative Method for Magnetohydrodynamics Based on HLL and Roe Methods". *J. Comput. Phys.* 160 (2) (2000), pp. 649–661.

[13] R. J. LeVeque. "Large Time Step Shock-Capturing Techniques for Scalar Conservation Laws". *SIAM J. Numer. Anal.* 19 (6) (1982), pp. 1091–1109.

[14] R. J. LeVeque. "Convergence of a Large Time Step Generalization of Godunov's Method for Conservation Laws". *Comm. Pure Appl. Math.* 37 (4) (1984), pp. 463–477.

[15] R. J. LeVeque. "A Large Time Step Generalization of Godunov's Method for Systems of Conservation Laws". *SIAM J. Numer. Anal.* 22 (6) (1985), pp. 1051–1073.

[16] R. J. LeVeque. "High Resolution Finite Volume Methods on Arbitrary Grids via Wave Propagation". *J. Comput. Phys.* 78 (1) (1988), pp. 36–63.

[17] R.J. LeVeque. *Finite Volume Methods for Hyperbolic Problems*. Cambridge Texts in Applied Mathematics (Book 31). Cambridge University Press, 2002.

[18] S. Lindqvist and H. Lund. "A Large Time Step Roe Scheme Applied to Two-Phase Flow". In: *VII European Congress on Computational Methods in Applied Sciences and Engineering*. Ed. by M. Papadrakakis, V. Papadopoulos, G. Stefanou, and V. Plevris. Crete Island, Greece, 2016.

[19] S. Lindqvist, P. Aursand, T. Flåtten, and A. A. Solberg. "Large Time Step TVD Schemes for Hyperbolic Conservation Laws". *SIAM J. Numer. Anal.* 54 (5) (2016), pp. 2775–2798.

[20] H. Lochon, F. Daude, P. Galon, and J.-M Hérard. "HLLC-Type Riemann Solver with Approximated Two-Phase Contact for the Computation of the Baer–Nunziato Two-Fluid Model". *J. Comput. Phys.* 326 (2016), pp. 733–762.

[21] N. N. Makwana and A. Chatterjee. "Fast Solution of Time Domain Maxwell's Equations Using Large Time Steps". In: *2015 IEEE International Conference on Computational Electromagnetics (ICCEM 2015)*. Hong Kong, China: Institute of Electrical and Electronics Engineers (IEEE), 2015, pp. 330–332.

[22] T. Miyoshi and K. Kusano. "A Multi-State HLL Approximate Riemann Solver for Ideal Magnetohydrodynamics". *J. Comput. Phys.* 208 (1) (2005), pp. 315–344.

[23] M. Morales-Hernández, P. García-Navarro, and J. Murillo. "A Large Time Step 1D Upwind Explicit Scheme (CFL>1): Application to Shallow Water Equations". *J. Comput. Phys.* 231 (19) (2012), pp. 6532–6557.

[24] M. Morales-Hernández, M. Hubbard, and P. García-Navarro. "A 2D Extension of a Large Time Step Explicit Scheme (CFL>1) for Unsteady Problems with Wet/Dry Boundaries". *J. Comput. Phys.* 263 (2014), pp. 303–327.

[25] M. Morales-Hernández, J. Murillo, P. García-Navarro, and J. Burguete. "A Large Time Step Upwind Scheme for the Shallow Water Equations With Source Terms". In: *Numerical Methods for Hyperbolic Equations*. Ed. by Elena Vázquez Cendón, Arthuro Hidalgo, P. García-Navarro, and Luis Cea. CRC Press, 2012, pp. 141–148.

[26] M. Morales-Hernández, A. Lacasta, J. Murillo, and P. García-Navarro. "A Large Time Step Explicit Scheme (CFL>1) on Unstructured Grids for 2D Conservation Laws: Application to the Homogeneous Shallow Water Equations". *Appl. Math. Model.* 47 (2017), pp. 294–317.

[27] J. Murillo, P. García-Navarro, P. Brufau, and J. Burguete. "Extension of an Explicit Finite Volume Method to Large Time Steps (CFL>1): Application to Shallow Water Flows". *Int. J. Numer. Meth. Fluids* 50 (1) (2006), pp. 63–102.

[28] M. Pelanti and K.-M. Shyue. "A Mixture-Energy-Consistent Six-Equation Two-Phase Numerical Model for Fluids with Interfaces, Cavitation and Evaporation Waves". *J. Comput. Phys.* 259 (2014), pp. 331–357.

[29] M. Prebeg. "Numerical Viscosity in Large Time Step HLL-type Schemes". In: *Proceedings of the Sixteenth International Conference on Hyperbolic Problems, HYP2016*. Ed. by C. Klingenberg and M. Westdickenberg. Accepted for publication. Aachen, Germany, 2016.

[30] M. Prebeg, T. Flåtten, and B. Müller. "Large Time Step Roe Scheme for a Common 1D Two-Fluid Model". *Appl. Math. Model.* 44 (2017), pp. 124–142.

[31] Z. Qian and C.-H. Lee. "A Class of Large Time Step Godunov Schemes for Hyperbolic Conservation Laws and Applications". *J. Comput. Phys.* 230 (19) (2011), pp. 7418–7440.

[32] P. Roe. "Approximate Riemann Solvers, Parameter Vectors, and Difference Schemes". *J. Comput. Phys.* 43 (2) (1981), pp. 357–372.

[33] G. A. Sod. "A Survey of Several Finite Difference Methods for Systems of Nonlinear Hyperbolic Conservation Laws". *J. Comput. Phys.* 27 (1) (1978), pp. 1–31.

[34] E. Tadmor. "Numerical Viscosity and the Entropy Condition for Conservative Difference Schemes". *Math. Comp* 43 (168) (1984), pp. 369–381.

[35] K. Tang, A. Beccantini, and C. Corre. "Combining Discrete Equations Method and Upwind Downwind-Controlled Splitting for Non-Reacting and Reacting Two-Fluid Computations: One Dimensional Case". *Comput. Fluids* 93 (2014), pp. 74–90.

[36] B. Tian, E. F. Toro, and C. E. Castro. "A Path-Conservative Method for a Five-Equation Model of Two-Phase Flow with an HLLC-Type Riemann Solver". *Comput. Fluids* 46 (1) (2011), pp. 122–132.

[37] S. A. Tokareva and E. F. Toro. "HLLC-Type Riemann Solver for Baer–Nunziato Equations of Compressible Two-Phase Flow". *J. Comput. Phys.* 229 (10) (2010), pp. 3573–3604.

[38] E. F. Toro. *Riemann Solvers and Numerical Methods for Fluid Dynamics*. 3rd ed. Springer-Verlag Berlin Heidelberg, 2009.

[39] E. F. Toro, M. Spruce, and W. Speares. "Restoration of the Contact Surface in the HLL-Riemann Solver". *Shock Waves* 4 (1) (1994), pp. 25–34.

[40] P. Woodward and P. Colella. "The Numerical Simulation of Two-Dimensional Fluid Flow with Strong Shocks". *J. Comput. Phys.* 54 (1) (1984), pp. 115–173.

[41] R. Xu, D. Zhong, B. Wu, X. Fu, and R. Miao. "A Large Time Step Godunov Scheme for Free-Surface Shallow Water Equations". *Chinese Sci. Bull.* 59 (21) (2014), pp. 2534–2540.

[42] G.-S. Yeom and K.-S. Chang. "Two-Dimensional Two-Fluid Two-Phase Flow Simulation Using an Approximate Jacobian Matrix for HLL Scheme". *Numer. Heat Tr. B-Fund.* 56 (5) (2010), pp. 372–392.

Journal paper 3 (P4)

Monotonicity and positivity preservation in Large Time Step methods

Marin Prebeg, Tore Flåtten and Bernhard Müller

Preprint

Journal of Scientific Computing manuscript No.
(will be inserted by the editor)

Monotonicity and positivity preservation in Large Time Step methods

Marin Prebeg · Tore Flåtten · Bernhard Müller

Received: date / Accepted: date

Abstract We study the positivity preserving property of Large Time Step (LTS) finite volume methods. Herein, LTS denotes explicit methods stable for Courant numbers greater than one. LTS-Godunov and LTS-Roe schemes have been developed by LeVeque [*SIAM J. Numer. Anal.*, 22 (1985), pp. 1051–1073], while LTS extensions of the HLL (Harten-Lax-van Leer) and HLLC (HLL-Contact) schemes have recently been developed by Prebeg et al. [submitted, 2017]. In this paper, we determine the monotonicity conditions for LTS methods, and show that they are stronger than in standard (3-point) methods. We show that conditions for positivity preservation in LTS methods are also stronger than in standard methods. In particular, we show that the LTS-HLLE scheme is not positivity preserving and that the LTS-Lax-Friedrichs scheme is positivity preserving. We apply LTS methods to the one-dimensional Euler equations and consider the double rarefaction, LeBlanc's shock tube and the Sedov blast-wave problem. We numerically demonstrate that robustness of LTS methods can be increased by adding numerical diffusion.

Keywords Large Time Step · HLL · Positivity preservation · Euler equations · Riemann solver

Mathematics Subject Classification (2000) 65M08 · 35L65 · 65Y20

The authors were supported by the Research Council of Norway (234126/30) through the SIMCOFLOW project.

M. Prebeg
Department of Energy and Process Engineering, Norwegian University of Science and Technology, Kolbjørn Hejes vei 2, NO-7491 Trondheim, Norway
Tel.: +47-980-70-428. E-mail: marin.prebeg@ntnu.no, marin.prebeg@gmail.com

B. Müller
Department of Energy and Process Engineering, Norwegian University of Science and Technology, Kolbjørn Hejes vei 2, NO-7491 Trondheim, Norway. E-mail: bernhard.muller@ntnu.no

T. Flåtten
SINTEF Materials and Chemistry, P. O. Box 4760 Sluppen, NO-7465 Trondheim, Norway
E-mail: toref@math.uio.no

1 Introduction

We consider a hyperbolic system of conservation laws:

$$\mathbf{U}_t + \mathbf{F}(\mathbf{U})_x = 0, \qquad x \in \mathbb{R}, t \in \mathbb{R}^+, \tag{1.1a}$$

$$\mathbf{U}(x,0) = \mathbf{U}_0(x), \tag{1.1b}$$

where $\mathbf{U} \in \mathbb{R}^N$ is a vector of conserved variables, $\mathbf{F}(\mathbf{U}) : \mathbb{R}^N \to \mathbb{R}^N$ is a flux function and $\mathbf{U}_0$ is the initial data. We are interested in solving (1.1) with an explicit finite volume methods not limited by the CFL (Courant–Friedrichs–Lewy) condition, and we focus on the positivity preserving property of such methods.

When we use conservation laws to describe the real world, the conserved variables are representing some particular measurable properties of the nature. In addition to being conserved, these properties may have additional requirements imposed upon then. For example, when we solve the Euler equations it is required that the density is positive at all times:

$$\rho(x,t) > 0 \quad \forall x \in \mathbb{R}, t \in \mathbb{R}^+. \tag{1.2}$$

Does the numerical method ensure that the condition (1.2) is always satisfied on a discrete level? Namely, does the scheme enforce that:

$$\rho_j^n > 0 \quad \forall j, n. \tag{1.3}$$

To tackle this question, we start by considering a scalar conservation law. In this paper, we follow a common approach of treating monotonicity as a scalar counterpart of positivity preserving property [50]. Consider a one-dimensional initial value problem for the scalar conservation law:

$$u_t + f(u)_x = 0, \qquad x \in \mathbb{R}, t \in \mathbb{R}^+, \tag{1.4a}$$

$$u(x,0) = u_0(x), \tag{1.4b}$$

where $u \in \mathbb{R}$ is a conserved variable a $f(u) : \mathbb{R} \to \mathbb{R}$ is the flux function. A unique weak solution of (1.4) satisfies a strict *maximum principle*. Namely, if:

$$m = \min_x \left(u_0(x)\right), \quad M = \max_x \left(u_0(x)\right), \tag{1.5}$$

then:

$$u(x,t) \in [m, M] \quad \forall \quad x, t. \tag{1.6}$$

We want the numerical scheme to enforce this property on a discrete level. Define:

$$m = \min_j(u_j^0), \quad M = \max_j(u_j^0). \tag{1.7}$$

If the numerical scheme ensures that:

$$u_j^n \in [m, M] \quad \forall \quad j, n, \tag{1.8}$$

we say that the scheme is *maximum-principle-satisfying*. When we discuss systems of equations, it may be unreasonable to require that a certain variable remains bounded between its initial values at all time, but it might be necessary to require that a conserved variable remains bounded in some specific sense, such as for

example the positivity of the density and internal energy in the Euler equations. We then say that the scheme is *positivity preserving*.

The development of positivity preserving schemes has been an ongoing topic for many years now. For the standard methods, Einfeldt et al. [11] showed that the Godunov and the HLLE (HLL-Einfeldt) schemes are positivity preserving, while the Roe scheme is not. Batten et al. [3] showed that the HLLC (HLL-Contact) [44] scheme is positivity preserving with an appropriate choice of wave velocity estimates, and Bouchut [5] determined wave velocities estimates such that the HLLC scheme can also handle vacuum. Further, Perthame and Shu [33] established a general framework to achieve high-order positivity preserving methods for the Euler equations in one and two dimensions. Areas of interest include the Euler equations (Calgaro et al. [6], Hu et al. [16], Li et al. [23], Zhang and Shu [49–51]), shallow water equations [39,18,46,1], magnetohydrodynamics [2,17,12], multiphase flows (Chen and Shu [8]), unstructured meshes (Berthon [4]) and flux-vector splitting methods (Gressier et al. [13]), to name just a few. These papers consider standard methods and mostly tackle issues with positivity preservation that arise in high-order methods. This paper takes a different route and considers the issues with positivity preservation in Large Time Step (LTS) methods.

The LTS methods have been introduced by LeVeque [19–21], where the Godunov and Roe schemes were extended to the LTS-Godunov and LTS-Roe schemes, respectively, and applied to scalar conservation laws and the Euler equations. These ideas have been applied in different fields, including the shallow water equations (Murillo, Morales-Hernández and co-workers [32,28,31,29,30] and Xu et al. [47]), 3D Euler equations (Qian and Lee [37]), high speed combustion waves (Tang et al. [41]), Maxwell's equations (Makwana and Chatterjee [27]) and multiphase flows (Lindqvist and Lund [25] and Prebeg et al. [36]). Lindqvist et al. [24] studied the TVD properties of LTS methods and developed the LTS-Lax-Friedrichs scheme, while Prebeg et al. [35] developed an LTS extension of the HLL [15] and HLLC [44] schemes and applied them to the one-dimensional Euler equations. Prebeg [34] also used the modified equation analysis to show that the LTS-HLLE scheme yields entropy satisfying solutions.

The positivity preserving in the LTS-Roe scheme for the shallow water equations with source terms has been addressed by Morales-Hernández and co-workers [28,29], where they suggested to handle loss of positivity by reducing the Courant number when the it is likely to happen. In this paper, we focus on the LTS-HLLE scheme and consider scalar conservation laws and the Euler equations. Our first result are conditions on the numerical flux function of an LTS method that guarantees that the method is monotone. We show that the LTS-HLLE scheme is not monotone, and that the LTS-Lax-Friedrichs scheme is monotone. Next, we consider the Euler equations and the classical result by Einfeldt et al. [11] that states that the exact or approximate Riemann solver is positivity preserving if and only if the intermediate states generated by the Riemann solver are physically real. Our second result is showing that in the LTS framework this condition is necessary, but not sufficient for the positivity preservation. We then show that the LTS-HLLE scheme is not positivity preserving, and that the LTS-Lax-Friedrichs scheme is positivity preserving.

This paper is structured as follows. In section 2 we outline the problem we solve and the numerical methods we use. In order to investigate the monotonicity, we will interpret the HLL scheme as a numerical method for scalar conservation

laws. Extension to systems of equations is then obtained by a classical field-by-field decomposition. In section 3 we consider scalar conservation laws and how is monotonicity lost in LTS methods. In section 4 we move to systems of equations and investigate different ways how is positivity lost in the LTS-HLLE scheme when applied to the Euler equations. Section 5 presents numerical results, while section 6 closes with conclusions.

2 Preliminaries

2.1 Problem outline

As an example of (1.1) we consider the Euler equations. They can be written in the form (1.1) by defining:

$$\mathbf{U} = \begin{bmatrix} \rho \\ \rho v \\ E \end{bmatrix}, \qquad \mathbf{F}(\mathbf{U}) = \begin{bmatrix} \rho v \\ \rho v^2 + p \\ v(E+p) \end{bmatrix}, \tag{2.1}$$

where ρ, v, E, p denote the density, velocity, total energy density and pressure, respectively. The system is closed by the relation for the total energy density, $E = \rho e + \rho v^2/2$, an equation of state for perfect gas, $e = p/(\rho(\gamma - 1))$, and $\gamma > 1$ (we use $\gamma = 1.4$ for air). We can write (1.1) in a quasilinear form as:

$$\mathbf{U}_t + \mathbf{A}(\mathbf{U})\mathbf{U}_x = 0, \qquad \mathbf{A}(\mathbf{U}) = \partial\mathbf{F}(\mathbf{U})/\partial\mathbf{U}. \tag{2.2}$$

We assume that the system of equations (2.2) is hyperbolic, i.e. the Jacobian matrix $\mathbf{A}$ has real eigenvalues and linearly independent eigenvectors. The eigenvalues of the Euler equations (2.1) are:

$$\lambda^1 = v - a, \quad \lambda^2 = v, \quad \lambda^3 = v + a, \tag{2.3}$$

where a is the speed of sound:

$$a = \sqrt{\gamma p/\rho}. \tag{2.4}$$

2.2 Numerical methods

We start by presenting the standard HLL and the LTS-HLL schemes for scalar conservation laws, and then generalize them to systems of equations.

2.2.1 Standard (3-point) methods

We discretize (1.4) by the explicit Euler method in time and the finite volume method in space:

$$u_j^{n+1} = u_j^n - \frac{\Delta t}{\Delta x}\left(F_{j+1/2}^n - F_{j-1/2}^n\right), \tag{2.5}$$

where u_j^n is a piecewise constant approximation of u in the cell with center at x_j at time level n, and $F_{j+1/2}^n$ is a numerical approximation of the flux function at the cell interface $x_{j+1/2}$ at time level n. In the case that the numerical flux depends

only on the neighboring cell values, we can with no loss of generality write the scheme in the numerical viscosity form [14,40]:

$$F_{j+1/2} = \frac{1}{2}\left(f_j + f_{j+1}\right) - \frac{1}{2}Q_{j+1/2}\left(u_{j+1} - u_j\right), \tag{2.6}$$

where $f_j = f\left(u_j\right)$, $Q_{j+1/2}$ is the numerical viscosity coefficient and the temporal index n is from now on omitted because we consider only explicit methods. The choice of the numerical viscosity coefficient uniquely determines the choice of the numerical method. For the HLL scheme [15], the numerical viscosity coefficient is (see [10]):

$$Q_{\mathrm{HLL},j+1/2} = \frac{\left|S_{\mathrm{R}}\right|\left(\lambda - S_{\mathrm{L}}\right) + \left|S_{\mathrm{L}}\right|\left(S_{\mathrm{R}} - \lambda\right)}{S_{\mathrm{R}} - S_{\mathrm{L}}}, \tag{2.7}$$

where λ is the shock speed determined by the Rankine–Hugoniot condition, and S_{L} and S_{R} are the wave velocity estimates to be determined later.

An alternative way to discretize (1.4) is with the flux-difference splitting form:

$$u_j^{n+1} = u_j - \frac{\Delta t}{\Delta x}\left(A^+_{j-1/2}\left(u_j - u_{j-1}\right) + A^-_{j+1/2}\left(u_{j+1} - u_j\right)\right), \tag{2.8}$$

where $A^{\pm}_{j-1/2}$ are the flux-difference splitting coefficients. The choice of the method in this form is determined by the choice of the flux-difference splitting coefficients, where for the HLL scheme we have:

$$A^{\pm}_{\mathrm{HLL},j-1/2} = \frac{S^{\pm}_{\mathrm{R}}\left(\lambda - S_{\mathrm{L}}\right) + S^{\pm}_{\mathrm{L}}\left(S_{\mathrm{R}} - \lambda\right)}{S_{\mathrm{R}} - S_{\mathrm{L}}}, \tag{2.9}$$

where $S^+_{\mathrm{R}} = \max(0, S_{\mathrm{R}})$ and $S^-_{\mathrm{R}} = \min(0, S_{\mathrm{R}})$.

A third way to discretize (1.4) is the wave propagation form that will be used in this paper:

$$u_j^{n+1} = u_j - \frac{\Delta t}{\Delta x}\left(\sum_{p=1}^{m} S^{p,+}_{j-1/2}\mathcal{W}^p_{j-1/2} + \sum_{p=1}^{m} S^{p,-}_{j+1/2}\mathcal{W}^p_{j+1/2}\right), \tag{2.10}$$

where we replaced the discontinuity in the conserved variable by m waves. For the HLL scheme $m = 2$, and we define the velocities S^p as:

$$S^1_{j-1/2} = S_{\mathrm{L},j-1/2}, \quad S^2_{j-1/2} = S_{\mathrm{R},j-1/2}, \tag{2.11}$$

and the waves $\mathcal{W}^p$ as:

$$\mathcal{W}^1_{j-1/2} = u^{\mathrm{HLL}}_{j-1/2} - u_{j-1}, \quad \mathcal{W}^2_{j-1/2} = u_j - u^{\mathrm{HLL}}_{j-1/2}, \tag{2.12}$$

where $u^{\mathrm{HLL}}_{j-1/2}$ is the intermediate state determined from the integral form of the conservation law (3.17) (see [15,43]):

$$u^{\mathrm{HLL}}_{j-1/2} = \frac{S_{\mathrm{R}}u_j - S_{\mathrm{L}}u_{j-1} + f_{j-1} - f_j}{S_{\mathrm{R}} - S_{\mathrm{L}}}. \tag{2.13}$$

We refer to [15,9–11,3,43] for a more detailed derivation of the HLL scheme.

2.2.2 Large Time Step methods

For the standard methods above, the size of time step in discretizations (2.5), (2.8) and (2.10) is limited by the CFL condition:

$$C = \max_{p,x,t} |\lambda^p(x,t)| \frac{\Delta t}{\Delta x} \leq 1, \tag{2.14}$$

where λ is $\partial f(u)/\partial u$ if we consider (1.4), and the eigenvalues of $\mathbf{A}(\mathbf{U})$ (eq. (2.2)) if we consider (1.1). In this paper, we consider explicit Large Time Step (LTS) methods that are not limited by the condition (2.14), i.e. we relax the CFL condition so that:

$$C = \max_{p,x,t} |\lambda^p(x,t)| \frac{\Delta t}{\Delta x} \leq k, \quad k \in \mathbb{Z}^+. \tag{2.15}$$

Following Lindqvist et al. [24], the LTS extension of the numerical viscosity formulation (2.6) is:

$$F_{j+1/2} = \frac{1}{2}(f_j + f_{j+1}) - \frac{1}{2}\sum_{i=-\infty}^{\infty} Q^i_{j+1/2+i} \Delta u_{j+1/2+i}, \tag{2.16}$$

and the LTS extension of the flux-difference splitting formulation (2.8) is:

$$u_j^{n+1} = u_j - \frac{\Delta t}{\Delta x}\sum_{i=0}^{\infty}\left(A^{i+}_{j-1/2-i}\Delta u_{j-1/2-i} + A^{i-}_{j+1/2+i}\Delta u_{j+1/2+i}\right), \tag{2.17}$$

where we introduced the notation $\Delta u_{j-1/2} = u_j - u_{j-1}$ and the convention:

$$Q^{\pm i} = A^{i\pm} = 0 \quad \text{for} \quad i \geq k. \tag{2.18}$$

The LTS extension of the wave formulation (2.10) is:

$$u_j^{n+1} = u_j - \frac{\Delta t}{\Delta x}\sum_{i=0}^{\infty}\left(\sum_{p=1}^{m} S^{p,i+}_{j-1/2-i}\mathcal{W}^p_{j-1/2-i} + \sum_{p=1}^{m} S^{p,i-}_{j+1/2+i}\mathcal{W}^p_{j+1/2+i}\right). \tag{2.19}$$

We note that (2.16) differs from [24] in a sense that we scale Q^i by $\Delta x/\Delta t$. The newly introduced upper indices denote relative cell interfaces. For instance, $Q^i_{j+1/2+i}$ describes the contribution of the numerical viscosity coefficient Q from the cell interface $x_{j+1/2+i}$ to the numerical flux function $F_{j+1/2}$ which is $|i|$ cells away. From now on, we will suppress the subscript and our definition of Q will simply tell us how much does the numerical viscosity coefficient Q from an arbitrary interface contributes to the numerical flux function $|i|$ cells away. The same reasoning applies to the flux-difference splitting coefficients A and wave velocities S.

Lindquist et al. [24] determined the numerical viscosity and flux-difference splitting coefficients of the LTS-Godunov, LTS-Roe and LTS-Lax-Friedrichs schemes.

Prebeg et al. [35] determined the numerical viscosity coefficients of the LTS-HLL scheme as:

$$Q^0_{\mathrm{HLL}} = \frac{|S_{\mathrm{R}}|\,(\lambda - S_{\mathrm{L}}) + |S_{\mathrm{L}}|\,(S_{\mathrm{R}} - \lambda)}{S_{\mathrm{R}} - S_{\mathrm{L}}}, \tag{2.20a}$$

$$\begin{aligned} Q^{\mp i}_{\mathrm{HLL}} =& 2\frac{\lambda - S_{\mathrm{L}}}{S_{\mathrm{R}} - S_{\mathrm{L}}} \max\left(0, \pm S_{\mathrm{R}} - i\frac{\Delta x}{\Delta t}\right) \\ &+ 2\frac{S_{\mathrm{R}} - \lambda}{S_{\mathrm{R}} - S_{\mathrm{L}}} \max\left(0, \pm S_{\mathrm{L}} - i\frac{\Delta x}{\Delta t}\right) \quad \text{for} \quad i > 0, \end{aligned} \tag{2.20b}$$

and the flux-difference splitting coefficients of the LTS-HLL scheme as:

$$\begin{aligned} A^{i\pm}_{\mathrm{HLL}} =& \pm \frac{\lambda - S_{\mathrm{L}}}{S_{\mathrm{R}} - S_{\mathrm{L}}} \max\left(0, \min\left(\pm S_{\mathrm{R}} - i\frac{\Delta x}{\Delta t}, \frac{\Delta x}{\Delta t}\right)\right) \\ &\pm \frac{S_{\mathrm{R}} - \lambda}{S_{\mathrm{R}} - S_{\mathrm{L}}} \max\left(0, \min\left(\pm S_{\mathrm{L}} - i\frac{\Delta x}{\Delta t}, \frac{\Delta x}{\Delta t}\right)\right). \end{aligned} \tag{2.21}$$

The wave velocities in an arbitrary LTS method given by (2.19) are:

$$S^{p,i\pm} = \pm \max\left(0, \min\left(\pm S^p - i\frac{\Delta x}{\Delta t}, \frac{\Delta x}{\Delta t}\right)\right). \tag{2.22}$$

The derivation and a detailed analysis of equations (2.16) and (2.17) can be found in [24], while the derivation of (2.20) and (2.21) can be found in [35].

2.2.3 Systems of equations

In order to apply the methods discussed above to systems of equations, we follow the standard approach of applying the scalar method to a field-by-field decomposition obtained through the Roe linearization [38]. We refer to the books by LeVeque [22] and Toro [43] for the standard theory, and to Lindqvist et al. [24] and Prebeg et al. [35] for LTS methods considered in this paper.

The LTS extensions of the numerical viscosity (2.16), flux-difference splitting (2.17) and wave formulation (2.19) for systems of equations are:

$$\mathbf{F}_{j+1/2} = \frac{1}{2}\left(\mathbf{F}_j + \mathbf{F}_{j+1}\right) - \frac{1}{2}\sum_{i=-\infty}^{\infty} \mathbf{Q}^i_{j+1/2+i} \Delta \mathbf{U}_{j+1/2+i}, \tag{2.23}$$

for the numerical viscosity,

$$\mathbf{U}^{n+1}_j = \mathbf{U}_j - \frac{\Delta t}{\Delta x}\sum_{i=0}^{\infty}\left(\hat{\mathbf{A}}^{i+}_{j-1/2-i}\Delta \mathbf{U}_{j-1/2-i} + \hat{\mathbf{A}}^{i-}_{j+1/2+i}\Delta \mathbf{U}_{j+1/2+i}\right), \tag{2.24}$$

for the flux-difference splitting, and:

$$\mathbf{U}^{n+1}_j = \mathbf{U}_j - \frac{\Delta t}{\Delta x}\sum_{i=0}^{\infty}\left(\sum_{p=1}^{m} S^{p,i+}_{j-1/2-i}\mathcal{W}^p_{j-1/2-i} + \sum_{p=1}^{m} S^{p,i-}_{j+1/2+i}\mathcal{W}^p_{j+1/2+i}\right), \tag{2.25}$$

for the wave formulation. For the LTS-HLL scheme [35], the partial viscosity matrices $\mathbf{Q}^i$ are defined through their eigenvalues by diagonalizing them as:

$$\mathbf{Q}^i_{j+1/2} = (\hat{\mathbf{R}}\mathbf{\Omega}^i\hat{\mathbf{R}}^{-1})_{j+1/2}, \tag{2.26}$$

where $\hat{\mathbf{R}}$ is matrix of eigenvectors of the Roe scheme [38], and $\mathbf{\Omega}^i$ is the diagonal matrix with the eigenvalues:

$$\omega^0_{\mathrm{HLL}} = \frac{|S_{\mathrm{R}}|\,(\lambda - S_{\mathrm{L}}) + |S_{\mathrm{L}}|\,(S_{\mathrm{R}} - \lambda)}{S_{\mathrm{R}} - S_{\mathrm{L}}}, \tag{2.27a}$$

$$\begin{aligned}\omega^{\mp i}_{\mathrm{HLL}} =& 2\frac{\lambda - S_{\mathrm{L}}}{S_{\mathrm{R}} - S_{\mathrm{L}}}\max\left(0, \pm S_{\mathrm{R}} - i\frac{\Delta x}{\Delta t}\right)\\ &+2\frac{S_{\mathrm{R}} - \lambda}{S_{\mathrm{R}} - S_{\mathrm{L}}}\max\left(0, \pm S_{\mathrm{L}} - i\frac{\Delta x}{\Delta t}\right) \quad \text{for } i > 0,\end{aligned} \tag{2.27b}$$

and the flux-difference splitting matrices $\hat{\mathbf{A}}^{i\pm}$ are defined through their eigenvalues by diagonalizing them as:

$$\hat{\mathbf{A}}^{i\pm}_{j+1/2} = (\hat{\mathbf{R}}\hat{\mathbf{\Lambda}}^{i\pm}\hat{\mathbf{R}}^{-1})_{j+1/2}, \tag{2.28}$$

where $\hat{\mathbf{\Lambda}}^{i\pm}$ is the diagonal matrix with the eigenvalues:

$$\begin{aligned}\lambda^{i\pm}_{\mathrm{HLL}} =& \pm\frac{\lambda - S_{\mathrm{L}}}{S_{\mathrm{R}} - S_{\mathrm{L}}}\max\left(0, \min\left(\pm S_{\mathrm{R}} - i\frac{\Delta x}{\Delta t}, \frac{\Delta x}{\Delta t}\right)\right)\\ &\pm\frac{S_{\mathrm{R}} - \lambda}{S_{\mathrm{R}} - S_{\mathrm{L}}}\max\left(0, \min\left(\pm S_{\mathrm{L}} - i\frac{\Delta x}{\Delta t}, \frac{\Delta x}{\Delta t}\right)\right).\end{aligned} \tag{2.29}$$

For the wave formulation, the wave velocities are the same as in (2.22):

$$S^{p,i\pm} = \pm\max\left(0, \min\left(\pm S^p - i\frac{\Delta x}{\Delta t}, \frac{\Delta x}{\Delta t}\right)\right). \tag{2.30}$$

We refer to [35] for the detailed derivation of (2.27) and (2.29).

3 Scalar conservation law

We consider the scalar conservation law (1.4) and we want to construct an LTS method that will guarantee that the numerical solution respects the strict maximum principle (1.8). The condition (1.8) is guaranteed if the numerical method is monotone. We can determine if the scheme is monotone by the following result:

Lemma 1 (Trangenstein [45]) *Suppose that:*

$$u^{n+1}_j = \mathcal{H}(u_{j-k}, \ldots, u_{j+k}; \Delta x, \Delta t), \tag{3.1}$$

is a monotone scheme and that it is differentiable in each of its u_l arguments for $j - k \le l \le j + k$. Then:

$$\frac{\partial \mathcal{H}}{\partial u_l} \ge 0, \quad \forall \quad j - k \le l \le j + k. \tag{3.2}$$

Conversely, if:

$$\frac{\partial \mathcal{H}}{\partial u_l} \ge 0, \quad \forall \quad j - k \le l \le j + k, \tag{3.3}$$

then (3.1) *is monotone scheme.*

For standard methods, monotonicity can be also shown by considering the numerical flux function (2.6):

$$F(a,b) = \frac{1}{2}\left(f(a)+f(b)\right) - \frac{1}{2}Q(a,b)\,(b-a)\,. \tag{3.4}$$

The standard numerical method is monotone if the numerical flux function $F(a,b)$ is non-decreasing in its first argument, non-increasing in its second argument and the CFL condition (2.14) holds. Our first result is a set of conditions on the numerical flux function of an LTS method that yields a monotone scheme.

Proposition 1 *Suppose that an explicit* $(2k+1)$*-point scheme:*

$$u_j^{n+1} = \mathcal{H}\left(u_{j-k},\ldots,u_{j+k};\Delta x,\Delta t\right), \tag{3.5}$$

can be written in conservation form:

$$\begin{aligned} u_j^{n+1} = u_j + \frac{\Delta t}{\Delta x}\big(&F_{j-1/2}\big(u_{j-k},u_{j-k+1},\ldots,u_{j+k-1}\big) \\ &-F_{j+1/2}\big(u_{j-k+1},\ldots,u_{j+k-1},u_{j+k}\big)\big), \end{aligned} \tag{3.6}$$

where:

$$F = F\left(u^1,\ldots,u^{2k}\right), \tag{3.7}$$

is a Lipschitz continuous numerical flux function of $2k$ *arguments. The numerical method* (3.5) *is monotone if:*

$$\frac{\partial F}{\partial u^p} = \begin{cases} \dfrac{\partial F}{\partial u^p} \geq \dfrac{\partial F}{\partial u^{p-1}} \geq 0 & \text{for} \quad 1 < p \leq k, \\ \dfrac{\partial F}{\partial u^{p-1}} \leq \dfrac{\partial F}{\partial u^p} \leq 0 & \text{for} \quad k+1 < p \leq 2k; \end{cases} \tag{3.8}$$

and the condition:

$$\frac{\Delta t}{\Delta x}\left(\left|\frac{\partial F}{\partial u^k}\right| + \left|\frac{\partial F}{\partial u^{k+1}}\right|\right) \leq 1, \tag{3.9}$$

holds.

Remark 1 We note that we use lower indices to denote the absolute index position, $l \in [j-k,\ldots,j+k]$ for the numerical method $\mathcal{H}$ and the numerical flux function F, and upper indices to denote the relative (local) index position: $p \in [1,\ldots,2k+1]$ for the numerical method $\mathcal{H}$, and $p \in [1,\ldots,2k]$ for the numerical flux function F.

Proof We recall Lemma 1 and note that the scheme (3.5) is monotone iff:

$$\frac{\partial \mathcal{H}}{\partial u^p} \geq 0, \quad \forall \quad 1 \leq p \leq 2k+1. \tag{3.10}$$

By differentiating $\mathcal{H}$ with respect to its arguments u^p we obtain:

$$\frac{\partial \mathcal{H}}{\partial u^p} = \begin{cases} (a) & \frac{\Delta t}{\Delta x}\frac{\partial F}{\partial u^1} & \text{for} & p=1, \\ (b) & \frac{\Delta t}{\Delta x}\left(\frac{\partial F}{\partial u^p} - \frac{\partial F}{\partial u^{p-1}}\right) & \text{for} & 1 < p \leq k, \\ (c) & 1 + \frac{\Delta t}{\Delta x}\left(\frac{\partial F}{\partial u^p} - \frac{\partial F}{\partial u^{p-1}}\right) & \text{for} & p = k+1, \\ (d) & \frac{\Delta t}{\Delta x}\left(\frac{\partial F}{\partial u^p} - \frac{\partial F}{\partial u^{p-1}}\right) & \text{for} & k+1 < p \leq 2k, \\ (e) & -\frac{\Delta t}{\Delta x}\frac{\partial F}{\partial u^{2k}} & \text{for} & p = 2k+1; \end{cases} \tag{3.11}$$

We now show that (3.8) implies that all conditions (a–e) are ≥ 0.

– Conditions (a) and (e): Condition (a) is satisfied by (3.8) because $\partial F/\partial u^p \geq 0$ when $p = 1$. In the same manner, condition (e) is satisfied by (3.8) because $\partial F/\partial u^p \leq 0$ when $p = 2k$.
– Conditions (b) and (d):

$$\left(\frac{\partial F}{\partial u^p} - \frac{\partial F}{\partial u^{p-1}}\right) \geq 0, \tag{3.12}$$

can be satisfied by any of the following:

$$\frac{\partial F}{\partial u^p} \geq \frac{\partial F}{\partial u^{p-1}} \geq 0, \tag{3.13a}$$

$$\frac{\partial F}{\partial u^{p-1}} \leq \frac{\partial F}{\partial u^p} \leq 0. \tag{3.13b}$$

However, conditions (a) and (e) require that F is non-decreasing in its first argument and non-increasing in its last argument. Therefore, only condition (3.13a) holds for $1 < p \leq k$, which is satisfied by (3.8); and only condition (3.13b) holds for $k + 1 < p \leq 2k$, which is satisfied by (3.8).
– Condition (c) can be written as:

$$1 + \frac{\Delta t}{\Delta x}\left(\frac{\partial F}{\partial u^{k+1}} - \frac{\partial F}{\partial u^k}\right) \geq 0, \tag{3.14}$$

and since for $p = k+1$ we have $\partial F/\partial u^p \leq 0$, and for $p = k$ we have $\partial F/\partial u^p \geq 0$, we may rewrite this as:

$$\frac{\Delta t}{\Delta x}\left(\left|\frac{\partial F}{\partial u^k}\right| + \left|\frac{\partial F}{\partial u^{k+1}}\right|\right) \leq 1, \tag{3.15}$$

which is the condition (3.9). □

It was already pointed out by LeVeque [20] that the LTS-Godunov scheme is not monotone for $C > 1$. We now use LeVeque's argument to show that the LTS-HLLE scheme is not monotone by constructing a counter-example. The LTS-HLLE scheme is obtained by defining the wave velocity estimates S_{L} and S_{R} according to Einfeldt [10]:

$$S_{\mathrm{L},j+1/2} = \min\left(f'(u_j), \lambda_{j+1/2}\right), \tag{3.16a}$$

$$S_{\mathrm{R},j+1/2} = \max\left(\lambda_{j+1/2}, f'(u_{j+1})\right). \tag{3.16b}$$

Consider the initial value problem for the inviscid Burgers equations with the initial data:

$$u_i^0 = \begin{cases} 1 & \text{if} \quad i = j, \\ 0 & \text{if} \quad i \neq j. \end{cases} \tag{3.17}$$

We can see that for the initial data (3.17):

$$S_{\mathrm{R},j-1/2} = u_j > S_{\mathrm{R},j+1/2} = \lambda_{j+1/2}, \tag{3.18}$$

hence the wave from $x_{j-1/2}$ can pass the wave from $x_{j+1/2}$ at some finite time (see Fig. 1). Given enough time and a large enough Courant number, there will be a cell z in front of the shock such that (2.19) reduces to:

$$u_z^{n+1} = u_z - \frac{\Delta t}{\Delta x} S_{\mathrm{R},j-1/2} \mathcal{W}_{j-1/2}^2 = -\frac{\Delta t}{\Delta x} S_{\mathrm{R},j-1/2}\left(u_j - u_{j-1/2}^{\mathrm{HLLE}}\right) < 0. \tag{3.19}$$

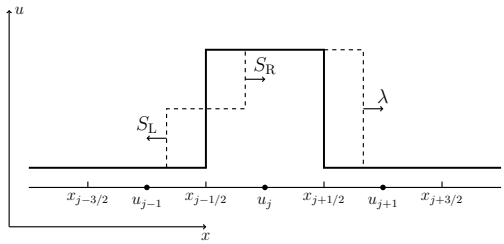

Fig. 1: Transport of initial data (3.17) with the LTS-HLLE scheme in the wave formulation (2.19)

Remark 2 We point out that both the LTS-Godunov and LTS-HLLE schemes are TVD (total variation diminishing). It is sometimes stated that the TVD methods are maximum-principle-satisfying, which we believe is due to the fact that authors implicitly assume standard methods. To the best of our knowledge, standard TVD methods are indeed maximum-principle-satisfying. However, as we showed above, that is not the case for the LTS TVD methods.

We now show that the LTS-Lax-Friedrichs scheme of Lindqvist et al. [24] is maximum-principle-satisfying by showing that it is monotone.

Proposition 2 *The LTS-Lax-Friedrichs scheme by Lindqvist et al. [24]:*

$$u_j^{n+1} = \mathcal{H}\left(u_{j-k}, u_{j+k}\right) = \frac{1}{2}\left(u_{j-k} + u_{j+k}\right) - \frac{\Delta t}{2k\Delta x}\left(f\left(u_{j+k}\right) - f\left(u_{j-k}\right)\right), \quad (3.20)$$

is monotone under the CFL condition:

$$C = \max_{x,t} |f'(u(x,t))| \frac{\Delta t}{\Delta x} \leq k. \quad (3.21)$$

Proof By differentiating (3.20) we have that:

$$\frac{\partial \mathcal{H}}{\partial u_l} = \begin{cases} \frac{1}{2}\left(1 + \frac{\Delta t}{k\Delta x} f'\left(u_{j-k}\right)\right) & l = j-k, \\ \frac{1}{2}\left(1 - \frac{\Delta t}{k\Delta x} f'\left(u_{j+k}\right)\right) & l = j+k, \\ 0 & \text{otherwise;} \end{cases} \quad (3.22)$$

which satisfies (3.3) if (3.21) holds. □

4 Systems of conservation laws

We begin by restating some existing results on positivity preservation in standard methods. We then move to LTS methods and outline how the loss of positivity occurs there.

4.1 Positivity preservation

We start by considering the existing result for positivity preserving properties of standard methods:

Definition 1 A class of schemes that always generate physical solutions from physical data is denoted as positivity preserving schemes.

This definition is due to Einfeldt et al. [11], where it is shown that the Godunov and HLLE schemes are positivity preserving, while the Roe scheme is not. Herein we outline the main points that will be used onwards. Consider a standard exact or approximate Riemann solver and note that the numerical algorithm may be seen as:

- (a) Solve the Riemann problem exactly or approximately to obtain the intermediate states in the Riemann fan.
- (b) Update the solution according to:

$$\mathbf{U}_j^{n+1} = \frac{1}{\Delta x}\int_0^{\frac{\Delta x}{2}} \widetilde{\mathbf{U}}_{j-1/2}\left(x/\Delta t\right)\mathrm{d}x + \frac{1}{\Delta x}\int_{-\frac{\Delta x}{2}}^{0} \widetilde{\mathbf{U}}_{j+1/2}\left(x/\Delta t\right)\mathrm{d}x, \quad (4.1)$$

where $\widetilde{\mathbf{U}}_{j\mp1/2}(x/\Delta t)$ is the exact or approximate solution to the Riemann problem at the cell interface $x_{j\mp1/2}$.

Einfeldt et al. [11] showed that if and only if step (a) generates physical states, then the scheme is positivity preserving. This is due to the fact that, given the physically admissible solutions to Riemann problems, the integration in (4.1) yields physical solutions. We have the following classical result:

Lemma 2 (Einfeldt et al. [11]) *An approximate Riemann solver leads to a positively conservative scheme if and only if all the states generated are physically real.*

Therefore, step (a) is the necessary and sufficient condition for the positivity preserving property of the scheme. Next, consider an exact or approximate LTS Riemann solver and note that the numerical algorithm may be seen as:

- (a) Solve the Riemann problem exactly or approximately to obtain the intermediate states in the Riemann fan
- (b) Update the solution according to:

$$\mathbf{U}_j^{n+1} = \frac{\Delta t}{\Delta x}\sum_{i=-\infty}^{\infty}\int_{(i-1)\frac{\Delta x}{\Delta t}}^{i\frac{\Delta x}{\Delta t}} \widetilde{\mathbf{U}}_{j-1/2-i}\left(\zeta_i\right)\mathrm{d}\zeta_i - \sum_{l=-\infty}^{\infty}\mathbf{U}_l, \quad (4.2)$$

where $\widetilde{\mathbf{U}}_{j-1/2}(\zeta_i)$ is the exact or approximate solution to the Riemann problem at the cell interface $x_{j-1/2-i}$ and $\zeta_i = (x - x_{j-1/2-i})/(t - t^n)$ (see [21,24] for details on (4.2)).

We observe that step (a) is the same for standard and LTS methods. We will show that in the LTS framework step (a) is only a necessary condition, i.e. (4.2) may yield non-physical states even when the solutions to the Riemann problems are physically real. In particular, we will show that:

Claim (1) The LTS-HLLE scheme is not positivity preserving.

Claim (2) The LTS-Lax-Friedrichs scheme is positivity preserving.

We will show that the LTS-HLLE is not positivity preserving by using the wave formulation (2.25) and by constructing a counter-example. General updating formula for an LTS method (4.2) can be rewritten as (2.23), (2.24) and (2.25). A nice feature of the wave formulation (2.25) is that we can decompose it to updating component by component. Since the wave velocity estimates are scalars, and the waves $\mathcal{W}$ are vectors, (2.25) allows us to treat the updating field-by-field as:

$$\theta_j^{n+1} = \theta_j^p - \frac{\Delta t}{\Delta x} \sum_{i=0}^{\infty} \left(\sum_{p=1}^{m} S^{p,i+}_{j-1/2-i} \theta^p_{j-1/2-i} + \sum_{p=1}^{m} S^{p,i-}_{j+1/2+i} \theta^p_{j+1/2+i} \right), \quad (4.3)$$

where θ is an arbitrary conserved variable from (2.1), and θ^p is the value of θ in the wave $\mathcal{W}^p$.

4.2 Loss of positivity with LTS-HLLE scheme in the Euler equations

We now consider two different ways how positivity can be lost in the Euler equations. The goal of this section is not to cover all possible ways how positivity can be lost. Instead, we aim to show that the LTS-HLLE scheme is not positivity preserving by constructing a counter-example, and we wish to illustrate the mechanism behind the loss of positivity. In particular, we consider only a class of initial data with the initial velocity:

$$v_0(x) = 0. \quad (4.4)$$

Further, we assume a special type of initial data where the perturbation of the data is limited to a single cell. Finally, the wave velocity estimates S_{L} and S_{R} in the HLLE scheme [10] are determined as the approximations to the smallest and the largest eigenvalues:

$$S_{\mathrm{L}} = \min\left(\lambda^1_j, \lambda^1_{j+1/2}\right), \quad (4.5a)$$

$$S_{\mathrm{R}} = \max\left(\lambda^3_{j+1/2}, \lambda^3_{j+1}\right), \quad (4.5b)$$

which for the one-dimensional Euler equations carry the indices 1 and 3, and where $\lambda^{1,3}_{j+1/2}$ are the Roe averaged eigenvalues [38].

4.2.1 Local collapse in density

Consider the initial data with a density spike in a single cell:

$$(\rho, v, p)^0_i = \begin{cases} (\rho_j, 0, 1) & \text{if} \quad i = j; \\ (\rho_0, 0, 1) & \text{if} \quad i \neq j, \end{cases} \quad (4.6)$$

with $\rho_j > \rho_0$. By using (2.3) and (2.4), the hierarchy of the eigenvalues in the neighborhood of the cell j is:

$$\lambda^1_{j-1} < \lambda^1_{j-1/2} < \lambda^1_j, \quad (4.7a)$$

$$\lambda^3_{j-1} > \lambda^3_{j-1/2} > \lambda^3_j, \quad (4.7b)$$

at the interface $x_{j-1/2}$ and:

$$\lambda_j^1 > \lambda_{j+1/2}^1 > \lambda_{j+1}^1, \tag{4.8a}$$

$$\lambda_j^3 < \lambda_{j+1/2}^3 < \lambda_{j+1}^3, \tag{4.8b}$$

at the interface $x_{j+1/2}$. For the density in the cell j, the LTS-HLLE scheme (4.3) yields:

$$\rho_j^{n+1} = \rho_j - \frac{\Delta t}{\Delta x}\left(S_{R,j-1/2}^{0+}\left(\rho_j - \rho_{j-1/2}^{\mathrm{HLLE}}\right) + S_{L,j+1/2}^{0-}\left(\rho_{j+1/2}^{\mathrm{HLLE}} - \rho_j\right)\right), \tag{4.9}$$

where we note that for the initial data (4.6) we have $\rho_{j-1/2}^{\mathrm{HLLE}} = \rho_{j+1/2}^{\mathrm{HLLE}}$ and $\rho_{j\mp1} = \rho_0$.

Lemma 3 *For the initial data* (4.6)*, the LTS-HLLE scheme preserves the positivity of the density in the cell j if:*

$$\rho_{j-1/2}^{HLLE} > \frac{1}{2}\rho_j. \tag{4.10}$$

Proof Both waves updating (4.9) reduce the density in the cell j. The decrease in the density is greatest when the Courant number C is large enough that (2.30) yields:

$$S_{R,j-1/2}^{0+} = \frac{\Delta x}{\Delta t}, \quad S_{L,j+1/2}^{0-} = -\frac{\Delta x}{\Delta t}. \tag{4.11}$$

Then (4.9) reduces to:

$$\rho_j^{n+1} = 2\rho_{j-1/2}^{\mathrm{HLLE}} - \rho_j, \tag{4.12}$$

which is positive when (4.10) holds. □

Lemma 4 *For the initial data* (4.6)*, the condition* (4.10) *holds for:*

$$\rho_j < b\rho_0, \tag{4.13}$$

where:

$$b = \frac{2}{3}\left(4 + \sqrt[3]{19 - 3\sqrt{33}} + \sqrt[3]{19 + 3\sqrt{33}}\right) \approx 5.6786. \tag{4.14}$$

Proof For the initial data (4.6), the intermediate state $\rho_{j-1/2}^{\mathrm{HLLE}}$ is determined by (2.13):

$$\rho_{j-1/2}^{\mathrm{HLLE}} = \frac{S_{\mathrm{R}}\rho_j - S_{\mathrm{L}}\rho_0}{S_{\mathrm{R}} - S_{\mathrm{L}}}. \tag{4.15}$$

By using (4.7) in (4.5) we have that at $x_{j-1/2}$:

$$S_{\mathrm{L}} = \lambda_0^1 = -a_0 = -\sqrt{\gamma p/\rho_0}, \tag{4.16a}$$

$$S_{\mathrm{R}} = \lambda_{j-1/2}^3 = a_{j+1/2} = \sqrt{\gamma p/\sqrt{\rho_0\rho_j}}, \tag{4.16b}$$

where $a_{j-1/2}$ is the Roe averaged speed of the sound (see for instance [22]). The intermediate state (4.15) now becomes:

$$\rho_{j-1/2}^{\mathrm{HLLE}} = \frac{\sqrt{\frac{1}{\sqrt{\rho_0\rho_j}}}\rho_j + \sqrt{\frac{1}{\rho_0}}\rho_0}{\sqrt{\frac{1}{\sqrt{\rho_0\rho_j}}} + \sqrt{\frac{1}{\rho_0}}}. \tag{4.17}$$

Then we can rewrite the condition (4.10) as:

$$\frac{1}{2}\rho_j\sqrt{\frac{1}{\sqrt{\rho_0\rho_j}}}-\sqrt{\frac{1}{\rho_0}}\left(\frac{1}{2}\rho_j-\rho_0\right)>0. \tag{4.18}$$

We know that $\rho_0<\rho_j$, i.e. we may write $\rho_j=b\rho_0$, $b>1$. By using this in (4.18) we obtain:

$$b^{3/4}-b+2>0, \tag{4.19}$$

which is a decreasing function of $b\in(1,\infty)$ and becomes negative when b exceeds the condition (4.14). □

4.2.2 Local collapse in internal energy

Consider the initial data with a pressure spike in a single cell:

$$(\rho,v,p)_i^0=\begin{cases}(1,0,p_j) & \text{if} \quad i=j;\\ (1,0,p_0) & \text{if} \quad i\neq j,\end{cases} \tag{4.20}$$

with $p_j>p_0$. By using (2.3) and (2.4), the hierarchy of the eigenvalues in the neighborhood of the cell j is:

$$\lambda^1_{j-1}>\lambda^1_{j-1/2}>\lambda^1_j, \tag{4.21a}$$
$$\lambda^3_{j-1}<\lambda^3_{j-1/2}<\lambda^3_j, \tag{4.21b}$$

at the interface $x_{j-1/2}$ and:

$$\lambda^1_j<\lambda^1_{j+1/2}<\lambda^1_{j+1}, \tag{4.22a}$$
$$\lambda^3_j>\lambda^3_{j+1/2}>\lambda^3_{j+1}, \tag{4.22b}$$

at the interface $x_{j+1/2}$. For the total energy density in the cell j, the LTS-HLLE scheme (4.3) yields:

$$E_j^{n+1}=E_j-\frac{\Delta t}{\Delta x}\left(S^{0+}_{R,j-1/2}\left(E_j-E^{\mathrm{HLLE}}_{j-1/2}\right)+S^{0-}_{L,k+1/2}\left(E^{\mathrm{HLLE}}_{j+1/2}-E_j\right)\right). \tag{4.23}$$

By using the following relations (superscript denotes the time step):

$$E_j^0=\rho_j^0e_j^0+\frac{1}{2}\rho_j^0[v_j^0]^2=\rho_j^0e_j^0, \tag{4.24a}$$
$$E_j^1=\rho_j^1e_j^1+\frac{1}{2}\rho_j^1[v_j^1]^2, \tag{4.24b}$$
$$\rho_j^1=\rho_j^0, \quad \forall j, \tag{4.24c}$$

we can obtain from (4.23) that the internal energy is:

$$\begin{aligned}e_j^{n+1}=&e_j-\frac{\Delta t}{\Delta x}\left(S^{0+}_{R,j-1/2}\left(e_j-e^{\mathrm{HLLE}}_{j-1/2}\right)+S^{0-}_{L,k+1/2}\left(e^{\mathrm{HLLE}}_{j+1/2}-e_j\right)\right)\\ &-\frac{1}{2}\left[v_j-\frac{\Delta t}{\Delta x}\left(S^{0+}_{R,j-1/2}\left(v_j-v^{\mathrm{HLLE}}_{j-1/2}\right)+S^{0-}_{L,k+1/2}\left(v^{\mathrm{HLLE}}_{j+1/2}-v_j\right)\right)\right]^2.\end{aligned} \tag{4.25}$$

We note that for the initial data (4.20) we have $e^{\mathrm{HLLE}}_{j-1/2}=e^{\mathrm{HLLE}}_{j+1/2}$, $v^{\mathrm{HLLE}}_{j-1/2}=-v^{\mathrm{HLLE}}_{j+1/2}$ and $p_{j\mp1}=p_0$.

Lemma 5 *For the initial data* (4.20)*, the LTS-HLLE scheme preserves the positivity of the internal energy in the cell* j*.*

Proof Both waves associated with the internal energy and the term associated with the kinetic energy reduce the internal energy in the cell j, eq. (4.25). The decrease in the internal energy is greatest when the Courant number C is large enough that (2.30) yields:

$$S^{0+}_{R,j-1/2} = \frac{\Delta x}{\Delta t}, \quad S^{0-}_{L,j+1/2} = -\frac{\Delta x}{\Delta t}. \tag{4.26}$$

Then (4.25) reduces to:

$$e_j^{n+1} = 2e^{\mathrm{HLLE}}_{j-1/2} - e_j - \frac{1}{2}\left[v^{\mathrm{HLLE}}_{j-1/2} + v^{\mathrm{HLLE}}_{j+1/2}\right]^2 = 2e^{\mathrm{HLLE}}_{j-1/2} - e_j, \tag{4.27}$$

which is always positive, as we will show next. For the initial data (4.20), the intermediate state $e^{\mathrm{HLLE}}_{j-1/2}$ is:

$$e^{\mathrm{HLLE}}_{j-1/2} = \frac{S_{\mathrm{R}} e_j - S_{\mathrm{L}} e_0}{S_{\mathrm{R}} - S_{\mathrm{L}}}. \tag{4.28}$$

By using (4.21) in the (4.5) we have that at $x_{j-1/2}$:

$$S_{\mathrm{L}} = \lambda^1_{j-1/2} = -a_{j-1/2} = -\sqrt{\gamma\left(p_0 + p_j\right)/\left(2\rho\right)}, \tag{4.29a}$$

$$S_{\mathrm{R}} = \lambda^3_j = a_j = \sqrt{\gamma p_j/\rho}. \tag{4.29b}$$

The intermediate state (4.28) now becomes:

$$e^{\mathrm{HLLE}}_{j-1/2} = \frac{1}{\gamma - 1}\frac{\sqrt{p_j}p_j + \sqrt{\frac{p_0+p_j}{2}}p_0}{\sqrt{p_j} + \sqrt{\frac{p_0+p_j}{2}}}. \tag{4.30}$$

We wish to show that (4.27) is always positive, i.e. $e^{\mathrm{HLLE}}_{j-1/2} > \frac{1}{2}e_j$ always holds:

$$\begin{aligned} &\frac{1}{\gamma - 1}\frac{\sqrt{p_j}p_j + \sqrt{\frac{p_0+p_j}{2}}p_0}{\sqrt{p_j} + \sqrt{\frac{p_0+p_j}{2}}} > \frac{1}{2}\frac{p_j}{\gamma - 1}, \\ &\frac{1}{2}p_j\sqrt{p_j} + \sqrt{\frac{p_0+p_j}{2}}\left(p_0 - \frac{1}{2}p_j\right) > 0. \end{aligned} \tag{4.31}$$

We know that $p_0 < p_j$, i.e. we may write $p_j = bp_0$, $b > 1$. By using this in (4.31) we obtain:

$$\frac{1}{2}b\sqrt{b} + \sqrt{\frac{1+b}{2}}\left(1 - \frac{1}{2}b\right) > 0, \tag{4.32}$$

which is an increasing function of $b \in (1, \infty)$, hence the inequality (4.27) always holds. □

4.2.3 Nonlocal collapse in density

In the section above we described how positivity can be lost in the cell where there is a spike in the initial data. We now show that a spike in the initial data in one cell can also cause loss of positivity in other cells as well. Such collapse will be denoted as a *nonlocal collapse*. It is this type of loss of positivity that in a system of equations is equivalent to the loss of monotonicity described in section 3.

Consider the initial data with a density spike in a single cell:

$$(\rho, v, p)_i^0 = \begin{cases} (\rho_j, 0, 1) & \text{if} \quad i = j; \\ (\rho_0, 0, 1) & \text{if} \quad i \neq j, \end{cases} \tag{4.33}$$

with $\rho_j > \rho_0$. The hierarchy of the eigenvalues in the neighborhood of cell j is the same as earlier, see (4.7) and (4.8). We note that the problem is symmetric and focus on the right side. There is a cell z to the right of cell j such that $z > j$ for which the LTS-HLLE scheme (4.3) yields:

$$\rho_z^{n+1} = \rho_z - \frac{\Delta t}{\Delta x}\left(S_{R,j-1/2}^{(z-j)+}\left(\rho_j - \rho_{j-1/2}^{\text{HLLE}}\right) + S_{R,j+1/2}^{(z-j-1)+}\left(\rho_{j+1} - \rho_{j+1/2}^{\text{HLLE}}\right)\right), \tag{4.34}$$

where we note that for the initial data (4.33) we have $\rho_{j-1/2}^{\text{HLLE}} = \rho_{j+1/2}^{\text{HLLE}}$ and $\rho_{j\mp1} = \rho_z = \rho_0$.

Lemma 6 *For the initial data* (4.33) *the LTS-HLLE scheme preserves the positivity of the density in the cell z if:*

$$\rho_{j-1/2}^{HLLE} > \frac{1}{2}\rho_j. \tag{4.35}$$

Proof We consider (4.34) and note that the wave from $x_{j-1/2}$ decreases the density in the cell z, while the wave from $x_{j+1/2}$ increases the density in the cell z. By using (4.7) and (4.8) in (4.5) we find out that the waves are moving with velocities:

$$S_{\text{R},j-1/2} = \lambda_{j-1/2}^3 = \lambda_{j+1/2}^3 < S_{\text{R},j+1/2} = \lambda_{j+1}^3, \tag{4.36}$$

hence the waves updating (4.34) cannot pass each other. The critical case is when the Courant number C is large enough that (2.30) yields:

$$S_{R,j-1/2}^{(z-j)+} = \frac{\Delta x}{\Delta t}, \qquad S_{R,j+1/2}^{(z-j-1)+} = \frac{\Delta x}{\Delta t}. \tag{4.37}$$

Then (4.34) reduces to:

$$\rho_z^{n+1} = 2\rho_{j-1/2}^{\text{HLLE}} - \rho_j, \tag{4.38}$$

which is positive when (4.35) holds. □

We note that the condition (4.35) holds under the same condition as in Lemma 4.

4.2.4 Nonlocal collapse in internal energy

Consider the initial data with a pressure spike in a single cell:

$$(\rho, v, p)_i^0 = \begin{cases} (1, 0, p_j) & \text{if} \quad i = j; \\ (1, 0, p_0) & \text{if} \quad i \neq j, \end{cases} \tag{4.39}$$

with $p_j > p_0$. The hierarchy of the eigenvalues in the neighborhood of cell j is the same as earlier, see (4.21) and (4.22). We note that the problem is symmetric and focus on the right side. There is a cell z to the right of cell j such that $z > j$ for which the LTS-HLLE scheme (4.3) yields:

$$E_z^{n+1} = E_z - \frac{\Delta t}{\Delta x}\left(S_{R,j-1/2}^{(z-j)+}\left(E_j - E_{j-1/2}^{\mathrm{HLLE}}\right) + S_{R,j+1/2}^{(z-j-1)+}\left(E_{j+1} - E_{j+1/2}^{\mathrm{HLLE}}\right)\right). \tag{4.40}$$

By using the relations given in (4.24), we can obtain from (4.40) that the internal energy is:

$$\begin{aligned} e_z^{n+1} =& e_z - \frac{\Delta t}{\Delta x}\left(S_{R,j-1/2}^{(z-j)+}\left(e_j - e_{j-1/2}^{\mathrm{HLLE}}\right) + S_{R,j+1/2}^{(z-j-1)+}\left(e_{j+1} - e_{j+1/2}^{\mathrm{HLLE}}\right)\right) \\ & -\frac{1}{2}\left[v_z - \frac{\Delta t}{\Delta x}\left(S_{R,j-1/2}^{(z-j)+}\left(v_j - v_{j-1/2}^{\mathrm{HLLE}}\right) + S_{R,j+1/2}^{(z-j-1)+}\left(v_{j+1} - v_{j+1/2}^{\mathrm{HLLE}}\right)\right)\right]^2. \end{aligned} \tag{4.41}$$

We note that for the initial data (4.39) we have $e_{j-1/2}^{\mathrm{HLLE}} = e_{j+1/2}^{\mathrm{HLLE}}$, $v_{j-1/2}^{\mathrm{HLLE}} = -v_{j+1/2}^{\mathrm{HLLE}}$ and $p_{j\mp1} = p_0$.

Lemma 7 *For the initial data* (4.39)*, the LTS-HLLE scheme preserves positivity of the internal energy in the cell z if:*

$$e_{j-1/2}^{HLLE} > e_j - e_0 + \frac{1}{2}[v_{j-1/2}^{HLLE}]^2. \tag{4.42}$$

Proof We consider (4.41) and note that the wave from $x_{j-1/2}$ decreases the internal energy in cell z, the wave from $x_{j+1/2}$ increases the internal energy in the cell z, and the term corresponding to kinetic energy decreases the internal energy in the cell z. By using (4.21) and (4.22) in (4.5) we find out that the waves are moving with velocities:

$$S_{\mathrm{R},j-1/2} = \lambda_j^3 > S_{\mathrm{R},j+1/2} = \lambda_{j+1/2}^3, \tag{4.43}$$

hence the waves updating (4.40) can pass each other. The critical case is when the Courant number C is such that (2.30) yields:

$$S_{R,j-1/2}^{(z-j)+} = \frac{\Delta x}{\Delta t}, \qquad S_{R,j+1/2}^{(z-j-1)+} = 0, \tag{4.44}$$

i.e. the wave decreasing the internal energy completely passes through the cell z, and the wave increasing the internal energy does not reach the cell z. Then (4.41) reduces to:

$$e_z^{n+1} = e_0 - e_j + e_{j-1/2}^{\mathrm{HLLE}} - \frac{1}{2}[v_{j-1/2}^{\mathrm{HLLE}}], \tag{4.45}$$

which is positive when (4.42) holds. □

Lemma 8 *For the initial data* (4.39)*, the condition* (4.42) *holds for:*

$$p_j < 3.09224 p_0. \tag{4.46}$$

Proof For the initial data (4.39), the intermediate state $e^{\mathrm{HLLE}}_{j-1/2}$ was already defined in (4.30), while the intermediate state $v^{\mathrm{HLLE}}_{j-1/2}$ can be determined in a similar manner as:

$$v^{\mathrm{HLLE}}_{j-1/2} = \frac{p_0 - p_j}{\sqrt{\gamma p_0} + \sqrt{\gamma \frac{p_0+p_j}{2}}}. \tag{4.47}$$

Then we can rewrite the condition (4.42) as:

$$\frac{1}{\gamma-1}\frac{\sqrt{p_j}p_j + \sqrt{\frac{p_0+p_j}{2}}p_0}{\sqrt{p_j}+\sqrt{\frac{p_0+p_j}{2}}} + \frac{p_0}{\gamma-1} - \frac{p_j}{\gamma-1} - \frac{1}{2}\left[\frac{p_0-p_j}{\sqrt{\gamma p_0}+\sqrt{\gamma\frac{p_0+p_j}{2}}}\right]^2 > 0 \tag{4.48}$$

We know that $p_0 < p_j$, i.e. we may write $p_j = bp_0$ and $b > 1$. By using that we have:

$$\sqrt{\frac{1+b}{2}}(2-b) + \sqrt{b} - \frac{\gamma-1}{2\gamma}\left(\frac{1-2b+b^2}{b+2\sqrt{b}\sqrt{\frac{(1+b)}{2}}+\frac{(1+b)}{2}}\right)\left(\sqrt{b}+\sqrt{\frac{1+b}{2}}\right) > 0. \tag{4.49}$$

This is a decreasing function of $b \in (1,\infty)$ and becomes negative when $b = 3.09224$. □

We showed four different examples how positivity of density and internal energy can be lost when we use the LTS-HLLE scheme. We note that these examples are limited to very special types of the initial data, and it is reasonable to expect that arbitrary initial data might lead to more ways to lose positivity, especially if the velocity differences between the cells would be very large.

We now proceed to show that the LTS-Lax-Friedrichs scheme by Lindqvist et al. [24] is positivity preserving.

4.3 LTS-Lax-Friedrichs scheme for the Euler equations

Proposition 3 *The LTS-Lax-Friedrichs scheme by Lindqvist et al. [24]:*

$$\mathbf{U}^{n+1}_j = \frac{1}{2}\left(\mathbf{U}_{j-k} + \mathbf{U}_{j+k}\right) - \frac{\Delta t}{2k\Delta x}\left(\mathbf{F}_{j+k} - \mathbf{F}_{j-k}\right), \tag{4.50}$$

is positivity preserving for the one-dimensional Euler equations under the CFL condition:

$$C = \max_{p,x,t}\left|\lambda^p(x,t)\right|\frac{\Delta t}{\Delta x} \le k, \quad k \in \mathbb{Z}^+. \tag{4.51}$$

Our proof is based on the paper by Zhang and Shu [49] where it is shown that the standard Lax-Friedrichs scheme is positivity preserving for the Euler equations under the standard CFL condition (2.14). We follow their proof and generalize it to hold under the relaxed CFL condition (4.51). We start with the following result:

Lemma 9 (Zhang and Shu [49]) *Define the set of admissible states by:*

$$G = \left\{ \mathbf{U} = \begin{bmatrix} \rho \\ \rho u \\ E \end{bmatrix} \middle| \, \rho > 0, \quad \text{and} \quad p = (\gamma - 1)\left(E - \tfrac{1}{2}\rho v^2\right) > 0 \right\}, \tag{4.52}$$

then G is a convex set.

Proof (Proposition 3) We can rewrite (4.50) as:

$$\mathbf{U}_j^{n+1} = \frac{1}{2}\left(\mathbf{U}_{j-k} + \frac{\Delta t}{k\Delta x}\mathbf{F}_{j-k}\right) + \frac{1}{2}\left(\mathbf{U}_{j+k} - \frac{\Delta t}{k\Delta x}\mathbf{F}_{j+k}\right). \tag{4.53}$$

We assume that $\mathbf{U}_{j-k}$ and $\mathbf{U}_{j+k}$ are in the set G, and we want to show that $\mathbf{U}_j^{n+1} \in G$ under the CFL condition (4.51). We start by observing that $\mathbf{U}_j^{n+1}$ is a convex combination of vectors:

$$\mathbf{U}_{j-k} + \frac{\Delta t}{k\Delta x}\mathbf{F}_{j-k}, \quad \text{and} \quad \mathbf{U}_{j+k} - \frac{\Delta t}{k\Delta x}\mathbf{F}_{j+k}. \tag{4.54}$$

Therefore, we only need to show that these vectors are in the set G. For the first component of $\mathbf{U}$ (the density) we obtain:

$$\left(1 \pm \frac{\Delta t}{k\Delta x} v_{j\mp k}\right) \rho_{j\mp k} > 0, \tag{4.55}$$

which is satisfied when (4.51) holds. The next step is showing the positivity of pressure. By dropping subscripts, the pressure ($p = (\gamma - 1)\rho e$) can be written as a function of conserved variables:

$$\begin{aligned} p\left(\mathbf{U} \pm \frac{\Delta t}{k\Delta x}\mathbf{F}\right) =& p\left(\left[\rho \pm \frac{\Delta t}{k\Delta x}\rho v, \rho v \pm \frac{\Delta t}{k\Delta x}(\rho v^2 + p), E \pm \frac{\Delta t}{k\Delta x} v(E+p)\right]^{\mathrm{T}}\right) \\ =& p\left(1 \pm \frac{\Delta t}{k\Delta x} v\right)\left(1 - \frac{p}{\rho}\frac{\gamma - 1}{2\left(\frac{k\Delta x}{\Delta t} \pm v\right)^2}\right). \end{aligned} \tag{4.56}$$

The first bracket is positive since it is equal to the bracket in (4.55), while the second bracket can be rewritten as:

$$\left(1 - \frac{p}{\rho}\frac{\gamma - 1}{2\left(\frac{k\Delta x}{\Delta t} \pm v\right)^2}\right) > 0 \quad \longrightarrow \quad \sqrt{\frac{2\gamma}{\gamma - 1}}\left(\frac{k\Delta x}{\Delta t} \pm v\right) > \sqrt{\gamma\frac{p}{\rho}}, \tag{4.57}$$

which always holds under the CFL condition (4.51). □

4.4 Towards a positivity preserving LTS method

In the existing literature, two main ways to tackle the loss of positivity are:

– Constructing an unconditionally positivity preserving scheme (see references in section 1). This approach is currently available only for standard methods, and at the moment it seems unattainable for a wide class of LTS methods because of lack of full understanding of all possible ways the positivity can be lost. Currently, the LTS-Lax-Friedrichs scheme is the only known positivity preserving LTS method.

– Reducing the Courant number. This approach works for LTS methods as well, and it has been exploited by Morales-Hernández and co-workers [28,29]. The straightforward way to do this is by repeating the time step with a reduced Courant number when the positivity is lost, while more sophisticated approaches include determining if the loss of positivity is likely to happen at the beginning of each time step.

Herein, we propose a very general way to increase the robustness of the LTS method and its ability to preserve positivity by adding numerical diffusion. We start by observing that by defining the wave velocity estimates as $S_{\mathrm{L}} = -k\Delta x/\Delta t$ and $S_{\mathrm{R}} = k\Delta x/\Delta t$ in the LTS-HLL scheme we recover the LTS-Lax-Friedrichs scheme of Lindquist et al. [24]. Since the LTS-Lax-Friedrichs scheme is positivity preserving, we propose to parametrize the wave velocity estimates as a convex combination between the HLLE and Lax-Friedrichs schemes:

$$S_{\mathrm{L}} = (1-\beta)\, S_{\mathrm{L}}^{\mathrm{E}} + \beta S_{\mathrm{L}}^{\mathrm{LxF}}, \qquad S_{\mathrm{R}} = (1-\beta)\, S_{\mathrm{R}}^{\mathrm{E}} + \beta S_{\mathrm{R}}^{\mathrm{LxF}}, \tag{4.58}$$

where $S_{\mathrm{L,R}}^{\mathrm{E}}$ are the wave velocity estimates according to Einfeldt (4.5). We will denote this method as the LTS-HLLEβ.

5 Numerical results

In this section we present numerical results for three test cases commonly used to test the robustness of numerical methods. The input discretization parameters are the Courant number C and Δx. Then, the time step Δt is evaluated at each time step according to:

$$\Delta t = \frac{C\Delta x}{\max\limits_{p,j} |\lambda_j^p|}\,. \tag{5.1}$$

5.1 Double rarefaction

As the first test case we consider the double rarefaction test case already considered by Prebeg [34], with initial data $\mathbf{V}(x,0) = (\rho, v, p)^{\mathrm{T}}$:

$$\mathbf{V}(x,0) = \begin{cases} (1,-2,0.4)^{\mathrm{T}} & \text{if} \quad x < 0, \\ (1,2,0.4)^{\mathrm{T}} & \text{if} \quad x > 0, \end{cases} \tag{5.2}$$

where the solution is evaluated at $t = 0.05$ on a grid with 100 cells in the interval $[-0.2, 0.2]$. Figure 2 shows that the LTS-HLLE scheme successfully resolves problem (5.2) at the Courant number $C = 5$. Further, we observe that the LTS-HLLEβ scheme yields smoother profiles of all variables. We note that the LTS-HLLE scheme preserves positivity for the problem (5.2) for all Courant numbers we tried.

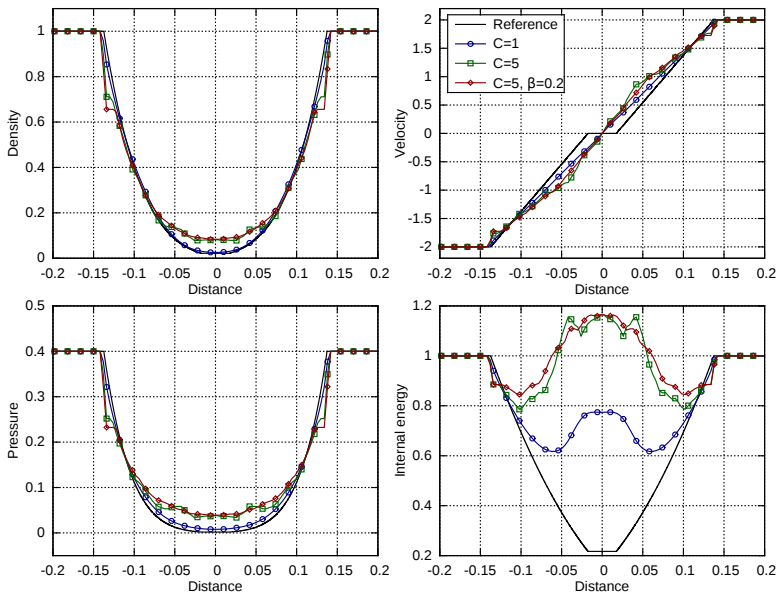

Fig. 2: The HLLE and LTS-HLLE(β) schemes for the problem (5.2)

5.2 LeBlanc's shock tube

As the second test case we consider LeBlanc's shock tube with initial data $\mathbf{V}(x,0) = (\rho, v, p)^{\mathrm{T}}$:

$$\mathbf{V}(x,0) = \begin{cases} (1, 0, (2/3)0.1)^{\mathrm{T}} & \text{if} \quad x < 3, \\ (0.001, 0, (2/3)10^{-7})^{\mathrm{T}} & \text{if} \quad x > 3, \end{cases} \tag{5.3}$$

and $\gamma = 5/3$, where the solution is evaluated at $t = 6$ on a grid with 600 cells in the interval $[0, 9]$. Figure 3 shows that both LTS-HLLE(β) schemes perform better than the LTS-Roe scheme. This becomes even more notable as we increase the Courant number, and the LTS-Roe scheme losses positivity and crashes for $C \geq 10$, while the LTS-HLLE(β) schemes preserve positivity for all Courant numbers we tried. Introducing numerical diffusion smoothened the profiles, but also calculated position of the right shock even further to the right. We note that large errors observed in velocity and internal energy (even with the standard methods) have been reported by other authors as well, see for instance [26,7,48].

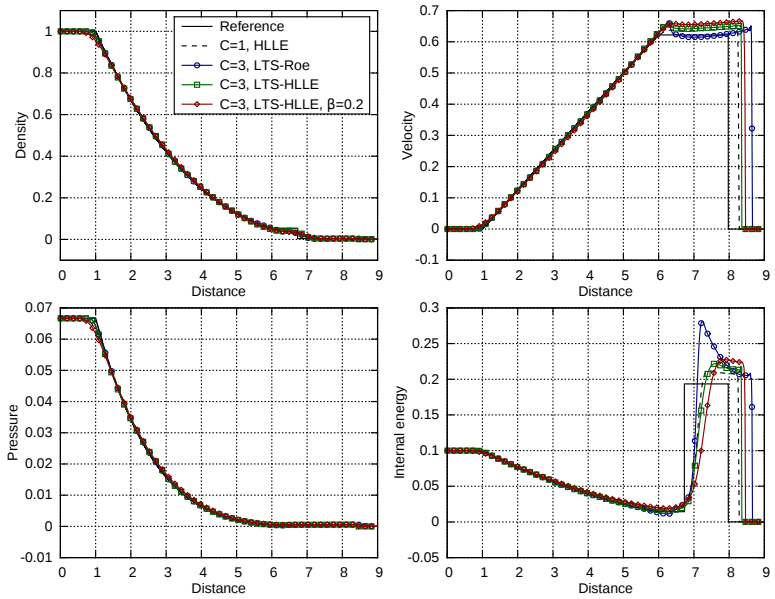

Fig. 3: The HLLE, LTS-Roe and LTS-HLLE(β) schemes for the problem (5.3)

5.3 Sedov blast-wave

As the last test case we consider the planar Sedov blast-wave problem with the initial data $\mathbf{V}(x,0) = (\rho, v, p)^{\mathrm{T}}$:

$$\mathbf{V}(x,0) = \begin{cases} (1, 0, 4 \times 10^{-13}) & \text{if} \quad -2 < x < -0.5\Delta x, \quad 0.5\Delta x < x < 2 \\ (1, 0, 2.56 \times 10^{8}) & \text{if} \quad -0.5\Delta x < x < 0.5\Delta x, \end{cases} \tag{5.4}$$

where the solution is evaluated at $t = 10^{-3}$ on a grid with 800 cells in the interval $[-2, 2]$. The exact solution is obtained with free software [42]. In the previous two test cases, the LTS-HLLE scheme preserved positivity for any Courant number we tried. For the Sedov blast-wave, the LTS-HLLE scheme loses positivity for $C > 4$, but we were able to use $C > 4$ by adding numerical diffusion, see Fig. 4. The loss of positivity for the LTS-HLLE scheme is expected because the initial data (5.4) closely resembles the initial data studied in section 4.

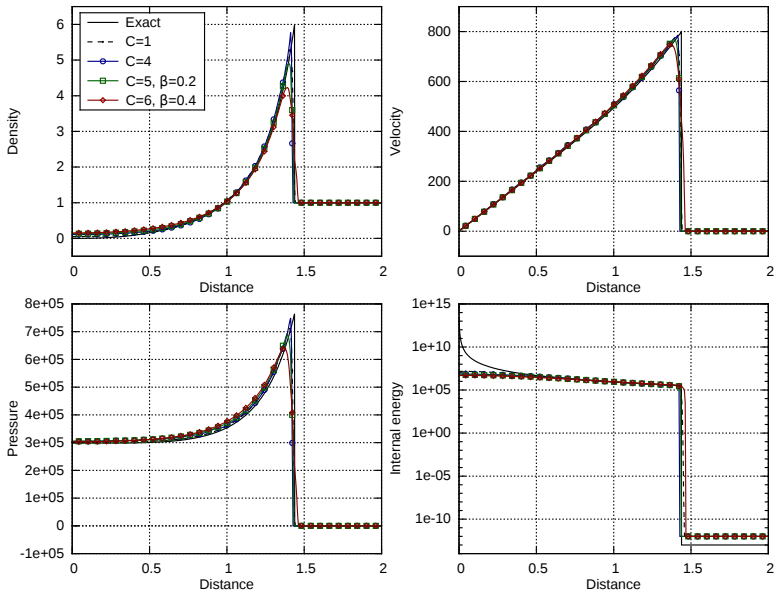

Fig. 4: The HLLE and LTS-HLLE(β) schemes for the problem (5.4)
(the solution is symmetric and only the right half of the domain is shown)

6 Conclusions

We have investigated the monotonicity and positivity preserving properties in LTS methods, with a special focus on the LTS-HLLE scheme for the Euler equations. In particular, we have determined the monotonicity conditions on the numerical flux function of the LTS method for scalar conservation laws (Proposition 1), and we showed that the LTS-HLLE scheme is not positivity preserving. Further, we showed that the LTS-Lax-Friedrichs scheme for scalar conservation laws is monotone (Proposition 2) and that the LTS-Lax-Friedrichs scheme for the Euler equations is positivity preserving (Proposition 3).

We applied the LTS-HLLE(β) schemes to three test cases commonly used to test the positivity preserving property. Even though the LTS-HLLE scheme is not positivity preserving, numerical investigations suggest that it always preserves positivity for the double rarefaction and LeBlanc's shock tube. The LTS-HLLE scheme lost positivity for the Sedov blast-wave when we increased the Courant number above certain values. We proposed a very simple way to make the schemes more robust by adding numerical diffusion, which allowed us to increase the Courant number used for the Sedov blast-wave. Unfortunately, increased robustness obtained by adding numerical diffusion results in less accurate solutions.

We believe that the decrease in accuracy due to additional diffusion can be reduced by more sophisticated ways of introducing numerical diffusion. In our

investigations the parameter β is constant across the whole domain and at all time steps. By selectively introducing numerical diffusion we could introduce a minimal amount of numerical diffusion required to ensure positivity preservation, while keeping the solution as sharp as possible. The development of such methods requires further insight into the ways positivity is lost, and at the moment it remains outside the scope of this paper.

References

1. Audusse, E., Bristeau, M.O.: A well-balanced positivity preserving second-order scheme for shallow water flows on unstructured meshes. J. Comput. Phys. **206**(1), 311–333 (2005). DOI 10.1016/j.jcp.2004.12.016
2. Balsara, S.D., Spicer, D.: Maintaining pressure positivity in magnetohydrodynamic simulations. J. Comput. Phys. **148**(1), 133–148 (1999). DOI 10.1006/jcph.1998.6108
3. Batten, P., Clarke, N., Lambert, C., Causon, D.M.: On the choice of wavespeeds for the HLLC Riemann solver. SIAM J. Sci. Comput. **18**(6), 1553–1570 (1997). DOI 10.1137/S1064827593260140
4. Berthon, C.: Robustness of MUSCL schemes for 2D unstructured meshes. J. Comput. Phys. **218**(2), 495–509 (2006). DOI 10.1016/j.jcp.2006.02.028
5. Bouchut, F.: Nonlinear Stability of Finite Volume Methods for Hyperbolic Conservation Laws, 1 edn. Frontiers in Mathematics. Birkhäuser Basel (2004). DOI 10.1007/b93802
6. Calgaro, C., Creusé, E., Goudon, T., Penel, Y.: Positivity-preserving schemes for Euler equations: Sharp and practical CFL conditions. J. Comput. Phys. **234**, 417–438 (2013). DOI 10.1016/j.jcp.2012.09.040
7. Cheng, J., Shu, C.W.: A high order ENO conservative Lagrangian type scheme for the compressible Euler equations. J. Comput. Phys. **227**(2), 1567–1596 (2007). DOI 10.1016/j.jcp.2007.09.017
8. Cheng, J., Shu, C.W.: Positivity-preserving Lagrangian scheme for multi-material compressible flow. J. Comput. Phys. **257**(A), 143–168 (2014). DOI 10.1016/j.jcp.2013.09.047
9. Davis, S.: Simplified second-order Godunov-type methods. SIAM J. Sci. Stat. Comput. **9**(3), 445–473 (1988). DOI 10.1137/0909030
10. Einfeldt, B.: On Godunov-type methods for gas dynamics. SIAM J. Numer. Anal. **25**(2), 294–318 (1988). DOI 10.1137/0725021
11. Einfeldt, B., Munz, C.D., Roe, P., Sjögreen, B.: On Godunov-type methods near low densities. J. Comput. Phys. **92**(2), 273–295 (1991). DOI 10.1016/0021-9991(91)90211-3
12. Gallice, G.: Positive and entropy stable Godunov-type schemes for gas dynamics and MHD equations in Lagrangian or Eulerian coordinates. Numer. Math. **94**(4), 673–713 (2003). DOI 10.1007/s00211-002-0430-0
13. Gressier, J., Villedieu, P., J.-M., M.: Positivity of flux vector splitting schemes. J. Comput. Phys. **155**(1), 199–220 (1999). DOI 10.1006/jcph.1999.6337
14. Harten, A.: High resolution schemes for hyperbolic conservation laws. J. Comput. Phys. **49**(3), 357–393 (1983). DOI 10.1016/0021-9991(83)90136-5
15. Harten, A., Lax, P.D., van Leer, B.: On upstream differencing and Godunov-type schemes for hyperbolic conservation laws. SIAM Rev. **25**(1), 35–61 (1983). DOI 10.1137/1025002
16. Hu, X.Y., Adams, N.A., Shu, C.W.: Positivity-preserving method for high-order conservative schemes solving compressible Euler equations. J. Comput. Phys. **242**, 169–180 (2013). DOI 10.1016/j.jcp.2013.01.024
17. Janhunen, P.: A positive conservative method for magnetohydrodynamics based on HLL and Roe methods. J. Comput. Phys. **160**(2), 649–661 (2000). DOI 10.1006/jcph.2000.6479
18. Kurganov, A., Petrova, G.: A second-order well-balanced positivity preserving central-upwind scheme for the Saint-Venant system. Commun. Math. Sci. **5**(1), 133–160 (2007)
19. LeVeque, R.J.: Large time step shock-capturing techniques for scalar conservation laws. SIAM J. Numer. Anal. **19**(6), 1091–1109 (1982). DOI 10.1137/0719080
20. LeVeque, R.J.: Convergence of a large time step generalization of Godunov's method for conservation laws. Comm. Pure Appl. Math. **37**(4), 463–477 (1984). DOI 10.1002/cpa.3160370405
21. LeVeque, R.J.: A large time step generalization of Godunov's method for systems of conservation laws. SIAM J. Numer. Anal. **22**(6), 1051–1073 (1985). DOI 10.1137/0722063

22. LeVeque, R.J.: Finite Volume Methods for Hyperbolic Problems, 1 edn. Cambridge Texts in Applied Mathematics (Book 31). Cambridge University Press (2002). DOI 10.1017/CBO9780511791253
23. Li, P., Don, W.S., Wang, C., Gao, Z.: High order positivity- and bound-preserving hybrid compact-WENO finite difference scheme for the compressible Euler equations. J. Sci. Comput. pp. 1–27 (2017). DOI 10.1007/s10915-017-0452-5
24. Lindqvist, S., Aursand, P., Flåtten, T., Solberg, A.A.: Large Time Step TVD schemes for hyperbolic conservation laws. SIAM J. Numer. Anal. **54**(5), 2775–2798 (2016). DOI 10.1137/15M104935X
25. Lindqvist, S., Lund, H.: A Large Time Step Roe scheme applied to two-phase flow. In: M. Papadrakakis, V. Papadopoulos, G. Stefanou, V. Plevris (eds.) VII European Congress on Computational Methods in Applied Sciences and Engineering. ECCOMAS, Crete Island, Greece (2016)
26. Loubére, R., Shashkov, M.J.: A subcell remapping method on staggered polygonal grids for arbitrary-Lagrangian-Eulerian methods. J. Comput. Phys. **209**(1), 105–138 (2005). DOI 10.1016/j.jcp.2005.03.019
27. Makwana, N.N., Chatterjee, A.: Fast solution of time domain Maxwell's equations using large time steps. In: 2015 IEEE International Conference on Computational Electromagnetics (ICCEM 2015), pp. 330–332. Institute of Electrical and Electronics Engineers (IEEE), Hong Kong, China (2015). DOI 10.1109/COMPEM.2015.7052651
28. Morales-Hernández, M., García-Navarro, P., Murillo, J.: A large time step 1D upwind explicit scheme (CFL>1): Application to shallow water equations. J. Comput. Phys. **231**(19), 6532–6557 (2012). DOI 10.1016/j.jcp.2012.06.017
29. Morales-Hernández, M., Hubbard, M.E., García-Navarro, P.: A 2D extension of a Large Time Step explicit scheme (CFL>1) for unsteady problems with wet/dry boundaries. J. Comput. Phys. **263**, 303–327 (2014). DOI 10.1016/j.jcp.2014.01.019
30. Morales-Hernández, M., Lacasta, A., Murillo, J., García-Navarro, P.: A Large Time Step explicit scheme (CFL>1) on unstructured grids for 2D conservation laws: Application to the homogeneous shallow water equations. Appl. Math. Model. **47**, 294–317 (2017). DOI 10.1016/j.apm.2017.02.043
31. Morales-Hernández, M., Murillo, J., García-Navarro, P., Burguete, J.: A large time step upwind scheme for the shallow water equations with source terms. In: E.V. Cendón, A. Hidalgo, P. García-Navarro, L. Cea (eds.) Numerical Methods for Hyperbolic Equations, pp. 141–148. CRC Press (2012). DOI 10.1201/b14172-17
32. Murillo, J., García-Navarro, P., Brufau, P., Burguete, J.: Extension of an explicit finite volume method to large time steps (CFL>1): Application to shallow water flows. Int. J. Numer. Meth. Fluids **50**(1), 63–102 (2006). DOI 10.1002/fld.1036
33. Perthame, B., Shu, C.W.: On positivity preserving finite volume schemes for Euler equations. Numer. Math. **73**(1), 119–130 (1996). DOI 10.1007/s002110050187
34. Prebeg, M.: Numerical viscosity in Large Time Step HLL-type schemes. In: C. Klingenberg, M. Westdickenberg (eds.) Proceedings of the Sixteenth International Conference on Hyperbolic Problems, HYP2016. Aachen, Germany (2017). Accepted for publication.
35. Prebeg, M., Flåtten, T., Müller, B.: Large Time Step HLL and HLLC schemes (2017). Submitted
36. Prebeg, M., Flåtten, T., Müller, B.: Large Time Step Roe scheme for a common 1D two-fluid model. Appl. Math. Model. **44**, 124–142 (2017). DOI 10.1016/j.apm.2016.12.010
37. Qian, Z., Lee, C.H.: A class of large time step Godunov schemes for hyperbolic conservation laws and applications. J. Comput. Phys. **230**(19), 7418–7440 (2011). DOI 10.1016/j.jcp.2011.06.008
38. Roe, P.: Approximate Riemann solvers, parameter vectors, and difference schemes. J. Comput. Phys. **43**(2), 357–372 (1981). DOI 10.1016/0021-9991(81)90128-5
39. Shirkhani, H., Mohammadian, A., Seidou, O., Kurganov, A.: A well-balanced positivity-preserving central-upwind scheme for shallow water equations on unstructured quadrilateral grids. Comput. Fluids **121**, 25–40 (2016). DOI 10.1016/j.compfluid.2015.11.017
40. Tadmor, E.: Numerical viscosity and the entropy condition for conservative difference schemes. Math. Comp **43**(168), 369–381 (1984). DOI 10.1090/s0025-5718-1984-0758189-x
41. Tang, K., Beccantini, A., Corre, C.: Combining Discrete Equations Method and upwind downwind-controlled splitting for non-reacting and reacting two-fluid computations: One dimensional case. Comput. Fluids **93**, 74–90 (2014). DOI 10.1016/j.compfluid.2014.01.017
42. Timmes, F.X., Gisler, G., Hrbek, G.M.: Automated analyses of the tri-lab verification test suite on uniform and adaptive grids for code project A. Tech. rep., Los Alamos National Laboratory (2005). URL http://cococubed.asu.edu/research_pages/sedov.shtml

43. Toro, E.F.: Riemann Solvers and Numerical Methods for Fluid Dynamics, 3 edn. Springer-Verlag Berlin Heidelberg (2009). DOI 10.1007/b79761
44. Toro, E.F., Spruce, M., Speares, W.: Restoration of the contact surface in the HLL-Riemann solver. Shock Waves **4**(1), 25–34 (1994). DOI 10.1007/BF01414629
45. Trangenstein, J.A.: Numerical Solution of Hyperbolic Partial Differential Equations. Cambridge University Press (2009)
46. Xing, Y., Zhang, X., Shu, C.W.: Positivity-preserving high order well-balanced discontinuous Galerkin methods for the shallow water equations. Adv. Water Resour. **33**(12), 1476–1493 (2010). DOI 10.1016/j.advwatres.2010.08.005
47. Xu, R., Zhong, D., Wu, B., Fu, X., Miao, R.: A large time step Godunov scheme for free-surface shallow water equations. Chinese Sci. Bull. **59**(21), 2534–2540 (2014). DOI 10.1007/s11434-014-0374-7
48. Zanotti, O., Dumbser, M.: Efficient conservative ADER schemes based on WENO reconstruction and space-time predictor in primitive variables. Comput. Astrophys. **3**(1) (2016). DOI 10.1186/s40668-015-0014-x
49. Zhang, X., Shu, C.W.: On positivity-preserving high order discontinuous Galerkin schemes for compressible Euler equations on rectangular meshes. J. Comput. Phys. **229**(23), 8918–8934 (2010). DOI 10.1016/j.jcp.2010.08.016
50. Zhang, X., Shu, C.W.: Maximum-principle-satisfying and positivity-preserving high-order schemes for conservation laws: Survey and new developments. Proc. Math. Phys. Eng. Sci. **467**(2134), 2752–2776 (2011). DOI 10.1098/rspa.2011.0153
51. Zhang, X., Shu, C.W.: Positivity-preserving high order finite difference WENO schemes for compressible Euler equations. J. Comput. Phys. **231**(5), 2245–2258 (2012). DOI 10.1016/j.jcp.2011.11.020

Conference paper 1 (P5)

Boundary and source term treatment in the Large Time Step method for a common two-fluid model

Marin Prebeg, Tore Flåtten and Bernhard Müller

In: Proceedings of the 11th International Conference on CFD in the Minerals and Process Industries. Melbourne, Australia, 2015.

Eleventh International Conference on CFD in the Minerals and Process Industries
CSIRO, Melbourne, Australia
7-9 December 2015

BOUNDARY AND SOURCE TERM TREATMENT IN THE LARGE TIME STEP METHOD FOR A COMMON TWO-FLUID MODEL

Marin PREBEG[1]*, **Tore FLÅTTEN**[2], **Bernhard MÜLLER**[1]

[1]Department of Energy and Process Engineering, Norwegian University of Science and Technology, NO-7491 Trondheim, NORWAY

[2]SINTEF Materials and Chemistry, P. O. Box 4760 Sluppen, NO-7465 Trondheim, NORWAY

* Corresponding author, E-mail address: marin.prebeg@ntnu.no

ABSTRACT

In this paper we present the Large Time Step method based on the Roe scheme applied to a standard two-fluid model. The Large Time Step method was originally developed in the nineteen eighties by Randall LeVeque and has enjoyed increasing popularity in the CFD community in recent years due to its attractive features such as increased accuracy and efficiency compared to its standard low time step counterparts. In terms of efficiency and computation time, one of the main disadvantages in common explicit schemes is the limited time step size imposed by the CFL condition. The idea behind the Large Time Step method is to increase the domain of dependence which leads to a relaxation of the CFL condition, allowing us to use Courant numbers larger than one, i.e. using very large time steps compared to standard explicit methods. It is shown that such an approach notably reduces the computation time and increases the accuracy of the solution. However, the idea of increasing the domain of dependence causes difficulties when it comes to boundary treatment, especially in the presence of source terms. In this paper, we describe and address these difficulties. We extend the standard Roe scheme with the Large Time Step method and apply it to the standard two-fluid model for the water faucet test case, focusing on the treatment of the boundary conditions. Furthermore, we compare the performance of the scheme with the classical Roe scheme in terms of computational time.

Keywords: Two-fluid model, Large Time Step, Boundary treatment, Source term.

NOMENCLATURE

a	speed of sound, $[m/s]$
$\mathbf{A}$	coefficient matrix
$\hat{\mathbf{A}}$	Roe matrix
$\mathbf{F}$	flux vector
g	gravitational acceleration, $[m/s^2]$
k	phase index, g - gas, l - liquid
p	pressure, $[Pa]$
p^i	interface pressure, $[Pa]$
$\mathbf{Q}$	source term
$\hat{\mathbf{R}}$	matrix of right eigenvectors of Roe matrix
t	time, $[s]$
$\mathbf{U}$	vector of evolved variables
v	velocity, $[m/s]$
x	spatial coordinate, $[m]$
α	volume fraction
λ	eigenvalue of coefficient matrix
$\hat{\Lambda}$	diagonal matrix of eigenvalues of Roe matrix
ρ	density, $[kg/m^3]$

INTRODUCTION

The two-fluid model is a mathematical model in widespread use for the simulation of two-phase flow. The model contains difficulties associated with a complicated eigenstructure and non-conservative terms (Jones and Prosperetti, 1985; Flåtten and Morin, 2012; Morin *et al.*, 2013). Despite these difficulties the model has been successfully used in many applications, such as oil & gas (Larsen *et al.*, 1997; Bendiksen *et al.*, 1991) and the nuclear industry (Barre and Bernard, 1990). Current research and improvements of the two-fluid model are based on resolving the mathematical difficulties and further improving the computational performance, in terms of new numerical schemes which aim to increase the accuracy of the solution or reduce the computational time. In the present work we show that the computational time can be reduced and the accuracy can be improved by the Large Time Step (LTS) scheme. The basic idea is to formulate an explicit scheme which will not be limited by the CFL condition, thereby allowing us to use time steps much larger than usually associated with explicit schemes. Such schemes were first introduced by Randall LeVeque in the nineteen eighties (LeVeque, 1985), but have recently seen a revival with applications to the Euler equations (Qian and Lee, 2012) and the shallow water equations (Morales-Hernández *et al.*, 2014; Xu *et al.*, 2013). To the best of our knowledge no application of LTS to two-phase flows has yet been published.

Although the results obtained with the LTS method are promising, there are certain difficulties when it comes to the treatment of boundary conditions, especially in presence of source terms, such as gravity. In this paper we present two different approaches to treat the boundaries. We show the effect of the different treatments of boundary conditions on the accuracy of the solution depending on the choice of the time step

and the grid size. A performance study demonstrates how the computational time is reduced by increasing the time step in the LTS method.

MODEL DESCRIPTION

We consider a one-dimensional isentropic equal-pressure two-fluid model without energy equations (Evje and Flåtten, 2003), where we solve separate evolution equations for mass and momentum of two fluids ($k = g, l$):

$$\frac{\partial(\rho_k \alpha_k)}{\partial t} + \frac{\partial(\rho_k \alpha_k v_k)}{\partial x} = 0 \tag{1}$$

$$\frac{\partial(\rho_k \alpha_k v_k)}{\partial t} + \frac{\partial\left(\rho_k \alpha_k v_k^2 + (p - p^i)\alpha_k\right)}{\partial x} + \alpha_k \frac{\partial p^i}{\partial x} = Q_k. \tag{2}$$

Closure relations and thermodynamic submodel

The model is closed by a basic relation between volume fractions:

$$\alpha_g + \alpha_l = 1 \tag{3}$$

and by equation of state for each phase k:

$$\rho_k = \rho_{k,0} + \frac{p - p_{k,0}}{a_k^2} \tag{4}$$

where the speed of sound a is defined as $a_k^2 = \partial p / \partial \rho_k$. The parameters are defined as:

$$\begin{aligned} p_{l,0} &= 10^5 \text{ Pa} & p_{g,0} &= 0 \\ \rho_{l,0} &= 1000 \text{ kg/m}^3 & \rho_{g,0} &= 0 \\ a_l &= 10^3 \text{ m/s} & a_g &= \sqrt{10^5} \text{ m/s}. \end{aligned}$$

Although the model assumes equality of phase pressures, $p_g = p_l$, we need to define an interface pressure term to ensure that the system is hyperbolic:

$$\Delta p = p - p^i = \delta \frac{\alpha_g \alpha_l \rho_g \rho_l}{\rho_g \alpha_l + \rho_l \alpha_g} (v_g - v_l)^2 \tag{5}$$

with $\delta = 1.2$. For details on closure relations and interface pressure modeling we refer to Evje and Flåtten (2003).

NUMERICAL MODEL

The system of equations (1)–(2) can be written in quasilinear form as:

$$\frac{\partial \mathbf{U}}{\partial t} + \mathbf{A}(\mathbf{U}) \frac{\partial \mathbf{U}}{\partial x} = \mathbf{Q}(\mathbf{U}). \tag{6}$$

This system is discretized by the explicit Euler method in time and the Roe scheme in non-conservative form in space:

$$\mathbf{U}_j^{n+1} = \mathbf{U}_j^n - \frac{\Delta t}{\Delta x}\left(\Delta \mathbf{F}_{j-1/2}^+ + \Delta \mathbf{F}_{j+1/2}^-\right) + \Delta t \mathbf{Q}_j^n \tag{7}$$

where the flux differences $\Delta \mathbf{F}^+$ and $\Delta \mathbf{F}^-$ are:

$$\Delta \mathbf{F}_{j+1/2}^{\pm} = \Delta \mathbf{F}_{j+1/2}^{\pm}\left(\mathbf{U}_j, \mathbf{U}_{j+1}\right) = \hat{\mathbf{A}}_{j+1/2}^{\pm}\left(\mathbf{U}_{j+1} - \mathbf{U}_j\right) \tag{8}$$

Herein, the fundamental component is the construction of a *Roe matrix* $\hat{\mathbf{A}}$ (see Evje and Flåtten (2003) for details), and we define

$$\hat{\mathbf{A}}^{\pm} = \hat{\mathbf{R}} \hat{\Lambda}^{\pm} \hat{\mathbf{R}}^{-1} \tag{9}$$

where $\hat{\mathbf{R}}$ is the matrix of eigenvectors of $\hat{\mathbf{A}}$ and $\hat{\Lambda}$ is the diagonal matrix of eigenvalues. Herein,

$$\lambda^+ = \max(0, \lambda), \tag{10}$$

$$\lambda^- = \min(0, \lambda). \tag{11}$$

In this paper we will refer to this formulation and results obtained with it as "the standard Roe scheme".
A known limititation of this scheme is that the time step must satisfy the constraint $C \leq 1$, where C is the *Courant number*:

$$C = \max|\lambda| \frac{\Delta t}{\Delta x}. \tag{12}$$

Herein, the maximum is taken over all eigenvalues in all computational cells.
In the following, we will describe an extension of the Roe scheme that gets rid of this limitation.

Large Time Step Scheme

To extend the standard Roe scheme to the LTS Roe scheme we use the approach proposed by LeVeque (1985).
As stated earlier, the basic idea of the LTS method is to increase the domain of dependence. Since the information from the domain of dependence with which we update cell state $\mathbf{U}_j^{n+1}$ is delivered in terms of fluxes through the cell faces, we reformulate the flux differences to include all flux differences in the domain of dependence. Hence we modify (8) as follows:

$$\Delta \mathbf{F}_{j+1/2}^+ = \sum_{i=0}^{\infty} \hat{\mathbf{A}}_{j+1/2-i}^{i+} \left(\mathbf{U}_{j+1-i} - \mathbf{U}_{j-i}\right) \tag{13}$$

$$\Delta \mathbf{F}_{j+1/2}^- = \sum_{i=0}^{\infty} \hat{\mathbf{A}}_{j+1/2+i}^{i-} \left(\mathbf{U}_{j+1+i} - \mathbf{U}_{j+i}\right) \tag{14}$$

where the matrices $\hat{\mathbf{A}}^{i\pm}$ are defined as:

$$\hat{\mathbf{A}}^{i\pm} = \hat{\mathbf{R}}^{i\pm} \hat{\Lambda}^{i\pm} \left(\hat{\mathbf{R}}^{i\pm}\right)^{-1} \tag{15}$$

$$\hat{\Lambda}^{i\pm} = \text{diag}\left(\lambda^{i\pm}\right) \tag{16}$$

$$\lambda^{i+} = \max\left(0, \min\left(\lambda - i\frac{\Delta x}{\Delta t}, \frac{\Delta x}{\Delta t}\right)\right) \tag{17}$$

$$\lambda^{i-} = \min\left(0, \max\left(\lambda + i\frac{\Delta x}{\Delta t}, -\frac{\Delta x}{\Delta t}\right)\right). \tag{18}$$

The infinite sum from equations (13) and (14) will contain only a finite number of nonzero terms, because the term $\lambda - i\frac{\Delta x}{\Delta t}$ becomes negative, and the term $\lambda + i\frac{\Delta x}{\Delta t}$ becomes positive at some point.
Due to limited length of the paper the reader is referred to the forthcoming journal article for more extensive explanation of the LTS method.

BOUNDARY CONDITIONS

Increasing the domain of dependence leads to a difficulty when it comes to the definition of boundary cells. In the standard Roe scheme we must provide only one boundary cell at each boundary, because the first cell in the domain is updated only from its neighboring cells, i.e. the Roe scheme is a three-point scheme:

$$\mathbf{U}_j^{n+1} = \mathbf{U}\left(\mathbf{U}_{j-1}^n, \mathbf{U}_j^n, \mathbf{U}_{j+1}^n\right) \tag{19}$$

For the first cell in the domain this leads to:

$$\mathbf{U}_1^{n+1} = \mathbf{U}\left(\mathbf{U}_{LBC}, \mathbf{U}_1^n, \mathbf{U}_2^n\right) \tag{20}$$

with $\mathbf{U}_{LBC}$ being $\mathbf{U}$ in the left boundary cell. From the way the LTS Roe scheme is formulated it is clear that the value at any cell may depend on more than three cells:

$$\mathbf{U}_j^{n+1} = \mathbf{U}\left(..., \mathbf{U}_{j-2}^n, \mathbf{U}_{j-1}^n, \mathbf{U}_j^n, \mathbf{U}_{j+1}^n, \mathbf{U}_{j+2}^n, ...\right) \tag{21}$$

where the particular size of the domain of dependence depends on the local Courant number. Clearly, this leads to a difficulty when it comes to the definition of numerical boundary conditions, since (for example at the left boundary) we do not have cells associated with $\mathbf{U}_{j-2}^n$, $\mathbf{U}_{j-3}^n$, etc. We now suggest two different ways to define these boundary cells in the presence of source terms.

Extrapolated boundary conditions

Assume that we apply a Courant number C, i.e. we will need $M = \text{ceil}(C)$ numerical ghost cells at each boundary to directly apply the LTS Roe scheme. The straightforward way to provide these additional cells is to simply extrapolate the values of the original boundary condition cell. In this way, all additional cells in the boundary zone will have the same values as the original boundary cell:

$$\mathbf{U}_p^n = \mathbf{U}_{LBC}^n \quad \forall \quad p < LBC \tag{22}$$

$$\mathbf{U}_p^n = \mathbf{U}_{RBC}^n \quad \forall \quad p > RBC \tag{23}$$

where *LBC* and *RBC* denote the indices of the left and right boundary cells, respectively. Assuming N cells in the interior domain, we will use the convention that $LBC = 0$ and $RBC = N+1$.

We will refer to this formulation as EBC, i.e. extrapolated boundary conditions. If there are no source terms present in the computational domain this approach will be very effective, and very accurate results may be obtained. For reference we advise the reader of the forthcoming journal article by the same authors.

Herein, there are a number of ways of constructing the values of the primary *LBC* and *RBC* cells, depending on the physics of the prescribed problem. Most rigorous are the *characteristic boundary conditions*, see for instance Fjelde and Karlsen (2002).

However, regardless of our choice of updating $\mathbf{U}_{LBC}$ and $\mathbf{U}_{RBC}$ we are left with a central problem associated with the EBC as given by (22)–(23) in the presence of source terms. Assuming the constant boundary conditions, the assumption of locally uniform data corresponds to a valid steady-state solution in the *absence* of source terms. Consequently, the application of (22)–(23) may be viewed as follows:

- Calculate $\mathbf{U}_{LBC}$ and $\mathbf{U}_{RBC}$ by some boundary scheme, for instance by extrapolation of the characteristic or primitive variables.
- Solve the steady-state *homogeneous* problem

$$\frac{\partial \mathbf{U}}{\partial t} + \mathbf{A}(\mathbf{U})\frac{\partial \mathbf{U}}{\partial x} = 0 \tag{24}$$

  in an artifical domain extended at the boundaries (the solution is simply $\mathbf{U} = \text{const.}$)
- Transport the solution in this artificial domain into the actual computational domain through the LTS method.

Comparing (6) to (24), we see that under this point of view the EBC approach introduces an *artifical discontinuity* of the source term at the boundaries. Applying a Courant number $C > 1$, we will then see this manifest itself as a discontinuity in the numerical solution, propagating C cells per time step away from the boundary. Clearly, this is a numerical artifact arising from our extrapolation being faster than the interaction between transport and source term effects in each cell. This issue is the main topic of our current paper, and we will illustrate this phenomenon in the numerical section. We now proceed to propose a natural modification that will remedy this.

Steady-state boundary condition

To overcome the problem discussed above, we simply replace our equation (24) by (6) to instead solve the steady-state problem:

$$\mathbf{A}(\mathbf{U})\frac{d\mathbf{U}}{dx} = \mathbf{Q}(\mathbf{U}). \tag{25}$$

By solving this for $\frac{d\mathbf{U}}{dx}$ we obtain:

$$\frac{d\mathbf{U}}{dx} = (\mathbf{A}(\mathbf{U}))^{-1}\mathbf{Q}(\mathbf{U}). \tag{26}$$

Now, by solving this equation at the left and the right boundary cells we obtain the slopes $\delta_x\mathbf{U}_L$ and $\delta_x\mathbf{U}_R$ (left and right, respectively) which we then use to formulate the additional boundary cells as:

$$\mathbf{U}_{-q}^n = \mathbf{U}_{LBC}^n - q\Delta x\delta_x\mathbf{U}_L \quad \forall \quad q \in [0,\ldots,M] \tag{27}$$

at the left boundary zone and:

$$\mathbf{U}_{N+q}^n = \mathbf{U}_{RBC}^n + (q-1)\Delta x\delta_x\mathbf{U}_R \quad \forall \quad q \in [1,\ldots,M] \tag{28}$$

at the right boundary zone. These equations then replace our previous equation (22) and (23). We will refer to this formulation as SSBC, i.e. steady-state boundary conditions.
In the following, we will present some numerical simulations highlighting the differences between EBC and SSBC.

NUMERICAL RESULTS

As a test case to compare our implementations of the boundary conditions we use a simplified water faucet problem proposed by Ransom (1987). We consider a vertical pipe 12 meters long with initial data:

$$\alpha_l = 0.8, \quad v_l = 10 \text{ m/s}, \quad v_g = 0 \text{ m/s}, \quad p = 10^5 \text{ Pa}.$$

The source term Q_k is limited to gravity and defined as:

$$Q_k = \rho_k \alpha_k g.$$

The following boundary conditions are given:

$$\begin{aligned} &\text{Inlet:} && \alpha_l = 0.8, \quad v_l = 10 \text{ m/s}, \quad v_g = 0 \text{ m/s}, \\ &\text{Outlet:} && p = 10^5 \text{ Pa}. \end{aligned}$$

Boundary values are then simply obtained by extrapolating the missing variables from the computational domain, more precisely

$$\mathbf{W}^n_{LBC} = \begin{bmatrix} p \\ \alpha_l \\ v_g \\ v_l \end{bmatrix}_{LBC} = \begin{bmatrix} p^n_1 \\ 0.8 \\ 0 \\ 10 \text{ m/s} \end{bmatrix} \tag{29}$$

and

$$\mathbf{W}^n_{RBC} = \begin{bmatrix} p \\ \alpha_l \\ v_g \\ v_l \end{bmatrix}_{RBC} = \begin{bmatrix} 10^5 \text{ Pa} \\ (\alpha_l)^n_N \\ (v_g)^n_N \\ (v_l)^n_N \end{bmatrix}. \tag{30}$$

All the results discussed above are computed at time $t = 0.6s$. The analytical solution for the liquid volume fraction and liquid velocity can be found in Evje and Flåtten (2003), while the complete procedure is available in Trapp and Riemke (1986). The reference solution for the remaining variables is obtained by the standard Roe scheme with superbee wave limiter on a mesh with 10 000 cells and $\Delta t = 3.5294 \cdot 10^{-6}$.
For the actual Roe scheme, we use the exactly the same procedure as described in Evje and Flåtten (2003). Herein, we replace the original discretization (8) by our Large Time Step extension (13)–(18). Note in particular that (13)–(18) reduces to (8) in the event that $C \leq 1$.

Effect of time step

We consider a domain with a fixed number of cells (100) and compare the pressure, volume fraction and velocity profiles for different time steps and different implementations of the boundary conditions, see figure 1.

It can be seen that the solution obtained with SSBC is smoother than the solution obtained with EBC for corresponding time steps, especially for larger time steps. That is expected since the boundaries defined with SSBC introduce a smaller error and provide a smoother transition between the boundary zone and the rest of the domain.
The solutions for the gas volume fraction are very similar among each other which is not surprising because the liquid and gas velocities are more than an order of magnitude smaller than the velocity of the pressure waves. Because of that, the Courant number corresponding to the volume fraction waves is actually smaller than 1 at all times. Further, it can be seen that the accuracy of the solution for the gas volume fraction and liquid velocity is actually *increased*. This is because the larger time step leads to fewer time steps in total, which reduces the numerical diffusion introduced each time we average a cell state. More rigorous insight can be gained through the modified equation analysis, see for instance Harten *et al.* (1976).

Effect of mesh refinement

We also compare the effect of grid refinement starting with a mesh of 100 cells and a time step $\Delta t = 0.00176$ which corresponds to $C \approx 5$. For each refined mesh we keep the Courant number constant, i.e. the ratio $\Delta t / \Delta x = 0.01467 =$ const., see figure 2.
We again note the SSBC provides smoother profiles than EBC. However, this effect becomes less significant as the mesh is refined. This is to be expected, as the number of boundary cells remains constant as the total number of grid cells is increased. Hence their relative influence becomes smaller.
Nevertheless, practical simulations are often performed on coarse grids due to computational efficiency constraints. Here the results may be sensitive to the different treatments of the boundary conditions presented here.

Performance analysis

The last numerical experiment (see figure 3) shows how the computational time depends on the increased time steps for different grid sizes. The abscissa shows the Courant number. The ordinate shows the relative computational time normalized to one for $C = 1$. The approach used for the treatment of the boundary conditions is SSBC.
Each profile is the averaged results of 10 simulations performed in MATLAB.
It can be seen that the gain in computational time for different mesh sizes shows a similar trend, with the gain being smaller for larger meshes. A precise explanation of this phenomenon would require a careful code profiling beyond the scope of the current paper. However, it should be noted that a relative slow-down

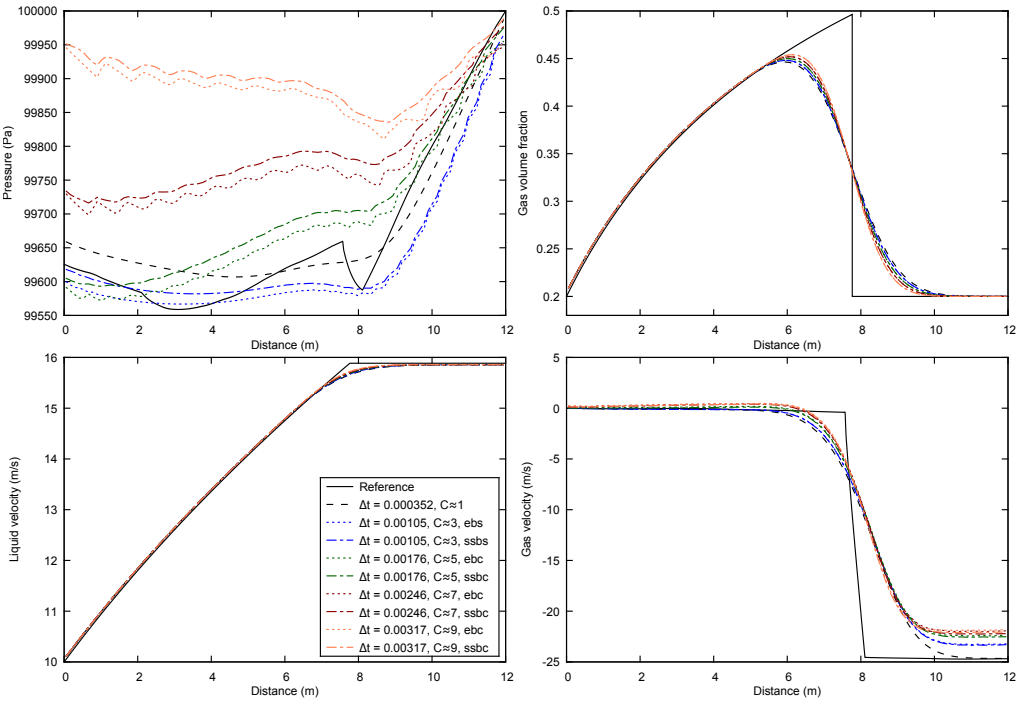

Figure 1: Effect of increasing time step on mesh with 100 cells

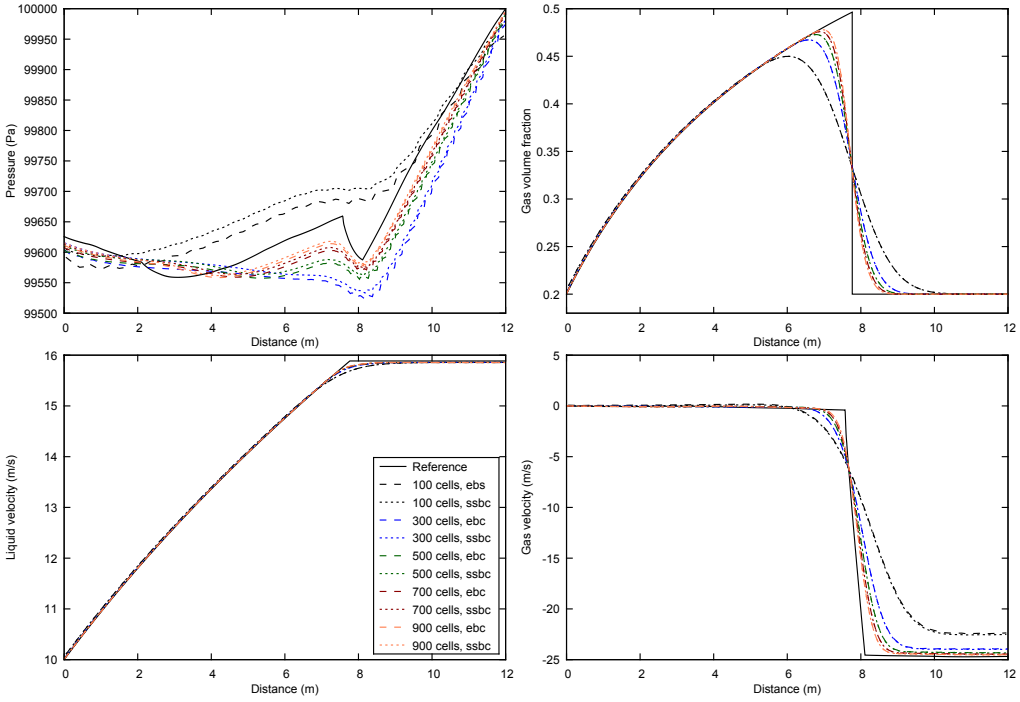

Figure 2: Effect of mesh refinement with $\Delta t/\Delta x =$ const., (C $\approx$ 5)

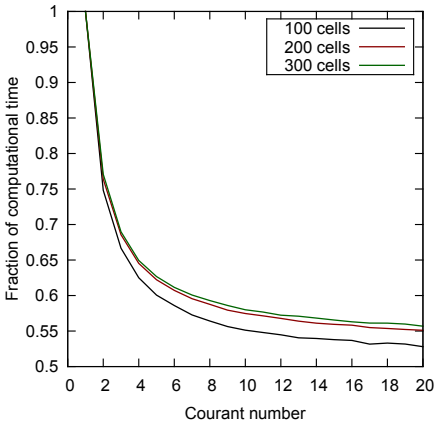

Figure 3: Relative computational time with respect to $C = 1$ vs. Courant number

of the code would be expected for high Courant numbers for coarse meshes, as the values in the artificial boundary cells will then influence a significant part of the domain. The figure indicates that this effect is not detrimental.

CONCLUSION

We extended the standard Roe scheme to a Large Time Step Roe scheme and showed that the two-fluid model can be resolved with an explicit method not limited by the CFL condition.

Increasing the time step size leads to less accurate pressure and gas velocity, but to increased accuracy in volume fractions and liquid velocity. The numerical error associated with pressure waves can be partially reduced by imposing steady-state boundary conditions (SSBC) to determine the flow variables in the ghost cells compared to a simple extrapolation boundary treatment. In particular, the SSBC approach will reduce oscillations and lead to smoother profiles. This observation is the main contribution of the current paper.

Grid refinement shows that the error introduced by a larger time step decreases with decreased grid spacing.

A performance study shows that the relative gain in computational time is highly dependent on the Courant number, and that the gain is largest immediately after increasing the time step above the CFL limit.

The proposed method shows promising potential, especially in the two following cases. First, in problems with a large number of grid cells where additional ghost cells introduced by the LTS method cause relatively small increase in computational time compared to the reduction of computational time gained by increasing the time step (i.e. reducing the number of time steps). Second, in problems where the velocities of the phases are much smaller than the acoustic wave speeds and we are not interested in maximum accuracy of the pressure field compared to the accuracy required for volume fractions and velocities.

REFERENCES

BARRE, F. and BERNARD, M. (1990). "The CATHARE code strategy and assessment". *Nucl. Eng. Des.*, **124**, 257–284.

BENDIKSEN, K.H. *et al.* (1991). "The Dynamics Two-Fluid Model OLGA: Theory and Application". *SPE Prod. Eng.*, **6**, 171–180.

EVJE, S. and FLÅTTEN, T. (2003). "Hybrid flux-splitting schemes for a common two-fluid model". *J. Comput. Phys.*, **192**, 175–210.

FJELDE, K.K. and KARLSEN, K.H. (2002). "High-resolution hybrid primitive-conservative upwind schemes for the drift flux model". *Comput. Fluids*, **31**, 335–367.

FLÅTTEN, T. and MORIN, A. (2012). "On interface transfer terms in two-fluid models". *Int. J. Multiph. Flow*, **45**, 24–29.

HARTEN, A. *et al.* (1976). "On Finite-Difference Approximations and Entropy Conditions for Shocks". *Comm. Pure Appl. Math.*, **29**, 297–322.

JONES, A.V. and PROSPERETTI, A. (1985). "On the suitability of first-order differential models for two-phase flow prediction". *Int. J. Multiph. Flow*, **11**, 133–148.

LARSEN, M. *et al.* (1997). "PeTra: A Novel Computer Code for Simulation of Slug Flow". *SPE Annual Technical Conference and Exhibition*. SPE 38841.

LEVEQUE, R.J. (1985). "A Large Time Step Generalization of Godunov's Method for Systems of Conservation Laws". *SIAM J. Numer. Anal.*, **22**, 1051–1073.

MORALES-HERNáNDEZ, M. *et al.* (2014). "A 2D extension of a Large Time Step explicit scheme (CFL>1) for unsteady problems with wet/dry boundaries". *J. Comput. Phys.*, **263**, 303–327.

MORIN, A. *et al.* (2013). "A Roe scheme for a compressible six-equation two-fluid model". *Int. J. Numer. Meth. Fluids*, **72**, 478–504.

QIAN, Z. and LEE, C.H. (2012). "On large time step TVD scheme for hyperbolic conservation laws and its efficiency evaluation". *J. Comput. Phys.*, **231**, 7415–7430.

RANSOM, V.H. (1987). "Numerical benchmark tests". *Multiphase Sci. Tech.*, **3**, 465–473.

TRAPP, J.A. and RIEMKE, R.A. (1986). "A nearly-implicit hydrodynamic numerical scheme for two-phase flows". *J. Comput. Phys.*, **66**, 62–82.

XU, R. *et al.* (2013). "LTS in Shallow Flows with RCM and Multi-wave Approximation". *Chin. J. Comput. Phys.*, **30**, 649–658.

Conference paper 2 (P1)

Numerical Viscosity in Large Time Step HLL-type Schemes

Marin Prebeg

Proceedings of the Sixteenth International Conference on Hyperbolic Problems, HYP2016. Accepted for publication. Aachen, Germany, 2016.

Numerical Viscosity in Large Time Step HLL-type Schemes

Marin Prebeg

Abstract We consider Large Time Step (LTS) methods, i.e. the explicit finite volume methods not limited by the CFL (Courant–Friedrichs–Lewy) condition. The original LTS method [R. J. LeVeque, *SIAM J. Numer. Anal.*, (22) 1985] was constructed as an extension of the Godunov scheme, and successive versions have been developed in the framework of Roe's approximate Riemann solver. Recently, Prebeg et al. [submitted, 2017] developed the LTS extension of the HLL and HLLC schemes. We perform the modified equation analysis and demonstrate that for the appropriate choice of the wave velocity estimates the LTS-HLL scheme yields entropy satisfying solutions. We apply the LTS-HLL(C) schemes to the one-dimensional Euler equations and consider the Sod shock tube, double rarefaction and Woodward-Colella blast-wave problem.

1 Introduction

We consider the hyperbolic system of conservation laws:

$$\mathbf{U}_t + \mathbf{F}(\mathbf{U})_x = 0 \,, \tag{1a}$$

$$\mathbf{U}(x,0) = \mathbf{U}_0(x) \,, \tag{1b}$$

where $\mathbf{U} \in \mathbb{R}^m$, $\mathbf{F} : \mathbb{R}^m \to \mathbb{R}^m$, $x \in \mathbb{R}$ and $t \in \mathbb{R}^+$. We are interested in solving (1) with an explicit finite volume method not limited by the CFL (Courant–Friedrichs–Lewy) condition.

A class of such methods has been proposed by LeVeque [1, 2, 3]. Therein, the Godunov scheme was extended to the LTS-Godunov and LTS-Roe schemes and applied to the one-dimensional Euler equations. Most recent applications of

Marin Prebeg
Department of Energy and Process Engineering, Norwegian University of Science and Technology, Kolbjørn Hejes vei 2, NO-7491 Trondheim, Norway, e-mail: marin.prebeg@ntnu.no

these ideas include shallow water equations (Murillo, Morales-Hernández and coworkers [4, 5, 6, 7, 8] and Xu et al. [9]), three-dimensional Euler equations (Qian and Lee [10]), high speed combustion waves (Tang et al. [11]), Maxwell's equations (Makwana and Chatterjee [12]) and two-phase flows (Lindqvist and Lund [13] and Prebeg et al. [14]). All the methods discussed above share the feature of starting from a Godunov or Roe-type Riemann solver and extending it to the LTS framework. In addition to these applications, Lindqvist et al. [15] studied the TVD properties of LTS methods and introduced the LTS-Lax-Friedrichs scheme. Several authors [1, 3, 5, 9, 10, 13, 15] reported that the LTS-Roe scheme yields entropy violating solutions even more often than the standard Roe scheme. Therein, this issue is solved by splitting the rarefaction wave into several expansion shocks [1, 3, 5, 9, 10] or by varying the time step [13, 15].

Prebeg et al. [16] developed the LTS extension of the HLL (Harten–Lax–van Leer) [17, 18, 19] and HLLC (HLL–Contact) [20] schemes and applied them to a one-dimensional Euler equations. They observed that the LTS-HLL(C) schemes with the wave velocity estimates according to Einfeldt [18] yield entropy satisfying solutions. This observation motivates the present paper, which is structured as follows: in Sect. 2 we outline the problem and the numerical methods we will consider, most importantly the LTS-HLL(C) schemes; in Sect. 3 we discuss the entropy violation associated with the LTS methods and use the modified equation analysis to demonstrate that the LTS-HLL scheme with the choice of the wave velocities estimates according to Einfeldt [18] yields entropy satisfying solutions; in Sect. 4 we perform numerical investigations; while in Sect. 5 we end with conclusions.

2 Preliminaries

We specify the particular hyperbolic conservation law we will investigate and outline the framework of the numerical methods we will use.

2.1 Problem Outline

As an example of (1) we consider the one-dimensional Euler equations where:

$$\mathbf{U} = (\rho, \rho u, E)^{\mathrm{T}} , \tag{2a}$$

$$\mathbf{F}(\mathbf{U}) = \big(\rho u, \rho u^2 + p, u(E+p)\big)^{\mathrm{T}} , \tag{2b}$$

where ρ, u, E, p denote the density, velocity, total energy density and pressure, respectively. The system is closed by the definition of the total energy density, $E = \rho e + \rho u^2/2$, where e is the internal energy given by the equation of state as $e = p/(\rho(\gamma-1))$. We use $\gamma = 1.4$ for air. We can also write (1) in a quasilinear form as:

$$\mathbf{U}_t + \mathbf{A}(\mathbf{U})\mathbf{U}_x = 0\,, \qquad \mathbf{A}(\mathbf{U}) = \frac{\partial \mathbf{F}(\mathbf{U})}{\partial \mathbf{U}}\,. \tag{3}$$

We assume that the system of Eqs. (3) is hyperbolic, i.e. the Jacobian matrix $\mathbf{A}$ has real eigenvalues and linearly independent eigenvectors.

2.2 Numerical Methods

We discretize (1) by the explicit Euler method in time and the finite volume method in space:

$$\mathbf{U}_j^{n+1} = \mathbf{U}_j^n - \frac{\Delta t}{\Delta x}\left(\mathbf{F}_{j+1/2}^n - \mathbf{F}_{j-1/2}^n\right)\,, \tag{4}$$

where $\mathbf{U}_j^n$ is an approximation of the average of $\mathbf{U}$ in the cell j at time level n and $\mathbf{F}_{j+1/2}^n$ is a numerical approximation of the flux function at the cell interface $x_{j+1/2}$ at time level n. In standard (3-point) methods the numerical flux depends only on the neighboring cell values and we may write the numerical fluxes in the numerical viscosity form:

$$\mathbf{F}_{j+1/2}^n = \frac{1}{2}\left(\mathbf{F}_j^n + \mathbf{F}_{j+1}^n\right) - \frac{1}{2}\mathbf{Q}_{j+1/2}^n\left(\mathbf{U}_{j+1}^n - \mathbf{U}_j^n\right)\,, \tag{5}$$

where $\mathbf{F}_j^n = \mathbf{F}(\mathbf{U}_j^n)$ and $\mathbf{Q}_{j+1/2}^n$ is the numerical viscosity matrix. To simplify the notation, the time level n will be implicitly assumed in the absence of a temporal index. In the numerical viscosity framework (5) the HLL scheme is obtained by setting:

$$\mathbf{Q}_{\mathrm{HLL}} = \frac{S_{\mathrm{R}}^+ + S_{\mathrm{L}}^-}{S_{\mathrm{R}}^+ - S_{\mathrm{L}}^-}\hat{\mathbf{A}} - 2\frac{S_{\mathrm{L}}^- S_{\mathrm{R}}^+}{S_{\mathrm{R}}^+ - S_{\mathrm{L}}^-}\mathbf{I}\,, \tag{6}$$

where $\hat{\mathbf{A}}$ is the Roe matrix [21], S_{R} and S_{L} are the wave velocity estimates, and the superscripts denote $S_{\mathrm{R}}^+ = \max(0, S_{\mathrm{R}})$ and $S_{\mathrm{L}}^- = \min(0, S_{\mathrm{L}})$. The choice of the wave velocity estimates will be addressed in Sect. 2.3. We note that $\mathbf{Q}$ can be diagonalized as:

$$\mathbf{Q} = \hat{\mathbf{R}}\boldsymbol{\Omega}\hat{\mathbf{R}}^{-1}\,, \tag{7}$$

where $\hat{\mathbf{R}}$ is the matrix of the right eigenvectors of the Roe matrix, and $\boldsymbol{\Omega} = \mathrm{diag}\left(\omega^1, \ldots, \omega^m\right)$ is the matrix of the eigenvalues of $\mathbf{Q}$, where the superscript denotes the particular characteristic field. Then we may define the HLL scheme through the diagonal entries of $\boldsymbol{\Omega}$ as:

$$\omega_{\mathrm{HLL}} = \frac{S_{\mathrm{R}}^+(\hat{\lambda} - S_{\mathrm{L}}^-) - S_{\mathrm{L}}^-(S_{\mathrm{R}}^+ - \hat{\lambda})}{S_{\mathrm{R}}^+ - S_{\mathrm{L}}^-}\,, \tag{8}$$

where $\hat{\lambda}$ are the eigenvalues of the Roe matrix $\hat{\mathbf{A}}$. For more details on the derivation of the HLL scheme we refer to [17, 18, 19, 22].

For the 3-point method (5) the time step Δt is limited by the CFL condition:

$$C = \max_{p,j} |\lambda_j^p| \frac{\Delta t}{\Delta x} \leq 1 \,, \tag{9}$$

where λ_j^p are the eigenvalues of the Jacobian matrix $\mathbf{A}(\mathbf{U}_j)$ in (3), and the superscript p denotes the particular characteristic field, $p = 1, \ldots, m$. We are interested in explicit methods not limited by the condition (9).

2.2.1 Large Time Step HLL Scheme

The natural LTS extension of the numerical viscosity formulation (5) is [15]:

$$\mathbf{F}_{j+1/2} = \frac{1}{2}\left(\mathbf{F}_j + \mathbf{F}_{j+1}\right) - \frac{1}{2}\sum_{i=-\infty}^{\infty} \mathbf{Q}^i_{j+1/2+i}\left(\mathbf{U}_{j+1+i} - \mathbf{U}_{j+i}\right) \,. \tag{10}$$

We note that (10) differs from [15] in the sense that we scale $\mathbf{Q}^i$ with $\Delta x/\Delta t$. By using the results from [16] we write the LTS-HLL scheme in the numerical viscosity form (10) by defining:

$$\mathbf{Q}^i_{j+1/2} = \left(\hat{\mathbf{R}}\boldsymbol{\Omega}^i\hat{\mathbf{R}}^{-1}\right)_{j+1/2} \,, \tag{11}$$

where the diagonal entries of $\boldsymbol{\Omega}$ are defined as:

$$\omega^0_{\mathrm{HLL}} = \frac{S_{\mathrm{R}}^+(\hat{\lambda} - S_{\mathrm{L}}^-) - S_{\mathrm{L}}^-(S_{\mathrm{R}}^+ - \hat{\lambda})}{S_{\mathrm{R}}^+ - S_{\mathrm{L}}^-} \,, \tag{12a}$$

$$\begin{aligned} \omega^{\mp i}_{\mathrm{HLL}} &= 2\frac{\hat{\lambda} - S_{\mathrm{L}}}{S_{\mathrm{R}} - S_{\mathrm{L}}} \max\left(0, \pm S_{\mathrm{R}} - i\frac{\Delta x}{\Delta t}\right) \\ &\quad + 2\frac{S_{\mathrm{R}} - \hat{\lambda}}{S_{\mathrm{R}} - S_{\mathrm{L}}} \max\left(0, \pm S_{\mathrm{L}} - i\frac{\Delta x}{\Delta t}\right) \quad \text{for} \quad i > 0 \,. \end{aligned} \tag{12b}$$

We refer to [16] for the derivation of these formulae.

2.2.2 Large Time Step HLLC Scheme

The HLL scheme assumes a two-wave structure of the solution and leads to poor resolution of the contact discontinuity in the one-dimensional Euler equations (2). Toro et al. [20] introduced the HLLC solver where the missing contact wave is restored. Following [22], the main idea consists of assuming a three-wave structure of the solution, thus splitting the Riemann fan into two intermediate states:

$$\widetilde{\mathbf{U}}(x,t) = \begin{cases} \mathbf{U}_j & \text{if} \quad x < S_{\mathrm{L}} t \,, \\ \mathbf{U}_{\mathrm{L}}^{\mathrm{HLLC}} & \text{if} \quad S_{\mathrm{L}} t < x < S_{\mathrm{C}} t \,, \\ \mathbf{U}_{\mathrm{R}}^{\mathrm{HLLC}} & \text{if} \quad S_{\mathrm{C}} t < x < S_{\mathrm{R}} t, \\ \mathbf{U}_{j+1} & \text{if} \quad x > S_{\mathrm{R}} t \,, \end{cases} \tag{13}$$

where the intermediate states are:

$$\mathbf{U}_{\mathrm{K}}^{\mathrm{HLLC}} = \rho_{\mathrm{K}} \left(\frac{S_{\mathrm{K}} - u_{\mathrm{K}}}{S_{\mathrm{K}} - S_{\mathrm{C}}} \right) \begin{bmatrix} 1 \\ S_{\mathrm{C}} \\ \frac{E_{\mathrm{K}}}{\rho_{\mathrm{K}}} + (S_{\mathrm{C}} - u_{\mathrm{K}}) \left(S_{\mathrm{C}} + \frac{p_{\mathrm{K}}}{\rho_{\mathrm{K}} (S_{\mathrm{K}} - u_{\mathrm{K}})} \right) \end{bmatrix} , \tag{14}$$

where index K denotes left (L) or right (R) state in (13). The contact discontinuity velocity is given by:

$$S_{\mathrm{C}} = \frac{p_{\mathrm{R}} - p_{\mathrm{L}} + \rho_{\mathrm{L}} u_{\mathrm{L}} (S_{\mathrm{L}} - u_{\mathrm{L}}) - \rho_{\mathrm{R}} u_{\mathrm{R}} (S_{\mathrm{R}} - u_{\mathrm{R}})}{\rho_{\mathrm{L}} (S_{\mathrm{L}} - u_{\mathrm{L}}) - \rho_{\mathrm{R}} (S_{\mathrm{R}} - u_{\mathrm{R}})} \,. \tag{15}$$

For details on the derivation of these formulae we refer to the book by Toro [22]. Herein, we present the LTS-HLLC scheme in the conservation form as derived in [16]. The numerical flux to be used in (4) is:

$$\mathbf{F}_{j+1/2}^{\text{LTS-HLLC}} = \mathbf{F}_{j+1/2}^{0} + \sum_{i=1}^{\infty} \mathbf{F}_{j+1/2-i}^{-i} + \sum_{i=1}^{\infty} \mathbf{F}_{j+1/2+i}^{+i} \,, \tag{16}$$

where $\mathbf{F}_{j+1/2}^{0}$ is defined as:

$$\mathbf{F}_{j+1/2}^{0} = \begin{cases} \mathbf{F}_j & \text{if} \quad 0 < S_{\mathrm{L}} \,, \\ \mathbf{F}_{\mathrm{L},j+1/2}^{\mathrm{HLLC}} & \text{if} \quad S_{\mathrm{L}} < 0 < S_{\mathrm{C}} \,, \\ \mathbf{F}_{\mathrm{R},j+1/2}^{\mathrm{HLLC}} & \text{if} \quad S_{\mathrm{C}} < 0 < S_{\mathrm{R}} \,, \\ \mathbf{F}_{j+1} & \text{if} \quad 0 > S_{\mathrm{R}} \,. \end{cases} \tag{17}$$

In the interesting case, $S_{\mathrm{L}} < 0 < S_{\mathrm{R}}$, the numerical flux function has the form:

$$\mathbf{F}_{\mathrm{L},j+1/2}^{\mathrm{HLLC}} = \mathbf{F}_j + S_{\mathrm{L}} \left(\mathbf{U}_{\mathrm{L},j+1/2}^{\mathrm{HLLC}} - \mathbf{U}_j \right) \,, \tag{18}$$

$$\mathbf{F}_{\mathrm{R},j+1/2}^{\mathrm{HLLC}} = \mathbf{F}_{j+1} + S_{\mathrm{R}} \left(\mathbf{U}_{\mathrm{R},j+1/2}^{\mathrm{HLLC}} - \mathbf{U}_{j+1} \right) \,. \tag{19}$$

The remaining terms in (16) are:

$$\begin{aligned} \mathbf{F}_{j+1/2-i}^{-i} = {} & S_{\mathrm{R},j+1/2-i}^{-i} \left(\mathbf{U}_{\mathrm{R},j+1/2-i}^{\mathrm{HLLC}} - \mathbf{U}_{j+1-i} \right) \\ & + S_{\mathrm{C},j+1/2-i}^{-i} \left(\mathbf{U}_{\mathrm{L},j+1/2-i}^{\mathrm{HLLC}} - \mathbf{U}_{\mathrm{R},j+1/2-i}^{\mathrm{HLLC}} \right) \\ & + S_{\mathrm{L},j+1/2-i}^{-i} \left(\mathbf{U}_{j-i} - \mathbf{U}_{\mathrm{L},j+1/2-i}^{\mathrm{HLLC}} \right) \,, \end{aligned} \tag{20}$$

$$\begin{aligned}\mathbf{F}^{+i}_{j+1/2+i} = & S^{+i}_{\mathrm{L},j+1/2+i}\left(\mathbf{U}^{\mathrm{HLLC}}_{\mathrm{L},j+1/2+i} - \mathbf{U}_{j+i}\right) \\ & + S^{+i}_{\mathrm{C},j+1/2+i}\left(\mathbf{U}^{\mathrm{HLLC}}_{\mathrm{R},j+1/2+i} - \mathbf{U}^{\mathrm{HLLC}}_{\mathrm{L},j+1/2+i}\right) \\ & + S^{+i}_{\mathrm{R},j+1/2+i}\left(\mathbf{U}_{j+1+i} - \mathbf{U}^{\mathrm{HLLC}}_{\mathrm{R},j+1/2+i}\right) . \end{aligned} \tag{21}$$

Herein, the modified velocities are:

$$S^{-i}_{[\mathrm{L,C,R}],j+1/2-i} = \max\left(S_{[\mathrm{L,C,R}],j+1/2-i} - i\frac{\Delta t}{\Delta x}, 0\right) , \tag{22}$$

$$S^{+i}_{[\mathrm{L,C,R}],j+1/2+i} = \min\left(S_{[\mathrm{L,C,R}],j+1/2+i} + i\frac{\Delta t}{\Delta x}, 0\right) . \tag{23}$$

We refer to [16] for the derivation of these formulae.

2.3 Estimates for Wave Velocities S_{L} and S_{R}

In the present paper, the choice of the wave velocity estimates is made according to Einfeldt [18]:

$$S_{\mathrm{L},j+1/2} = \min\left(\lambda^1(\mathbf{U}_j), \hat{\lambda}^1(\widehat{\mathbf{U}}_{j+1/2})\right) , \tag{24a}$$

$$S_{\mathrm{R},j+1/2} = \max\left(\hat{\lambda}^3(\widehat{\mathbf{U}}_{j+1/2}), \lambda^3(\mathbf{U}_{j+1})\right) , \tag{24b}$$

where $\widehat{\mathbf{U}}$ denotes the Roe average of conserved variables. The HLL scheme with (24) is usually denoted as the HLLE scheme. Einfeldt et al. [23] showed that the standard (3-point) HLLE scheme yields entropy satisfying solutions and preserves positivity. Batten et al. [24] showed that the HLLC scheme [20] with (24) also preserves positivity. In the following section we demonstrate that the LTS-HLLE scheme yields entropy satisfying solutions.

3 Entropy Violation

A weak solution to a conservation law is not necessary unique [25, p. 217]. For the numerical scheme to select the physically relevant solution, we need to impose so-called *entropy conditions*. Entropy violation is most commonly associated and discussed as it appears in the Roe scheme [21]. We start by following the same approach and consider the *numerical viscosity* interpretation of the entropy violation [25].

Consider a standard (3-point) Roe scheme written in the numerical viscosity formulation (5). The eigenvalues of the numerical viscosity matrix $\mathbf{Q}_{\mathrm{Roe}}$ are given by:

$$\omega_{\text{Roe}} = |\hat{\lambda}| \,. \tag{25}$$

In the transonic case a particular eigenvalue ω^p_{Roe} ($p = 1,\ldots,m$) may be close to zero, corresponding to no viscosity in the field p associated with the eigenvalue ω^p. We define the interface Courant number $C^p_{j+1/2} = \omega^p_{j+1/2}\Delta t/\Delta x$ and observe that if:

$$C^p_{j+1/2} = 0 \,, \tag{26}$$

we may expect an entropy violation in the particular field p. For the standard (3-point) method these situations are well understood and we refer to [25] and references therein for a detailed discussion.

Lindqvist et al. [15] showed that for the LTS-Roe scheme the entropy violation may also appear when:

$$C^p_{j+1/2} = -i \,, \quad \forall i \in \mathbb{Z} \,. \tag{27}$$

To clarify this phenomenon and to show how it is avoided in the LTS-HLL scheme we employ the modified equation analysis.

3.1 Modified Equation Analysis

For scalar conservation laws, Lindqvist et al. [15] showed that the LTS method (10) gives a second-order accurate approximation to the equation:

$$u_t + f(u)_x = \frac{1}{2}\Delta x \left[\frac{\Delta x}{\Delta t} \left(\sum_{i=1-k}^{k-1} \bar{Q}^i \frac{\Delta t}{\Delta x} - c^2 \right) u_x \right]_x \,, \tag{28}$$

where $\bar{Q}^i = Q^i(u,\ldots,u)$ is the numerical viscosity coefficient of the $(2k+1)$-point method, and $c = f'(u)\Delta t/\Delta x$. Therein, the expression:

$$D(u) = \sum_{i=1-k}^{k-1} \bar{Q}^i \frac{\Delta t}{\Delta x} - c^2 \,, \tag{29}$$

is interpreted as the amount of numerical diffusion inherent to the scheme. In [15] $D(u)$ for the LTS-Roe scheme is determined as:

$$D_{\text{LTS-Roe}} = \left(\lceil |c| \rceil - |c|\right)\left(1 + |c| - \lceil |c| \rceil\right) \,, \tag{30}$$

where $\lceil c \rceil = \min\{n \in \mathbb{Z} \,|\, n \geq c\}$ is the ceiling function. We may observe that D vanishes when (27) is satisfied. If the solution is supposed to be a rarefaction wave, this will lead to an entropy-violating expansion shock. We note that in [15] the modified equation (28) is defined for scalar conservation laws. Herein, we use it for systems of conservation laws by treating each characteristic field p separately.

Proposition 1. *The numerical diffusion D^p in the p-th characteristic field for the LTS-HLL scheme* (11)–(12) *is:*

$$\begin{aligned} D^p_{\text{LTS-HLL}} = &\frac{c-c_{\text{L}}}{c_{\text{R}}-c_{\text{L}}}\left(\lceil|c_{\text{R}}|\rceil-|c_{\text{R}}|\right)\left(1+|c_{\text{R}}|-\lceil|c_{\text{R}}|\rceil\right) \\ &+\frac{c_{\text{R}}-c}{c_{\text{R}}-c_{\text{L}}}\left(\lceil|c_{\text{L}}|\rceil-|c_{\text{L}}|\right)\left(1+|c_{\text{L}}|-\lceil|c_{\text{L}}|\rceil\right) \\ &+(c-c_{\text{L}})(c_{\text{R}}-c)\ , \end{aligned} \tag{31}$$

where $c_{\text{L}} = S_{\text{L}}\Delta t/\Delta x$, $c_{\text{R}} = S_{\text{R}}\Delta t/\Delta x$ and $c = \hat{\lambda}^p\Delta t/\Delta x$.

Proof. Use (12) in (29). □

Proposition 2. *If the exact solution in the p-th field is a rarefaction wave, i.e.:*

$$\lambda^p_j < \hat{\lambda}^p_{j+1/2} < \lambda^p_{j+1}\ , \tag{32}$$

the numerical diffusion D^p for the LTS-HLLE scheme satisfies:

$$D^p_{\text{LTS-HLLE}} > 0\ . \tag{33}$$

Proof. If (32) holds, Eq. (24) yields:

$$S_{\text{L},j+1/2} < \hat{\lambda}^p_{j+1/2} < S_{\text{R},j+1/2}\ . \tag{34}$$

By using this in (31) we observe that:

$$D^p_{\text{LTS-HLLE}} \geq (c-c_{\text{L}})(c_{\text{R}}-c) > 0\ . \quad \square \tag{35}$$

Numerical investigations in the following section suggest that the above also applies to the LTS-HLLC scheme with the wave velocity estimates according to [18].

4 Results

In this section we compare the LTS-HLL(C) schemes with their non-LTS counterparts and the LTS-Roe scheme. We note that all the results presented for LTS-HLL(C) schemes are obtained with the wave velocity estimates (24). Further, the input discretization parameters are the Courant number C and Δx. Then, the time step Δt is evaluated at each time step according to:

$$\Delta t = \frac{C\Delta x}{\max\limits_{p,j}|\lambda^p_j|}\ . \tag{36}$$

4.1 Sod Shock Tube

We consider the Sod shock tube problem [26] with initial data:

$$\mathbf{U}(x,0) = \begin{cases} (1,0,2.5)^{\mathrm{T}} & \text{if} \quad x < 0\,, \\ (0.125,0,0.25)^{\mathrm{T}} & \text{if} \quad x > 0\,, \end{cases} \tag{37}$$

with the solution evaluated at $t = 0.4$ on a grid with 200 cells. Figure 1 shows the comparison between LTS methods. We observe that the LTS-HLL(C) schemes yield entropy satisfying solutions, while the LTS-Roe scheme leads to an entropy violation at $x \approx -0.25$.

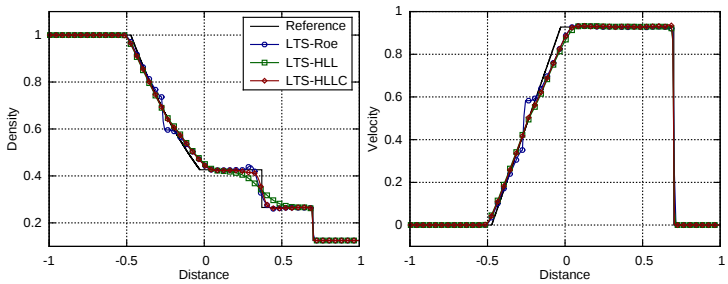

Fig. 1 Comparison between different LTS methods at $C = 3.5$ for problem (37)

4.2 Double Rarefaction Problem

Next, we consider the double rarefaction test case which is often used as a benchmark test case for the positivity preserving. The initial data is:

$$\mathbf{U}(x,0) = \begin{cases} (1,-2,1)^{\mathrm{T}} & \text{if} \quad x < 0\,, \\ (1,2,1)^{\mathrm{T}} & \text{if} \quad x > 0\,, \end{cases} \tag{38}$$

with the solution evaluated at $t = 0.05$ on a grid with 200 cells. Figure 2 shows that the LTS-HLL(C) schemes successfully handle the near-vacuum conditions. In addition, the accuracy is very close to that of the non-LTS methods.

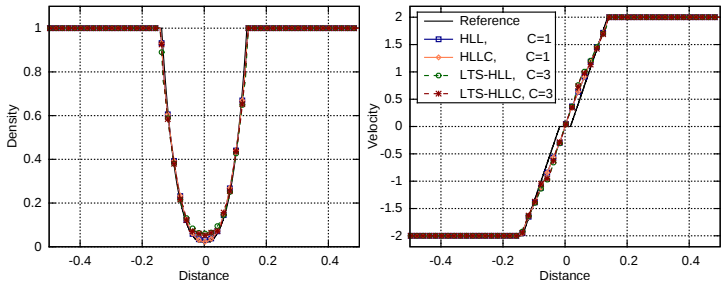

Fig. 2 Comparison between the standard HLL(C) and LTS-HLL(C) schemes for problem (38)

4.3 Woodward-Colella Blast-wave Problem

As the last test case we consider the Woodward-Colella blast-wave problem [27]. The initial data is given by uniform density $\rho(x,0) = 1$, uniform velocity $u(x,0) = 0$, and two discontinuities in the pressure:

$$p(x,0) = \begin{cases} 1000 & \text{if} \quad 0 < x < 0.1\,, \\ 0.01 & \text{if} \quad 0.1 < x < 0.9\,, \\ 100 & \text{if} \quad 0.9 < x < 1\,, \end{cases} \tag{39}$$

with the solution evaluated at $t = 0.038$ on a grid with 1000 cells. The reference solution was obtained by the Roe scheme with the superbee wave limiter on the grid with 16000 cells. The boundary walls at $x = 0$ and $x = 1$ are treated as reflective boundary conditions. In Fig. 3 we can see that all LTS methods correctly capture positions of shocks and contact discontinuities. In the density plot, we observe that both the LTS-Roe and the LTS-HLLC are much more accurate than the standard HLLC scheme.

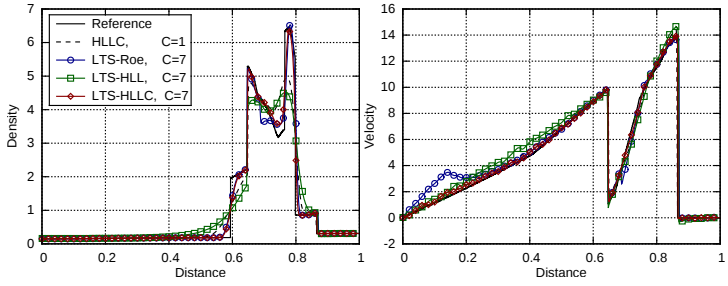

Fig. 3 Comparison between the standard HLLC and different LTS methods for problem (39)

However, the LTS-Roe scheme produces an entropy violation at $x \approx 0.69$, while LTS-HLL(C) schemes do not. This can be seen in Fig. 4 where we zoomed in the area of interest in the plot for the velocity.

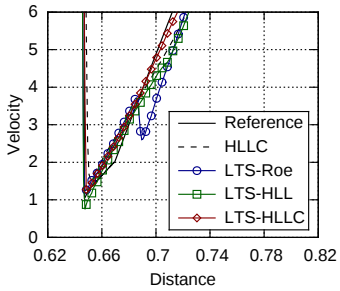

Fig. 4 Entropy violation with the LTS-Roe scheme for problem (39)

5 Conclusions

We used the modified equation analysis to demonstrate that the LTS-HLL scheme proposed by Prebeg et al. [16] with the choice of the wave velocity estimates according to Einfeldt [18] yields entropy satisfying solutions. We applied the scheme to the one-dimensional Euler equations and numerically demonstrated that the LTS-HLL(C) schemes with the same wave velocity choice also yield entropy satisfying solutions. In addition, we applied both schemes to the double rarefaction test case and showed that both schemes successfully handle near-vacuum conditions.

Acknowledgements The author was supported by the Research Council of Norway (234126/30) through the SIMCOFLOW project. I am grateful to my supervisors Tore Flåtten, Bernhard Müller and Marica Pelanti for fruitful discussions.

We would like to thank the anonymous reviewer for his helpful and constructive comments, which led to an improvement of the paper.

References

1. R. LeVeque, SIAM J. Numer. Anal. **19**(6), 1091 (1982). DOI 10.1137/0719080
2. R. LeVeque, Comm. Pure Appl. Math. **37**(4), 463 (1984). DOI 10.1002/cpa.3160370405
3. R. LeVeque, SIAM J. Numer. Anal. **22**(6), 1051 (1985). DOI 10.1137/0722063
4. J. Murillo, P. García-Navarro, P. Brufau, J. Burguete, Int. J. Numer. Meth. Fluids **50**(1), 63 (2006). DOI 10.1002/fld.1036

5. M. Morales-Hernández, P. García-Navarro, J. Murillo, J. Comput. Phys. **231**(19), 6532 (2012). DOI 10.1016/j.jcp.2012.06.017
6. M. Morales-Hernández, J. Murillo, P. García-Navarro, J. Burguete, in *Numerical Methods for Hyperbolic Equations*, ed. by E.V. Cendón, A. Hidalgo, P. García-Navarro, L. Cea (CRC Press, 2012), pp. 141–148. DOI 10.1201/b14172-17
7. M. Morales-Hernández, M. Hubbard, P. García-Navarro, J. Comput. Phys. **263**, 303 (2014). DOI 10.1016/j.jcp.2014.01.019
8. M. Morales-Hernández, A. Lacasta, J. Murillo, P. García-Navarro, Appl. Math. Model. **47**, 294 (2017). DOI 10.1016/j.apm.2017.02.043
9. R. Xu, D. Zhong, B. Wu, X. Fu, R. Miao, Chinese Sci. Bull. **59**(21), 2534 (2014). DOI 10.1007/s11434-014-0374-7
10. Z. Qian, C.H. Lee, J. Comput. Phys. **230**(19), 7418 (2011). DOI 10.1016/j.jcp.2011.06.008
11. K. Tang, A. Beccantini, C. Corre, Comput. Fluids **93**, 74 (2014). DOI 10.1051/m2an:2004016
12. N.N. Makwana, A. Chatterjee, in *2015 IEEE International Conference on Computational Electromagnetics (ICCEM 2015)* (Institute of Electrical and Electronics Engineers (IEEE), 2015), pp. 330–332. DOI 10.1109/COMPEM.2015.7052651
13. S. Lindqvist, H. Lund, in *VII European Congress on Computational Methods in Applied Sciences and Engineering, 5-10 June, Crete Island, Greece*, ed. by M. Papadrakakis, V. Papadopoulos, G. Stefanou, V. Pleveris (2016)
14. M. Prebeg, T. Flåtten, B. Müller, Appl. Math. Model. **44**, 124 (2017). DOI 10.1016/j.apm.2016.12.010
15. S. Lindqvist, P. Aursand, T. Flåtten, A.A. Solberg, SIAM J. Numer. Anal. **54**(5), 2775 (2016). DOI 10.1137/15M104935X
16. M. Prebeg, T. Flåtten, B. Müller, Large Time Step HLL and HLLC schemes (2017). Manuscript submitted for publication.
17. A. Harten, P.D. Lax, B. van Leer, SIAM Rev. **25**(1), 35 (1983). DOI 10.1137/1025002
18. B. Einfeldt, SIAM J. Numer. Anal. **25**(2), 294 (1988). DOI 10.1137/0725021
19. S. Davis, SIAM J. Sci. Stat. Comput. **9**(3), 445 (1988). DOI 10.1137/0909030
20. E.F. Toro, M. Spruce, W. Speares, Shock Waves **4**(1), 25 (1994). DOI 10.1007/BF01414629
21. P. Roe, J. Comput. Phys. **43**(2), 357 (1981). DOI 10.1016/j.jcp.2011.06.008
22. E.F. Toro, *Riemann Solvers and Numerical Methods for Fluid Dynamics*, 3rd edn. (Springer Berlin Heidelberg, 2009). DOI 10.1007/b79761
23. B. Einfeldt, C. Munz, P. Roe, B. Sjögreen, J. Comput. Phys. **92**(2), 273 (1991). DOI 10.1016/0021-9991(91)90211-3
24. P. Batten, N. Clarke, C. Lambert, D. Causon, SIAM J. Sci. Comput. **18**(6), 1553 (1997). DOI 10.1137/S1064827593260140
25. R. LeVeque, *Finite Volume Methods for Hyperbolic Problems* (Cambridge University Press, 2002). DOI 10.1017/CBO9780511791253
26. G.A. Sod, J. Comput. Phys. **27**(1), 1 (1978). DOI 10.1016/0021-9991(78)90023-2
27. P. Woodward, P. Colella, J. Comput. Phys. **54**(1), 115 (1984). DOI 10.1016/0021-9991(84)90142-6